# Transcriptome based analysis of starch metabolism in *Solanum tuberosum*

## Transkriptionelle Analyse des Stärkemetabolismus in *Solanum tuberosum*

Den Naturwissenschaftlichen Fakultäten
der Friedrich-Alexander-Universität Erlangen-Nürnberg
zur Erlangung des Doktorgrades Dr.rer.nat.

vorgelegt von
**Stephanus Johannes Ferreira**
aus Upington, Republik Südafrika

Als Dissertation genehmigt von der Naturwissenschaftlichen
Fakultät der Friedrich-Alexander-Universität
Erlangen-Nürnberg

Tag der mündlichen Prüfung:

Vorsitzender der Prüfungskommision: Prof. Dr. Rainer Fink

Erstberichterstatter: Prof. Dr. Uwe Sonnewald

Zweitberichterstatter: Prof. Dr. Jens Kossmann

After climbing a great hill, one only finds that there are many more hills to climb.

Nelson Mandela, *Long Walk to Freedom*

## Table of contents

# 1. Introduction

## 1.1. Central carbon metabolism and the production of starch

Central carbon metabolism concerns the reactions required for the fixation of carbon through photosynthesis and the production of carbon skeletons needed for all organic compounds, which includes storage carbohydrates. The most abundant storage carbohydrate in the world is starch, making it the most important energy source for the human diet. It consists of two major fractions, amylose and amylopectin. Amylose is essentially a linear polymer of glucose, whilst amylopectin has a higher percentage of branches. Due to its importance, crop plants producing starch in large quantities have been extensively researched. The fourth most important crop in the world in terms of total biomass produced is potato and this is due to its starchy tuber which can store up to 80% of its dry weight as starch (Kruger, 1997). It has also recently become attractive as a system for the production of valuable bio products, for instance vaccines (Streatfield, 2006) and antibodies (Ma et al., 2003; Obembe et al., 2011). Its ability to produce large quantities of carbohydrates makes it especially suited for the production of high value carbohydrates. Börnke et al. (2002) expressed a sucrose isomerase gene derived from bacteria in the apoplasmic space of potato tubers and were able to almost completely convert sucrose to the high value sucrose isomer trehalulose. The study was not only important in showing that potato tubers have the potential to be used as bioreactors for high-value sugars, but also served as an important research tool to study sugar signaling in potato tubers. For instance, Hajirezaei et al. (2003) observed increased respiration in these tubers. They also observed an increase in respiration when yeast invertase was expressed specifically in the cytosol of companion cells of potato tubers. In these lines there was also a reduction in sucrose, but in contrast to sucrose isomerase expression tubers (CW-ISO), which had a reduced glucose content, this was accompanied by an increase in glucose. The authors concluded from this study that it is rather the absence of sucrose, and not increased glucose, which leads to an increase in respiration.

Despite its potential for the production of novel products, the main economic benefit of potato remain its ability to produce starch and most research on potato have been aimed

at increasing potato tuber starch yield. Here, starch metabolism, with special emphasis on starch production in potato tubers, will be discussed.

### 1.1.1. Starch biosynthesis

In potato starch is either accumulated transiently in leaves or as storage starch in tubers. In leaves starch is synthesised in the chloroplast from triose-phosphates produced during photosynthesis. After several intermediate steps, glucose 6-phosphate is converted to glucose 1-phosphate by plastidial phosphoglucomutase (pPGM). Glucose 1-phosphate, along with ATP, serves as substrate for ADP-glucose production by ADP-glucose pyrophosphorylase (AGPase), which is the first reaction committed to starch biosynthesis (Müller-Röber et al., 1992). ADP-glucose is then the glycosyl donor for the various starch synthases forming linear glucans which are subsequently branched. The branch points, which are connected by alpha-1,6 bonds and not alpha 1,4 bonds as for the linear polymer, are produced by the starch branching enzymes. The orderly fashion in which these branch points occur is the primary reason for the semi-crystalline structure of starch, and what makes the molecule essentially insoluble in water. Recent studies have shown the importance of debranching enzymes in modifying starch branches to produce the structured starch molecule (Delatte et al., 2005; Streb et al., 2008). There are two classes of debranching enzymes in plants, limit dextrinase (LDE) and isoamylase. Isoamylase can be further divided into isoamylase 1 (ISA1), isoamylase 2 (ISA2) and isoamylase 3 (ISA3) (Hussain et al., 2003; Rahman et al., 2003). Although knowledge on LDE is incomplete, it seems to be mainly involved in starch degradation, where its role appears to be partly redundant with mutants showing no starch-related phenotype in Arabidopsis (Delatte et al., 2006). ISA1 and ISA2, which form a heterodimeric enzyme *in vivo*, are mainly involved in starch biosynthesis, where they hydrolyse wrongly positioned branches, producing a more structured starch molecule, as stated above. In Arabidopsis mutants lacking ISA1 or ISA2, starch structure is altered and contains a higher fraction of short branches. Furthermore, there is also accumulation of highly branched soluble glucan (Zeeman et al., 1998; Delatte et al., 2005; Streb et al., 2008).

For starch production in the tuber, photoassimilates in the form of sucrose must first be imported from photoautotrophic tissue via the phloem (Farrar, 1992). Despite some conflicting evidence (Sweetlove et al., 1998), it is generally accepted that starch biosynthesis in potato is sink limited (Zrenner et al., 1996). After the formation of tubers they represent the predominant sink in the plant. One of the major problems with potato research is that tuber growth and induction rates are not synchronised. Although tuber developmental stages are well defined (Kloosterman et al., 2005), this does not mean that tubers in the same stage have similar growth- or biochemical characteristics. Adding to this, tubers are underground organs making *in vivo* analysis without damaging the plant almost impossible. To date no study has determined the *in vivo* growth velocity of individual tubers.

The onset of tuberisation is marked by many physiological and biochemical changes in the stolons. The major changes, which are seen as markers of tuberisation, are the switch from apoplastic to symplastic sucrose unloading and the change from hydrolytic to sucrolytic cleavage of sucrose (Viola et al., 2001). Sucrose synthase (Susy) activity increases with the development of the tuber and it is believed that the rate of sucrose degradation, which under normal conditions is determined by Susy, is a major determinant of potato sink strength (Zrenner et al., 1995). In earlier attempts to increase sink strength by increasing the rate of sucrose degradation yeast invertase was expressed in potato tubers, where it was targeted to either the cytosol or apoplasm. Apoplasmic (U-IN-1) and cytosolic (U-IN-2) expression led to very different results. Cytosolic expression led to large changes in metabolite levels, reduced starch and, importantly, to an increase in respiration (Trethewey et al., 1998; Hajirezaei et al., 2000; Bologa et al., 2003). This increase in tuber respiration led to an acceleration of starch degradation during potato tuber storage. Apoplasmic expression led to an increase in tuber size and, under certain conditions, also tuber yield. This increase, however, was due to an increase in the water content, and there was no effect on the starch yield (Sonnewald et al., 1997; Hajirezaei et al., 2000). In later studies on U-IN-2, aiming to improve the starch yield, it was argued that the endogenous rates of hexokinase are not sufficient to convert the produced glucose to glucose-6-phosphate. To circumvent this problem a bacterial

glucokinase was over-expressed in the U-IN-2 background. Surprisingly, this led to a further increase in the levels of glycolytic metabolism and respiration, further reducing starch levels (Trethewey et al., 1998). Thus, despite the extensive research on yeast invertase expressing plants, the reasons for the shift to respiration in U-IN-2 are still not clear. Furthermore, it is also puzzling that such an increase in respiration is not observed in U-IN-1.

As mentioned, sucrose is primarily degraded by sucrose synthase in developing tubers, and after the degradation of sucrose to UDP-glucose and fructose, the two molecules must be converted to glucose 6-phosphate via different pathways for starch biosynthesis. The major difference between starch biosynthesis in tubers compared to leaves is that hexose-phosphates and ATP must be imported from the cytosol to the plastid. Although there is evidence that glucose 1-phosphate can also be transported across the plastid membrane and directly used for starch biosynthesis via starch phosporylase in potato tuber discs (Fettke et al., 2010), it seems that *in vivo* glucose 6-phosphate is the predominant form of hexose-phosphate transport across the amyloplast membrane. Transport of glucose 6-phosphate and ATP across the amyloplast membrane is facilitated by the plastidial glucose 6-phosphate translocator (GPT) (Kammerer et al., 1998), and the plastidial ATP/ADP translocator (NTT) (Tjaden et al., 1998), respectively. In fact, simultaneous over-expression of these transporters led to an increase in total starch yield per plant showing that starch biosynthesis is co-limited by hexose-phosphate and ATP in the plastid (Zhang et al., 2008). Glucose 6-phosphate is then converted to glucose 1-phosphate by plastidial PGM (pPGM). Silencing of plastidial PGM lead to a dramatic reduction in starch content of the tubers, illustrating not only the importance of this enzyme in starch biosynthesis, but provides compelling evidence that starch is synthesised from imported glucose 6-phosphate (Tauberger et al., 2000). As mentioned earlier, glucose 1-phosphate and ATP serve as substrates for ADP-glucose synthesis by AGPase and further starch biosynthesis is similar to leaves. Since large scale comparative transcriptome analysis comparing leaf and tuber starch biosynthesis have not been done, it is not known whether or not the same isoforms of these enzymes are active in both tissues. The importance of AGPase in starch biosynthesis has been shown on various

occasions and reduced activity lead to low starch, high sucrose containing tubers (Müller-Röber et al., 1992). As far as increasing starch biosynthesis by over-expression of AGPase is concerned, two studies over-expressing a non-regulated AGPase gave conflicting results. Stark et al. (1992) could increase starch content by over-expression but Sweetlove et al. (1996) showed that increased biosynthesis is accompanied by increased breakdown. There are mainly four soluble starch synthase enzymes responsible for biosynthesis, starch synthase I, II, III, IV and one that is exclusively granule bound, named granule bound starch synthase (GBSS). Soluble starch synthases and the branching enzymes, and also debranching enzymes as mentioned earlier, are believed to be responsible for amylopectin synthesis. The major starch synthases are starch synthase II and III and silencing of these two isoforms lead to greatly altered amylopectin structure (Lloyd et al., 1999). Granule bound starch synthase is exclusively responsible for the synthesis of amylose and a potato mutant lacking any activity produce amylose free starch (Hovenkamp-Hermelink et al., 1987). Starch synthase IV seems to be important for starch granule initiation and Arabidopsis mutants lacking this isoform do not only show changes in diurnal starch accumulation, but also have fewer, and bigger, starch granules (Roldán et al., 2007; Szydlowski et al., 2009). Despite the many isoforms of branching enzyme they can be grouped into starch branching enzyme A (SBEA) and B (SBEB). The majority of branching enzyme activity can be attributed to SBEB (Kossmann et al., 1991), but silencing of only SBEB did not lead to a change in starch structure. Simultaneous silencing of SBEA and SBEB, however, lead to production of high amylose potato starch (Schwall et al., 2000).

### 1.2. Starch degradation

In contrast to starch biosynthesis, the pathway of starch degradation in potato tubers is not well understood, although recent findings, especially in Arabidopsis, have greatly enhanced our understanding of starch degradation (Smith et al., 2005; Kötting et al., 2010). Currently it is believed that the major pathway of starch degradation in Arabidopsis and other organisms proceeds via β-amylase (Scheidig et al., 2002; Kaplan and Guy, 2005). Starch must first be phosphorylated by glucan-water dikinase (GWD),

and to a lesser extent phospho-glucan water dikinase (Ritte et al., 2002; Baunsgaard et al., 2005) before degradation can commence. Although the requirement of phosphorylation for starch degradation has been known for a while (Lorberth et al., 1998), the reason for this remained obscure. Recently, however, it has been shown that phosphorylation is important for the disruption, and by this solubilisation of glucans, making them accessible to the degrading enzymes (Hejazi et al., 2008). It is then either directly degraded to maltose by β-amylase or first to soluble glucans by Isoamylase 3 (Edner et al., 2007) and probably also other enzymes, for instance alpha-amylase. Despite the proven role of alpha-amylase during the mobilisation of starch reserves in cereal endosperms (Beck and Ziegler, 1989; Fincher, 1989), the role of the enzyme in dicots remains somewhat of a mystery. In Arabidopsis there are three alpha-amylase proteins (AAMY1, AAMY2 and AAMY3). Even though AAMY3 is located in the chloroplast and have amylolytic activity, single mutants of neither AAMY1, AAMY2 nor AAMY3 have a starch phenotype (Yu et al., 2005). However, *in vitro* the enzyme is capable of releasing glucans from the granule and its potential role in potato starch degradation cannot be ignored. Furthermore, in an Arabidopsis *isa1/isa2/isa3/lda* mutant background, which leads to the production of only soluble glucans, further removal of alpha-amylase 3 partly restores the wild type glucan phenotype. This suggests a role for alpha-amylase in degrading soluble glucans during starch biosynthesis (Streb et al., 2008).

Despite knowing for decades that ß-amylase cannot move pass phosphate residues and that glucan degradation is abolished when the enzyme encounters a phosphorylated glucose unit (Takeda and Hizukuri, 1981), the importance of dephosphorylation for the complete hydrolysis of glucans only recently became evident with the identification of a mutant with a starch excess phenotype, termed *sex4*. The mutation occurred in a specific phosphatase gene capable of removing phosphate groups from the glucan allowing for the complete hydrolysis by ß-amylase, producing maltose (Kötting et al., 2009). Maltose is subsequently exported to the cytosol via the maltose transporter (MEX1) (Niittylä et al., 2004) and it is believed that the disproportioning enzyme 2 (DPE2) plays an important role in its further degradation (Chia et al., 2004). Maltose can also be degraded by disproportioning enzyme 1 (DPE1) inside the plastid. For potato evidence has been

provided that DPE2 might be present inside the plastid (Lloyd et al., 2004), which questions the role of MEX1. A recent study, however, has shown that potato DPE2 is most probably also located outside the plastid (Lütken et al., 2010).

### 1.2.1. Starch degradation and long term tuber storage.

Since most potatoes are consumed fresh, long term storage of potato tubers is required to supply the demand all year long. After potato tubers are harvested they enter a period of dormancy in which very little metabolic activity takes place (Sonnewald, 2001). At the end of the dormancy period potato tubers start to sprout. The time and rate at which potato tubers sprout is dependent on various factors, one of which is the supply of soluble carbohydrates to the growing sprout. Under normal conditions, after soluble sugars are depleted, carbon supply for the growing sprout comes almost exclusively from the degradation of starch, a process which is partly dependent on the solubility of starch, as explained earlier. To extend the dormancy period, tubers are often stored under cold conditions, but this leads to other unwanted effects, for instance cold induced sweetening of tubers (Sonnewald, 2001). Although there is general agreement on the reasons for cold induced sweetening, very few attempts to reduce cold induced sweetening have been successful (Greiner et al., 1999), and only one study has been able to directly connect a starch degrading gene, GWD, to cold induced sweetening (Lorberth et al., 1998). Taken together, despite the clear role that starch degradation should play in the economically important processes of sprouting and cold induced sweetening, knowledge of the enzymes and regulatory mechanisms involved currently is inadequate.

### 1.3. Aims of the study

Despite the many studies done on starch biosynthesis in potato, and the vast knowledge gained, lack of knowledge on the regulatory mechanisms controlling it has hampered progress concerning the desire to increase potato tuber starch yield. In addition, individual potato tubers differ greatly in terms of initiation times and growth velocities, which cannot be studied since tubers are below-ground organs. Recent technological advancements regarding potato genomic (Xu et al., 2011) and transcriptional (Kloosterman et al., 2008) analysis have greatly enhanced our ability to study potato. Thus, this study, based on transcriptome analysis, aimed at identifying regulatory mechanisms underlying starch biosynthesis under various conditions, in different tissues, and also in transgenic plants with altered central carbon metabolism. Furthermore, it was aimed to develop a technique to study gene expression in relation to the specific growth rates of individual tubers. Secondly, aiming to influence starch degradation in terms of its role in sprouting and cold induced sweetening, specific genes were silenced and the results analysed. To conclude, an overview of the aims of this study is given in context of the various experimental chapters in which they are dealt with:

*1. Transcriptome analysis of starch metabolism in potato and the measurement of tuber growth velocity using X-ray computed tomography.*

The aim of this work was to investigate the transcriptional regulation of starch biosynthesis in potato tubers under various conditions. More specifically the similarties in gene expression between leaves and tubers were looked at. Furthermore a new technique, based on X-ray computed tomography, to determine tuber growth velocity *in vivo* was established and it was used to analyse gene expression in tubers growing at different velocities.

*2. Transciptional and metabolic profiling of yeast invertase expressing potato tubers.*

The aim of this chapter was to elucidate the metabolic pathways and signals responsible for the phenotypical changes occurring in potato tubers expressing yeast invertase in either the apoplasm (U-IN-1) or the cytosol (U-IN-2), with special emphasis on the

increase in tuber respiration at the expense of starch biosynthesis in U-IN-2. To this end gene expression analysis of growing U-IN-1 and U-IN-2 tubers was conducted in combination with metabolic data analysis.

*3. Transcriptional and metabolic profiling of sucrose isomerase expressing potato tubers.*
The aim of this chapter was to gain further insight into tubers expressing sucrose isomerase in either the apoplasmic space (CW-ISO) or the vacuole (NTTP) by conducting large scale transcriptional and metabolic profiling. Furthermore, transcriptional profiling was performed on potato leaf discs floated in different sugar solutions.

*4. Comparative transcriptome analysis towards the identification of regulatory genes*
The aim of this chapter was to identify through comparative transcriptome analysis regulatory genes involved in starch biosynthesis.

*5. Simultaneous silencing of isoamylases ISA1, ISA2 and ISA3 by multi-target RNAi in potato tubers.*
To enhance our understanding on the role of isoamylase in potato tuber sprouting, and starch metabolism in general, transgenic plants with reduced expression of all three isoamylases were created and the effect on starch degradation, and starch metabolism in general, was studied.

*6. Identification and RNAi silencing of alpha-amylase 23 in potato.*
The aim of this work was to identify, through microarray data analysis, starch degradation associated genes involved in potato tuber sprouting. Here the identification of a gene, annotated as alpha-amylase 23, which was strongly up-regulated at the time of sprouting during the sprout release assay (Hartmann et al., 2011) is shown. The gene was targeted by RNAi and the results are shown.

## 2. Results

### 2.1. Transcriptome analysis of starch metabolism in potato and the measurement of tuber growth velocity using X-ray computed tomography

In this chapter the transcriptional regulation of starch biosynthesis in potato tubers under various conditions was investigated. More specifically similarities between gene expression in leaves and tubers, and also the diurnal gene regulation in both tissues were analysed. Furthermore, a new technique using X-ray computed tomography to determine tuber growth velocity *in vivo* was established and used to analyse gene expression in tubers growing at different velocities. Table 1 contains all the genes involved in starch metabolism which will be further discussed in this chapter. The pathways in which these enzymes are involved are shown in figure 1.

**Table 1. List of genes involved in starch metabolism which will be discussed in this chapter.**

| Name | Abbreviated name | POCI identifier |
|---|---|---|
| Plastocyanin | Plastocyanin | Micro.4322.c1 |
| Chlorophyll a/b binding | CAB | Micro.4163.c1 |
| Ribulose 1,5 bisphosphate carboxylase oxygenase | Rubisco | Micro.4165.c3 |
| Triose phosphate translocator 1 | TPT | Micro.3160.c1 |
| Glucose 6-phosphate translocator 1 | GPT1 | Micro.4029.c2 |
| Glucose 6-phosphate translocator 2 | GPT2 | Micro.1076.c1 |
| Plastidial phosphoglucomutase | PGM | Micro.1743.c2 |
| ATP/ ADP translocator 1 | NTT1 | Micro.1831.c2 |
| ADP-glucose pyrophosphorylase large subunit | AGPase LS | Micro.2198.c1 |
| ADP-glucose pyrophosphorylase small subunit | AGPase SS | Micro.367.c1 |
| Starch synthase II | SSII | Micro.1850.c2 |
| Starch synthase III | SSIII | Micro.1658.c1 |
| Granule bound starch synthase | GBSS | Micro.920.c2 |
| Starch synthase IV | SSIV | Micro.16059.c1 |
| Starch branching enzyme A | SBEA | Micro.16220.c1 |
| Starch branching enzyme B | SBEB | Micro.1689.c1 |
| Isoamylase 1 | ISA1 | Micro.7513.c1 |
| Isoamylase 2 | ISA2 | Micro.13258.c1 |
| Cell wall invertase | Cw-Inv | Micro.4223.c2 |
| Fructokinase | FK | Bf_suspxxxx_0040h09.t3m.scf |
| Sucrose synthase 4 | Susy4 | Micro.196.c8 |
| Hexokinase 1 | HK1 | Micro.5594.c1 |
| Hexokinase 2 | HK2 | Micro.4130.c1 |

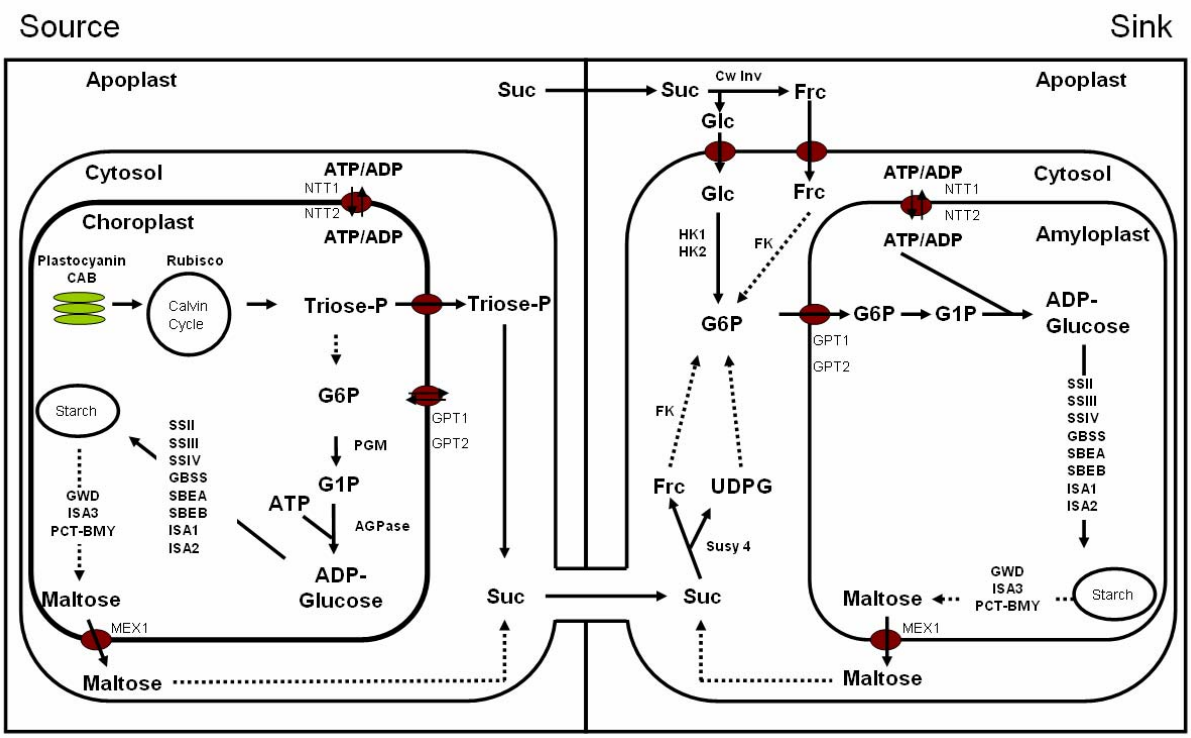


**Figure 1. Proposed pathways for starch biosynthesis in source and sink tissues.**

### 2.1.1. Microarray analysis of starch metabolism in potato leaves and tubers

Leaf samples for starch and RNA extractions were taken from four week old potato plants grown under a fourteen hour light and ten hour dark cycle. The light conditions were chosen to ensure diurnal turnover of transitory starch. As was expected, starch levels were the lowest at the start of the light period and accumulated during the day to a high at the end of the light period (figure 2A). The same pattern was observed for sucrose although the accumulation and decline was more rapid (figure 2B). The levels of starch and sucrose compared well to what was previously measured in potato leaves (Zrenner et al., 1996).

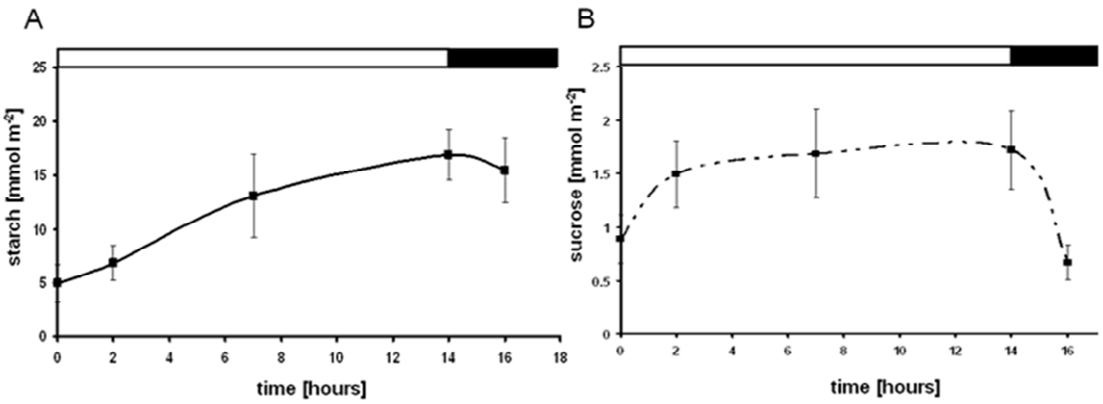


**Figure 2. Diurnal starch and sucrose content of leaves over a sixteen hour period.** A) Starch and B) sucrose content. Error bars indicate standard deviation (n=3).

After confirming that there was a turnover of transient starch under the specific light conditions used, gene expression at different times of the day was analysed by microarray. To this end, RNA samples were prepared from leaf discs taken at the same time-points as described for the starch and sucrose measurements above. For gene expression analysis, samples taken at the start of the light cycle, two hours into the light cycle, at the end of the light cycle and two hours into the dark cycle were hybridised to the Agilent 44k POCI array (Kloosterman et al., 2008), and data extracted using GeneSpring GX7.3.1 software as described in the materials and methods. To investigate how much similarity there is between leaf and tuber starch biosynthesis, the expression of genes known to be important for tuber starch biosynthesis was investigated in leaves. Most starch biosynthetic genes had a strong diurnal rhythm with expression increasing along with carbohydrate accumulation. Interestingly, genes involved in the import of glucose 6-phosphate and ATP into the plastid were co-regulated with ADP-glucose pyrophosphorylase (figure 3A). To rule out that the observed expression of GPT and NTT in leaf extracts was due to contaminating epidermis rather than mesophyll cells, cell-specific RNA analysis was performed. To this end epidermis stripes were harvested and expression of GPT and NTT were probed by quantitative real-time PCR (qRT-PCR). As shown in figure 4, GPT and NTT expression in epidermis cells was about ten fold lower compared to whole leaf extracts.

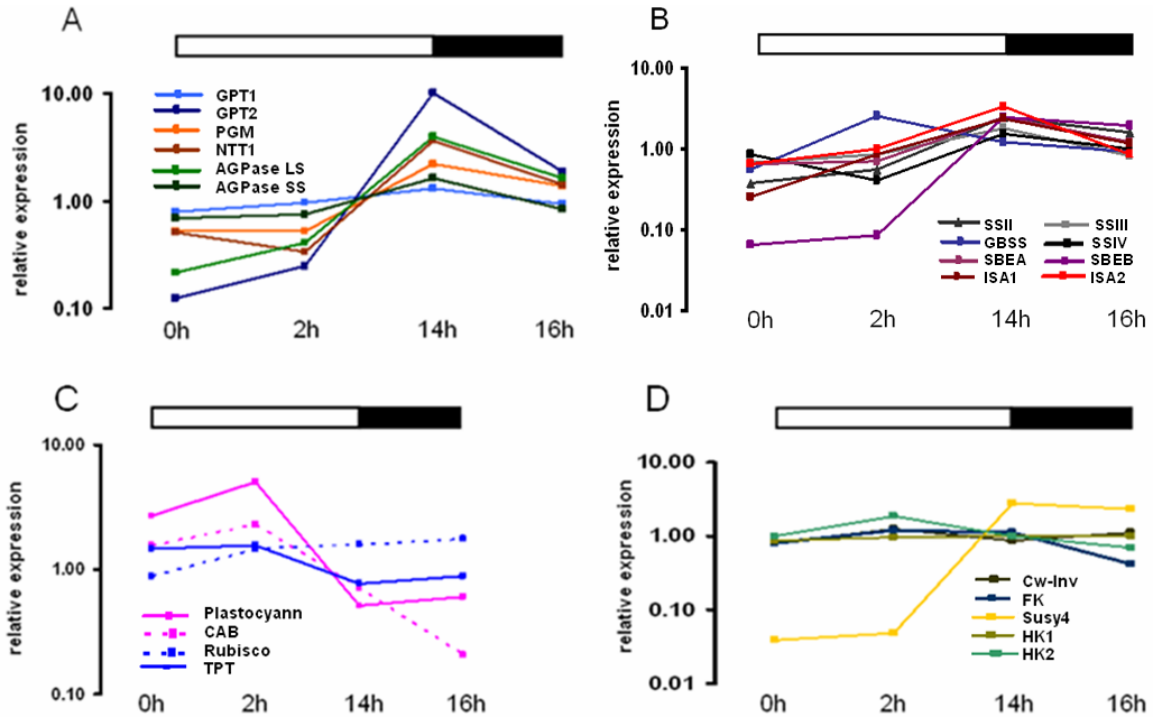


**Figure 3. Diurnal expression of genes known to be involved in starch biosynthesis.** A) Import of glucose 6-phosphate and ATP into the plastid and the conversion thereof to ADP-Glucose. B) Starch synthases and branching enzymes. C) Photosynthetic and Calvin cycle related genes. D) Sucrose cleavage and phosphorylation. Values are the mean of two replicates.

Most starch synthases and branching enzymes displayed a similar pattern to the above mentioned genes in figure 3A with the exception of GBSS, which was highest expressed two hours into the light period (figure 3B). Two genes involved in the light reaction of photosynthesis, plastocyanin and chlorophyll a/b binding protein, were already up-regulated at the first time point which was taken moments after the lights came on and were highest expressed two hours into the light. Ribulose 1,5 bisphosphate carboxylase oxygenase (Rubisco) had an expression pattern similar to that of starch biosynthetic genes (figure 3C). The sucrose cleavage enzymes cell wall-bound invertase and sucrose synthase had very different expression patterns with Susy 4 being much stronger regulated. Susy 4 increased during the light and went down in the dark. Hexokinase 1 was not diurnally regulated, whilst hexokinase 2 and fructokinase had a similar pattern of increasing early in the morning and declining at the end of the light period (figure 3D).

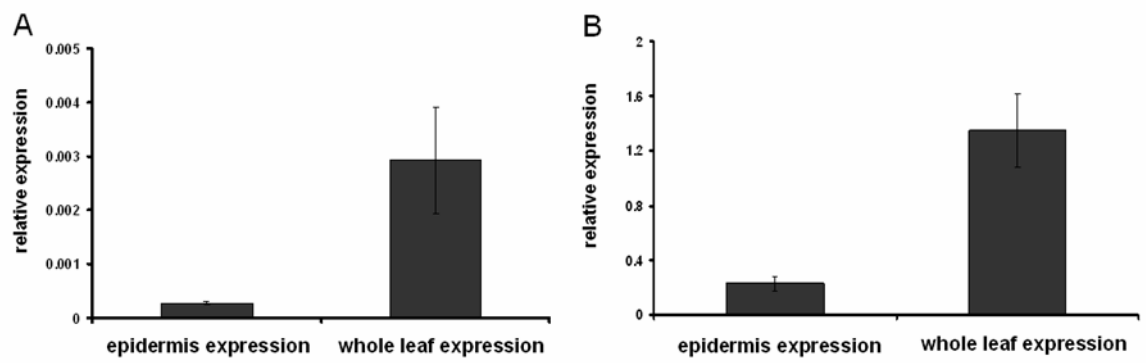


**Figure 4. Relative expression of GPT and NTT in epidermal and whole leaf tissue.** A) GPT and B) NTT. Error bars represent standard deviation (n = 3).

For analysis of gene expression during tuber induction, tuber developmental stages were designated according to Kloosterman (2005). Tuber samples taken from potato plants between four and six weeks old were hybridised to the Agilent 44k POCI array (Kloosterman et al., 2008), and data extracted using GeneSpring GX7.3.1 software as described in the materials and methods. Stage 1, representing an unswollen stolon, showed very low expression for all starch biosynthetic genes except starch synthase IV which was highest expressed at stage 1. From stages 3-5 there was an increase in the expression of all starch biosynthetic genes, again with the exception of starch synthase IV (figure 5A and B). As evidence that stage 1 was before the onset of tuberisation, cell wall-bound invertase expression was very high and sucrose synthase 4 (Susy 4), a tuber expressed isoform (Fu and Park, 1995; Zrenner et al., 1995; Ferreira et al., 2010), low. From stages 3-5 the expression cell wall-bound invertase went down and that of Susy 4 increased (figure 5C). The expression patterns compared well to earlier experiments (Kloosterman et al., 2008). qRT-PCR is a well accepted method for verifying microarray data and was used to validate the expression patterns of a selected number of genes in independent samples. The expression patterns and levels of Susy 4, GPT and GBSS compared well to the microarray data in both leaves and tubers and confirmed the accuracy of the microarray results (figure 6).

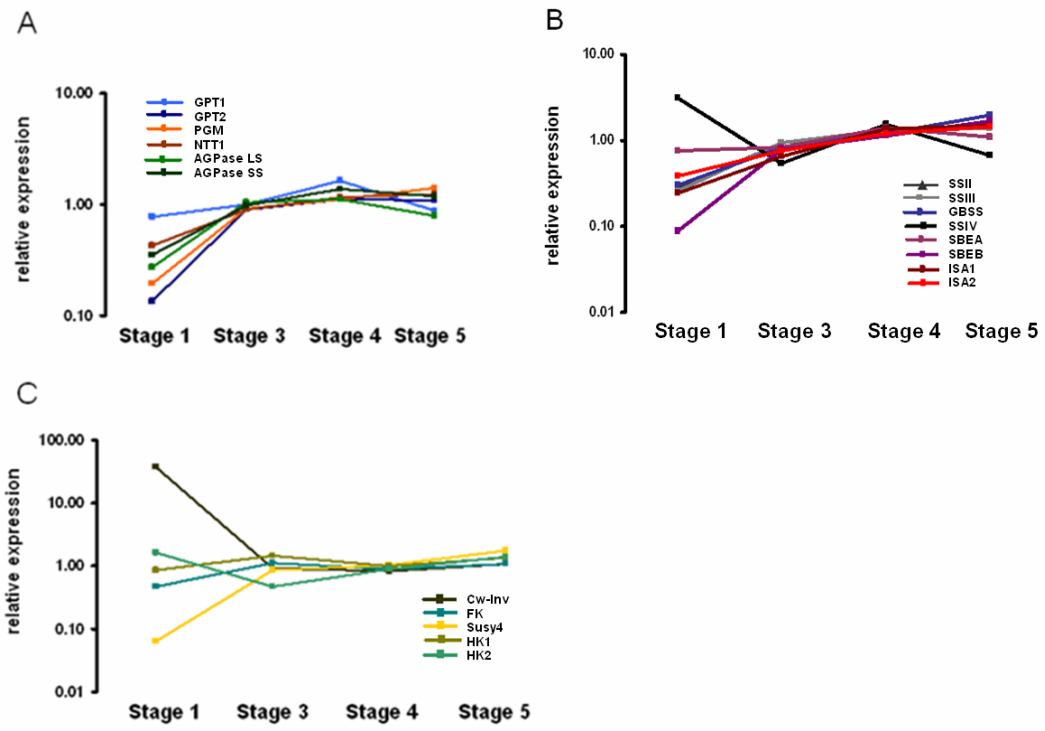


**Figure 5. Expression of genes known to be involved in starch biosynthesis during tuber induction.** A) Import of glucose 6-phosphate and ATP into the plastid and the conversion thereof to ADP-Glucose. B) Starch synthases and branching enzymes. C) Sucrose cleavage and phosphorylation. Values are the mean of two replicates.

The microarray datasets for both the diurnal leaf experiment and the tuber induction experiment have been deposited on ArrayExpress (accession numbers E- MEXP-2481 Ferreira et al. Potato diurnal leaf time- course and E-MEXP-2482 Ferreira et al. Potato tuber induction). POCI sequence and annotation data are available through the POCI online tool http://pgrc.ipk- gatersleben.de/poci

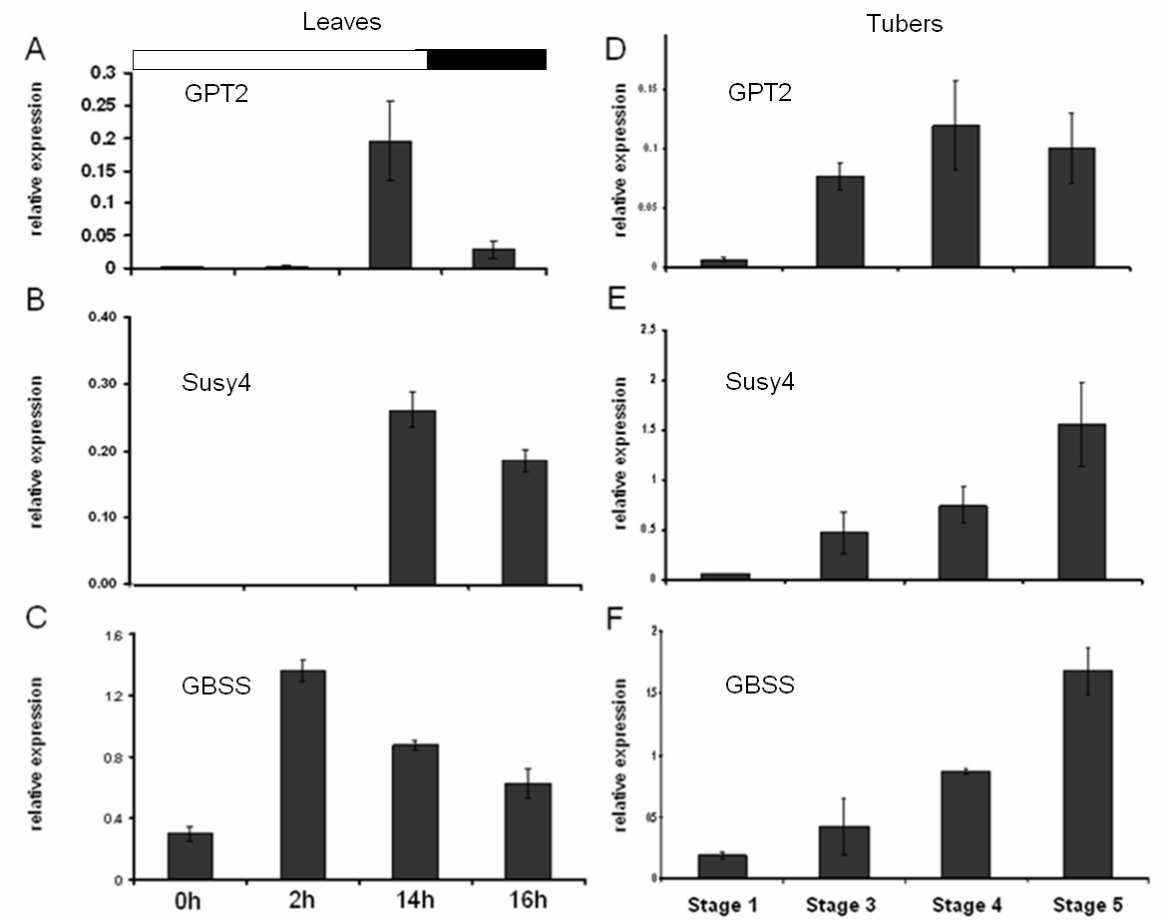


**Figure 6. Quantitative real time PCR confirmation of microarray results.** A-C) Relative expression of GPT2, Susy4 and GBSS diurnally in leaves. D-F) Relative expression of GPT2, Susy4 and GBSS in tubers. Error bars represent standard deviation (n = 3).

### 2.1.2. Diurnal gene expression analysis of GBSS in leaves and tubers.

Since GBSS is one of the strongest diurnally regulated genes involved in starch biosynthesis (Smith et al., 2004) (figure 6), it was investigated whether this gene is also diurnally regulated in tubers. GBSS expression was measured at different times of the day and under different light regimes. Plants were grown in a sixteen hour/ eight hour dark/ light regime and samples were taken from stolon-ends and tubers at different time-points of the diurnal cycle. GBSS expression in tubers oscillated during the day and was highest at the end of the light period and lowest 2 hours into the next light period (figure 7A). Expression was also significantly lower in tubers from plants kept in twenty four

hours of darkness compared to tubers from plants kept in a normal light/ dark cycle (figure 7B).

To examine whether oscillation of GBSS might be due to changes in sucrose supply from the source, sucrose content of stolon-ends attached to a tuber was measured. Phloem sucrose content is very high compared to those tissues surrounding it (Lohaus et al., 1995) and phloem signifies a large proportion of the total stolon tissue (Engels and Marschner, 1986). This makes it possible to determine sucrose import to the tuber by measuring sucrose content of the stolon-end (Sweetlove et al., 1998). Sucrose content differed significantly during the day and was highest at the end of the light and lowest at the end of the dark period. When plants were kept in constant darkness, sucrose content of stolon- ends declined linearly over time indicating that changes in sucrose supply from the leaves contributes to the oscillating expression of GBSS in tubers (figure 7C).

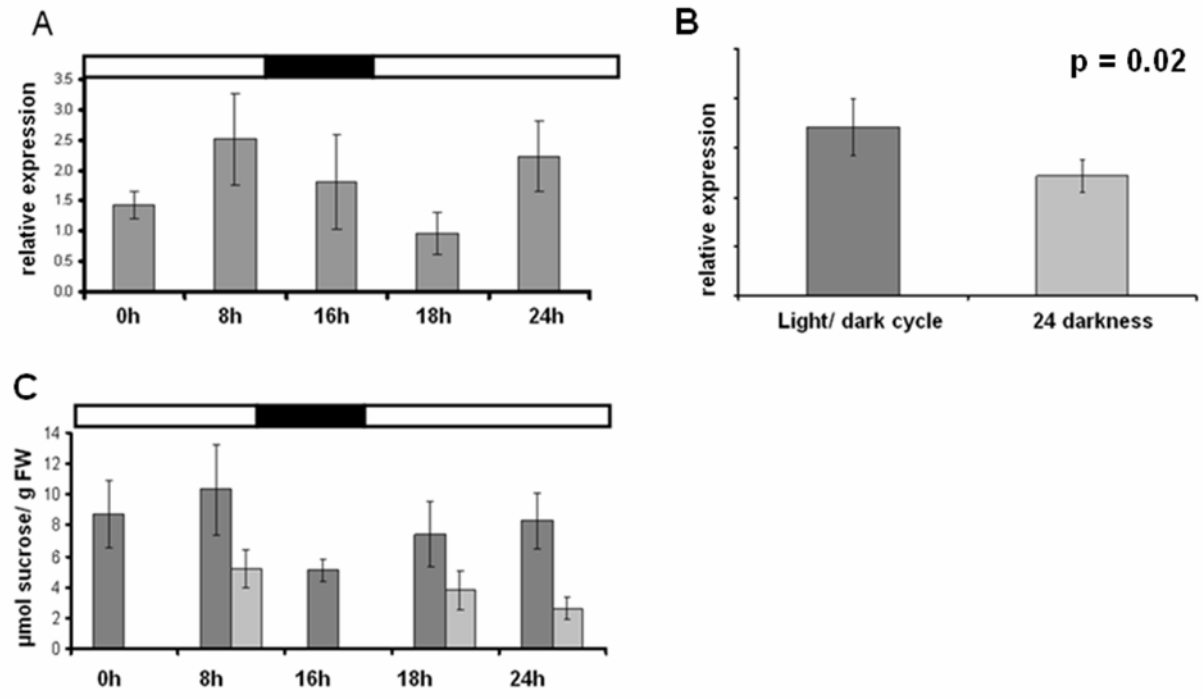


**Figure 7. GBSS relative expression and stolon sucrose content at different time-points of the day.** A) Diurnal expression of GBSS in tubers. B) GBSS expression at the 24 hour time-point from plants grown in light/dark cycle and from plants kept in twenty four hours of darkness. C) Stolon sucrose content at different time-points of the day (dark grey bars) and at the same time-points from plants kept in darkness from 0 hours onward (light grey bars). Error bars represent standard deviation (n = 3-7).

### 2.1.3. Measuring tuber growth velocity using X-ray CT.

Since tuber initiation and growth velocity differ greatly between tubers derived from the same plant, it was thought necessary to study gene expression in tubers growing at different velocities. To achieve this it was necessary to develop a method to view tuber initiation and growth rates without structural damage to the plant. To this end, X-ray Computed Tomography (X-ray CT) was used to determine tuber volume over a time course and then calculate the growth velocity. An overview of the method for calculating tuber volume using X-ray CT is given in figure 8.

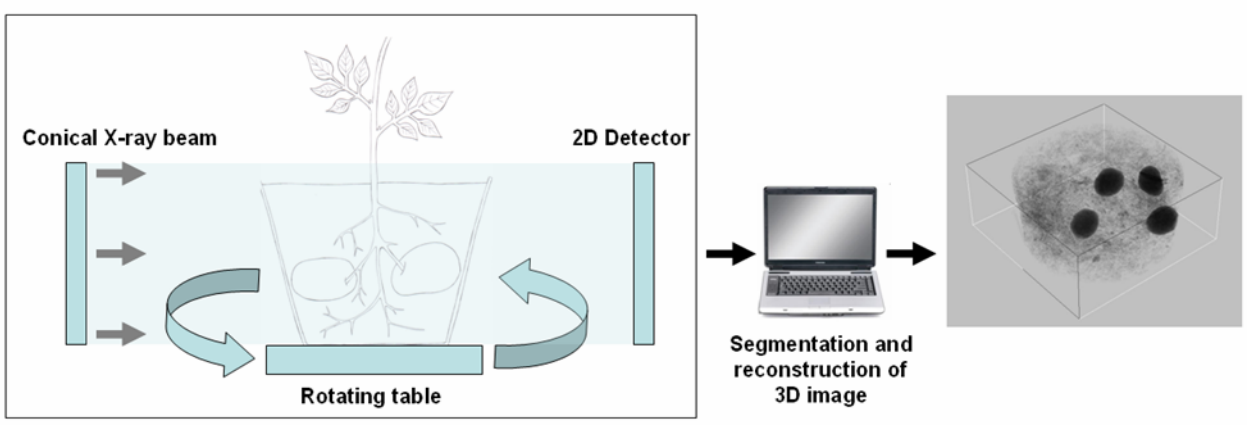


**Figure 8. Schematic scheme illustrating how tuber volume is measured using X-ray CT.** Potato plants are scanned with X-ray in a chamber containing an X-ray beam and a two dimensional detector. After projecting X-ray images of the potato plant on the detector at different angles, the projections are reconstructed *in silico* to create a three dimensional image. From this image the tuber volume can be calculated.

The accuracy of the growth velocity determination depends largely on how precise the volume can be calculated and it was crucial to establish whether tuber volume could be accurately calculated. figure 9A illustrates that potato tubers were clearly distinguishable from the surrounding soil, and a histogram demonstrated that segmentation of tuber material was possible. The software used for segmentation also allowed for manual correction of possible mistakes made during the automatic segmentation process. Tuber growth velocities were calculated for seventeen tubers. To validate the method, calculated tuber volumes were compared to measured tuber volumes after harvest. X-ray CT calculated volumes showed a correlation coefficient with experimental volume

measurements of 0.986, showing that X-ray CT calculated volumes were accurate (figure 9B).

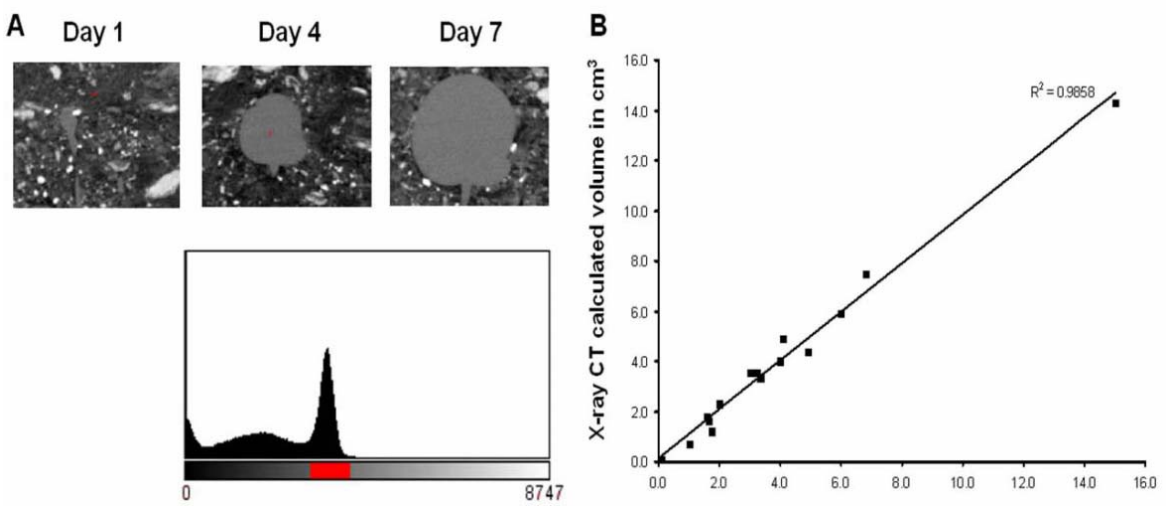


**Figure 9. Potato tuber segmentation and volume calculation.** A) Two dimensional X-ray images illustrating that potato tubers can be distinguished from the surrounding soil. The histogram shows that segmentation is possible. The red bar indicates the grey level threshold selected. B) Linear regression of X-ray calculated and real volume measurements confirming the accuracy of X-ray CT calculated volumes.

Six tubers with different growth velocities (figure 10) were selected for microarray hybridisation and the gene expression patterns were analysed. The expression of genes involved in starch biosynthesis is shown in figure 11. The expression of genes involved in starch biosynthesis did not show large differences in expression levels between tubers that were still growing, albeit at very different velocities. Gene expression however was much lower in tubers that have virtually stopped growing compared to tubers that still actively grow. This was especially true for Susy 4, a major determinant of tuber sink strength (Zrenner et al., 1996).

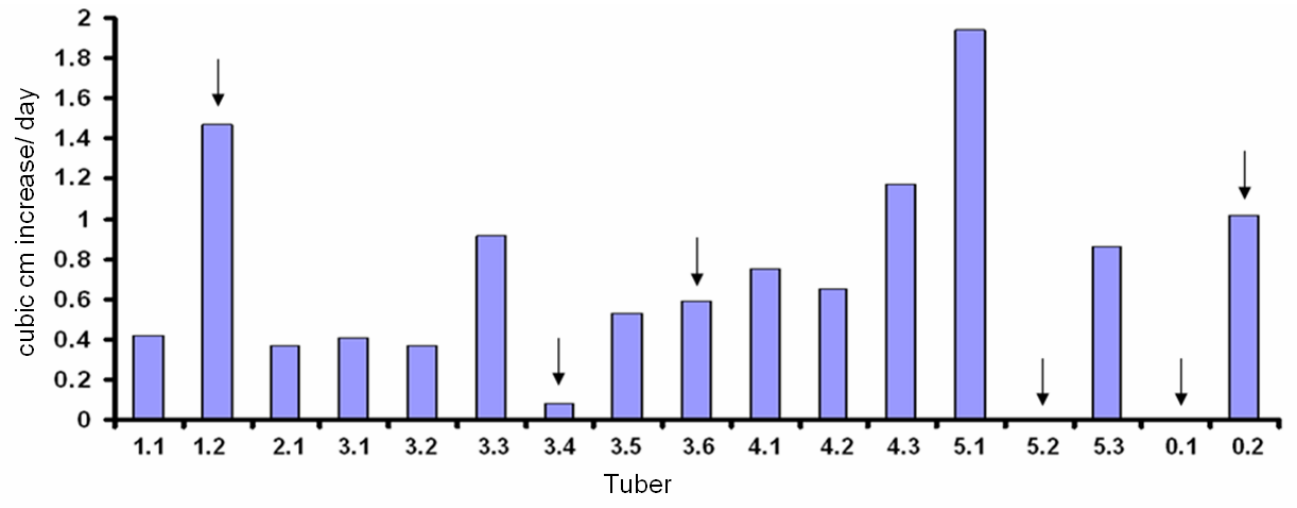


**Figure 10. Estimated growth velocity of tubers in cubic centimeter volume increase per day.** Tubers chosen for microarray hybridization are marked by arrow heads

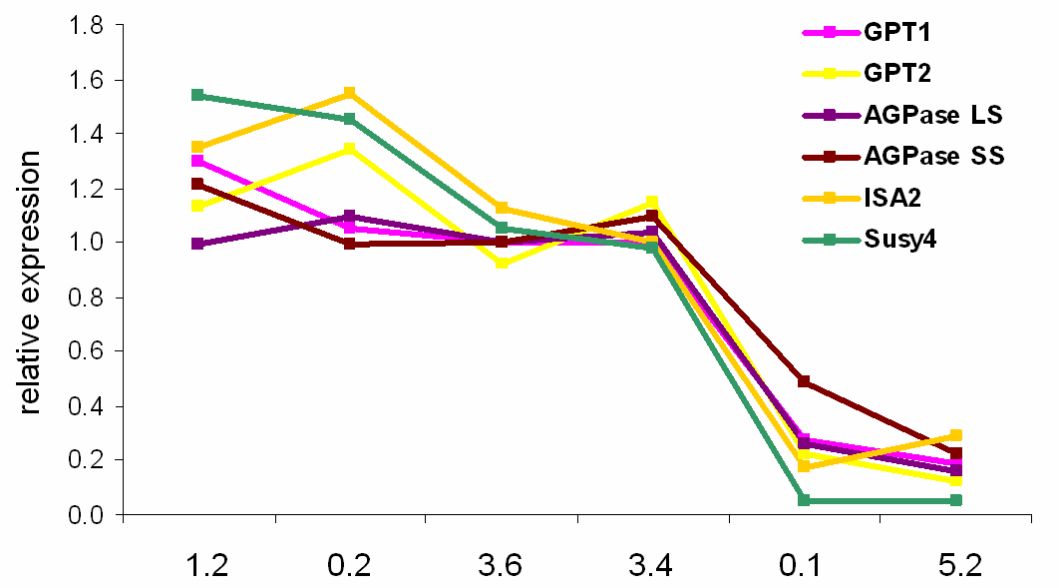


**Figure 11. Relative expression of starch biosynthetic genes in tubers growing at different velocities**. Values are the mean of two replicates.

Attempting to identify which processes were correlating to tuber growth velocity, the correlation coefficient (Pearson correlation) of all transctripts to growth velocity was calculated. Furthermore the relative functional enrichment of features correlating to growth velocity (correlation coefficient >0.5) was determined. Enrichment was based on

the percentage of features from a specific functional group in terms of the percentage which was expected by chance. The functional assignment was performed according to functional groupings defined previously (Hartmann et al., 2011). There was a more than two-fold relative enrichment of features associated with starch metabolism, storage proteins, translation, energy metabolism and cell wall metabolism. There was no functional group more than two-fold enriched amongst the negatively correlated features (figure 12).

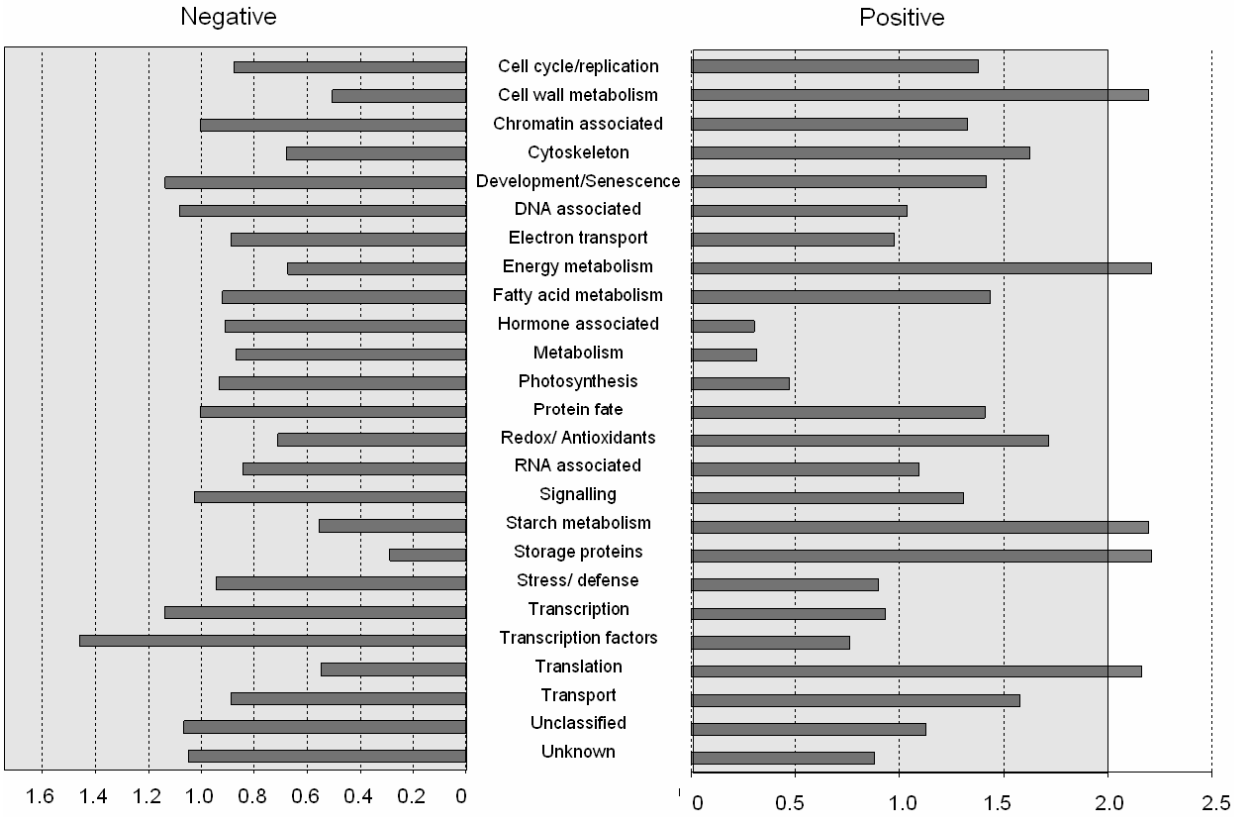


**Figure 12. Functional assignment of features correlating positively or negatively correlating to growth velocity.** Relative enrichment is based on features with a correlation coefficient (Pearson correlation) of either more than 0.5 or less than -0.5 to growth velocity.

The entire microarray dataset for the tuber growth velocity experiment has been deposited on ArrayExpress (accession number E- MEXP-2484 Ferreira et al. tuber growth velocity).

## 2.2. Transcriptional and metabolic profiling of yeast invertase expressing potato tubers

The aim of this chapter was to elucidate the metabolic pathways and signals responsible for the phenotypical changes occurring in potato tubers expressing yeast invertase in either the apoplasm (U-IN-1) or the cytosol (U-IN-2), with special emphasis on the increase in tuber respiration at the expense of starch biosynthesis in U-IN-2. To this end gene expression analysis of growing U-IN-1 and U-IN-2 tubers were conducted in combination with metabolic data analysis.

### 2.2.1. Global analysis of the transcripts and metabolites.

Potato plants were grown under greenhouse conditions for eight weeks after which tuber samples were taken and immediately frozen in liquid nitrogen. It can be assumed that the tubers were still actively growing at this stage. For gene expression analysis, RNA extracted from these samples were hybridised to the Agilent 44k POCI array (Kloosterman et al., 2008), and data extracted using GeneSpring 11 software as described in the materials and methods. As a starting point for the analysis, the global relationship between the different genotypes, based on expression data, was determined. To this end a principle component analysis was performed using either the individual replicates, or the mean expression values of each genotype. Genotypes could be separated on a PCA using expression data, with the replicates of each genotype clearly clustering into different groups. This was also true using the mean values (figure 13).

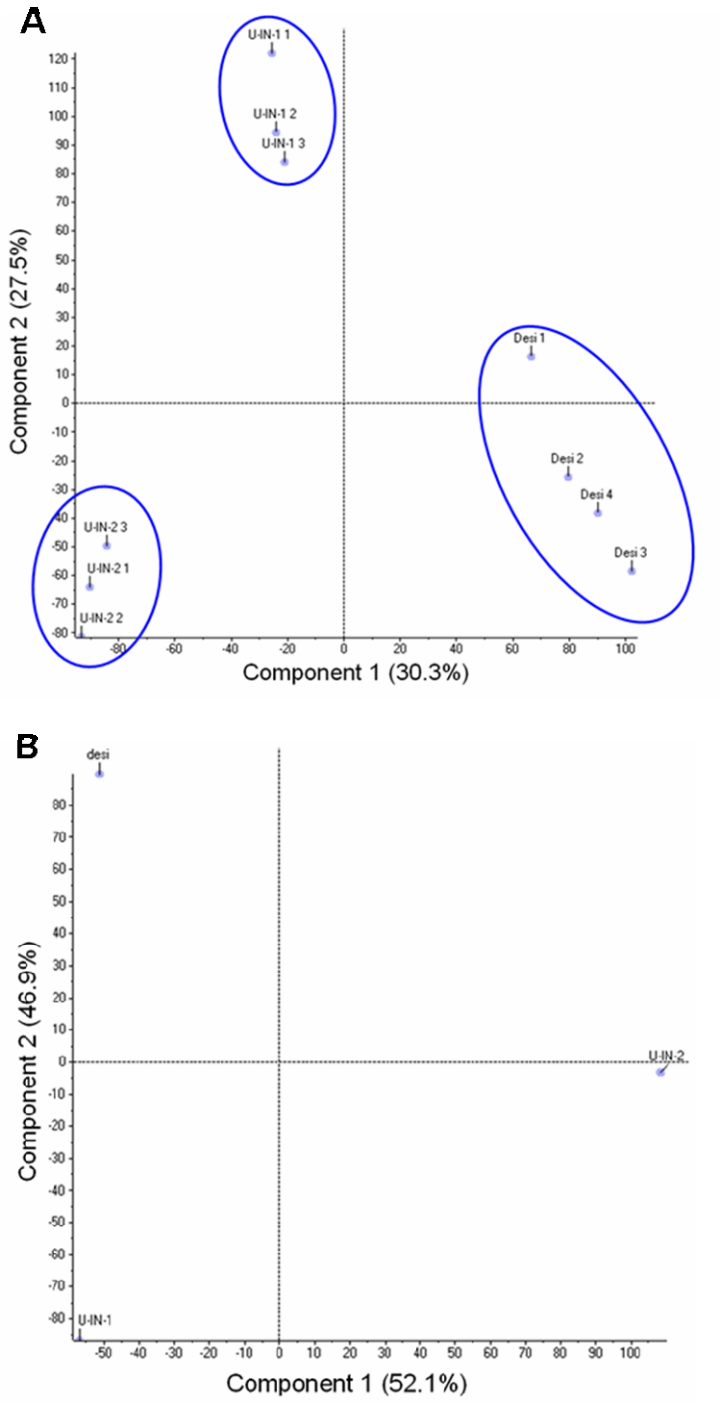


**Figure 13. Principle component analysis (PCA) of transcription data.** A) Individual replicates of each genotype clustered. B) PCA on the mean values of each genotype.

To determine which processes were mainly responsible for the observed phenotypes, a functional assignment of the features more than two-fold differentially expressed compared to the wild type (WT) was performed. Enrichment was based on the percentage

of features from a specific functional group in terms of the percentage which was expected by chance. The functional assignment was performed according to functional groupings defined previously (Hartmann et al., 2011). For U-IN-2 there was no functional group more than two-fold enriched amongst the up-regulated features. There was, however, a more than two-fold enrichment in the down-regulated features for storage proteins, fatty acid metabolism and cell wall metabolism (figure 14).

U-IN-1, despite showing a milder phenotype than U-IN-2 and clustering closer to WT in the PCA, showed far more changes in terms of the number of functional groups changed. Of the up-regulated features there was an enrichment of more than two-fold in development and senescence, whilst redox/ antioxidant, photosynthesis, fatty acid metabolism, cytoskeleton and cell wall metabolism related features were enriched amongst the down-regulated features (figure 14).

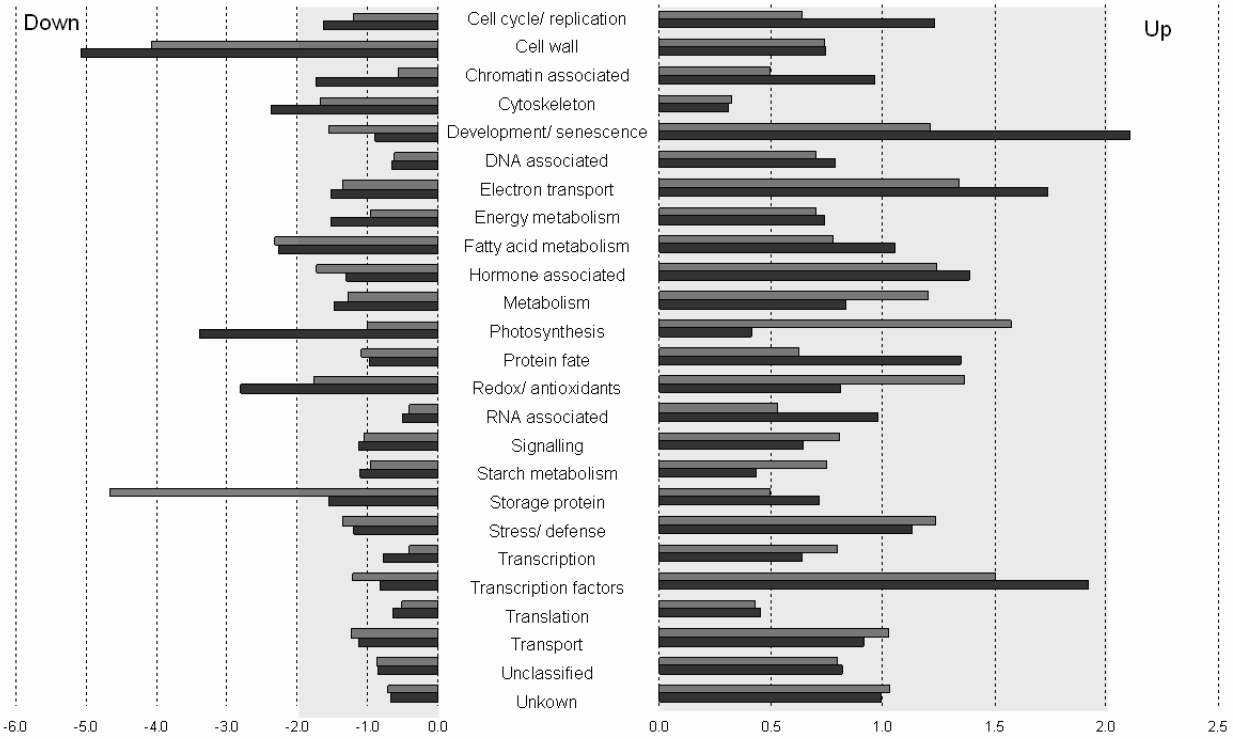


**Figure 14. Relative enrichment of functional groups in differentially expressed transcripts of U-IN-1 (black) and U-IN-2 (grey)**. Enrichment is based on the number of features present from a particular group as a fraction of the total number of features in a specific functional group

Parallel to the transcriptional analysis, metabolic profiling of the genotypes was also performed using the same sampling material. The metabolites measured included phosphorylated intermediates, organic acids, amino acids, major tuber carbohydrates (starch sucrose glucose and fructose), and carotenoids (table S1-S4).. PCA analysis showed that the genotypes could be separated and also provided clarity on which metabolites play the most significant role in the separation. Again, as with the transcripts component one, responsible for 71% of the variance, was able to separate U-IN-2 from the other genotypes, whilst component two, responsible for 29% of the variance, could separate all three genotypes with U-IN-1 the furthest from the control (figure 15). The metabolites most important for the variance in component one were sucrose, sucrose-6-phosphate (S6P), shikimate and glucose. For component two the carotenoid violaxanthin, inorganic pyrophosphate, fructose-6-phosphate and glucose had the biggest influence on the separation. Metabolic analysis revealed no significant change in total free amino acids in U-IN-2 and a strong reduction in U-IN-1 (table S2).

**A**

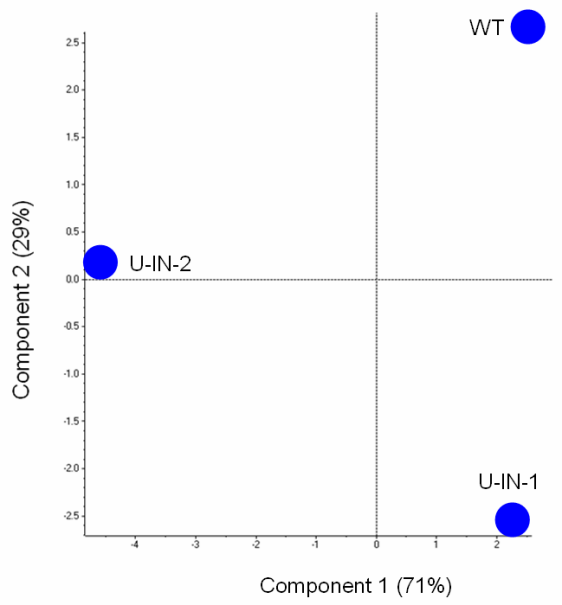


**B**

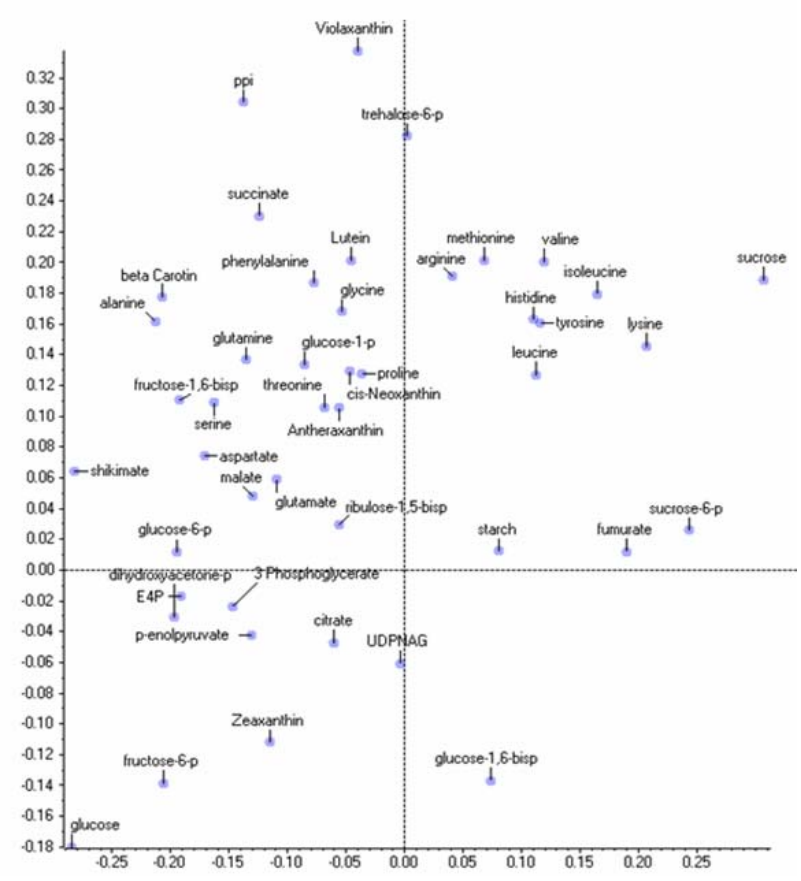


**Figure 15. Principle component analysis on metabolite levels.** A) The PCA separation of the genotypes and B) the loadings of the individual metabolites.

### 2.2.2. Pathway specific analysis.

#### 2.2.2.1. Cell wall and fatty acid biosynthesis.

To further enhance our understanding of what happened in the transgenic lines, pathway specific analysis of transcripts and metabolites were performed using Mapman software (Thimm et al., 2004). The first pathways analysed were cell wall and fatty acid biosynthesis, since global analysis revealed a down-regulation of transcripts associated with these in both U-IN-1 and U-IN-2. Using genomic (Xu et al., 2011) and expression data five differentially expressed isoforms of Susy could be identified, with the dominant isoform in tubers, Susy 4 (Fu and Park, 1995; Zrenner et al., 1995; Ferreira et al., 2010; Xu et al., 2011), strongly down-regulated in U-IN-1. It did not show any change in expression in U-IN-2. A striking aspect of Susy expression in U-IN-2 was the strong increase in expression of an isoform of Susy which is normally associated with stolons (Ferreira et al., 2010) (Figure 16 and 17).

From the transcription data it seems quite clear, especially for U-IN-2, that the reactions requiring UDP-glucose are all down-regulated. There also seems to be other pathways activated in order to produce the required UDP-glucose and UDP-glucuronate. UDP-glucuronate can also be produced via a bypass reaction through the myo-inositol pathway. There was not a strong, uniform up-regulation of this pathway in either U-IN-1 or U-IN-2, but myo-inositol-1-phosphate synthase (MI-1PS) was strongly up-regulated, especially in U-IN-2. Glucose-6-phosphate can also be converted to UDP-glucose via cytosolic phosphoglucomutase (cPGM) and UDP-glucose pyrophosphorylase (UGPase). In both transgenic lines there was increased cPGM expression, and in U-IN-2 there was also an increase in the expression of UGPase transcripts (figure 16 and 17).

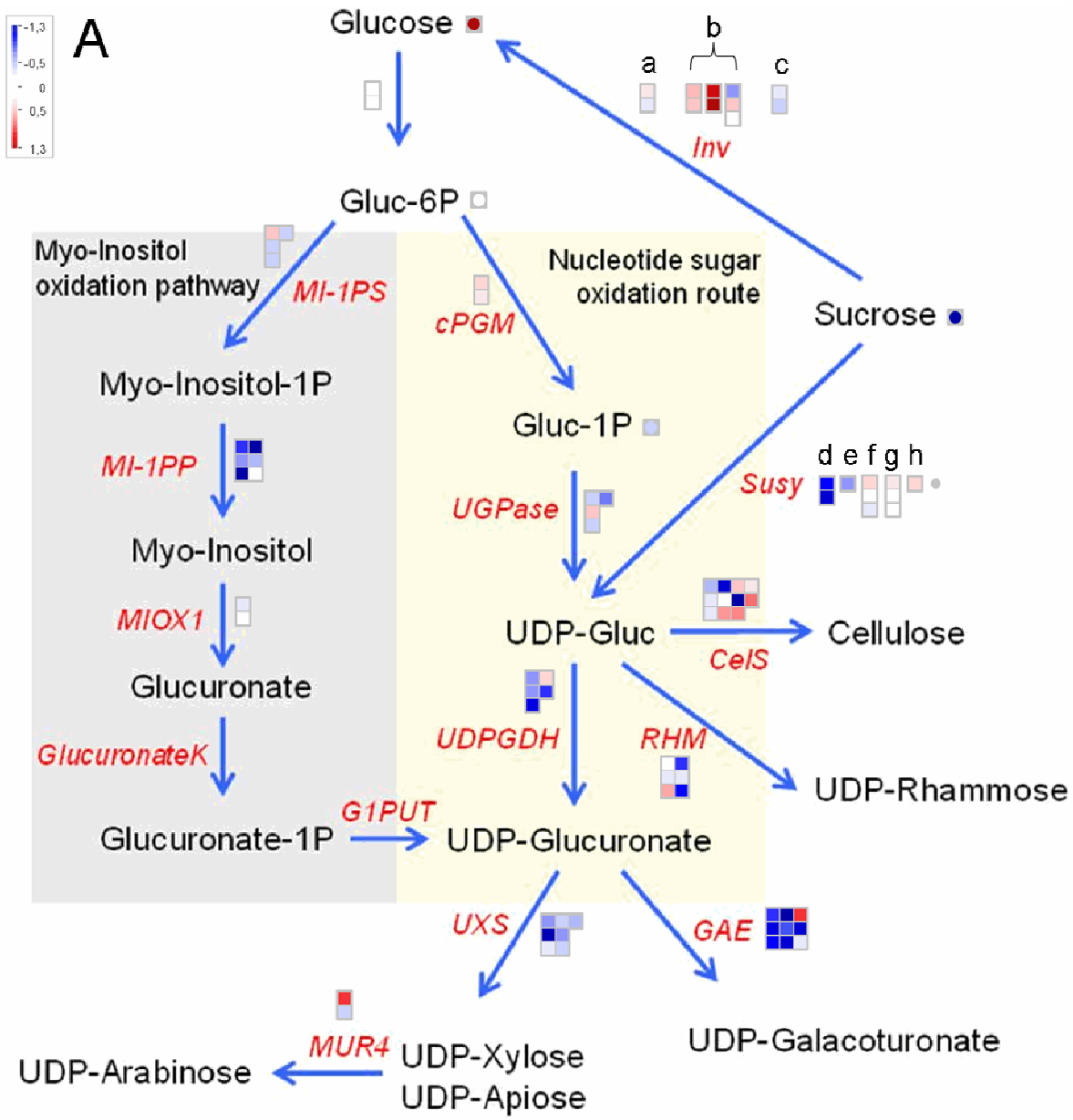


**Figure 16A.The production of UDP-glucose and UDP-glucuronate for cell wall biosynthesis in U-IN-1**. a) Neutral invertase. b) Cell wall invertase c) Vacuolar invertase. d-h) differentially expressed Susy isoforms with d) Susy4 and g) an isoform normally associated with stolons.

Gene name abbreviations: MI-1PP-Myo-inositol 1-phosphate phosphatase; GlucoronateK-gluconurate kinase; G1PUT-galactose-1-phosphate uridylytransferase; UXS- UDP-xylose synthase; GAE-UDP-glucuronate epimerase; RHM-rhamnose synthase; CelS-Cellulose synthase.

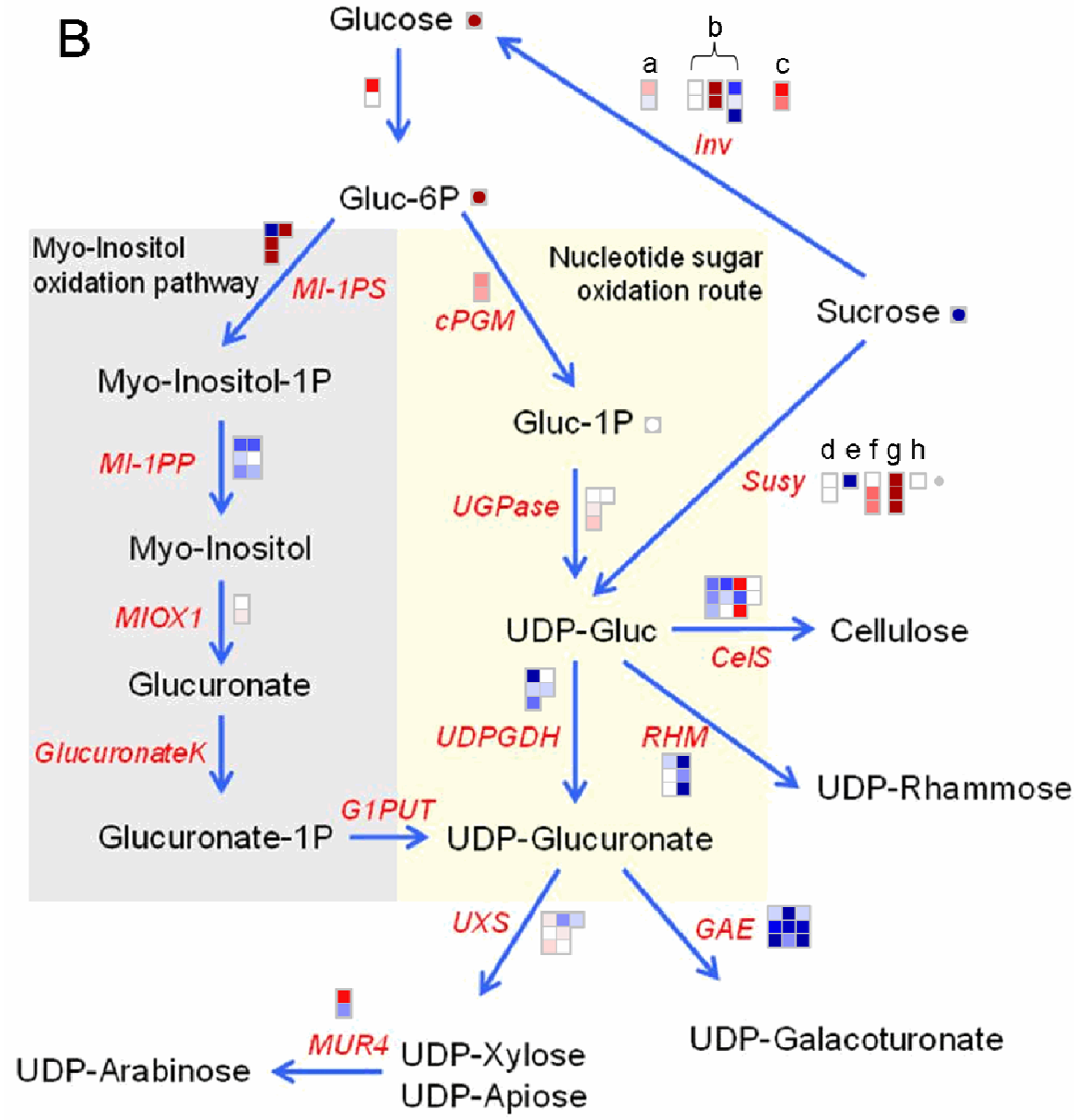


**Figure 16B.The production of UDP-glucose and UDP-glucuronate for cell wall biosynthesis in U-IN-2**. a) Neutral invertase. b) Cell wall invertase c) Vacuolar invertase. d-h) differentially expressed Susy Isoforms with d) Susy4 and g) an isoform normally associated with stolons.

Gene name abbreviations: MI-1PP-Myo-inositol 1-phosphate phosphatase; GlucoronateK-gluconurate kinase; G1PUT-galactose-1-phosphate uridylytransferase; UXS- UDP-xylose synthase; GAE-UDP-glucuronate epimerase; RHM-rhamnose synthase; CelS-Cellulose synthase.

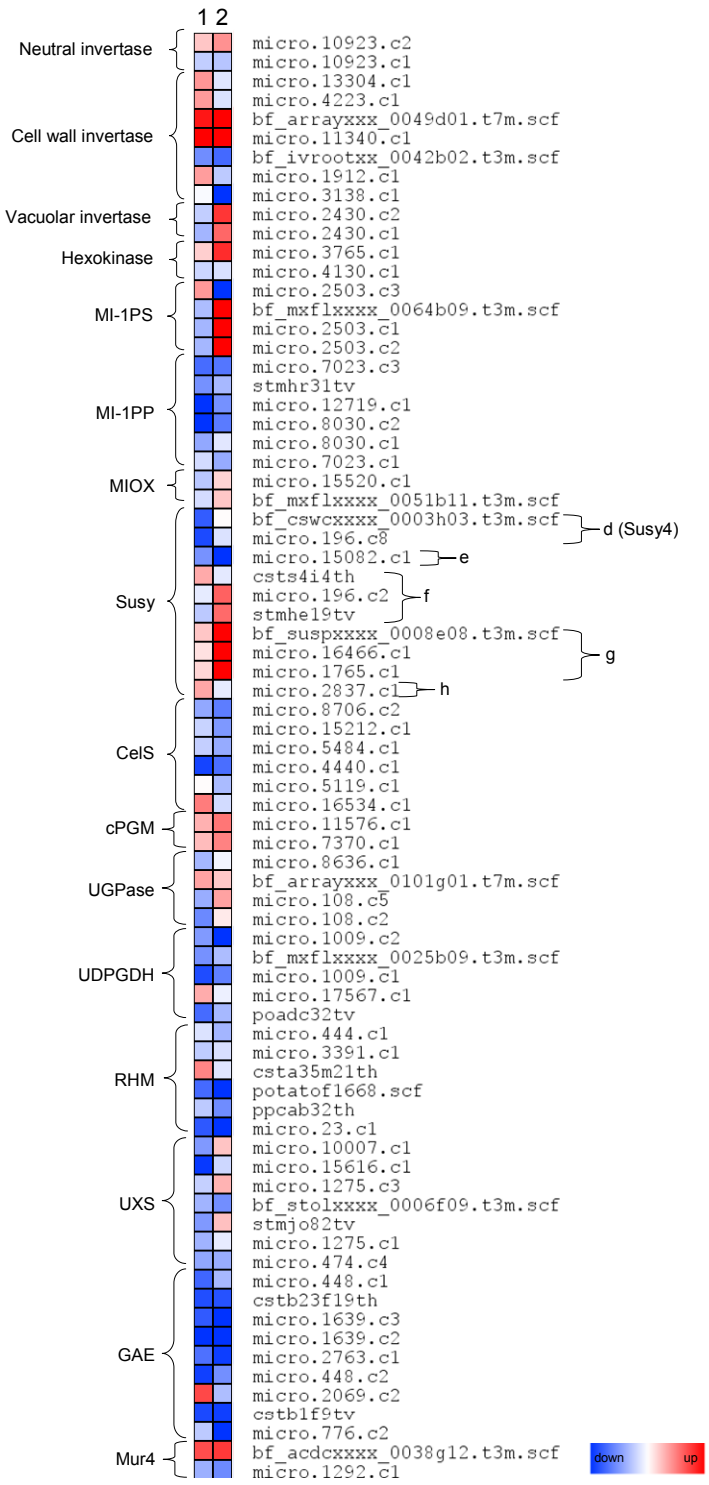


**Figure 17. Heatmap representation of features viewed in cell wall biosynthesis pathway.** Column 1 represents U-IN-1 and column 2 U-IN-2. Log2 values of the fold change compared to WT. Values are the mean of 3-4 replicates.

As mentioned, global analysis indicated a reduction in fatty acid metabolism in both U-IN-1 and U-IN-2. Closer inspection of the metabolic path leading to fatty acid biosynthesis revealed striking similarity between U-IN-1 and U-IN-2. Plastidial Acetyl-CoA, substrate for fatty acid biosynthesis, is produced from PEP by plastidial pyruvate kinase and pyruvate dehydrogenase. Despite an increase in PEP, there was a reduction in the expression of plastidial pyruvate kinase and pyruvate dehydrogenase. There was no such reduction for plastidial pyruvate kinase in U-IN-1, the only major difference in expression between the two genotypes regarding fatty acid biosynthesis. Plastidial Acetyl-CoA can also be produced from citrate by ATP: citrate lyase, either in the cytosol or in the plastid from imported citrate, with the distribution of cytosolic to plastidial activity varying greatly between *species* (Rangasamy and Ratledge, 2000) Although it was difficult to distinguish between cytosolic and plastidial isoforms in the study, it was quite clear that there is a significant reduction in expression of most of the transcripts encoding the different isoforms of this gene. Furthermore, there was also a strong reduction in the expression of genes involved in subsequent steps of fatty acid biosynthesis (figures 18 and 19).

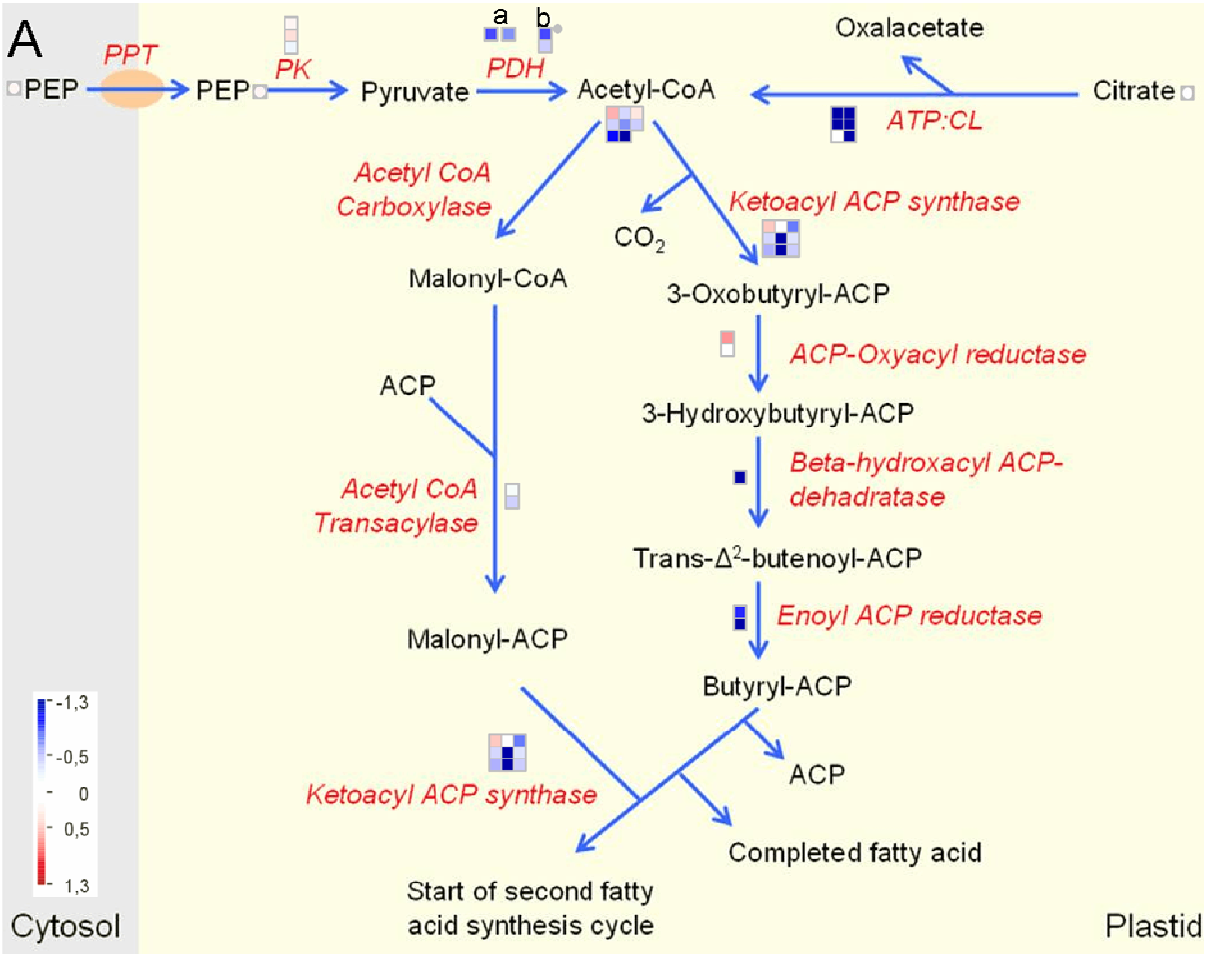


**Figure 18A.Fatty acid metabolism from imported PEP and citrate in U-IN-1**. Different subunits of the pyruvate dehydrogenate complex: a) E2. b) E3.

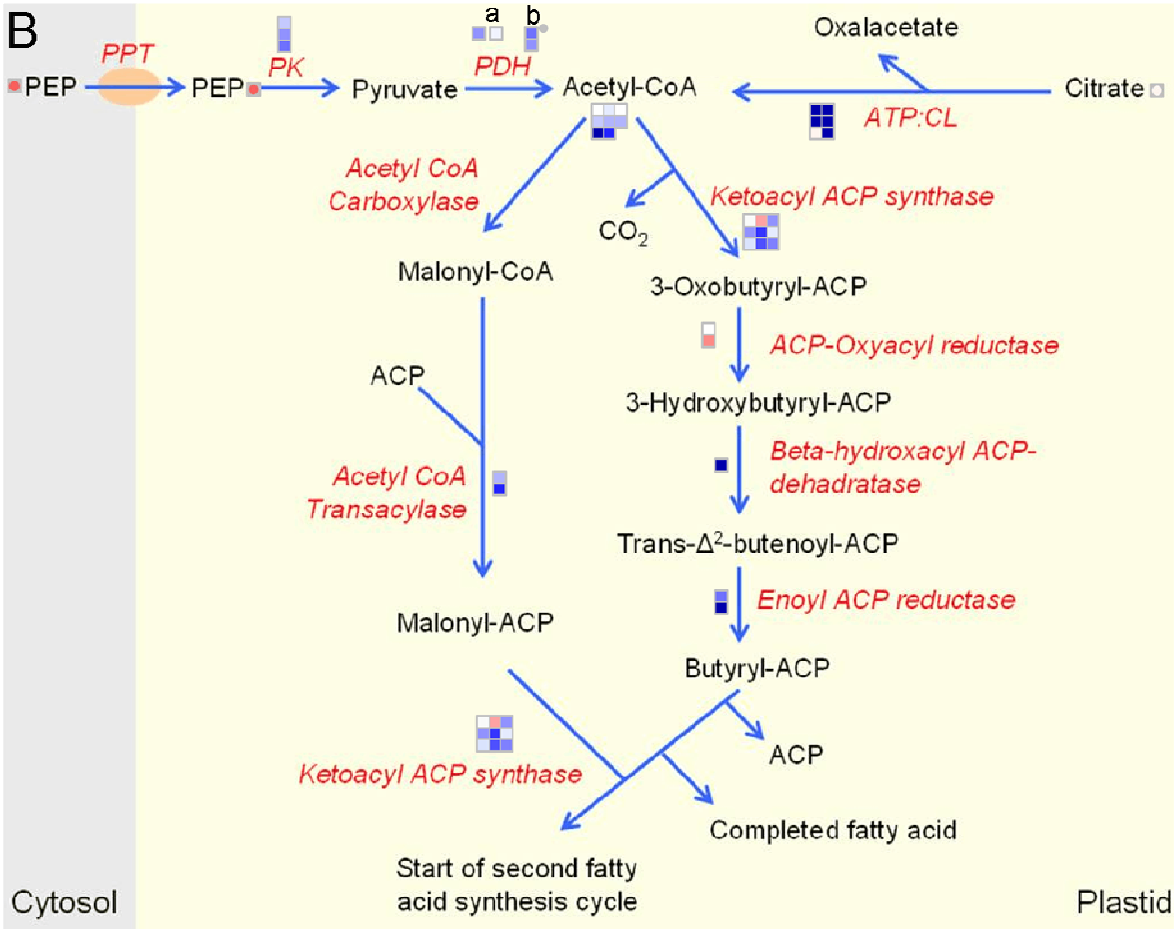


**Figure 18B.Fatty acid metabolism from imported PEP and citrate in U-IN-2**. Different subunits of the pyruvate dehydrogenate complex: a) E2. b) E3.

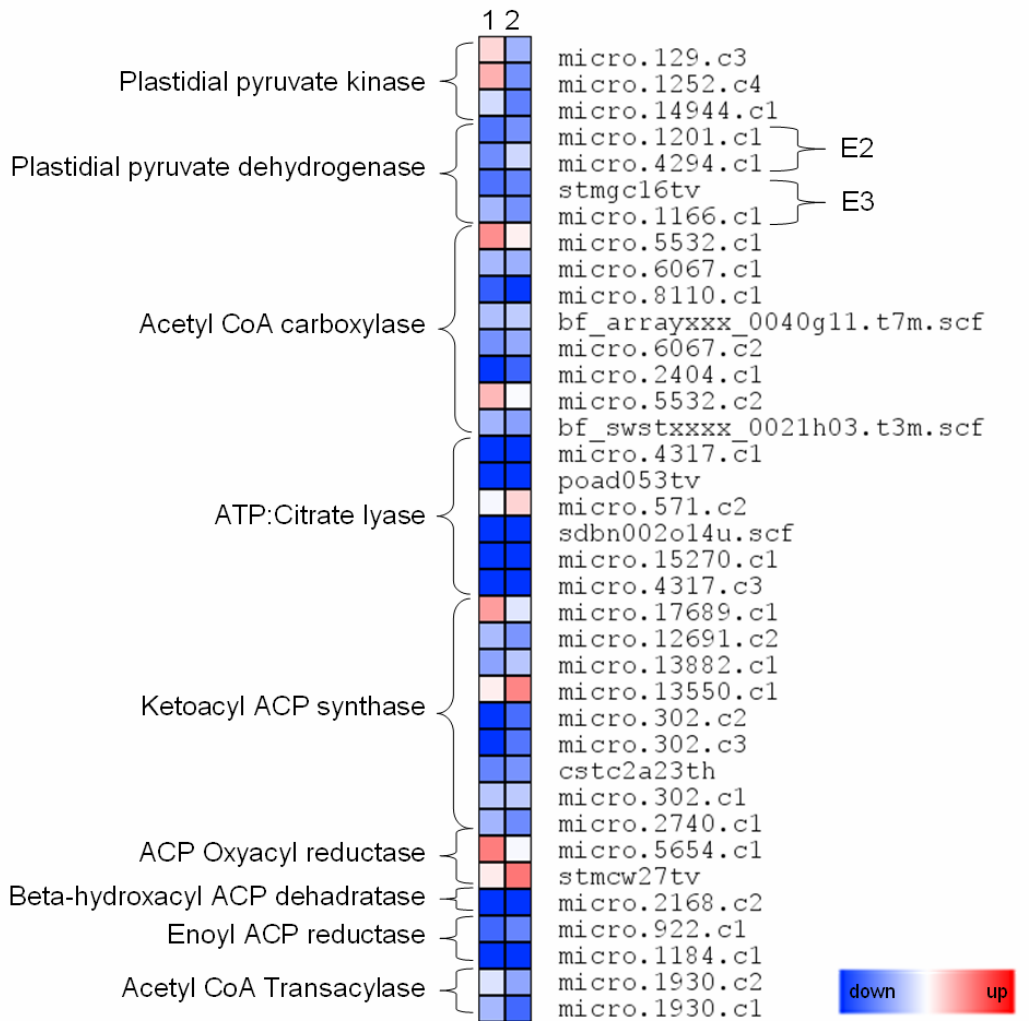


**Figure 19 Heatmap representation of features viewed in fatty acid biosynthesis pathway.** Log2 values of the fold change compared to WT. Column 1 represent U-IN-1 and column 2 U-IN-2. Values are the mean of 3-4 replicates.

### 2.2.2.2. Starch metabolism.

The next pathway analysed was starch biosynthesis, starting with the degradation of sucrose. Genomic alignment of EST sequences revealed three cell wall invertase genes differentially expressed. It was remarkable to note that despite the presence of a highly active transgenic invertase in the cell wall, the expression of endogenous invertases were up-regulated in U-IN-1. This was also the case for one isoform in U-IN-2. A third isoform present in potato tubers, fructokinase 3, was also reduced in both lines. Importantly, a change in the G6P/G1P ratio was observed in U-IN-2, and there was a

strong increase in the expression mitochondrial bound hexokinase 5 in U-IN-2 (figures 20 and 21).

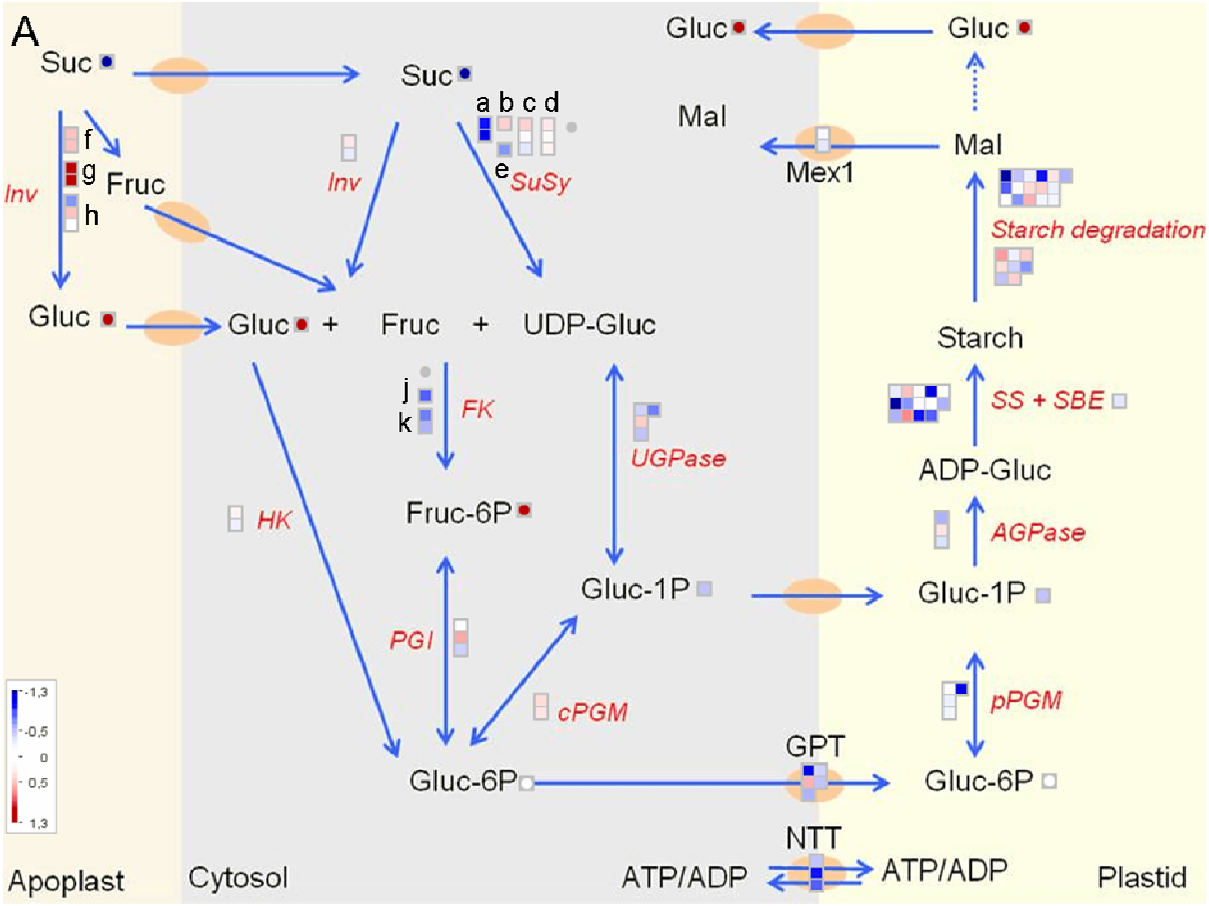


**Figure 20A.Starch biosynthesis with sucrose as primary substrate in U-IN-1**. Different isoforms of Susy is represented by a-e) with a) Susy4.

f-h) represent the differentially expressed cell wall invertase isoforms. j) fructokinase 2. k) fructokinase 3.

Gene name abbreviations: HK-hexokinase; PGI- phosphogluco isomerise; SS – starch synthase; SBE-starch branching enzymes; AGPase-ADP-glucose pyrophosphorylase.

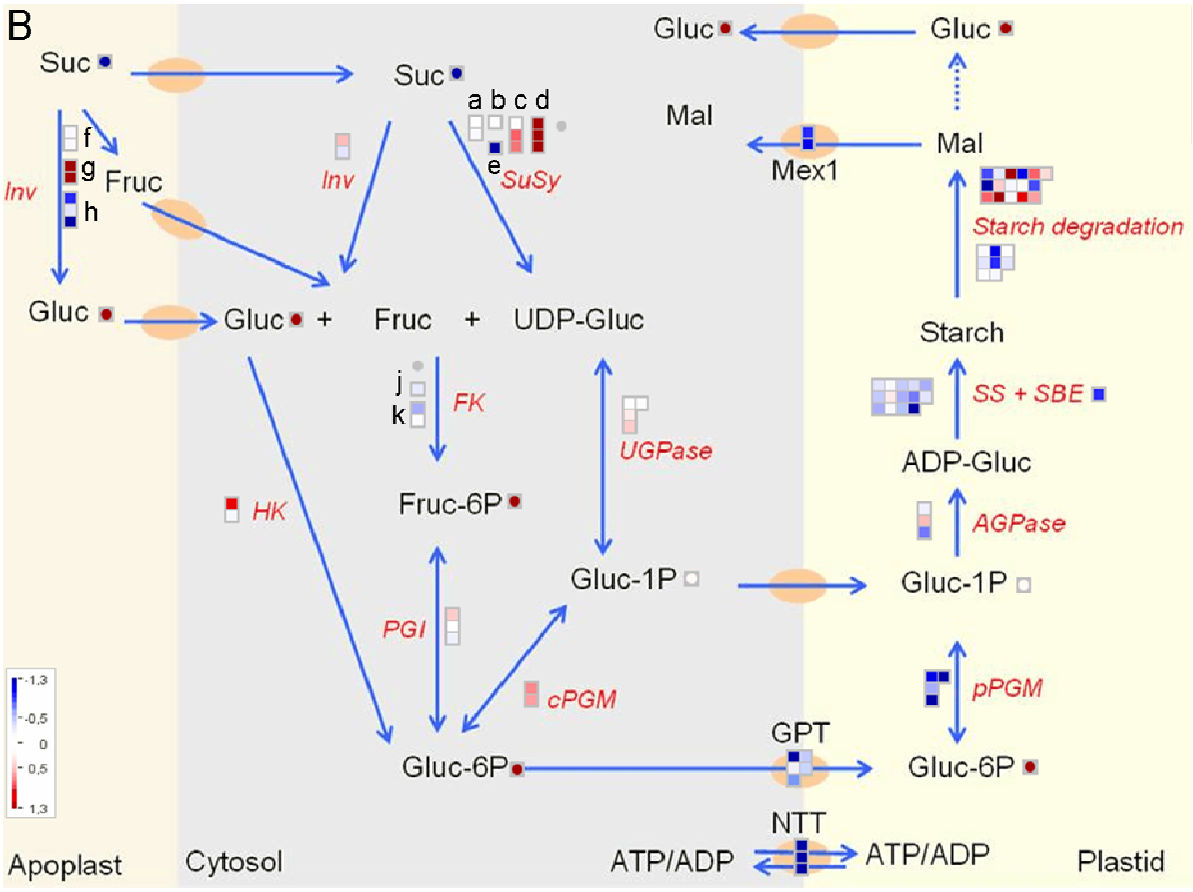


**Figure 20B.Starch biosynthesis with sucrose as primary substrate in U-IN-2**. Different isoforms of Susy is represented by a-e) with a) Susy4

f-h) represent the differentially expressed cell wall invertase isoforms. j) fructokinase 2. k) fructokinase 3. Gene name abbreviations: HK-hexokinase; PGI- phosphogluco isomerise; SS – starch synthase; SBE-starch branching enzymes; AGPase-ADP-glucose pyrophosphorylase.

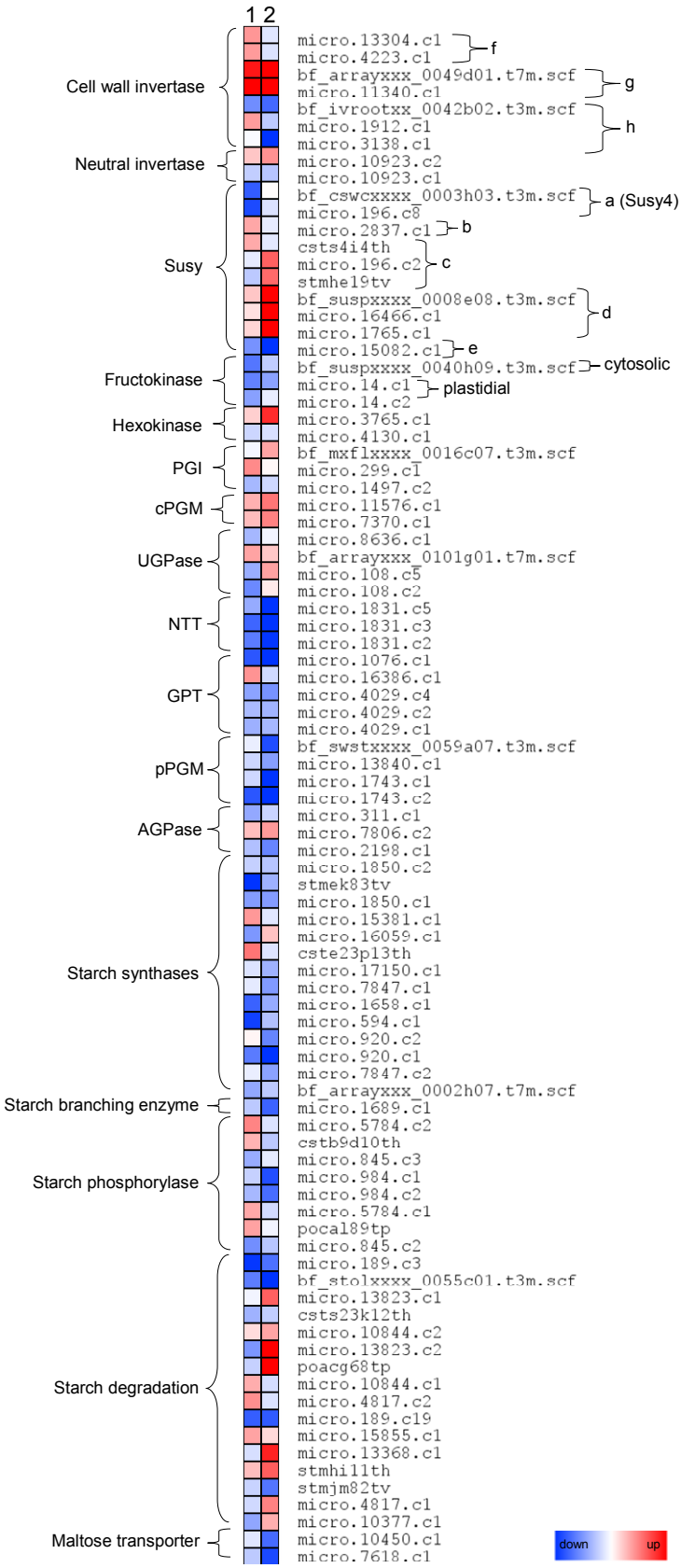


**Figure 21. Heatmap representation of features viewed in starch biosynthesis pathway.** Column 1 represents U-IN-1 and column 2 U-IN-2. Log2 values of the fold change compared to WT. values are the mean of 3-4 replicates.

In both U-IN-1 and U-IN-2 there was a strong reduction in the expression of the GPT transporter (figures 20 and 21). Combining our transcription data sets from growing U-IN-1 and U-IN-2 tubers and tubers growing at different velocities, a strict negative correlation between GPT2 and cell wall invertase gene expression could be observed (figure 22). This negative correlation was also observed in tubers expressing trehalulose 6-phosphate phosphatase (TPP) (figure 22). These tubers have altered carbon metabolism due to reduced levels of trehalose 6-phosphate and are very useful to study regulatory mechanisms controlling central carbon metabolism (Debast et al., 2011).

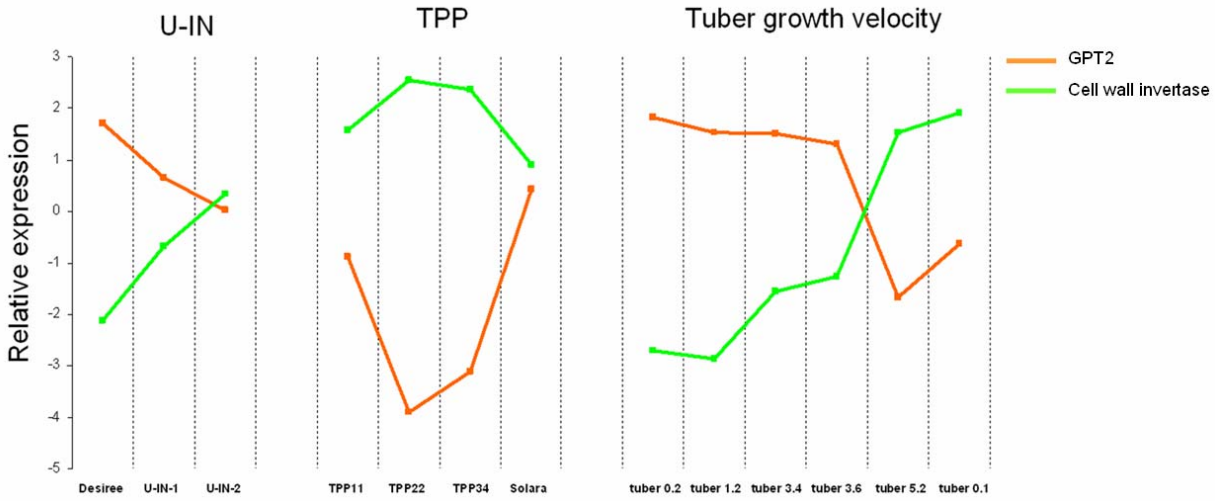


**Figure 22. Inverse correlation of GPT2 and Cell wall invertase gene expression.** The expression pattern of an EST derived from GPT2 (micro.1076.c1, orange) and cell wall invertase (micro.11340.c1, green) in different U-IN tubers, tubers with altered trehalose 6-phosphate (TPP) (Debast et al., 2011) and tubers growing at different velocities.

Aiming to identify possible regulators of this observation, genes showing a positive correlation to either invertase (Table S5) or GPT (Table S6) expression were identified. Amongst the genes positively correlating to invertase, several transcription factors could be identified and these are shown in figure 23.

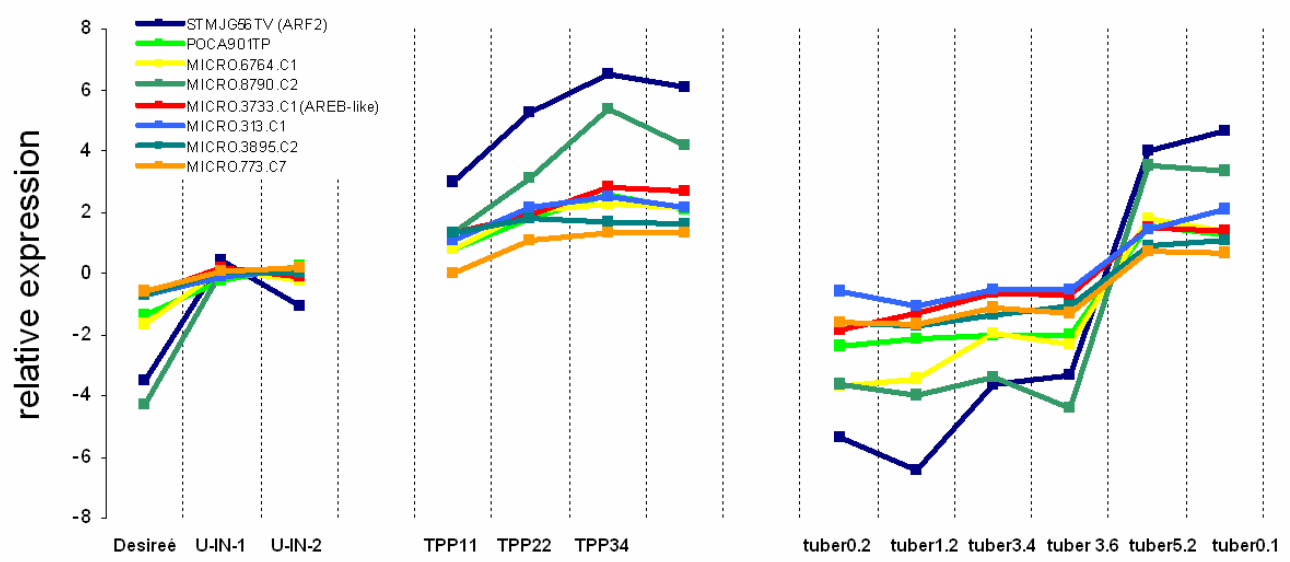


**Figure 23. Transcription factors positively correlating to cell wall invertase gene expression**. The conditions studies were U-IN tubers, tubers with altered trehalose 6-phosphate (TPP) (Debast et al., 2011) and tubers growing at different velocities.

Transcriptional data on starch degrading enzymes was not clear, but there was a reduction in the expression of MEX1 in U-IN-2, the transporter responsible for the export of the major starch degradation product, maltose, to the cytosol (figures 20 and 21).

### 2.2.2.3. Pentose phosphate pathway in U-IN-2

Metabolic analysis showed an increase in the levels of Erythrose 4-phosphate in U-IN-2, which pointed towards the activation of the pentose phosphate pathway, the metabolic route for Erythrose 4-phosphate synthesis. Indeed, both plastidial isoforms of the rate determining step in the reaction, Glucose-6-phosphate dehydrogenase (G6PDH) (Hauschild and von Schaewen, 2003), were strongly up-regulated in U-IN-2, whilst there was no change in the expression of the cytosolic form (figures 24 and 25).

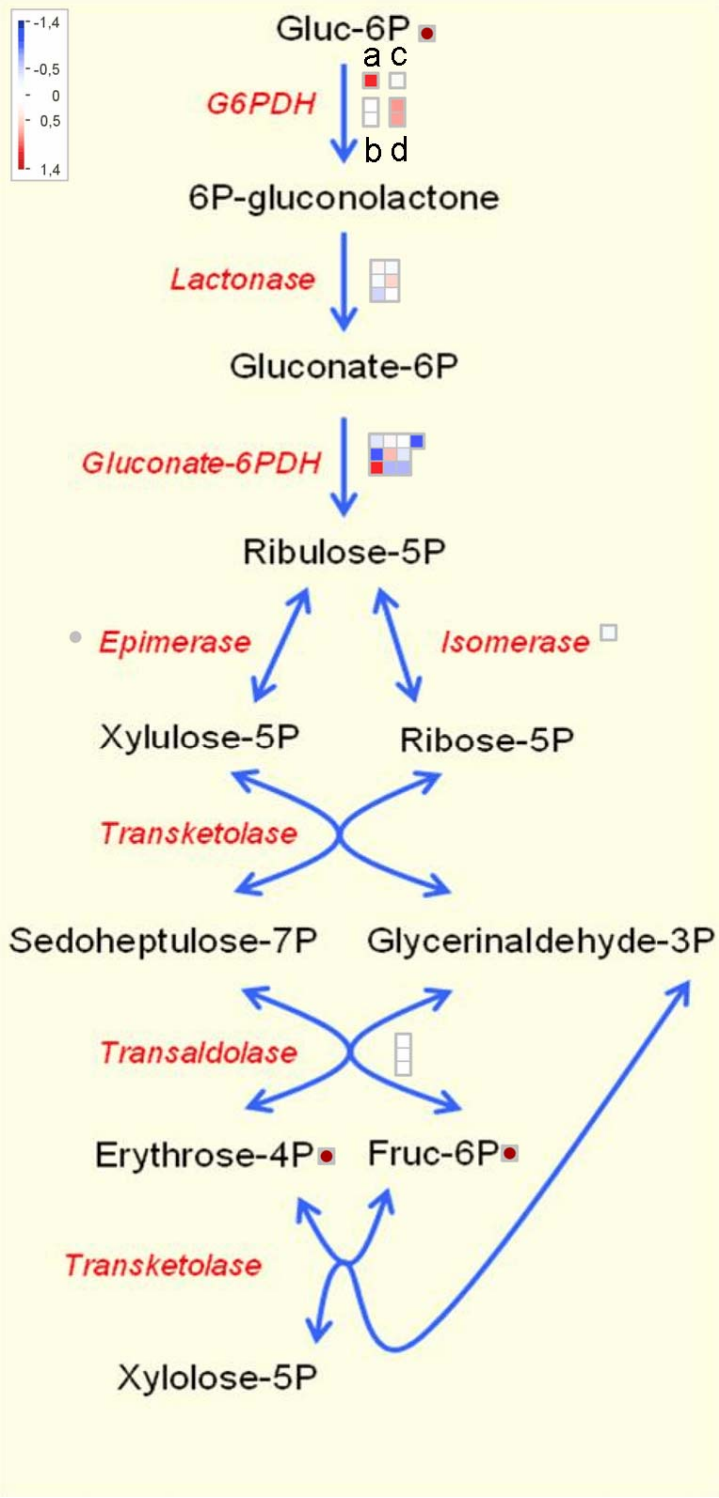


**Figure 24. Pentose phosphate pathway in U-IN-2**. a-d) Differentially expressed isoforms of G6PDH. a) and d) are plastidial isoforms.

Gene name abbreviations: Gluconate-6PDH-Gluconate 6-phosphate dehydrogenase

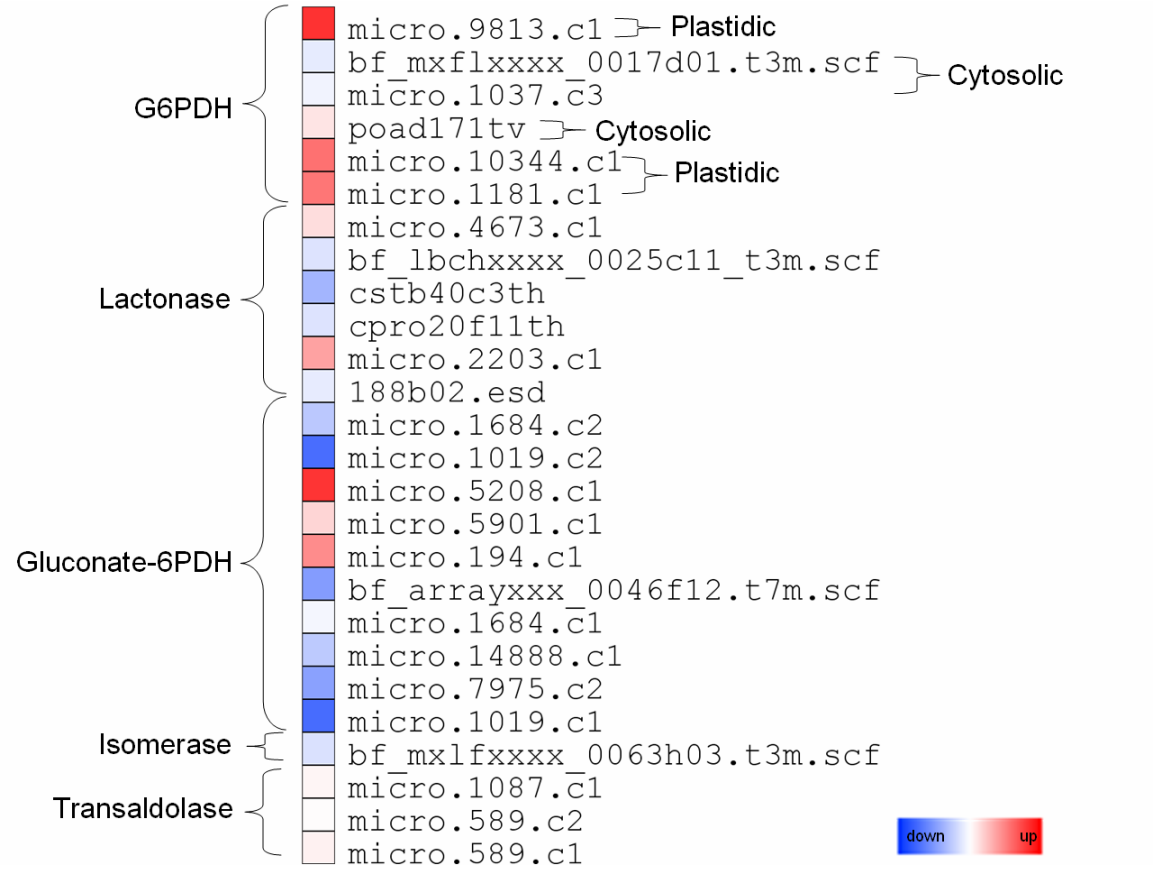


**Table 25. Heatmap representation of features viewed in pentose phosphate pathway pathway.** Log2 values of the fold change compared to WT. values are the mean of 3-4 replicates.

### 2.2.2.4. Shikimate pathway in U-IN-2

Despite an increase in shikimate and its precursors PEP, Erythrose-4-phosphate and 3-Deoxy-D-Arabino-Heptulosonate 7-Phosphate (DAHP) in U-IN-2, there was a general reduction in the expression levels of the enzymes in the pathway, and also of tyrosine, while phenylalanine remained unchanged. There was a strong down-regulation in most of the isoforms of the bifunctional enzyme 3-dehydroquinate dehydrogenase/ shikimate-5-dehydrogenase (3DHQ DH/ shikimate-5-DH). Furthermore, phenylalanine lyase (PAL), an enzyme present down-stream of phenylalanine towards lignin biosynthesis, was amongst the strongest down-regulated genes in the entire transcriptome analysis (figures 26 and 27).

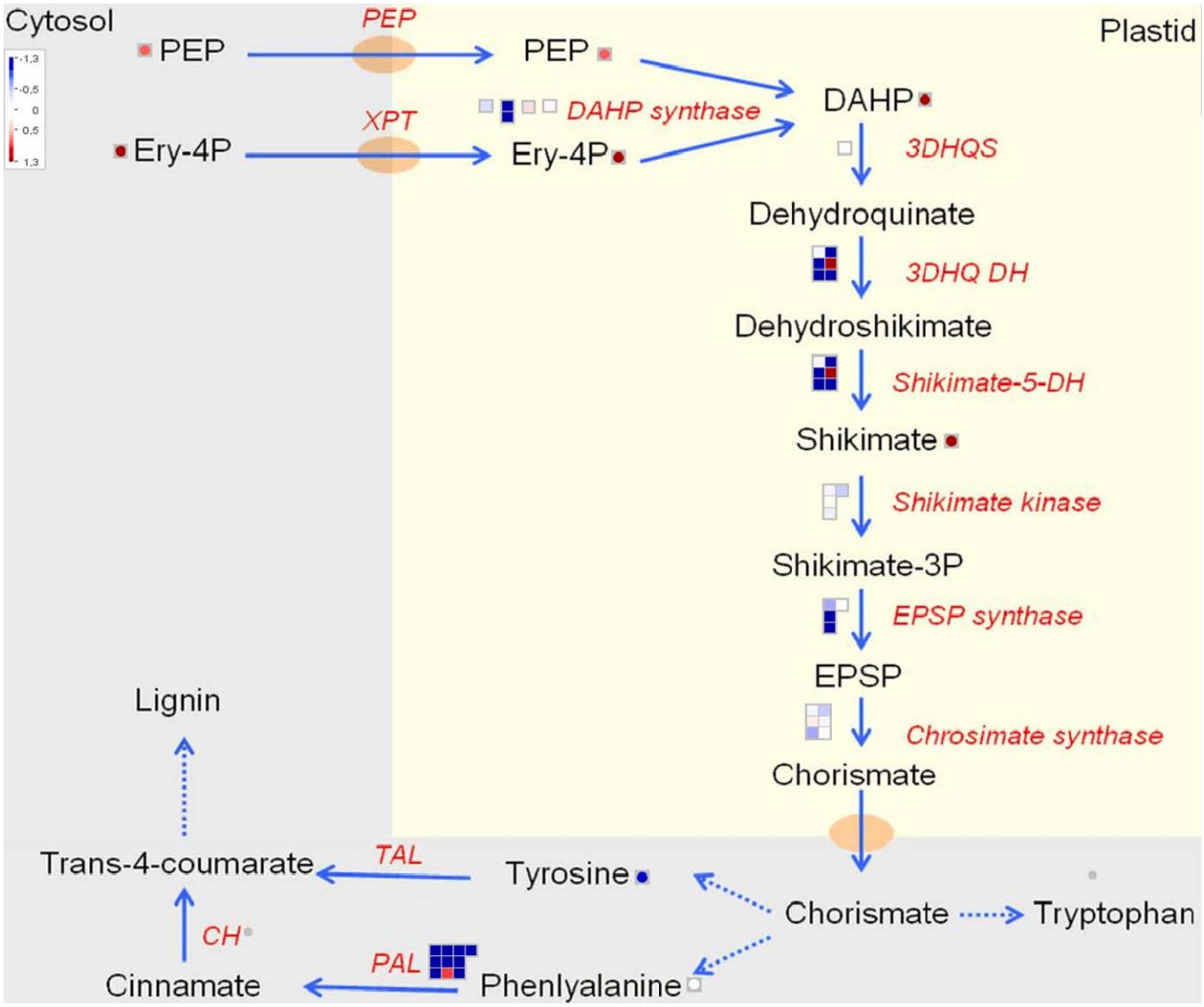


**Figure 26 Shikimate biosynthetic pathway producing aromatic amino acids and precursors for lignin in U-IN-2.**

Gene name abbreviations: DAHP synthase - 3-Deoxy-D-Arabino-Heptulosonate 7-Phosphate synhase; 3DHQS - 3-dehydroquinate synthase; 3DHQ DH - 3-dehydroquinate dehydrogenase ; Shikimate-5-DH - Shikimate 5-dyhydrogenase ; EPSP synthase – 5-Enolpyruvylshikimate 3-phosphate synthase; TAL – Tyrosine amminia lyase ; PAL – phenylalanine ammonia lyase ; CH – Cinnamate 4-hydroxylase.

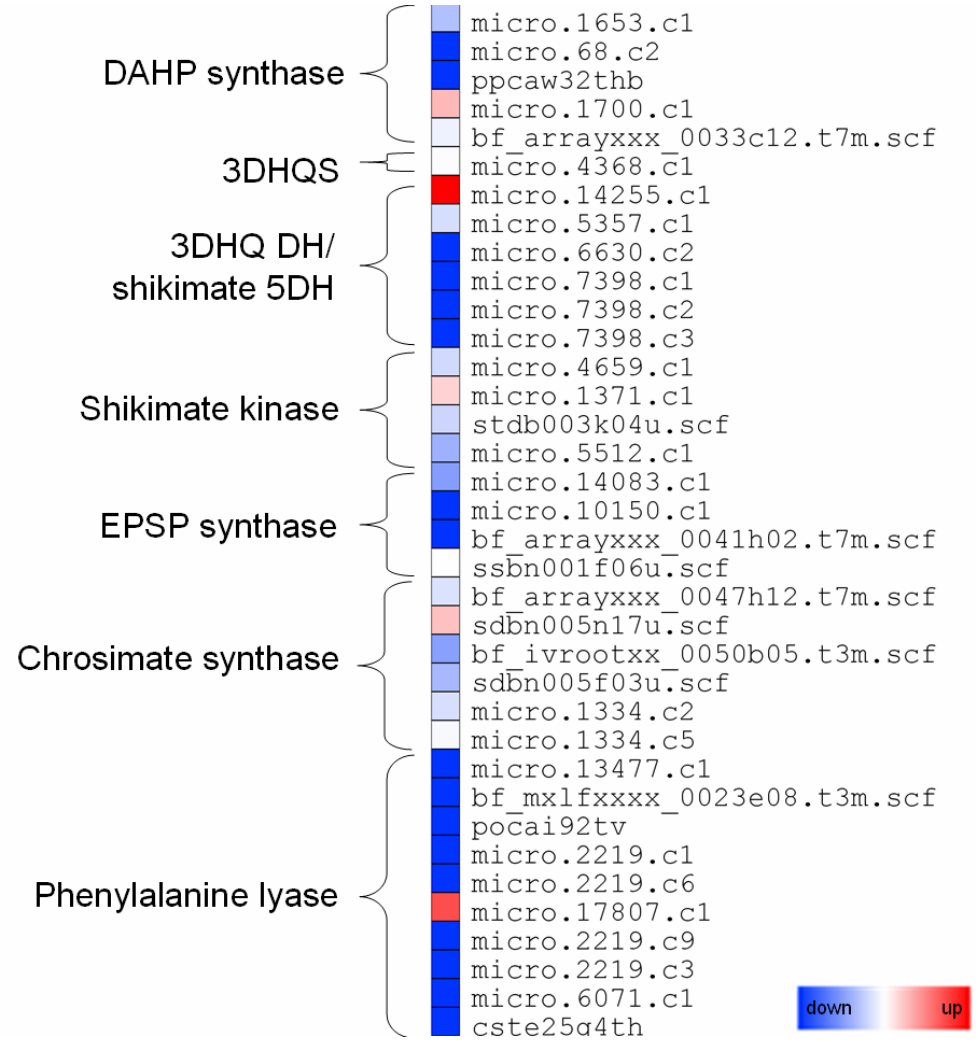


**Figure 27 Heatmap representation of the shikimate pathway.** Log2 values of the fold change compared to WT. values are the mean of 3-4 replicates.

### 2.2.2.5. TCA cycle and glycolysis in U-IN-2

Despite it being known that there is an increase in respiration in U-IN-2 (Trethewey et al., 1998; Hajirezaei et al., 2000; Bologa et al., 2003), expression data, in general, did not reveal a uniform up-regulation of TCA cycle enzymes, although several key metabolic steps were up-regulated. For instance, cytosolic pyruvate kinase and mitochondrial pyruvate dehydrogenase (mPDH) showed strong up-regulation, whilst the plastidial isoforms were strongly down-regulated, as was seen in the analysis of fatty acid metabolism. All the glycolytic and TCA cycle intermediate metabolites either were unchanged or increased in U-IN-2, with the exception of fumarate which was strongly

reduced. As mentioned earlier, there was no significant reduction in the levels of total amino acid contents, Importantly, there was an increase in the expression of fructose-2,6-bisphosphatase (F-2,6-BPase), known to be a potent regulator of glycolysis by inhibiting cytosolic fructose 1,6 bisphosphatase (FBPase) (Nielsen et al., 2004). (Figure 3.11).

Earlier studies have shown that conditions of hypoxia exist in U-IN-2, leading to anaerobic respiration (Bologa et al., 2003). Although transcription data did not reveal a strong and uniform increase in the expression of marker genes associated with anaerobic respiration, for instance alcohol dehydrogenase (ADH), lactate dehydrogenase (LDH) and glyceraldehyde 3-phosphate dehydrogenase (GA3PDH) (Bologa et al., 2003), there was accumulation of alanine, a marker metabolite for conditions of hypoxia (de Sousa and Sodek, 2003; Miyashita et al., 2007) (figure 28 and 29).

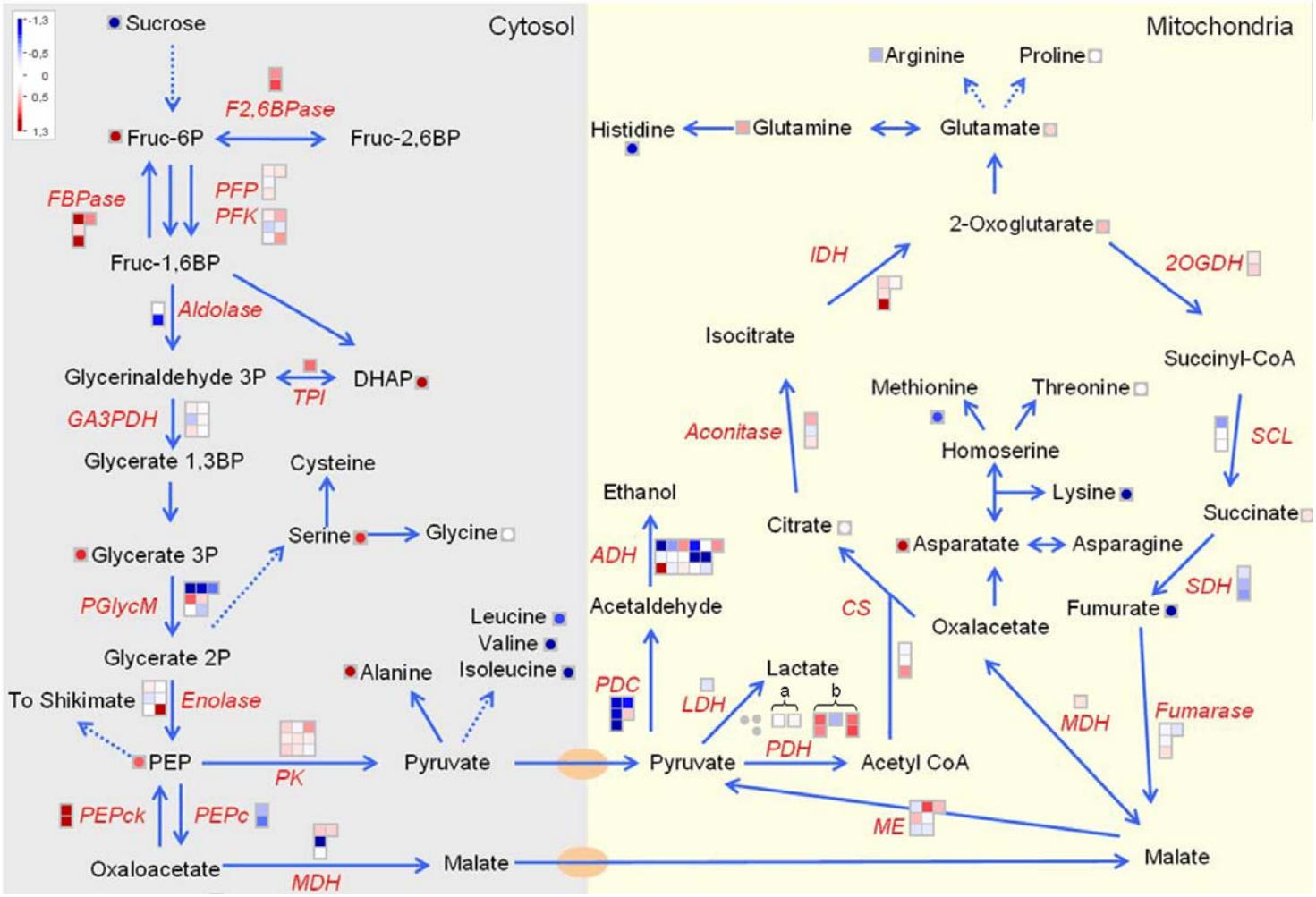


**Figure 28. TCA cycle and respiration in U-IN-2.** The E2 (a) and E3 (b) subunits of the mitochondrial pyruvate dehydrogenase complex.

Gene name abbreviations: TPI-Triose phosphate isomerise; GA3PDH-Glyceraldehyde 3-phosphate dehydrogenase;PGlycM-Phosphoglyceratemutase; PEPck-PEP carboxylase kinase; PEPc-PEP carboxylase; MDH-Malate dehydrogenase; ME-Malic enzyme; CS-citrate synthase; IDH-isocitrate dehydrogenase;2-oxoglutarate dehydrogenase; SCL- succinate CoA ligase; SDH - succinate dehydrogenase.

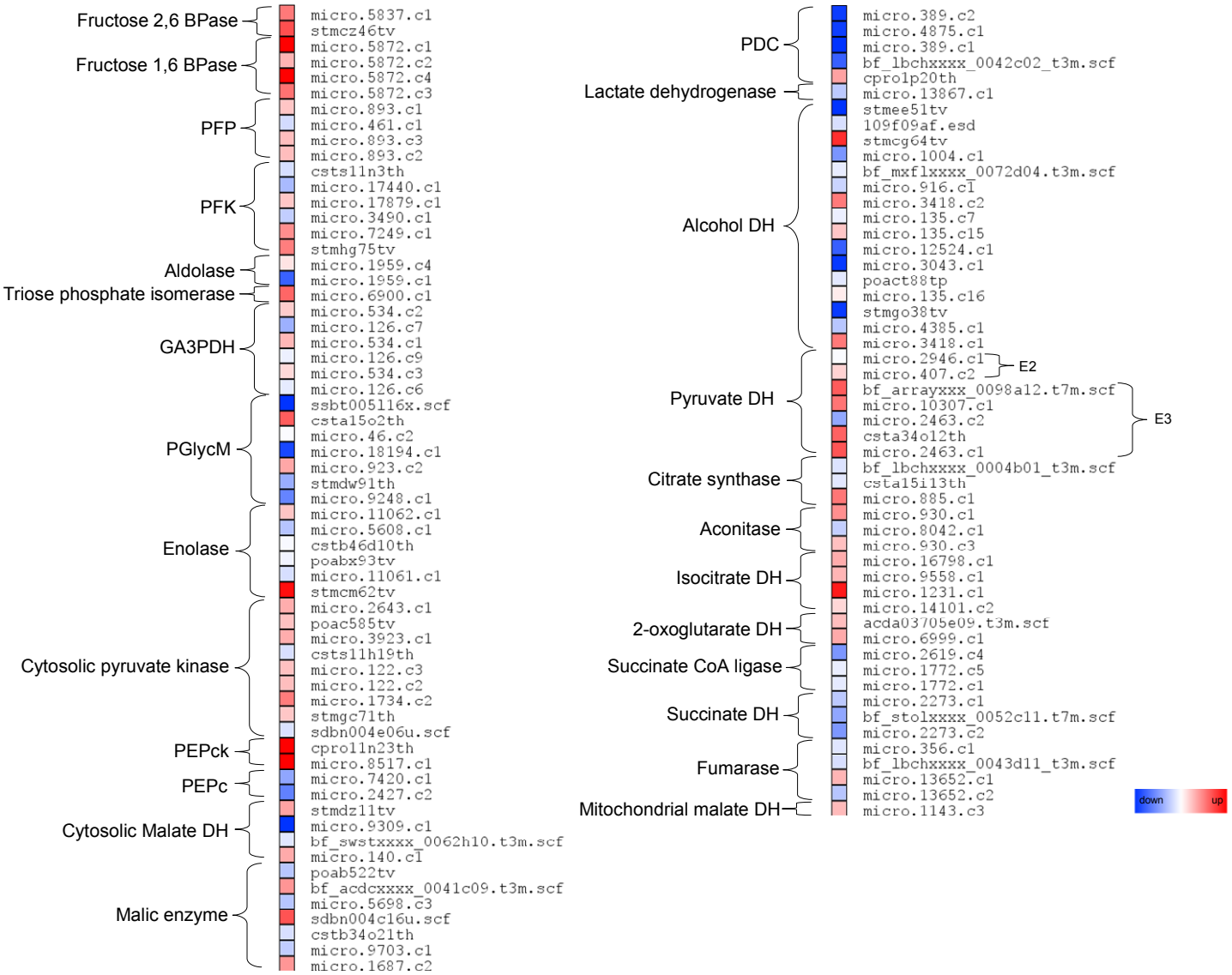


**Figure 29. Heatmap representation of features viewed in the glycolysis and TCA cycle pathway in U-IN-2.** Log2 values of the fold change compared to WT. values are the mean of 3-4 replicates.

### 2.2.3. Identification of genes expressed expressed specifically in U-IN-2

Inspired by the fact that elevated respiration is characteristic for U-IN-2 but not U-IN-1 tubers regulators highly expressed in in U-IN-2 but not in U-IN-1 were selected. This analysis revealed a significant list of differentially expressed genes but the gene showing the strongest induction in U-IN-2 tubers encodes for a catalytic trehalose phosphatase (figure 30), which would indicate the involvement of trehalose 6-phosphate as signalling molecule, as proposed by Debast et al. (2011). Attempts to measure T6P accumulation in both genotypes were, however, handicapped due to the very low T6P level, which was below detection limit for both transgenic genotypes (table S1.).

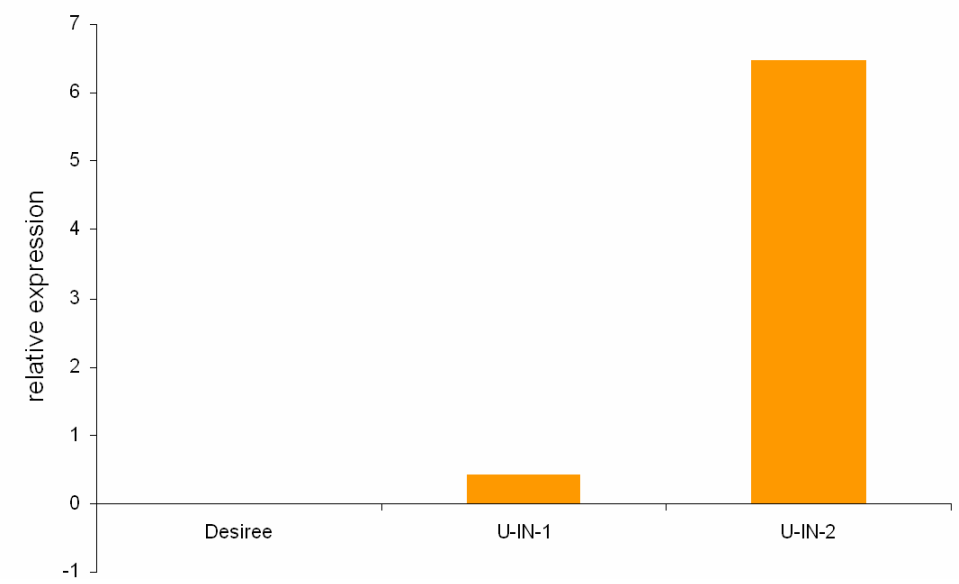


**Figure 30. Expression profile of catalytic trehalose phosphate (POCI identifier STMCN50TV_481) in growing Desiree, U-IN-1 and U-IN-2 tubers.** The expression profile represents the mean (n= 3-4 ).

## 2.3. Transcriptional and metabolic profiling of sucrose isomerase expressing potato tubers.

Potato tubers have the ability to store large amounts of carbohydrates, making them attractive bioreactors to produce high value carbohydrate or carbohydrate derived products. Börnke et al. (2002) successfully produced the sucrose isomer, trehalulose by expressing sucrose isomerase in the apoplasmic space (CW-ISO) of potato tubers. In a subsequent study, the enzyme was targeted to the vacuole (NTTP) (Börnke, unpublished data), but it was not determined whether this led to the production of trehalulose in this compartment. Not only did CW-ISO prove that it is possible to use potato tubers for trehalulose production, but CW-ISO also served as an attractive research model to study sugar signalling in tubers, as was shown by Hajirezaei et al.(2003), as discussed earlier. Furthermore, it is believed that despite trehalulose not being metabolisable by plants, the structural similarity to sucrose means that it could possibly be sensed in a sucrose-like manner. This would make it possible to study sucrose signalling uncoupled from the complications of sucrose also being a major plant metabolite. However, since trehalulose is not an endogenous plant sugar, and derived from bacteria, it could also be that it elicits a pathogen response signal rather than a sucrose response signal. A third possibly could be that trehalulose is sensed in a reducing sugar-like manner, for instance glucose, since it is a reducing sugar.

The aim of this chapter was to gain further insight into sugar signalling in potato tubers by conducting large scale transcriptional and metabolic profiling of growing potato tubers expressing sucrose isomerase in either the apoplasmic space (CW-ISO) or the vacuole (NTTP). Furthermore, feeding experiments were performed where potato leaf discs were fed with various sugars (sucrose, glucose, trehalulose) and gene expression probed by microarray.

### 2.3.1. Transcriptional and metabolic analysis of sucrose isomerase expressing plants.

#### 2.3.1.1. Global analysis of transcripts and metabolites.

Potato plants were grown under greenhouse conditions for eight weeks after which tuber samples were taken and immediately frozen in liquid nitrogen. It can be assumed that the tubers were still actively growing at this stage. For gene expression analysis, RNA extracted from these samples were hybridised to the Agilent 44k POCI array (Kloosterman et al., 2008), and data extracted using GeneSpring 11 software as described in the materials and methods. As a starting point, a principle component analysis (PCA) of the transcription profiles was performed and it was possible to clearly separate the replicates. This was also true using the mean values (figure 31).

A

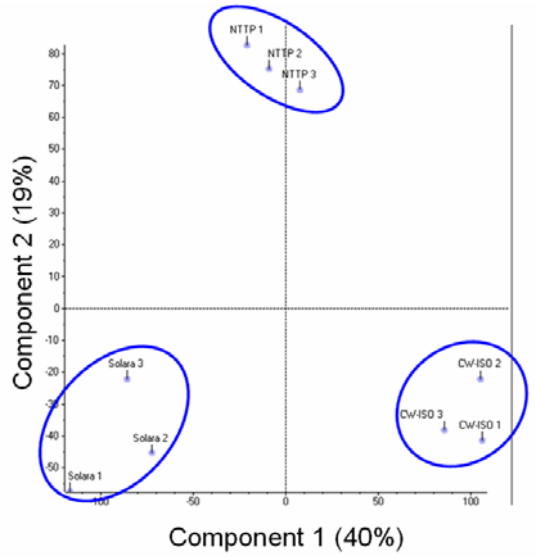


B

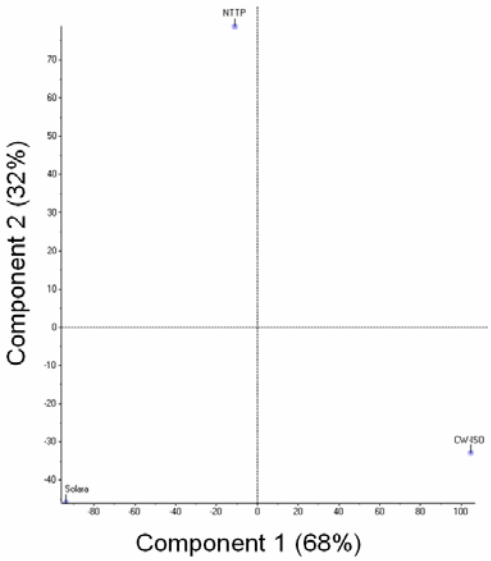


**Figure 31. Principle component analysis (PCA) of transcription data in sucrose isomerase expressing lines.** A) Replicates illustrating that the individual replicates of each genotype clustered. B) PCA on the mean values of each genotype.

The PCA was useful in illustrating that the expression of the transgene had large effects on transcription, and that different subcellular targeting leads to very different results. To determine which processes were mainly responsible for the separation, analyses of functional groupings were performed. To this end, the relative enrichment of features from different functional groups was performed as described in chapter 3. This revealed

that in CW-ISO only stress/ defence associated features were more than two-fold enriched amongst the down-regulated features, whilst no functional group was more than two-fold enriched amongst the down-regulated features for NTTP. For the up-regulated features, cell wall metabolism and photosynthesis was increased in both genotypes, storage proteins only in NTTP; and cytoskeleton, electron transport, fatty acid metabolism and redox/ antioxidant related features were more than two fold enriched only in CW-ISO (figure 32).

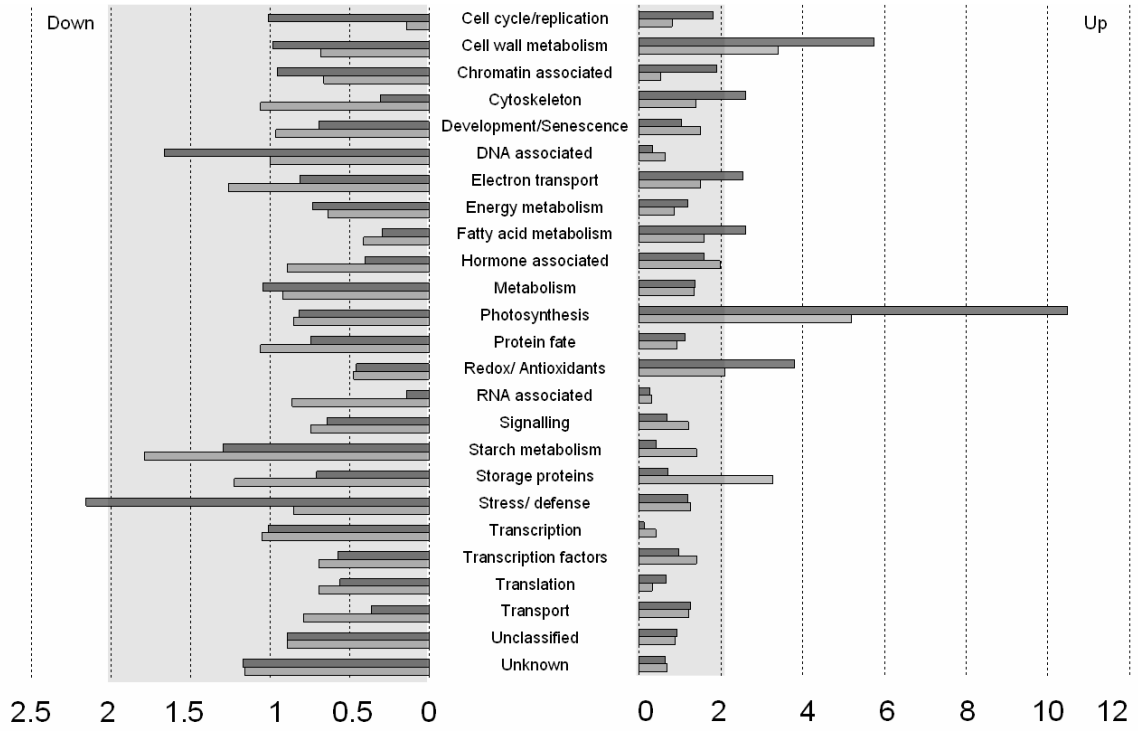


**Figure 32. Enrichment analysis of functional groupings amongst up- and down-regulated features in CW-ISO (dark grey) and NTTP (light grey).**

Parallel to transcriptional analysis, detailed metabolic profiling was also conducted using the same sampling material. Phosphorylated intermediates, organic acids, amino acids, major tuber carbohydrates (starch, sucrose, glucose and fructose) and carotenoids were measured (table S7-S10). Again, it was possible to separate the genotypes based on the metabolic profiles by a PCA (figure 33). The metabolites most important for the separation in component one, responsible for 76% of the variance, was fumarate,

glutamine, glucose and zeaxanthin; and for component two, responsible for 24% of the variance, fructose, shikimate, zeaxanthin and alanine was the most important.

A

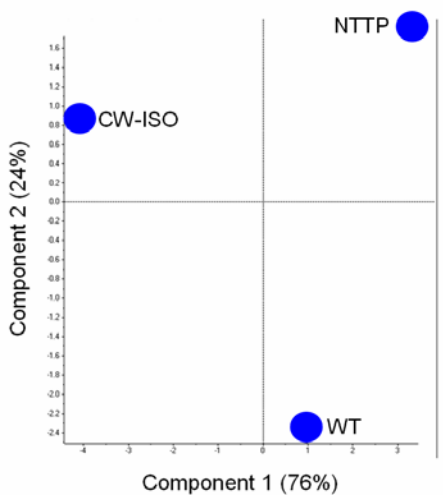


B

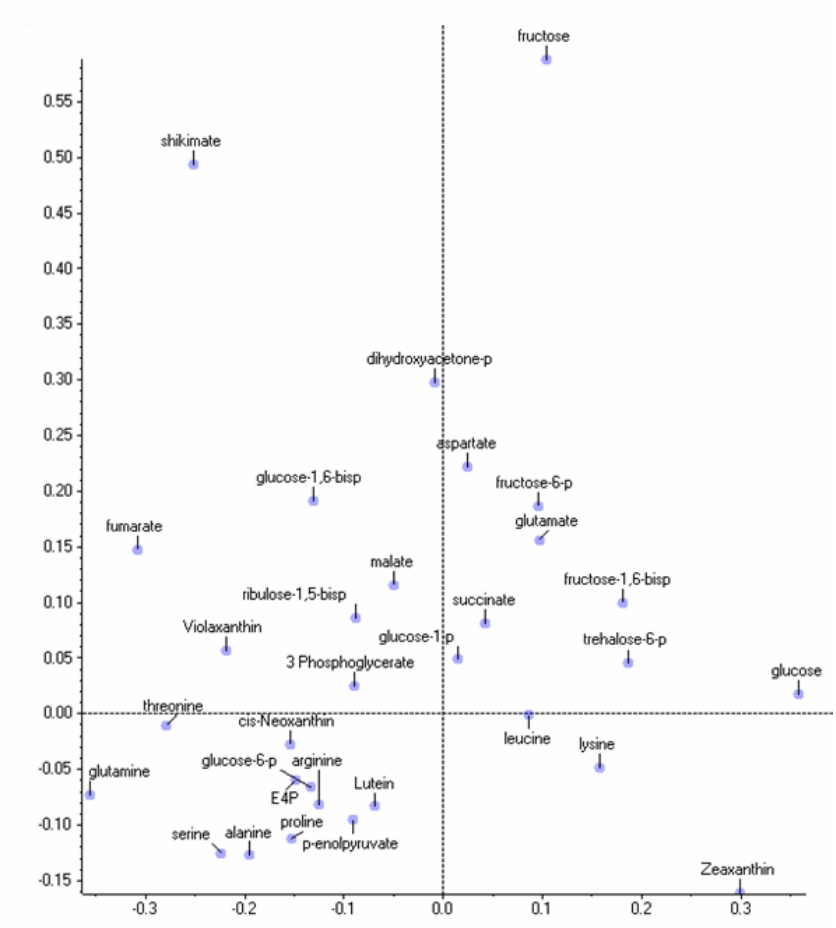


**Figure 33. Principle component analysis on metabolite levels in sucrose isomerase expressing plant and WT control.** A) The PCA separation of the genotypes and B) the loadings of the individual metabolites.

### 2.3.2. Pathway specific analysis.

#### 2.3.2.1. Photosynthesis.

To gain further insight into the phenotypical changes in both genotypes, pathway specific analysis of transcriptional and metabolic data was performed using Mapman software (Thimm et al., 2004). The first pathways analysed were those affected in both genotypes, starting with photosynthesis. The analysis revealed that the most striking increase was in the expression of chlorophyll a/b binding proteins whilst certain processes within the Calvin cycle were also up-regulated (figures 34 and 35).

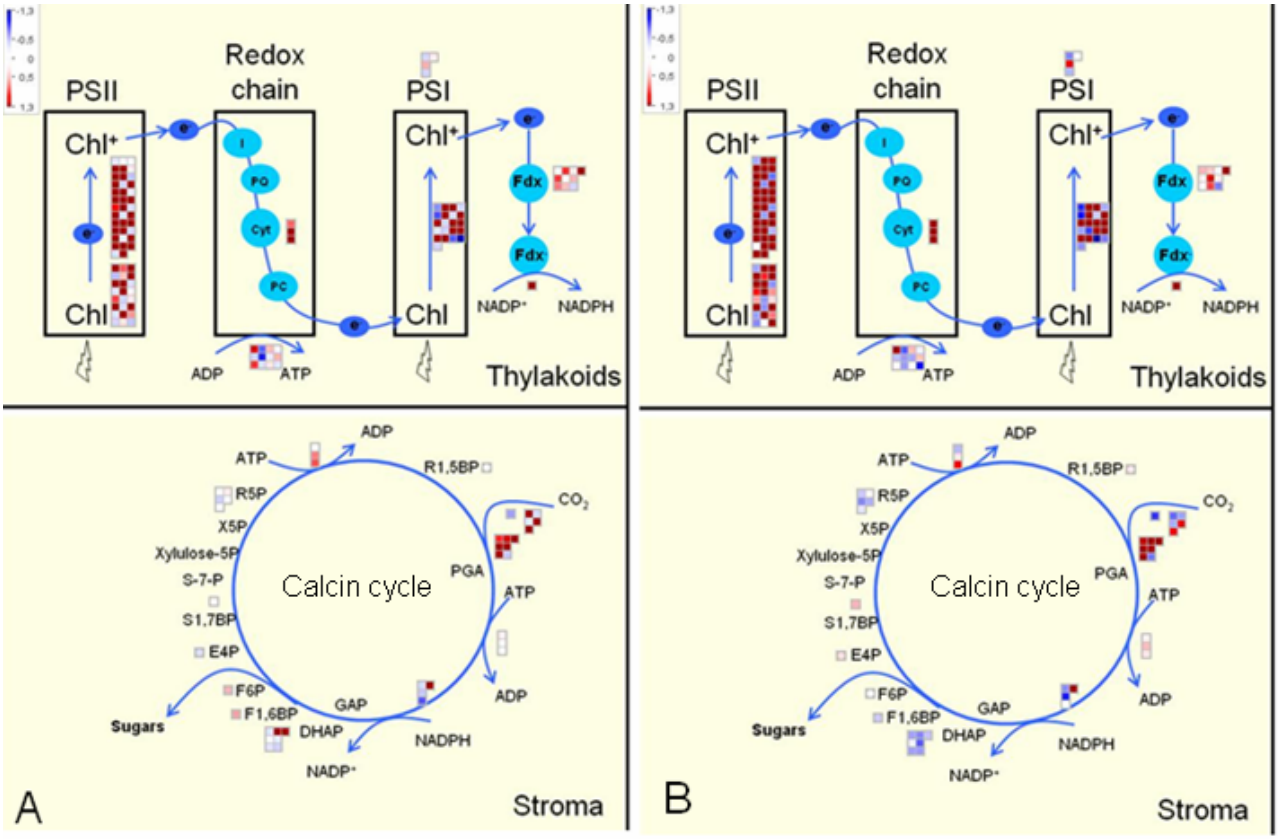


**Figure 34. Transcriptional and metabolic changes in reactions associated with photosynthesis in sucrose isomerase expression tubers**. A) NTTP and B) CW-ISO.

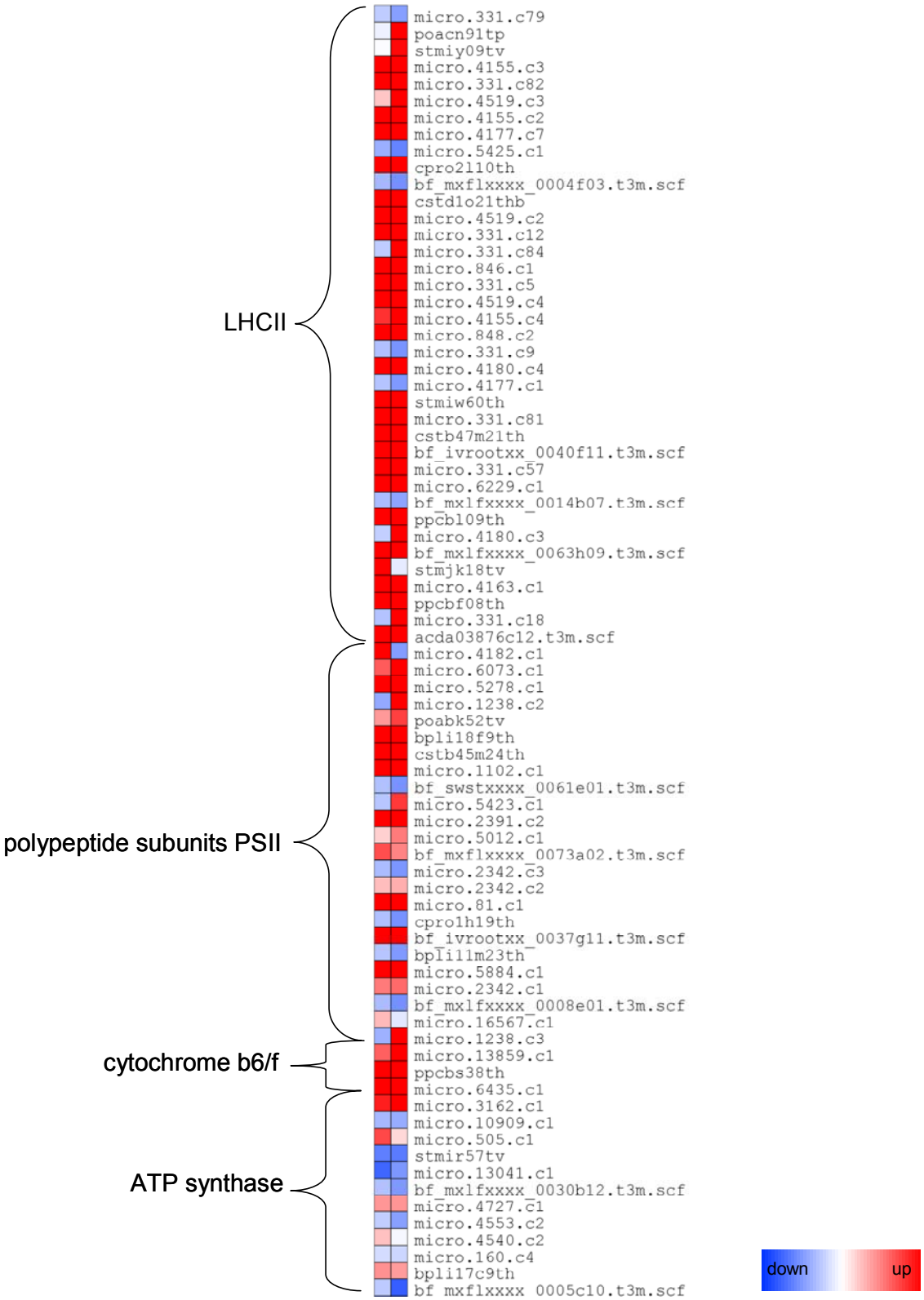
LHCII
polypeptide subunits PSII
cytochrome b6/f
ATP synthase
micro.331.c79
poacn91tp
stmiy09tv
micro.4155.c3
micro.331.c82
micro.4519.c3
micro.4155.c2
micro.4177.c7
micro.5425.c1
cpro2l10th
bf_mxflxxxx_0004f03.t3m.scf
cstd1o21thb
micro.4519.c2
micro.331.c12
micro.331.c84
micro.846.c1
micro.331.c5
micro.4519.c4
micro.4155.c4
micro.848.c2
micro.331.c9
micro.4180.c4
micro.4177.c1
stmiw60th
micro.331.c81
cstb47m21th
bf_ivrootxx_0040f11.t3m.scf
micro.331.c57
micro.6229.c1
bf_mxlfxxxx_0014b07.t3m.scf
ppcbl09th
micro.4180.c3
bf_mxlfxxxx_0063h09.t3m.scf
stmjk18tv
micro.4163.c1
ppcbf08th
micro.331.c18
acda03876c12.t3m.scf
micro.4182.c1
micro.6073.c1
micro.5278.c1
micro.1238.c2
poabk52tv
bpli18f9th
cstb45m24th
micro.1102.c1
bf_swstxxxx_0061e01.t3m.scf
micro.5423.c1
micro.2391.c2
micro.5012.c1
bf_mxflxxxx_0073a02.t3m.scf
micro.2342.c3
micro.2342.c2
micro.81.c1
cpro1h19th
bf_ivrootxx_0037g11.t3m.scf
bpli11m23th
micro.5884.c1
micro.2342.c1
bf_mxlfxxxx_0008e01.t3m.scf
micro.16567.c1
micro.1238.c3
micro.13859.c1
ppcbs38th
micro.6435.c1
micro.3162.c1
micro.10909.c1
micro.505.c1
stmir57tv
micro.13041.c1
bf_mxlfxxxx_0030b12.t3m.scf
micro.4727.c1
micro.4553.c2
micro.4540.c2
micro.160.c4
bpli17c9th
bf_mxflxxxx_0005c10.t3m.scf
down
up

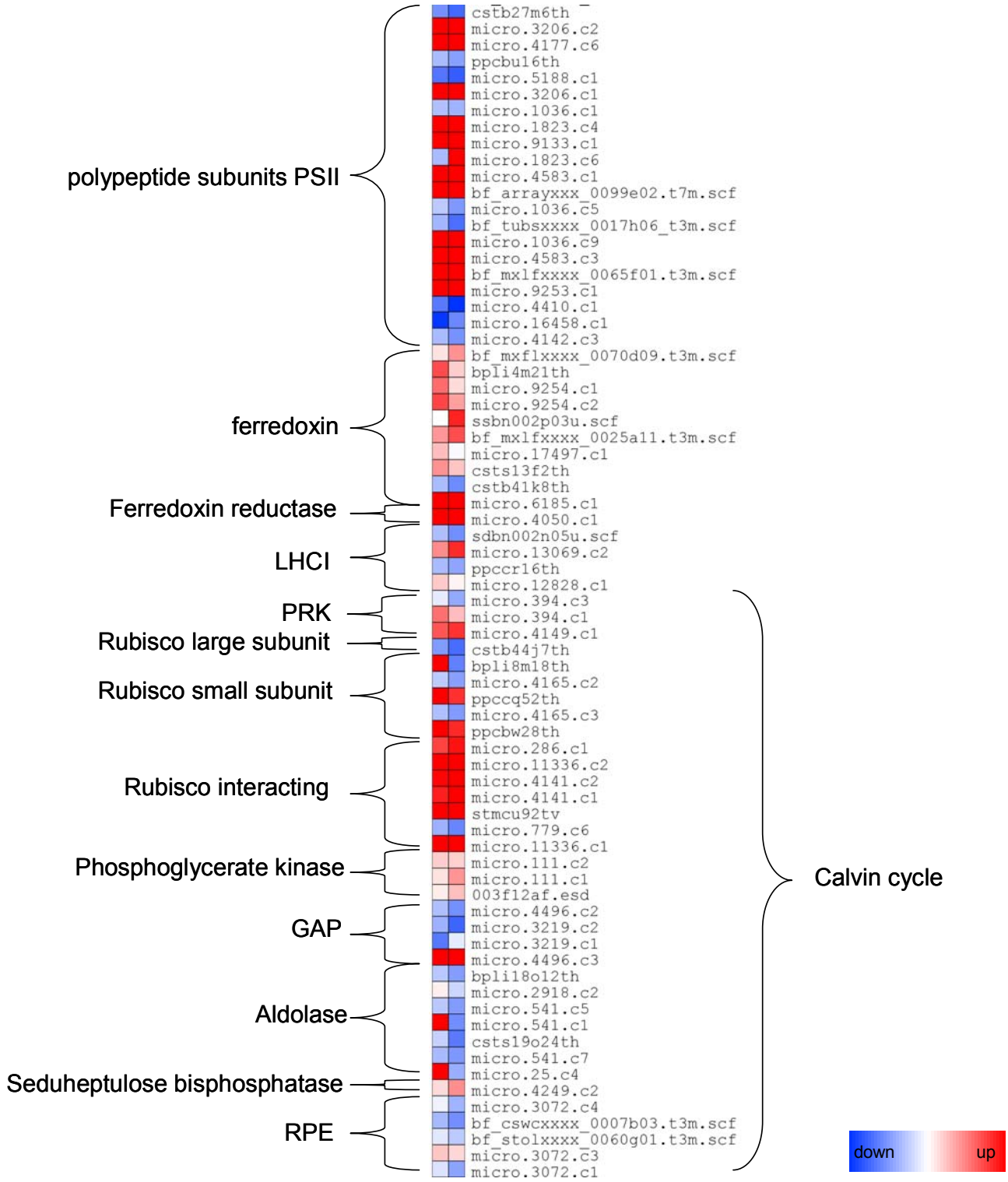


**Figure 35. Heat map representation of features presented in photosynthesis pathway analysis in sucrose isomerase expressing tubers**. Log2 values of fold change compared to WT control.

#### 2.3.2.2. Cell wall biosynthesis.

The second functional group increased in both genotypes was cell wall metabolism, and pathway analysis showed that this was indeed the case. The primary substrate for both cellulose and hemicellulose production is UDP-glucose, produced by sucrose synthase. Interestingly, despite significant reductions in sucrose in both transgenic lines, the expression of the major isoform in tubers, Susy 4, was strongly up-regulated. In both genotypes there was an overall increase in Myo-inositol pathway gene expression. This was especially true for the rate determining reaction in the pathway, myo-inositol 1-phosphate (Loewus and Loewus, 1980; Loewus et al., 1980). No isoform from cytosolic PGM was changed. In CW-ISO several isoforms of vacuolar invertase were up-regulated. The results for the two genotypes seemed to be very similar in terms of the effect on cell wall biosynthesis, and was more severe in CW-ISO, as was evident when the expression in NTTP was compared to CW-ISO (figures 36 and 37).

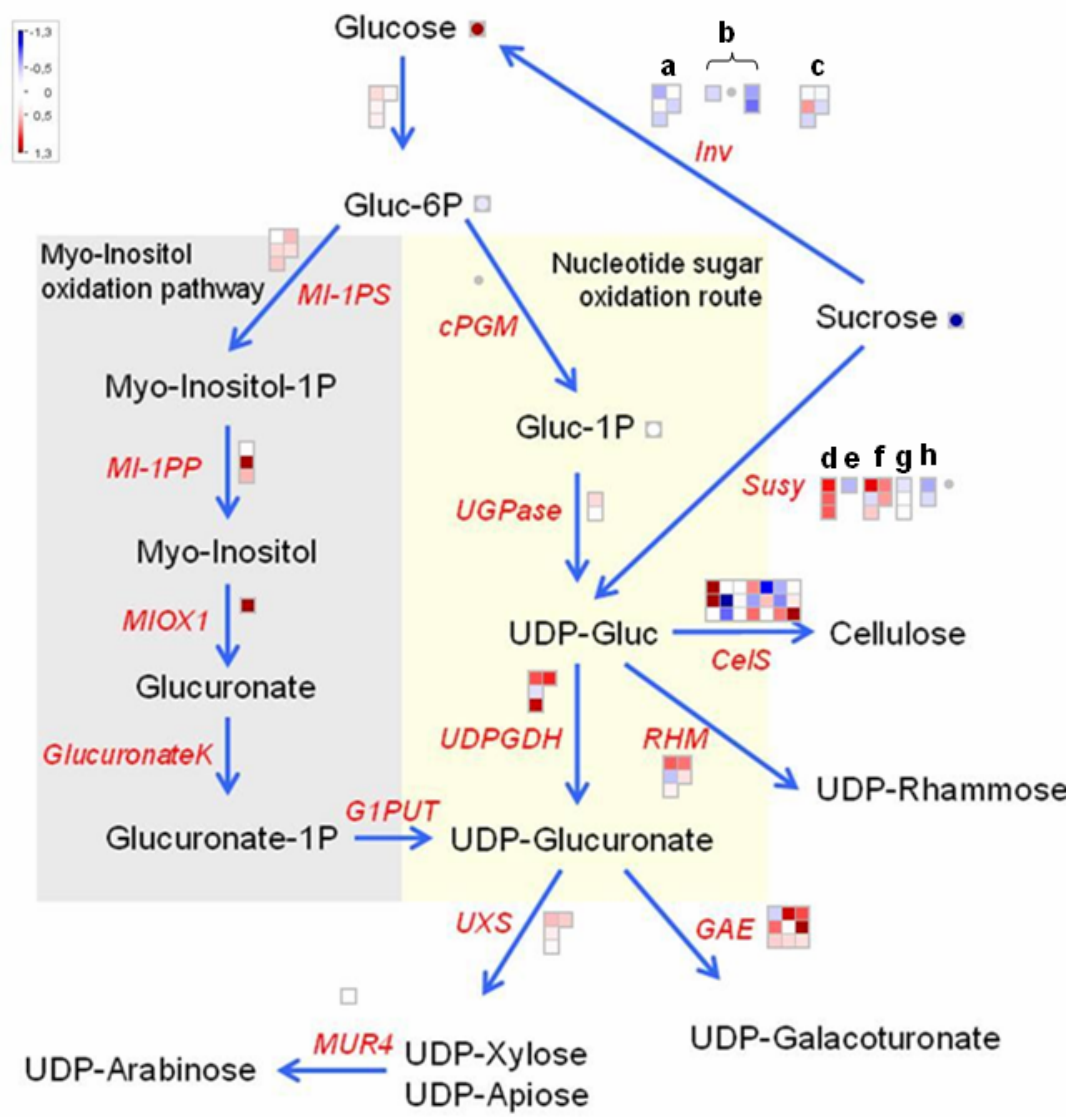


**Figure 36A. The production of UDP-glucose and UDP-glucuronate for cell wall biosynthesis in NTTP.** a) Neutral invertase. b) Cell wall invertase c) Vacuolar invertase. d-h) differentially expressed Susy Isoforms with d) Susy4.

Gene name abbreviations: MI-1PP-Myo-inositol 1-phosphate phosphatase; GlucoronateK - gluconurate kinase; G1PUT-galactose-1-phosphate uridylytransferase; UXS- UDP-xylose synthase; GAE-UDP-glucuronate epimerase; RHM-rhamnose synthase; CelS-Cellulose synthase.

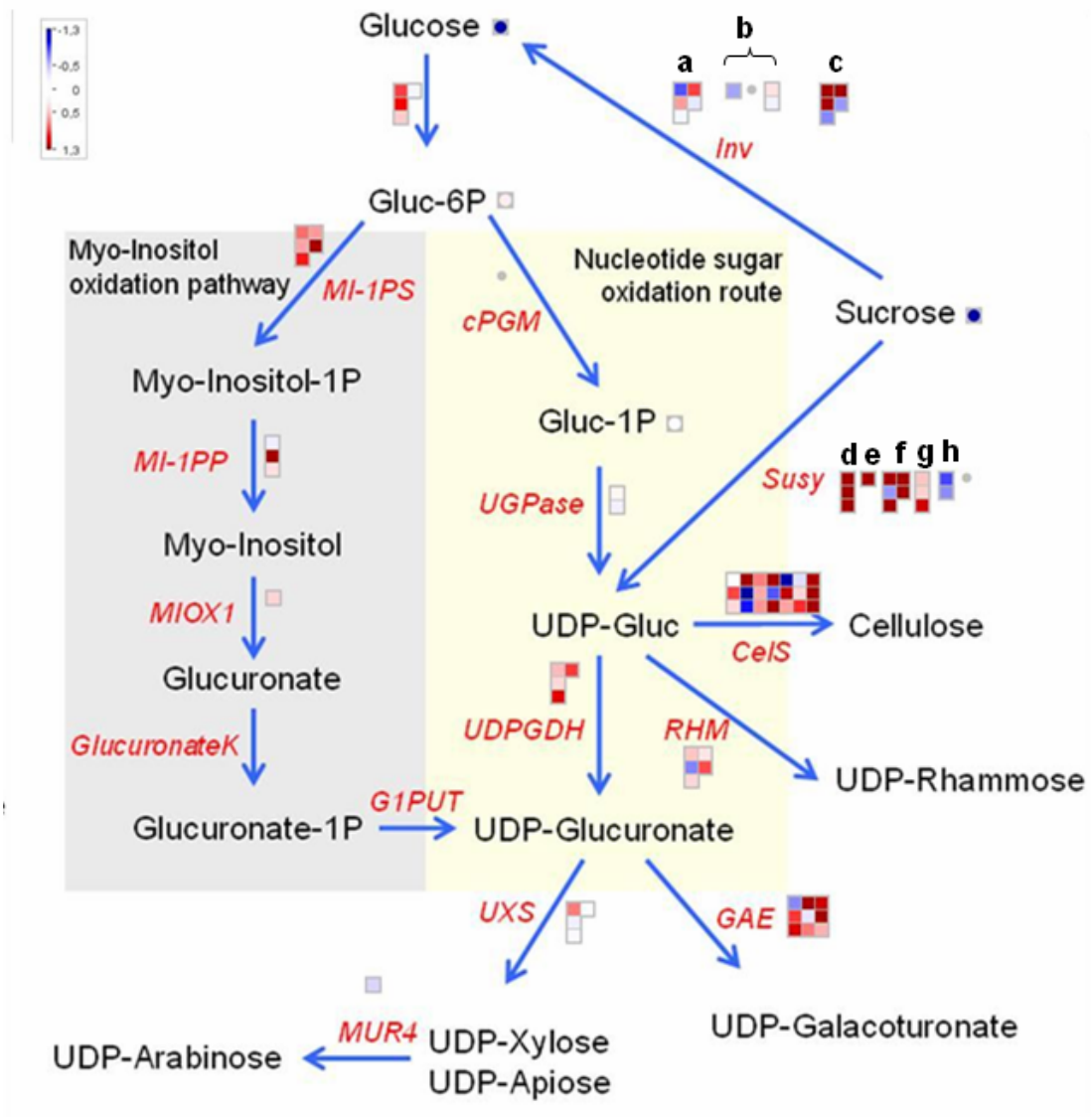


**Figure 36B. The production of UDP-glucose and UDP-glucuronate for cell wall biosynthesis in CW-ISO**. a) Neutral invertase. b) Cell wall invertase c) Vacuolar invertase. d-h) differentially expressed Susy Isoforms with d) Susy4.

Gene name abbreviations: MI-1PP-Myo-inositol 1-phosphate phosphatase; GlucoronateK - gluconurate kinase; G1PUT-galactose-1-phosphate uridylytransferase; UXS- UDP-xylose synthase; GAE-UDP-glucuronate epimerase; RHM-rhamnose synthase; CelS-Cellulose synthase.

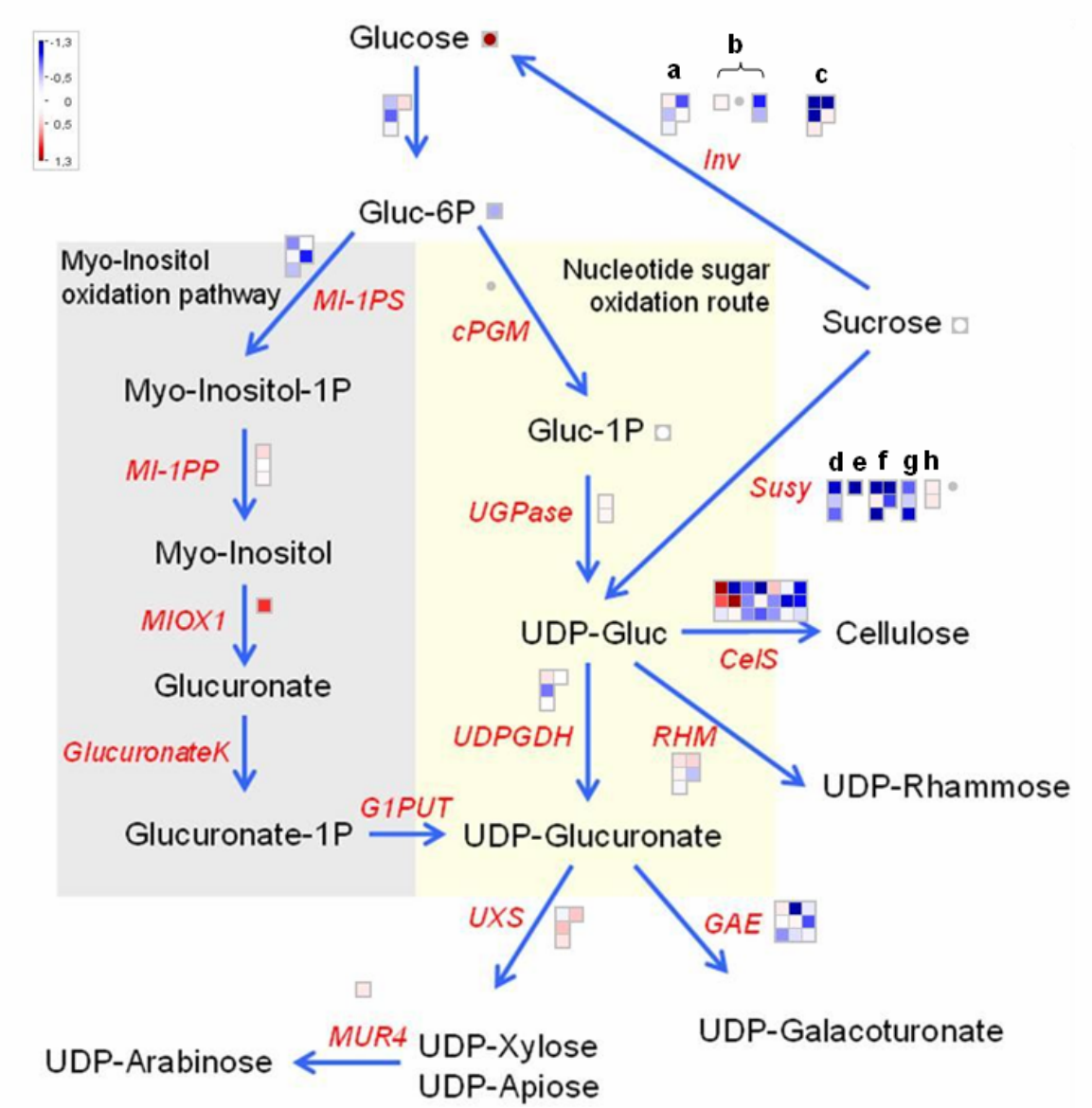


**Figure 36C. The production of UDP-glucose and UDP-glucuronate for cell wall biosynthesis in NTTP compared to CW-ISO**. a) Neutral invertase. b) Cell wall invertase c) Vacuolar invertase. d-h) differentially expressed Susy Isoforms with d) Susy4.

Gene name abbreviations: MI-1PP-Myo-inositol 1-phosphate phosphatase; GlucoronateK-gluconurate kinase; G1PUT-galactose-1-phosphate uridylytransferase; UXS- UDP-xylose synthase; GAE-UDP-glucuronate epimerase; RHM-rhamnose synthase; CelS-Cellulose synthase.

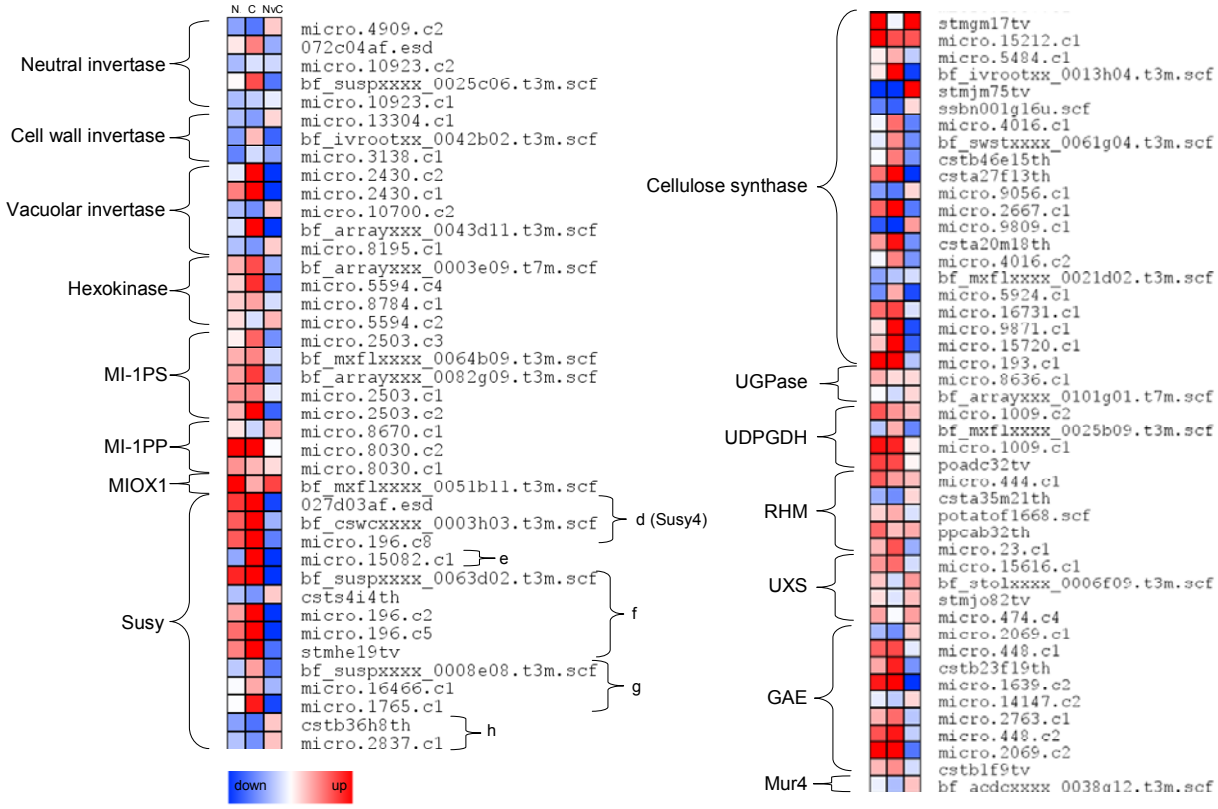


**Figure 37. Heatmap representation of features viewed in the photosynthesis pathway.** Log2 values of the fold change compared to WT; or NTTP compared to CW-ISO. Column N is NTTP, Column C is CW-ISO and column NvC is NTTP compared to CW-ISO. values are the mean of 3-4 replicates.

### 2.3.2.3. Glylolysis and TCA cycle.

As mentioned earlier, studies showed that CW-ISO had increased respiration rates (Hajirezaei, 2003), and it is not known whether this is the case for NTTP. Gene expression analysis did not reveal a clear increase in the expression of either glycolysis or the TCA cycle in CW-ISO, but there was huge increase in fumarate, intermediate of the TCA cycle (figures 38 and 39).

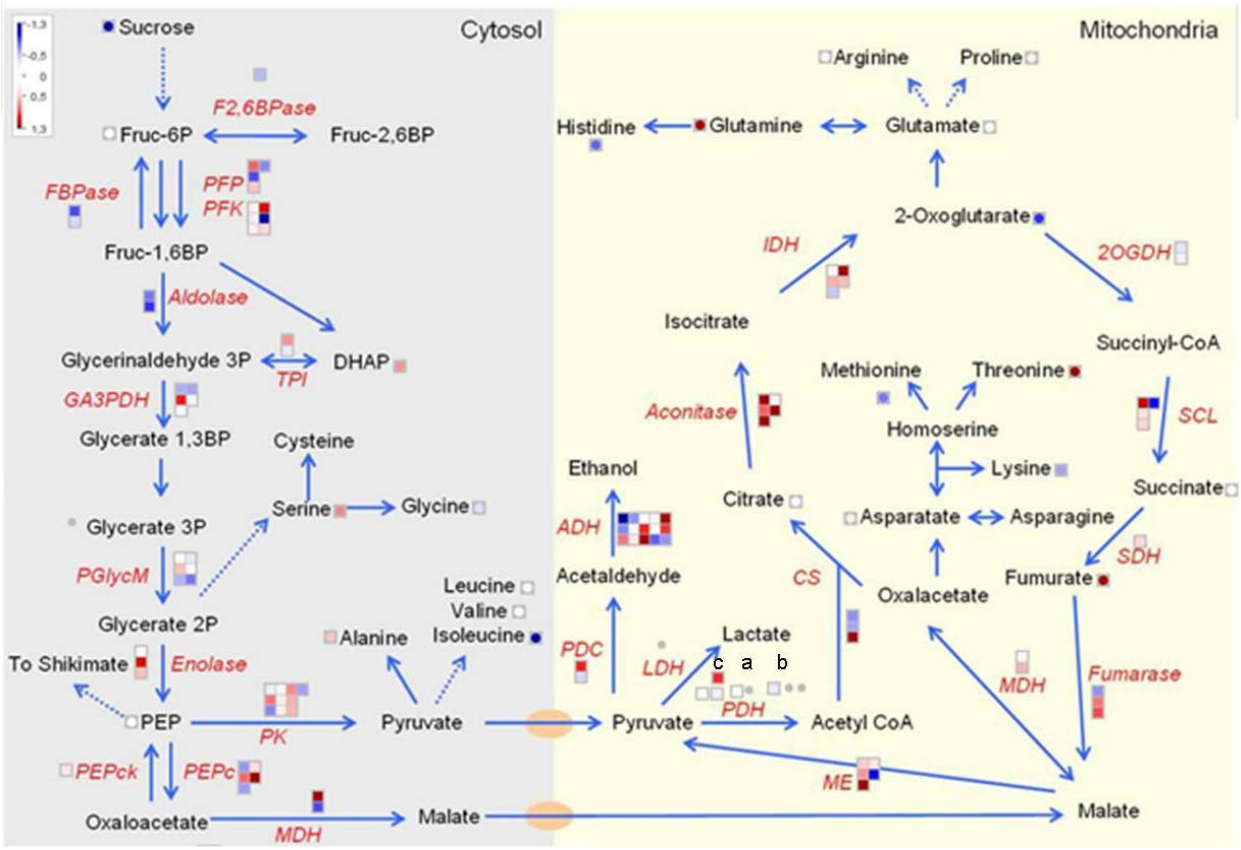


**Figure 38. TCA cycle and respiration in CW-ISO.** The E2 (a) and E3 (b) E1 (c) subunits of the mitochondrial pyruvate dehydrogenase complex.

Gene name abbreviations: TPI-Triose phosphate isomerise; GA3PDH-Glyceraldehyde 3-phosphate dehydrogenase;PGlycM-Phosphoglyceratemutase; PEPck-PEP carboxylase kinase; PEPc-PEP carboxylase; MDH-Malate dehydrogenase; ME-Malic enzyme; CS-citrate synthase; IDH-isocitrate dehydrogenase;2-oxoglutarate dehydrogenase; SCL- succinate CoA ligase; succinate dehydrogenase.

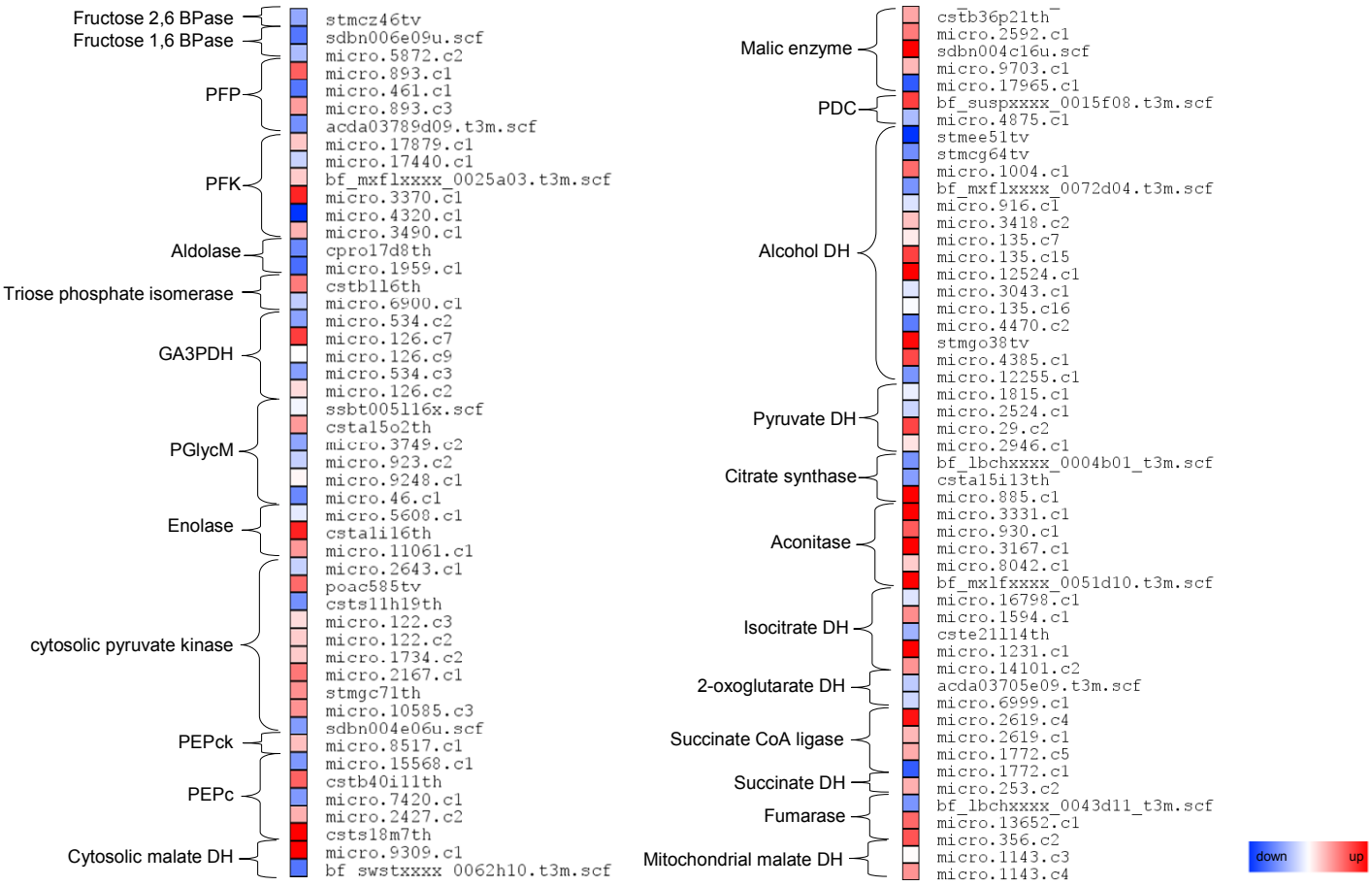


**Figure 39. Heatmap representation of features viewed in glycolysis and TCA cycle pathways for CW-ISO.** Log2 values of the fold change compared to WT. values are the mean of 3-4 replicates.

### 2.3.2.4. The Shikimate and pentose phosphate pathways.

One of the most striking aspects of CW-ISO was the accumulation of Shikimate and reduced levels of amino acids tyrosine and phenylalanine, similar to what was observed in U-IN-2. This was however, accompanied by a general increase in expression of genes in the pathway (figure 40 and 41), opposed to what was observed in U-IN-2.

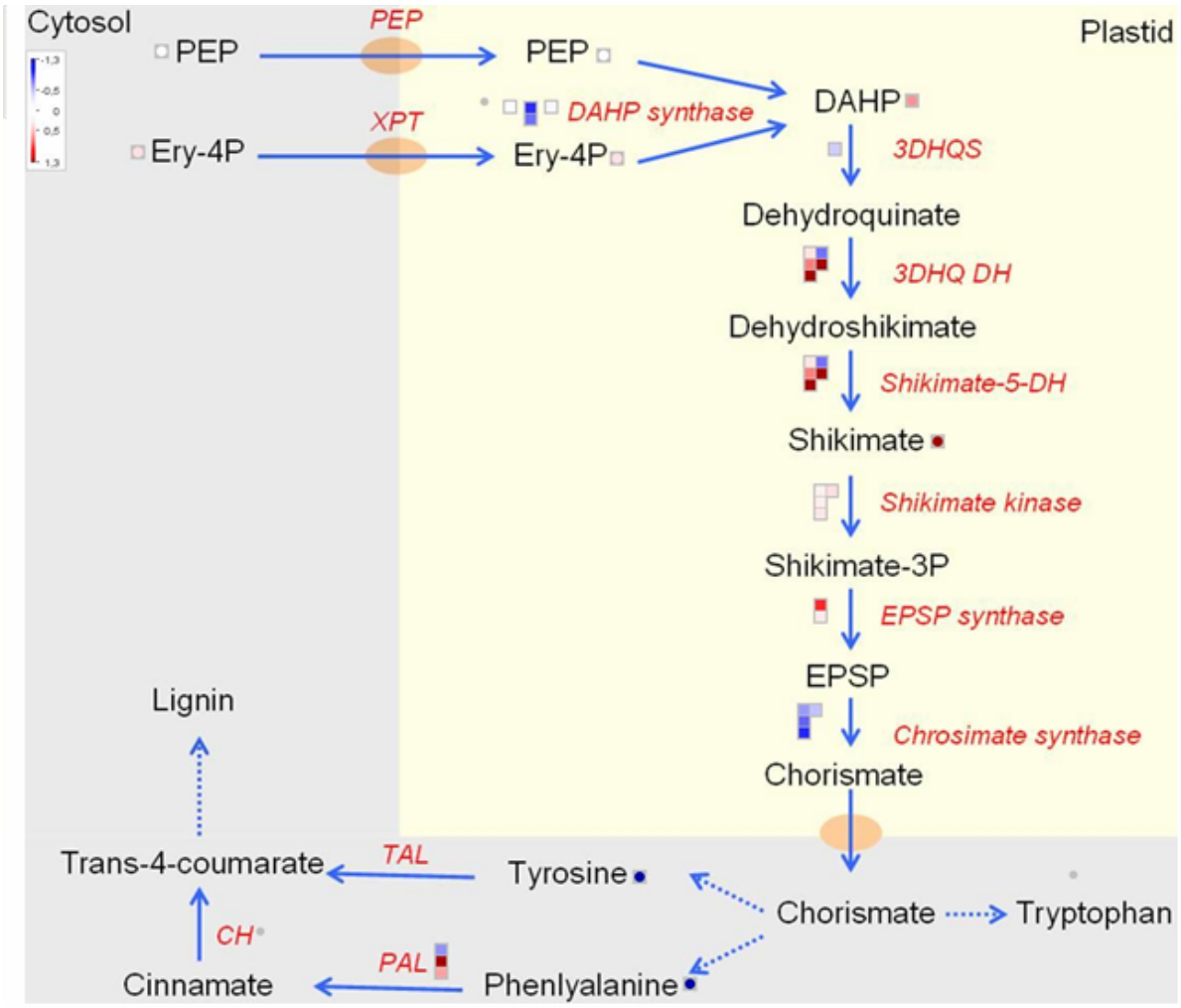


**Figure 40. Shikimate biosynthetic pathway producing aromatic amino acids and precursors for lignin in CW-ISO.**

Gene name abbreviations: DAHP synthase - 3-Deoxy-D-Arabino-Heptulosonate 7-Phosphate synhase; 3DHQS - 3-dehydroquinate synthase; 3DHQ DH - 3-dehydroquinate dehydrogenase ; Shikimate-5-DH - Shikimate 5-dyhydrogenase ; EPSP synthase – 5-Enolpyruvylshikimate 3-phosphate synthase; TAL – Tyrosine amminia lyase ; PAL – phenylalanine ammonia lyase ; CH – Cinnamate 4-hydroxylase.

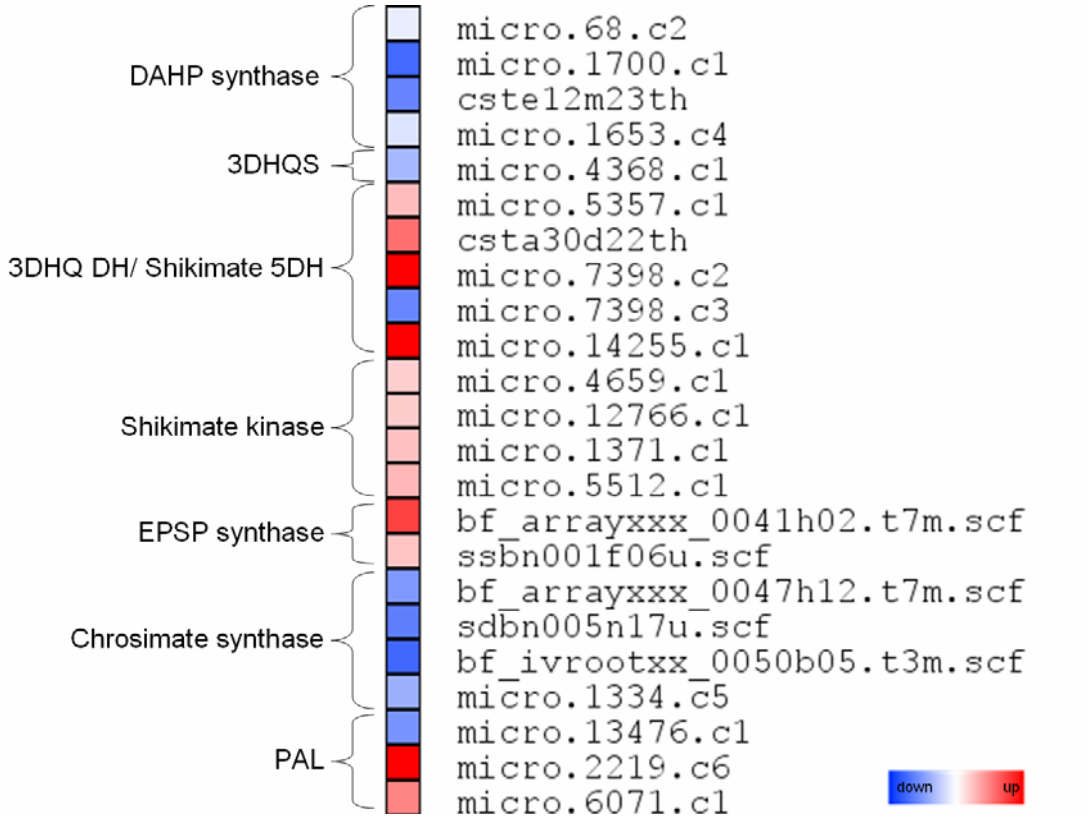


**Figure 41. Heatmap representation of features viewed in cell wall biosynthesis pathway in CW-ISO.** Log2 values of the fold change compared to WT. values are the mean of 3-4 replicates.

Furthermore, inspection of the pentose phosphate pathway showed that in CW-ISO an increase in the expression of the two plastid localised isoforms of G6PDH and this was accompanied by a significant increase in the levels of erythrose 4-phosphate (figures 42 and 43).

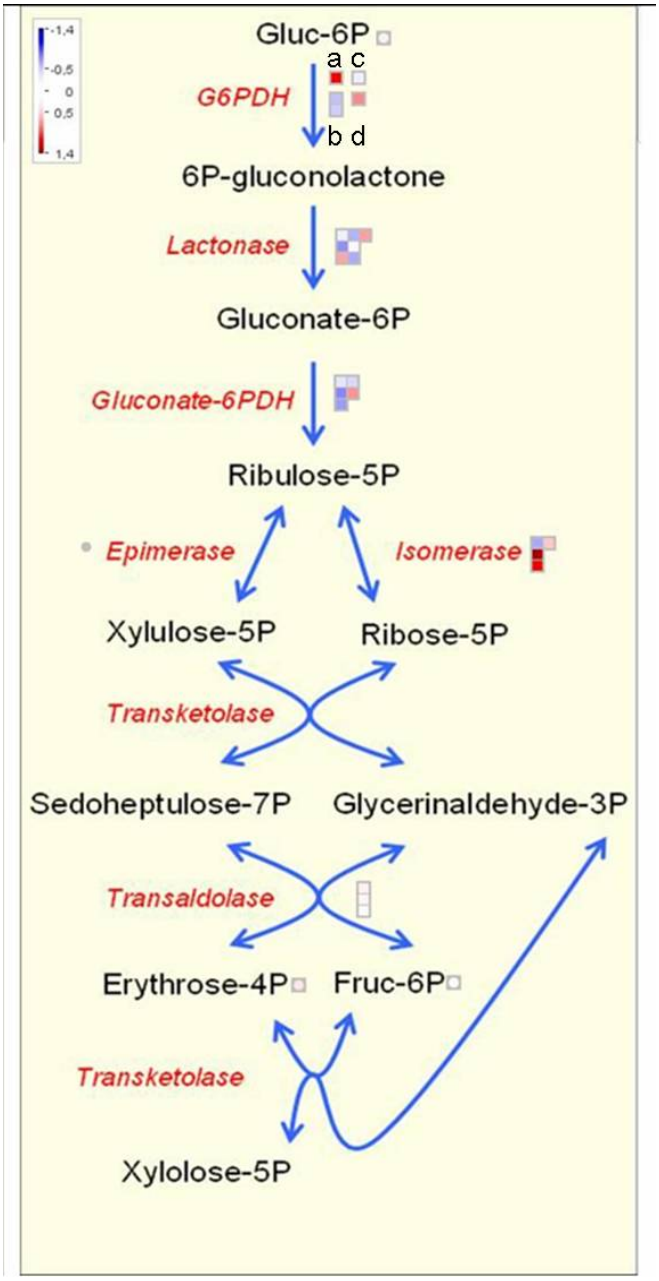


**Figure 42. Pentose phosphate pathway in CW-ISO**. a-d) Differentially expressed isoforms of G6PDH. a) and d) are plastidial isoforms.

Gene name abbreviations: Gluconate-6PDH-Gluconate 6-phosphate dehydrogenase

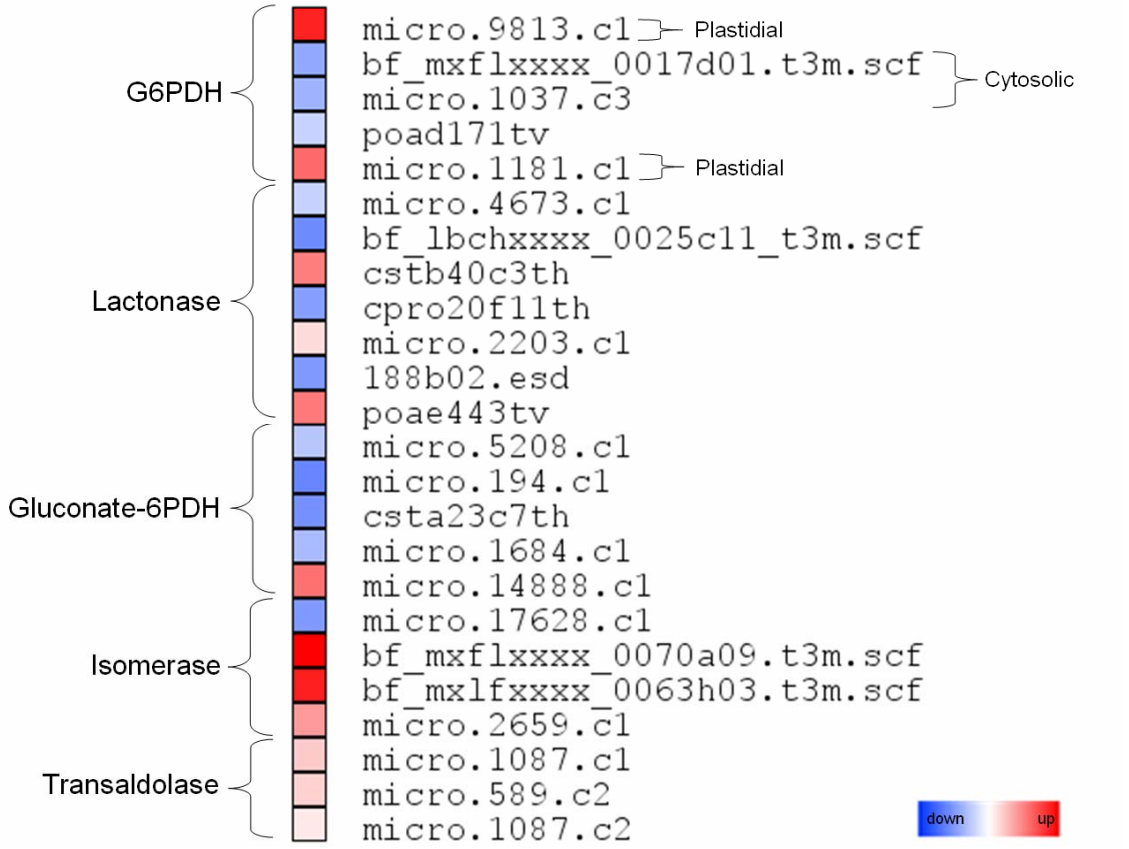


**Figure 43. Heatmap representation of features viewed in the pentose phsosphate pathway.** Log2 values of the fold change compared to WT. values are the mean of 3-4 replicates.

### 2.3.2.5. Starch metabolism.

Due to its importance in tubers, and also since there was a significant reduction in CW-ISO starch content, starch biosynthesis was investigated, starting with sucrose degradation. In both transgenic genotypes, there was either a reduction in cell wall invertase expression, or no real change. In CW-ISO, there was a strong induction in expression of most vacuolar invertase associated transcripts, whilst it was difficult to interpret the expression in NTTP. Despite the reduction in starch contents in CW-ISO, no clear reduction in the expression of starch biosynthetic genes could be observed in CW-ISO. There was, however, a general increase in the expression of starch degrading enzymes in both genotypes, but especially CW-ISO. As mentioned earlier, the strong increase in expression of Susy isoforms, especially Susy4, is interesting since there was reduced sucrose content. There was also an increase in the expression of fructokinase 1 and 2, thought to be negatively regulated by fructose, despite fructose increased in both

transgenic genotypes (table S9). In CW-ISO there was an increase in the hexokinase expression, and closer analysis revealed that the up-regulated isoform is homologous to the Arabidopsis gene, Hexokinase 1 (GIN2), thought to be an important regulator of central carbon metabolism (Rolland et al., 2006) (figures 44 and 45).

A

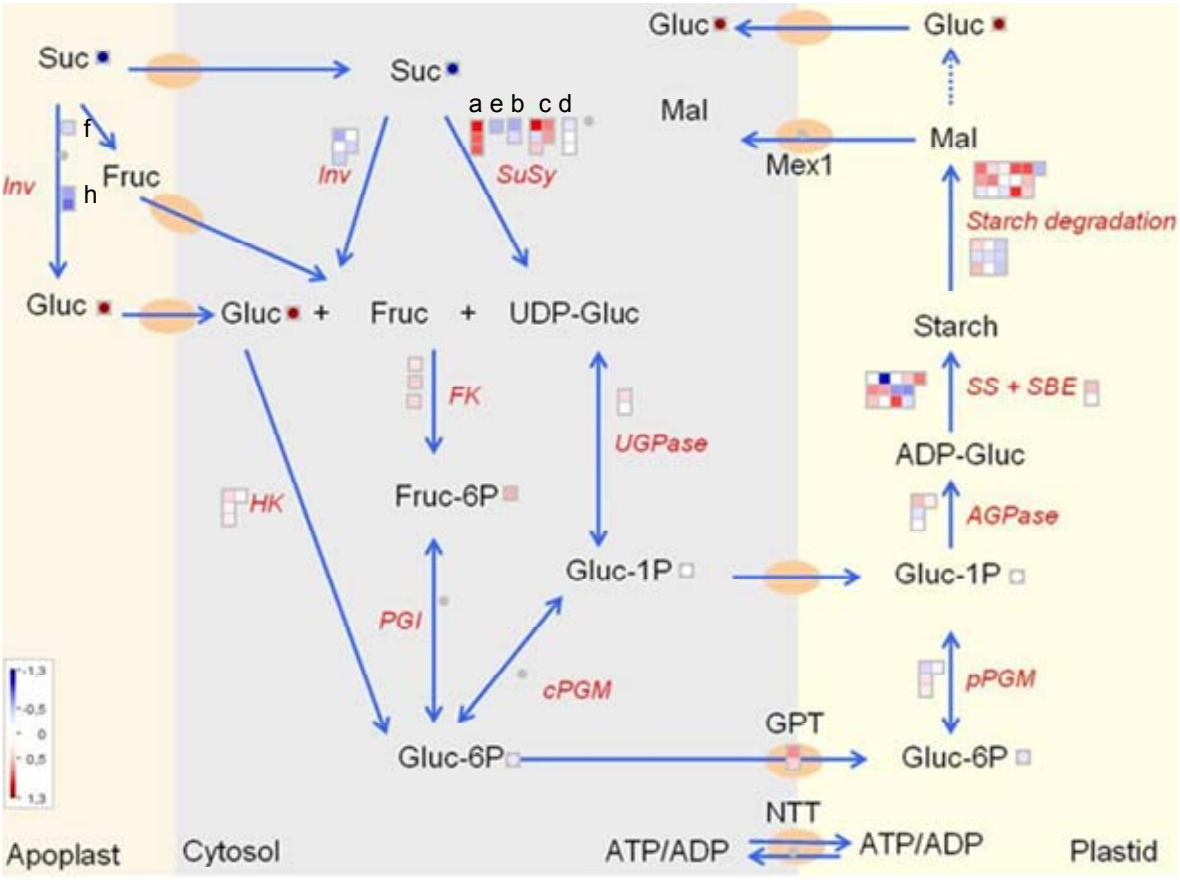


**Figure 44A. Starch biosynthesis with sucrose as primary substrate in A) NTTP**. Different subunits of Susy is represented by a-e) with a) Susy4.

f-h) represent the differentially expressed cell wall invertase isoforms. j) fructokinase 2. k) fructokinase 3.

Gene name abbreviations: HK-hexokinase; PGI- phosphogluco isomerise; SS – starch synthase; SBE-starch branching enzymes; AGPase-ADP-glucose pyrophosphorylase.

B

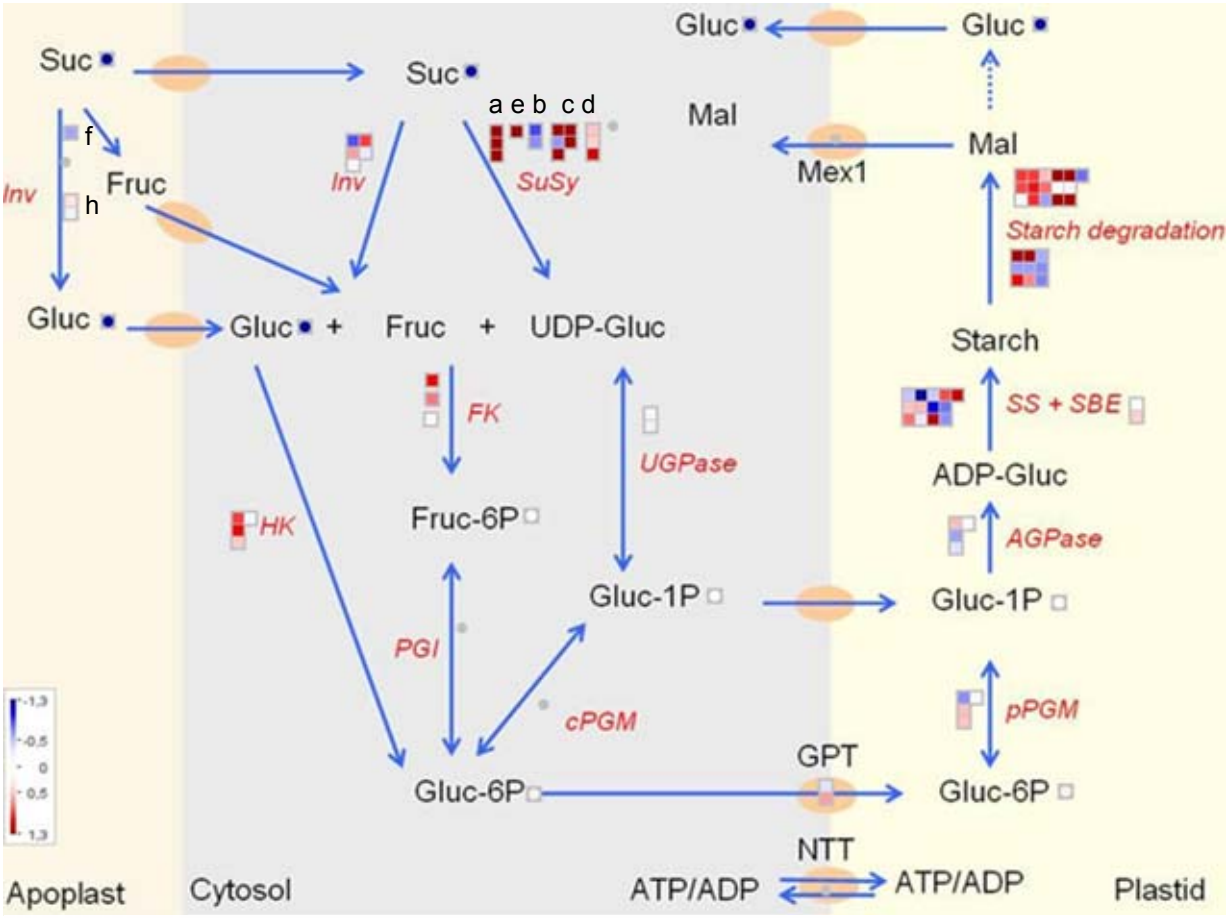


**Figure 44B. Starch biosynthesis with sucrose as primary substrate in CW-ISO**. Different subunits of Susy is represented by a-e) with a) Susy4 .

f-h) represent the differentially expressed cell wall invertase isoforms. j) fructokinase 2. k) fructokinase 3.

Gene name abbreviations: HK-hexokinase; PGI- phosphogluco isomerise; SS – starch synthase; SBE-starch branching enzymes; AGPase-ADP-glucose pyrophosphorylase.

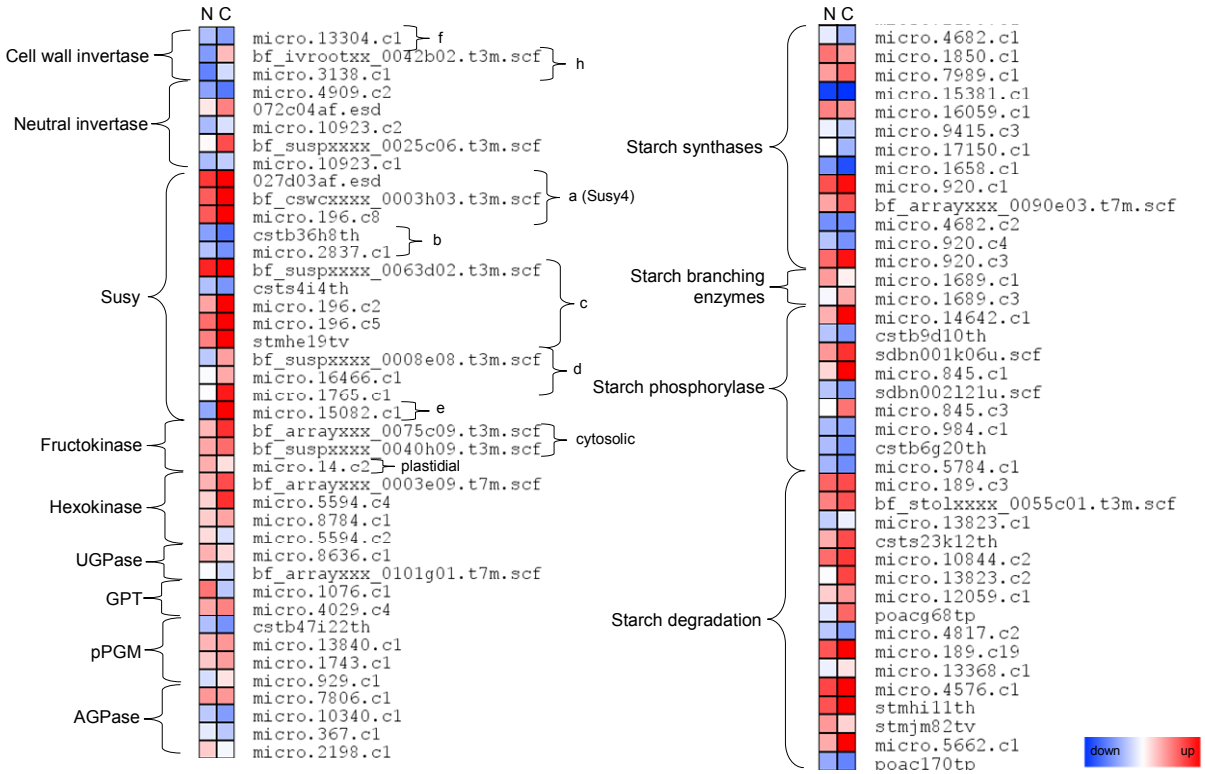


**Figure 45 Heatmap representation of features viewed in starch biosynthesis biosynthesis pathway for NTTP and CW-ISO.** Log2 values of the fold change compared to WT. values are the mean of 3-4 replicates.

### 2.3.3. Microarray analysis of leaf discs exogenously fed with sugars.

To further enhance our knowledge on sugar signalling in potato, microarray analysis of potato leaf discs floated in different sugar solutions were performed. Leaf discs were harvested from potato leaves two hours after illumination with supplementary light and immediately transferred to Petri dishes containing 250mM solutions of either sucrose, glucose or trehalulose in darkness. To verify whether trehalulose elicits a sugar or pathogen response signal, a salicylic acid floating experiment (1mM salicylic acid) was also performed as a control for pathogen response.

Samples were taken over a twenty four hour period and starch content of the leaves was determined. In plants fed with either sucrose or glucose, starch content increased drastically after twenty four hours. In the control samples and that of trehalulose, starch content was either reduced or unchanged (figure 46). Microarray hybridisation was

performed using RNA extracted from the same sample pool as what was used for starch measurements.

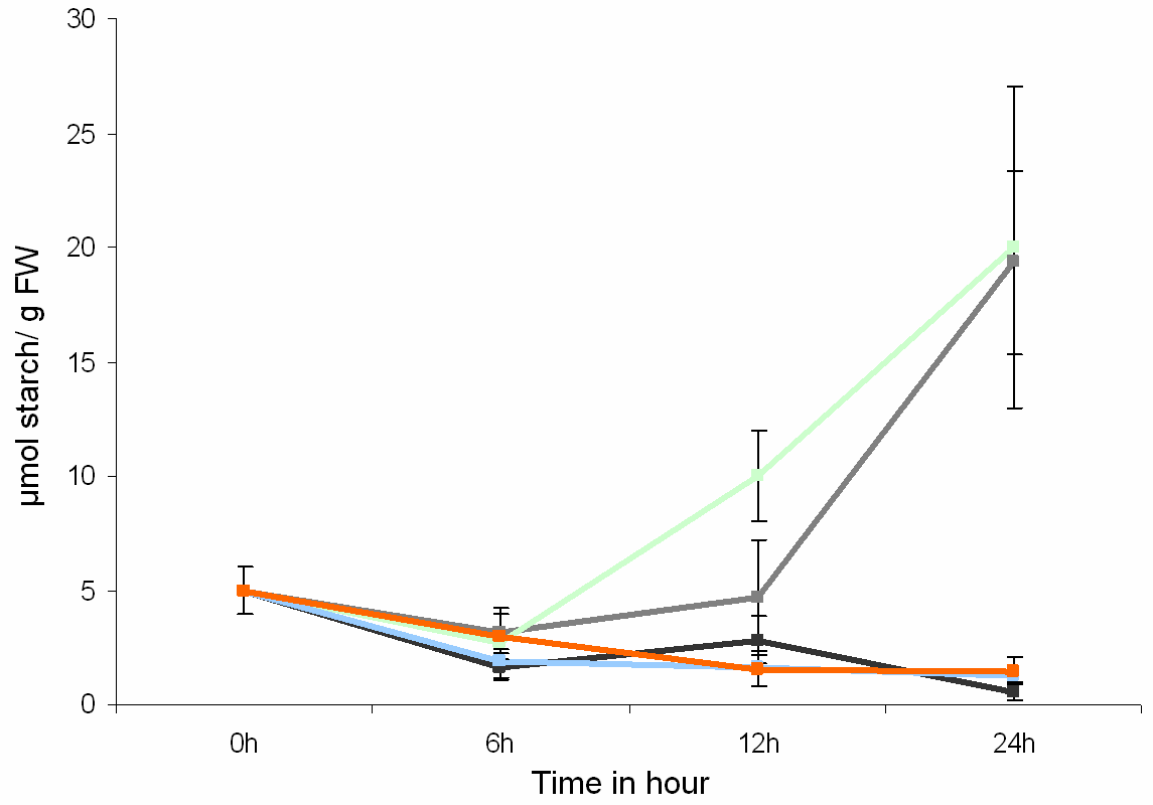


**Figure 46. Starch contents at different time-points in leaf discs floated on different solutions**. Water (black), sucrose (grey), glucose (green), trehalulose (blue) and salicylic acid (orange). Error bars represent standard deviation (n=4-5). Starch measurements performed by V. Scheuenstuhl

As mentioned, one of the reasons for floating experiments was to determine whether trehalulose elicits a sucrose-like or pathogen response-like (PR-like) signal. A PCA was performed to determine the relationship between the treatments. Treatments could clearly be separated by PCA, except for sucrose and glucose which had very similar transcript profiles. Trehalulose, however, was present between the metabolisable sugars sucrose and glucose, and salicylic acid. Thus, from a global perspective, it is unclear whether trehalulose elicits a sucrose- or reducing sugar-like, or a PR-like signal (figure 47).

A

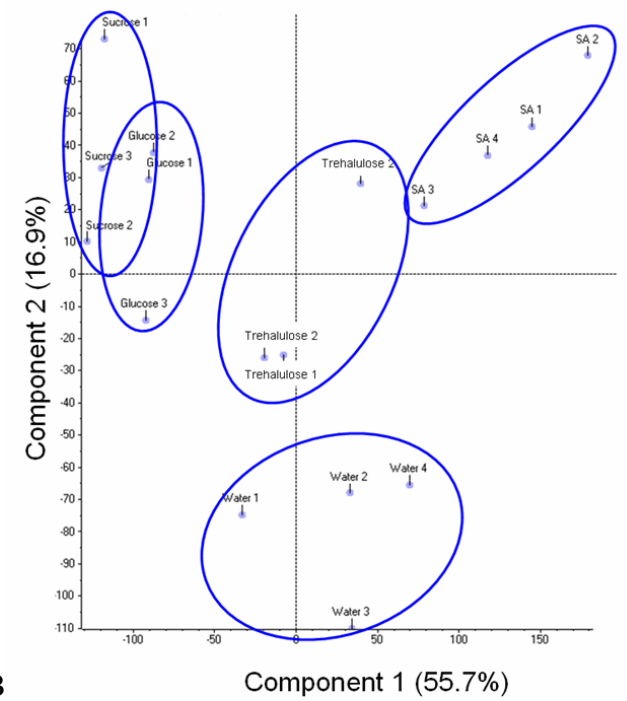


B

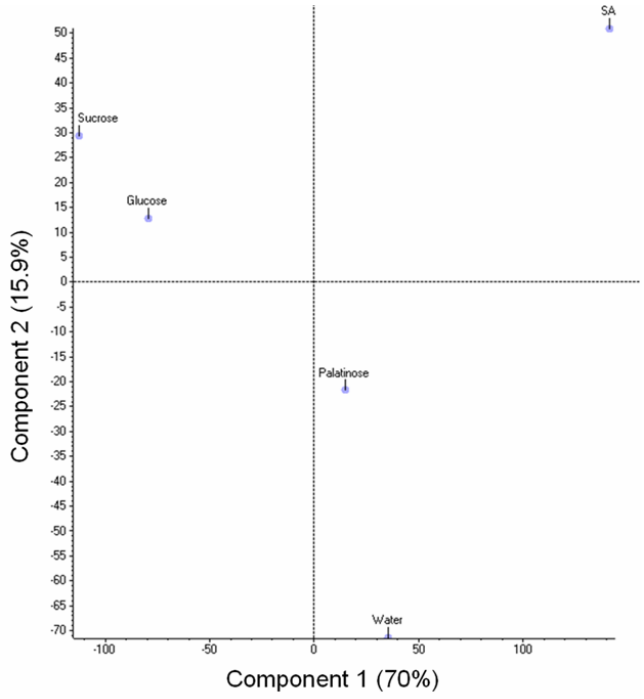


**Figure 47. Principle component analysis (PCA) of transcription data for leaf floating experiment.** A) Replicates illustrating that the individual replicates of each genotype clustered. B) PCA on the mean values of each genotype.

To determine which functional groups were mostly affected by the different treatments, functional enrichment amongst the up and down-regulated features was performed as described earlier (chapter 3). Amongst the down regulated features one functional group, photosynthesis, was affected in all treatments. There was also a more than two-fold enrichment of features associated with translation amongst the down-regulated features for salicylic acid treatment, the only further functional group affected for salicylic acid treatment in either the up- or down-regulated features. Amongst the up-regulated features, starch metabolism and storage protein associated features were more than two-fold enriched in sucrose and glucose treatment. Metabolism associated transcripts were increased in trehalulose- and glucose treatment, and there was a further enrichment for trehalulose in electron transport and also transport. Sucrose treatment also led to the more than two-fold enrichment in energy metabolism transcripts (figure 48).

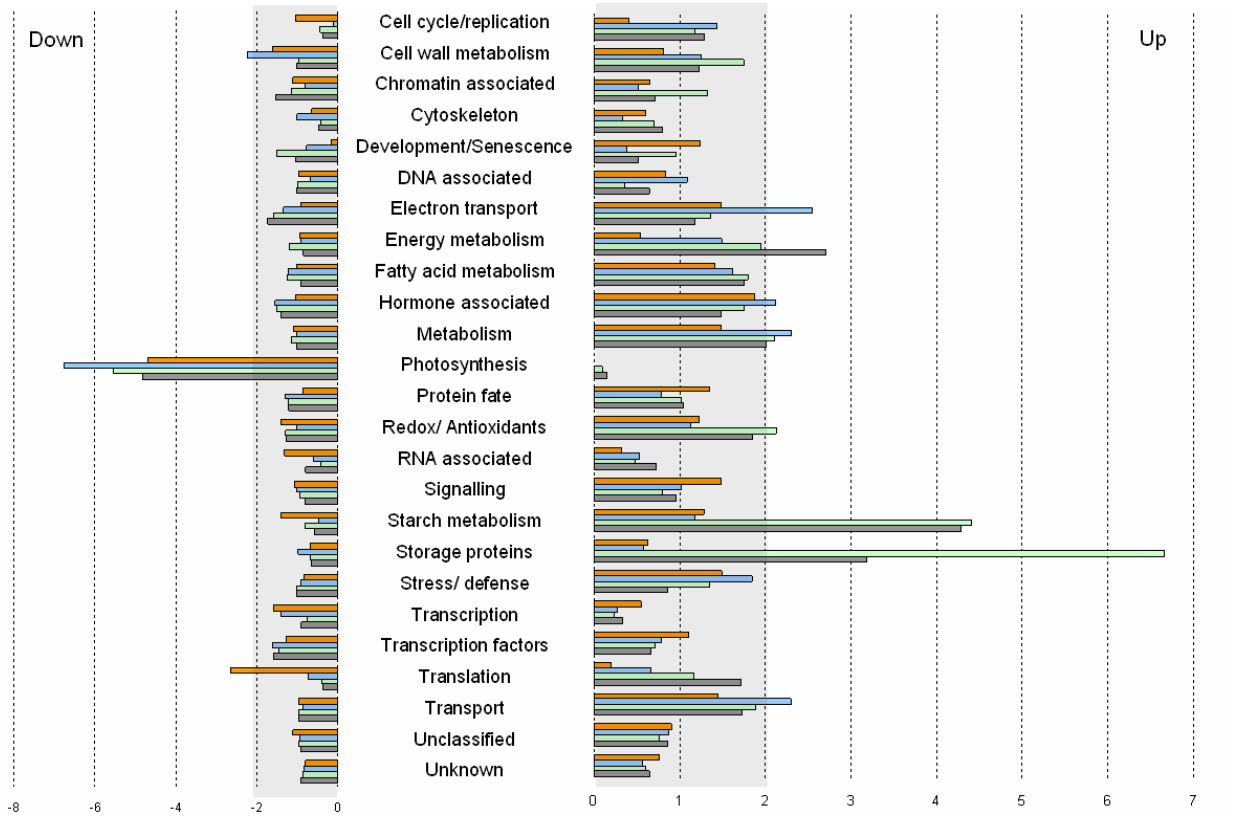


**Figure 48. Enrichment analysis of functional groupings amongst up- and down-regulated features comparing different treatments to the water floated control**. Sucrose (grey), glucose (green), trehalulose (blue) and salicylic acid (orange) floated leaf discs.

Qualitatively at least, the negative correlation observed earlier between cell wall invertase expression and GPT2 again held true (figure 49).

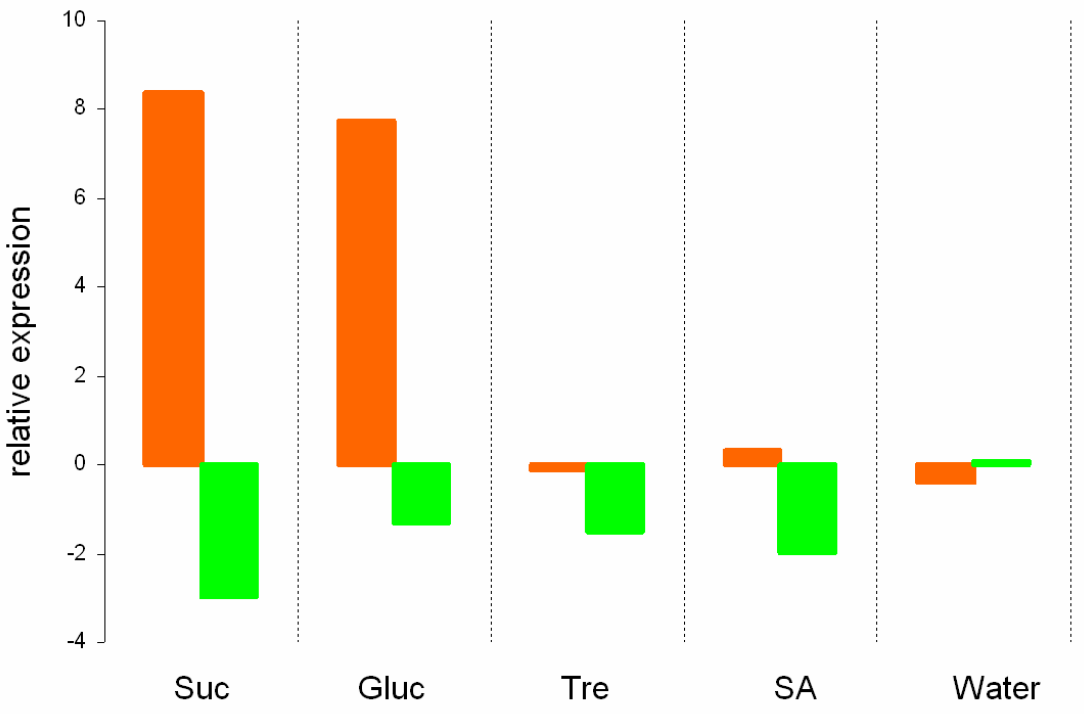


**Figure 49. GPT2 and cell wall invertase gene expression in floating experiments.** The expression pattern of an EST derived from GPT2 (micro.1076.c1, orange) and cell wall invertase (micro.11340.c1, green) in leaves treated with different solutions.

## 2.4. Comparative transcriptome analysis towards the identification of regulatory genes.

Comparative transcriptome analysis is a well-established method to identify new genes involved in a specific process. The rationale is that transcriptionally regulated genes involved would have similar expression patterns under various conditions. For instance, Sex4, a gene important for starch degradation as discussed earlier, was identified in this manner (Niittylä et al., 2006). Thus, the aim of this chapter was to identify through comparative transcriptome analysis regulatory genes putatively involved in starch biosynthesis.

### 2.4.1. Putative regulators of starch biosynthesis

To identify regulatory genes putatively involved in starch biosynthesis, genes up-regulated under the following conditions were chosen: Comparing either tuber induction stages 5 to stage 1; growing to non-growing tubers; sucrose floated leaf discs to water floated leaf discs and finally glucose floated leaf discs to water floated leaf discs. Furthermore, only features which were increased in all scenarios were selected. The mean expression profiles of the selected genes are shown in figure 50.

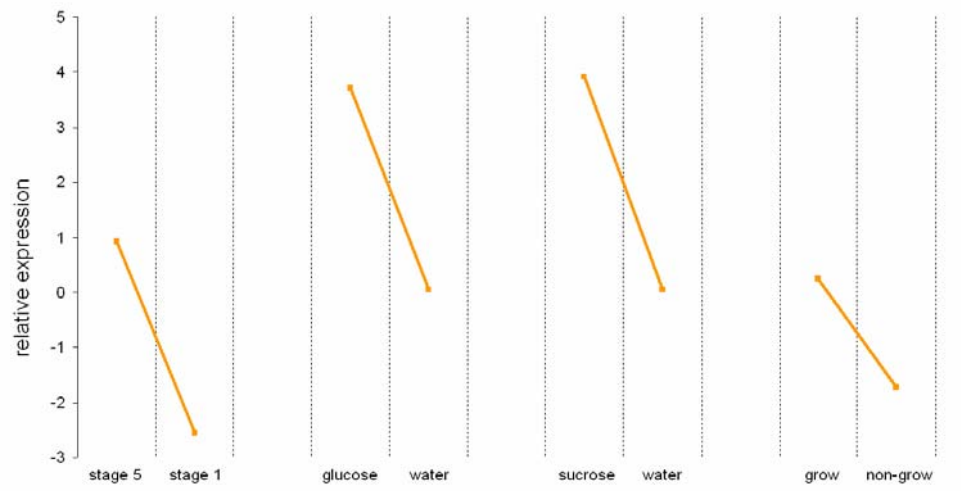


**Figure 50. Mean expression profile of genes up-regulated under conditions of active starch biosynthesis.** The conditions selected were tuber induction stage 5 and 1 (n=2), glucose and sucrose floating of leaf discs compared to the control (n=3-4), and growing and non-growing tubers (n=2).

Functional group analysis revealed that there was a stong enrichment of genes associated with storage proteins and starch biosynthesis (figure 51). This provided confirmation that the comparative analysis indeed selected for genes associated with the desired processes.

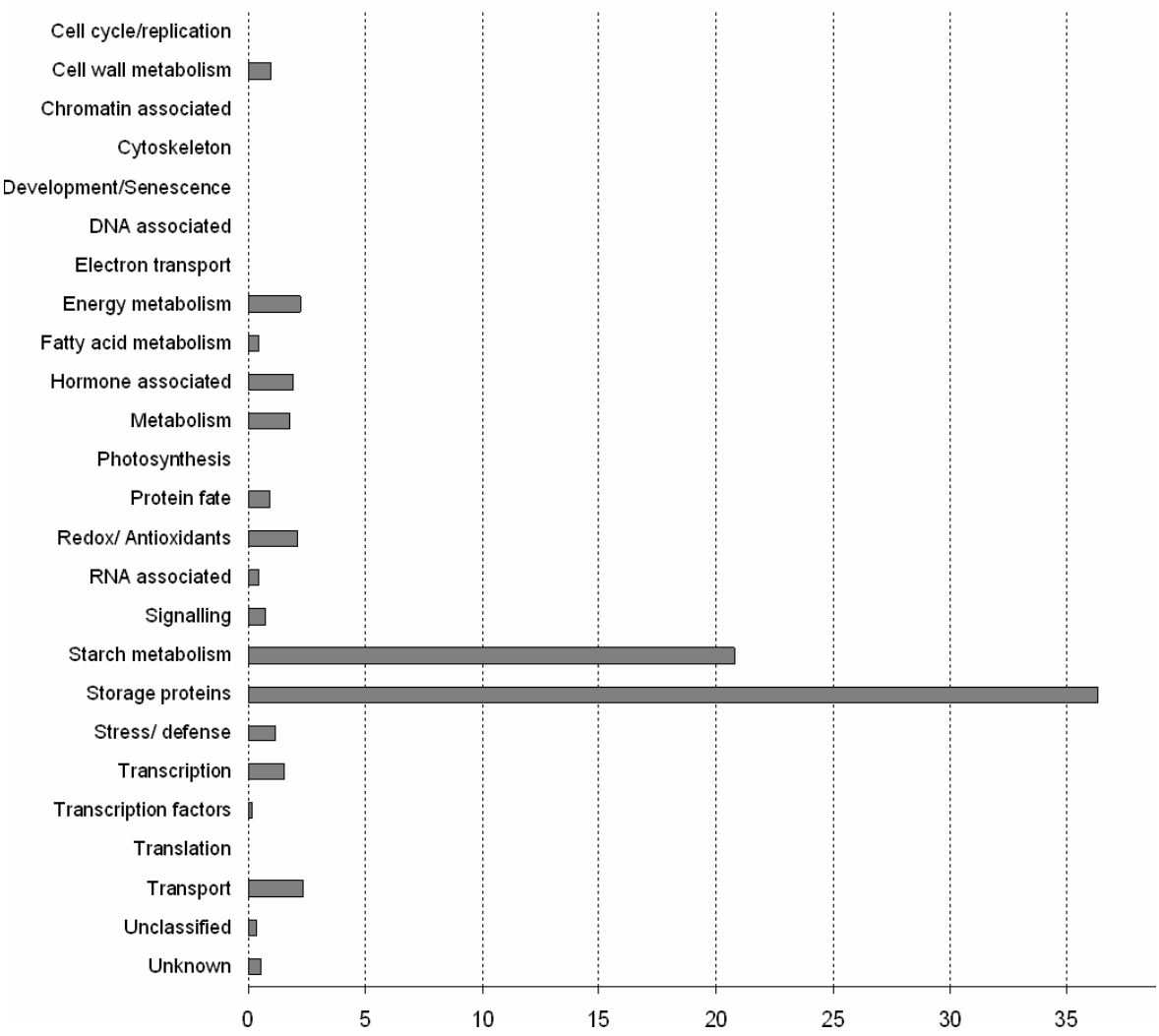


**Figure 51. Functional group enrichment analysis of genes expressed at times of active starch biosynthesis.**

This very strict selection identified one transcription factor (micro.5579.c2), annotated as bZIP transcription factor BZI-2. Closer inspection revealed that the bZIP protein belongs to the S group of bZipppers, known to possess a highly conserved open reading frame upstream of the coding sequence (uORF). Interestingly, this region is known to control translation in response to sucrose. The region is highly conserved between *species* and

has also been reported for potato (Genbank accession number BQ509423) (Wiese et al., 2004). Genomic alignment of this highly conserved uORF was used to identify other bZIP genes containing this uORF upstream of the coding sequence. Five more bZIP genes could be identified in the potato genome containing this uORF region and they were subsequently named St_bZIP 1, 2, 3, 8, 12 and 52. The amino acid sequence alignment of these identified bZIP proteins are shown in figure 52.


**Figure 52. Amino acid sequence alignment of St_bZIP proteins.** The genes have a highly conserved uORF region upstream of the coding sequence.

Furthermore, POCI identifiers for three of these genes were identified and expression profiles of these are shown in figure 53. St_bZIP2 and St_bZIP8 had very similar expression profiles and correlated to active starch biosynthesis. St_bZIP52, however, had almost exactly the opposite expression pattern and is seemingly antogonistically regulated to starch biosynthesis (figure 53.).

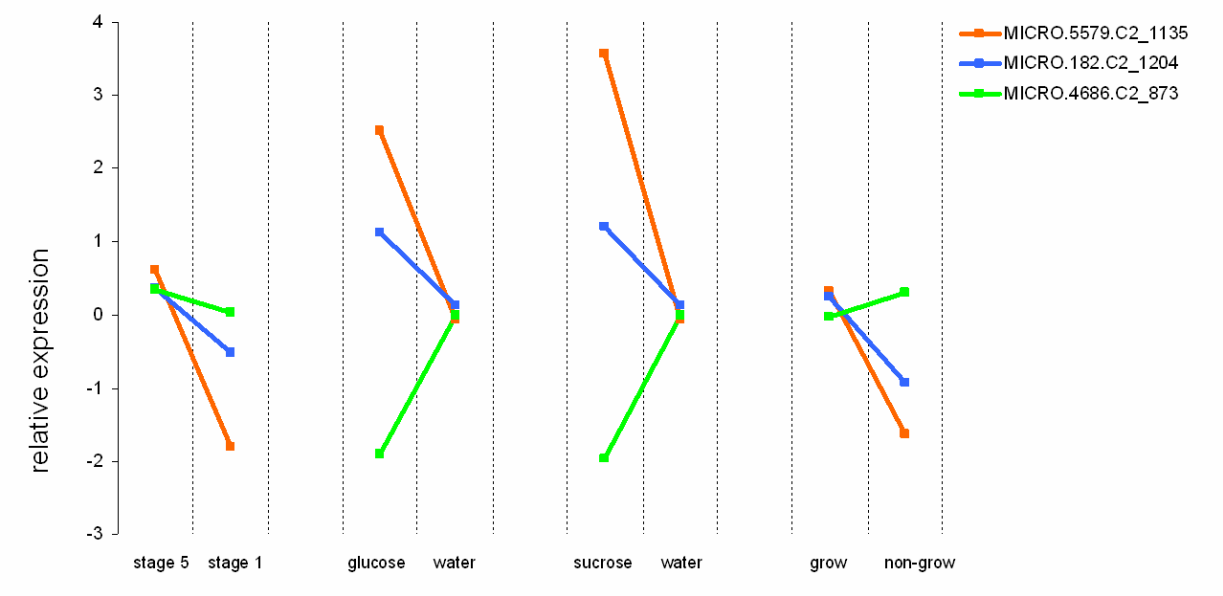


**Figure 53. Gene expression profile of uORF containing bZIP genes.** The conditions selected were tuber induction stage 5 and 1 (n=2), glucose and sucrose floating of leaf discs compared to the control (n=3-4), and growing and non-growing tubers (n=2).

## 2.5. Simultaneous silencing of isoamylases ISA1, ISA2 and ISA3 by multi-target RNAi in potato tubers.

To enhance our understanding on the role of isoamylase in potato tuber sprouting, and starch metabolism in general, transgenic plants with reduced expression of all three isoamylases were created and the consequences analysed.

### 2.5.1. Simultaneous silencing of all three isoamylase by RNAi

It was attempted to silence all three isoamylase genes by creating a single RNAi construct targeting all three genes. To achieve this, a chimeric PCR fragment was created and cloned into the gateway vector pK7GWIWG2(II), behind the ubiquitous 35S promoter (figure 54A). Initially northern blot hybridisation was used to screen for positive lines and revealed that in several lines the desired silencing was achieved. Lines 7, 16 and 39 were selected for subsequent studies (figure 54B).

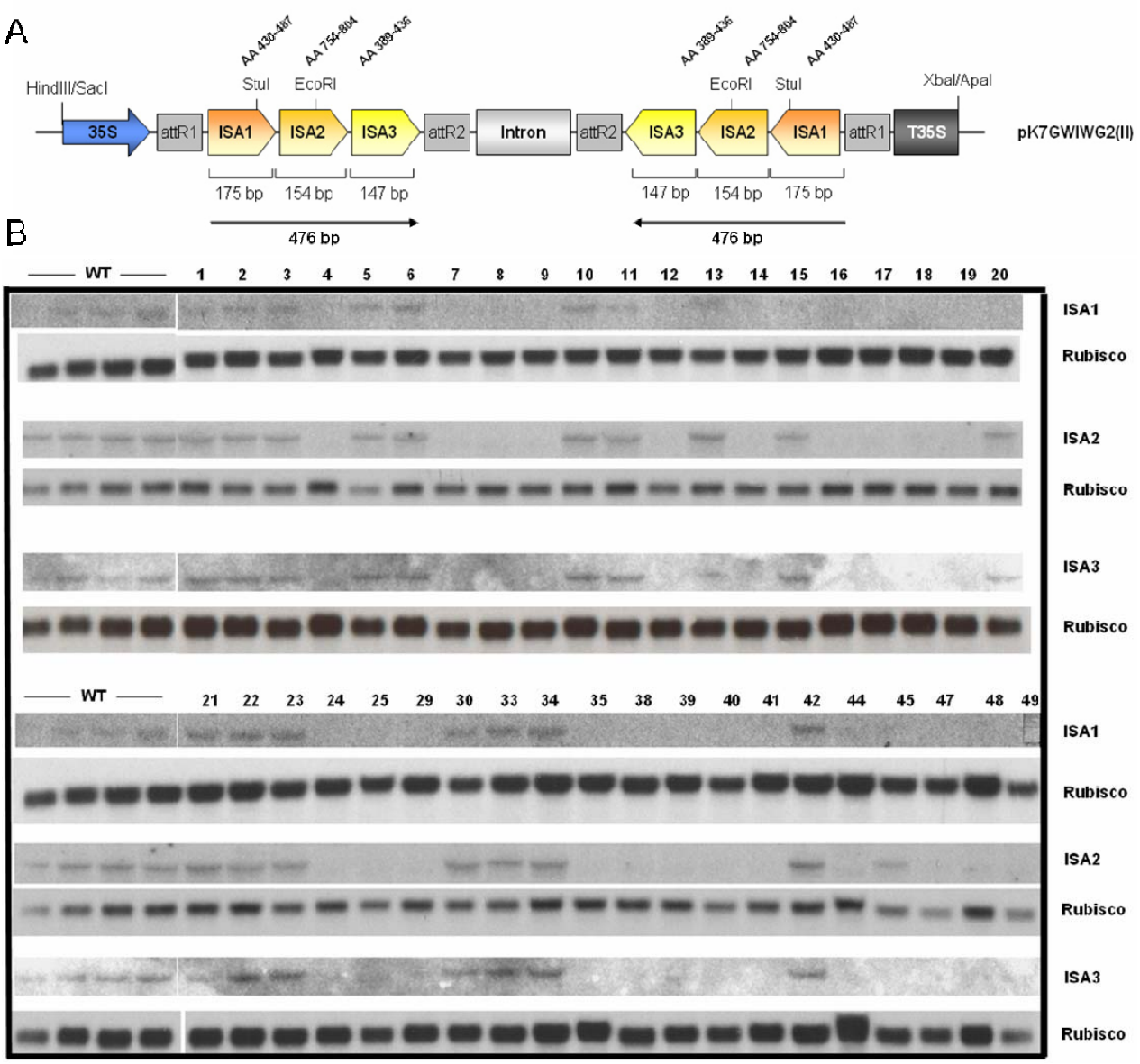


**Figure 54. Simultanious silencing of all three isoamylases.** A) Chimeric RNAi construct behind the 35S promoter. B) Northern hybridisation of ISA1, ISA2 and ISA3 of transgenic lines and WT control from RNA extracted in leaves. Lines 7, 16 and 39 were selected for subsequent studies. RNAi construct design and Northern blot performed by M. Senning.

### 2.5.2. Leaf carbohydrate content and analysis of transgenic tubers.

There were no visible phenotypical changes to the aerial parts of the plants, leaf glucan content was not affected and there were also no changes in the levels of sucrose or hexoses (figure 55).

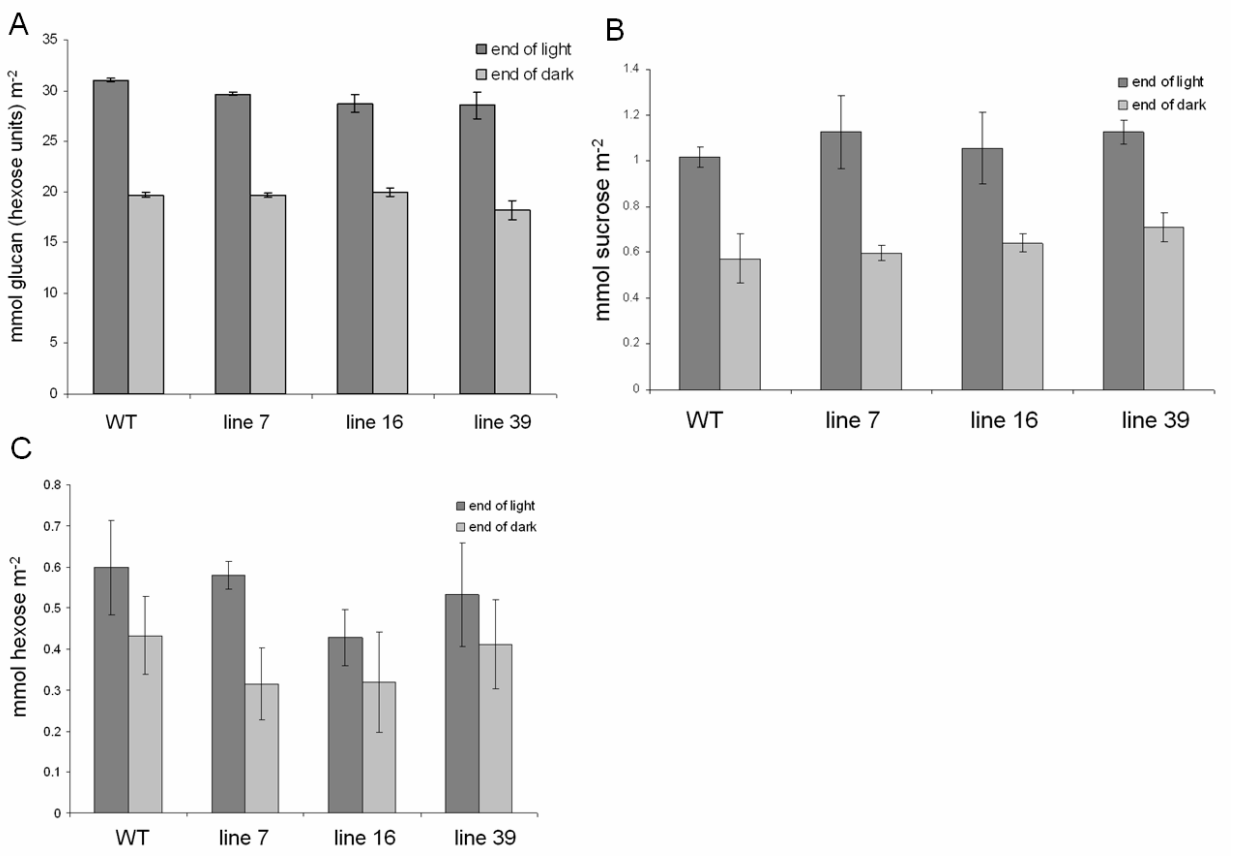


**Figure 55. Leaf glucan and soluble sugar contents at the end of the light period (light grey) and dark period (dark grey).** A) Total glucan, B) sucrose and C) hexose content. Error bars represent standard error (n=4-5).

To determine whether gene expression was altered in tubers, qRT-PCR was performed on tubers from the selected lines at harvest, which proved that gene expression was indeed reduced for all three isoamylases in the transgenic lines (figure 56).

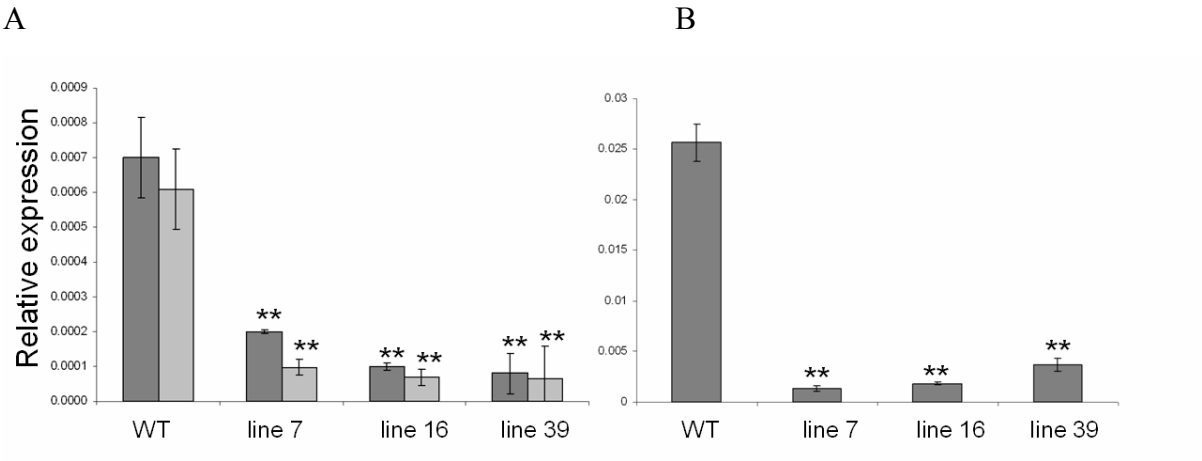


**Figure 56. Relative expression of isoamylase in WT and transgenic tubers at harvest.** A) Isoamylase 1 (dark grey) and Isoamylase 2 (light grey).B) Isoamlyase 3. The error bars represent standard error (n=3-4). ** indicates $p \leq 0.01$

At harvest there was no change in total tuber yield per plant (figure 57A), but there was a significant reduction in tuber starch content (figure 57B). This was accompanied by a reduction in the dry weight (DW) to fresh weight (FW) ratio (figure 57C) in the transgenic lines. Furthermore, there was no significant change to sucrose (figure 57D) or hexose (figure 57E) content in any of the transgenic lines at harvest.

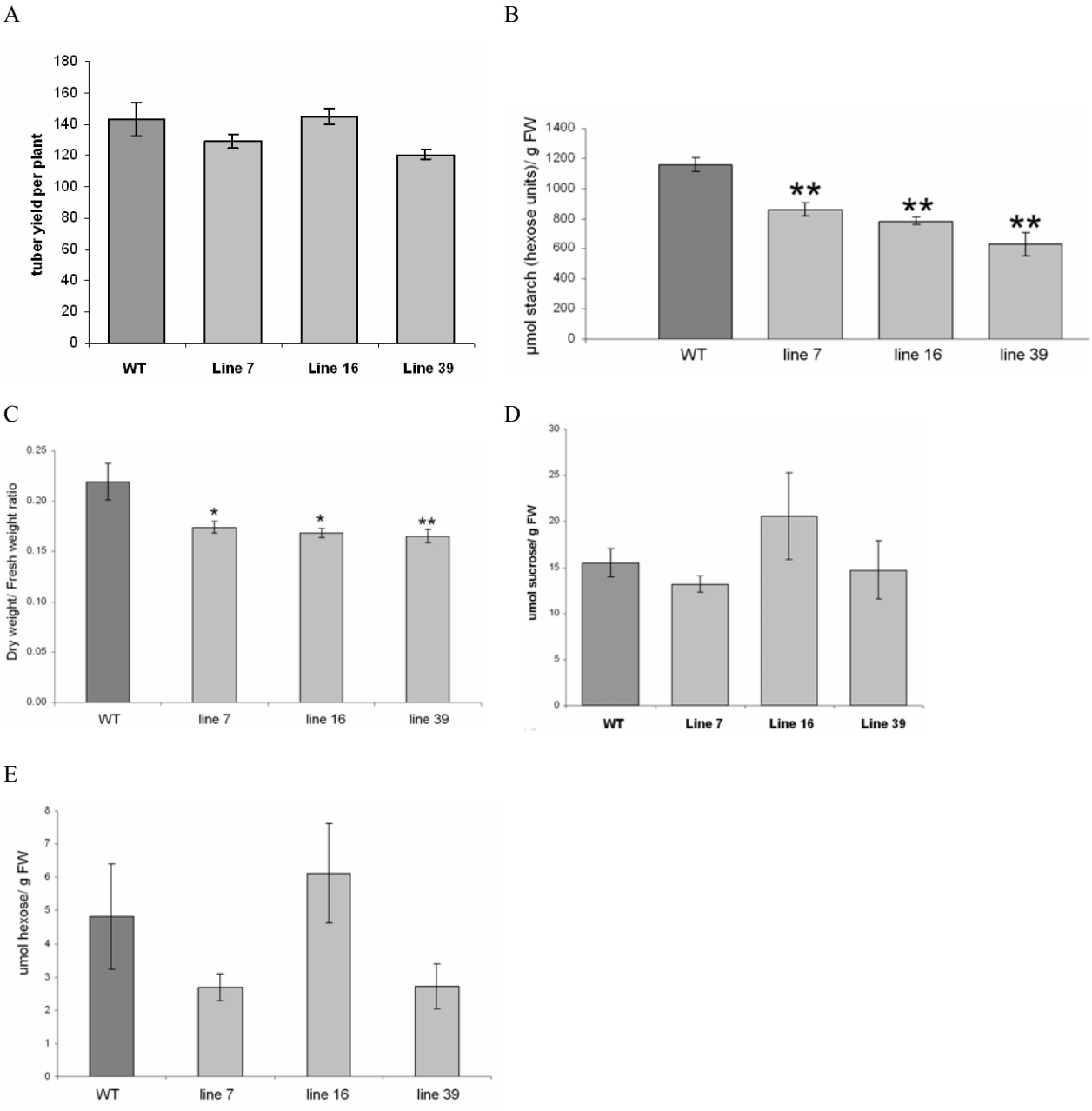


**Figure 57. Tubers at harvest.** A) tuber yield B) starch content C) DW/ FW ratio, D) sucrose content and E) hexose content. Error bars represent standard error (n=4-5). * indicates $p \leq 0.05$ and ** $p \leq 0.01$

### 2.5.3. Sprouting behaviour of transgenic and control plants.

Isoamylase silencing led to a change in sprouting behaviour, with the transgenic lines sprouting earlier than the control. In line 39, visible sprouts appeared after sixty eight

days and 100% sprouting was reached on day eighty five. The other transgenic lines sprouted between days seventy eight and eighty five, with 100% sprouting reached after ninety three days in the weakest line, line 7. For the control line, the first visible sprouts appeared after eighty eight days and 100% sprouting was reached after one hundred and three days (figure 58A and B). Sprouting behaviour was also changed in terms of the number of sprouts per tuber. The transgenic tubers had significantly more sprouts than the control tubers (figure 58C).

A

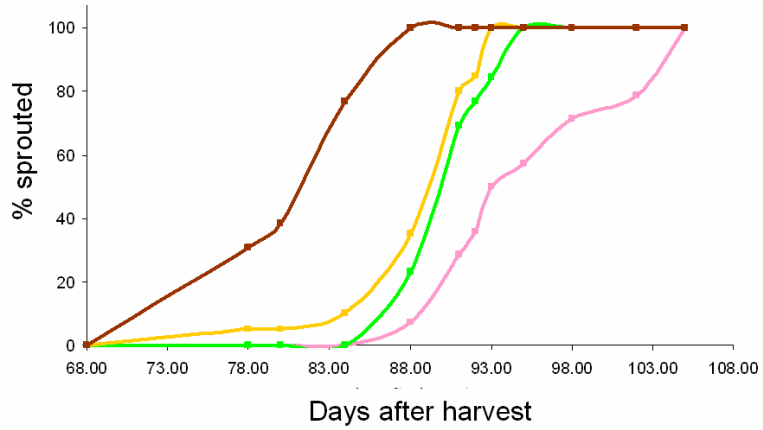


B


C

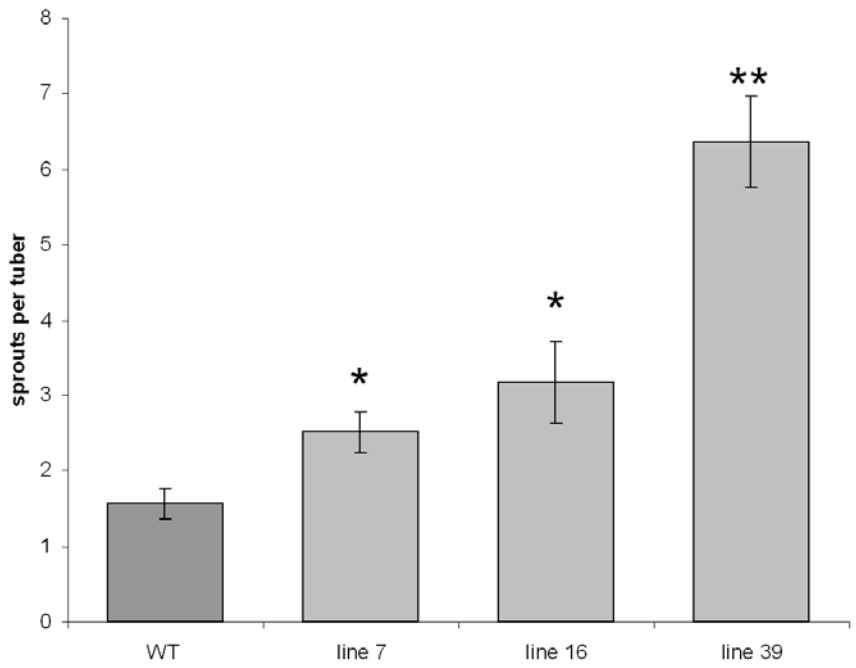


**Figure 58. Sprouting tubers.** A) Sprout kinetic. Line 7 (green), line 16 (yellow), line 39 (brown) and WT (pink). B) Trangenic and control lines showing that the transgenic lines sprout earlier than the WT control (Picture taken ~13 weeks). C) Number of sprouts per tuber. Error bars represent standard error (n=4-5).
* indicates $p > 0.05$ and ** $p > 0.01$

### 2.5.4. Carbohydrate contents of parenchyma around growing sprout

Since potato tubers have ample levels of starch and normally no reduction in starch content during storage can be observed, samples from parenchyma tissue directly associated with a sprout was taken (For sampling method see figure S1) at the time-point when sprouts became visible in the WT. In this tissue there was an increase in sucrose content which correlated with earlier sprouting (figure 59A). Surprisingly, the reduced starch phenotype observed at harvest was greatly diminished at sprouting and only line 39 still had significantly less starch (figure 59B). Earlier studies have shown that reduced ISA1/ ISA2 expression leads to the accumulation of soluble glucans (Bustos et al., 2004). This was also found in our study where soluble glucan content was higher in the transgenic lines at both harvest and sprouting, and increased during storage (figure 59C).

A

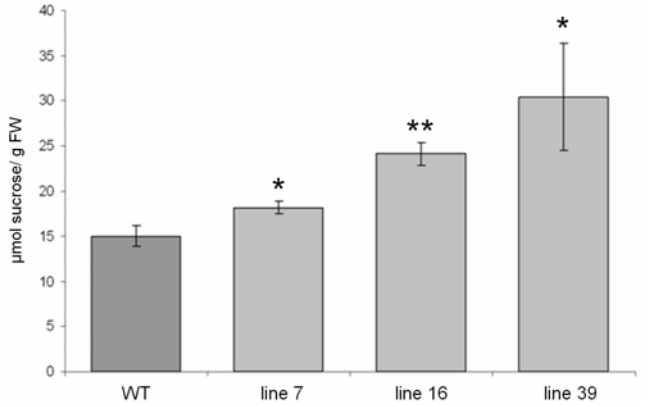


B

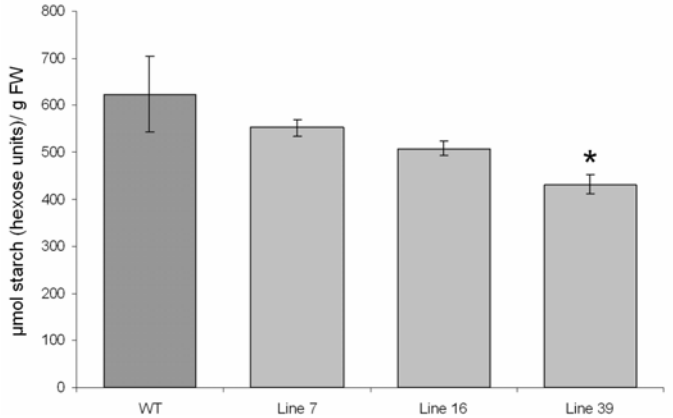


C

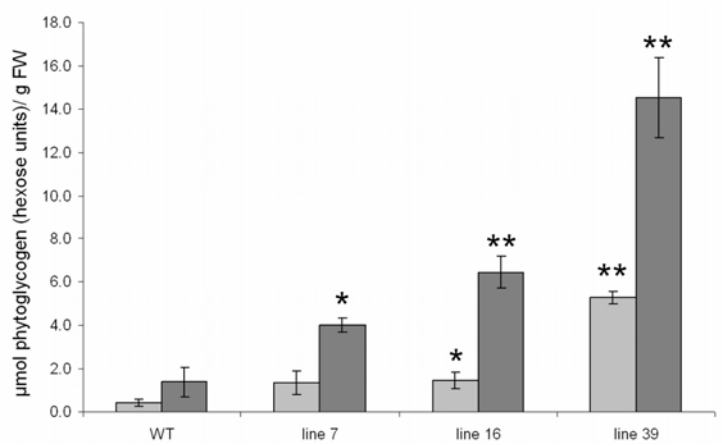


**Figure 59. Carbohydrate contents in parenchyma around growing sprout.** A) Sucrose content and B) starch content. C) Soluble glucan content at harvest (light grey) and parenchyma around growing sprout (dark grey). Error bars represent standard error (n=4-5). * indicates $p > 0.05$ and ** $p > 0.01$

### 2.5.5. Starch granule size and soluble and insoluble glucan structure.

To quantify granule size, starch granules from harvested tubers were isolated, stained with iodine and viewed under the microscope. Micrograph images were taken (figure 60A) and the relative granule size was determined using imaging software, ImageJ (http://rsbweb.nih.gov/ij) (figure 60B). By determining the accumulating percentage of starch granules in terms of granule size from small granules to bigger granules it was

revealed that there is a significant change in starch granule size, with transgenic lines accumulating higher amounts of small granules (figure 60C).

A

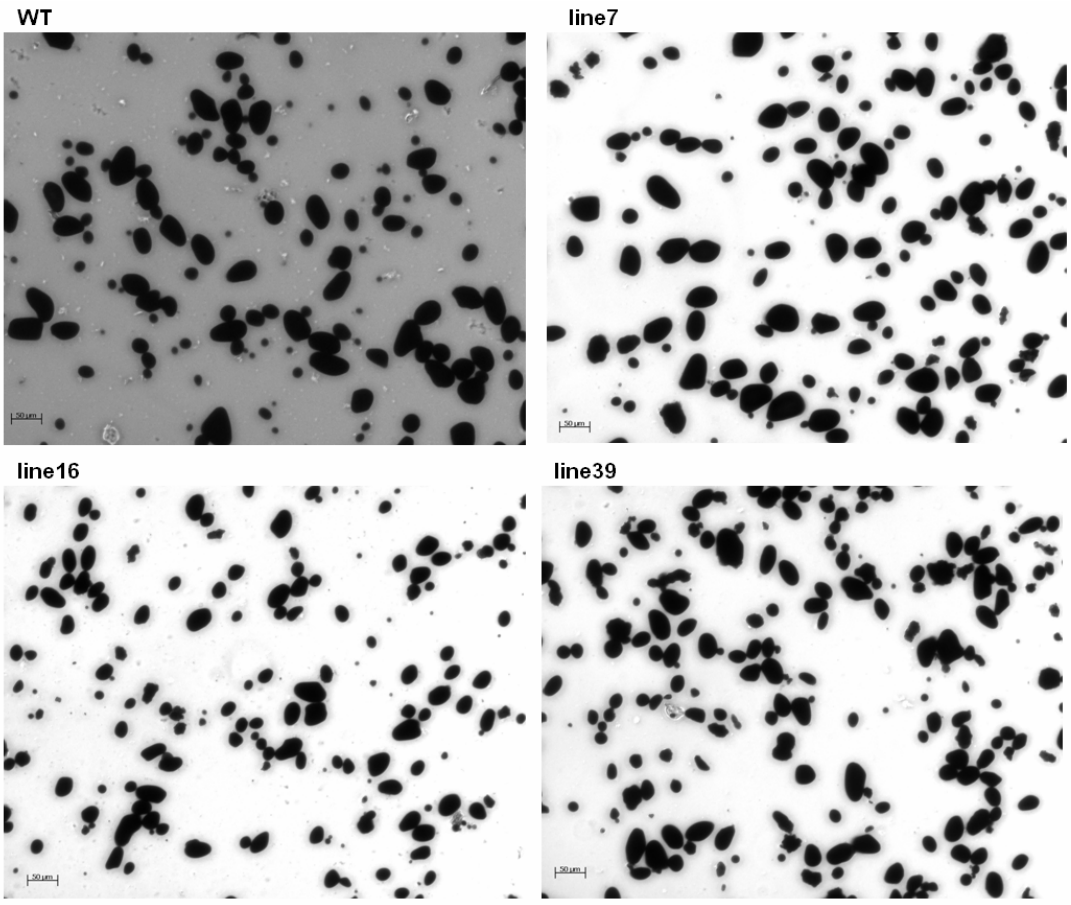

B

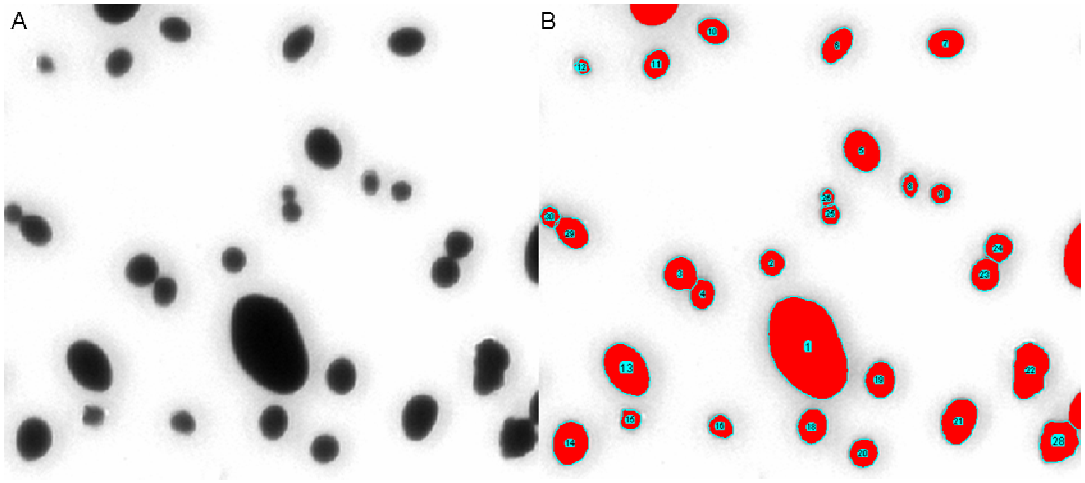


C

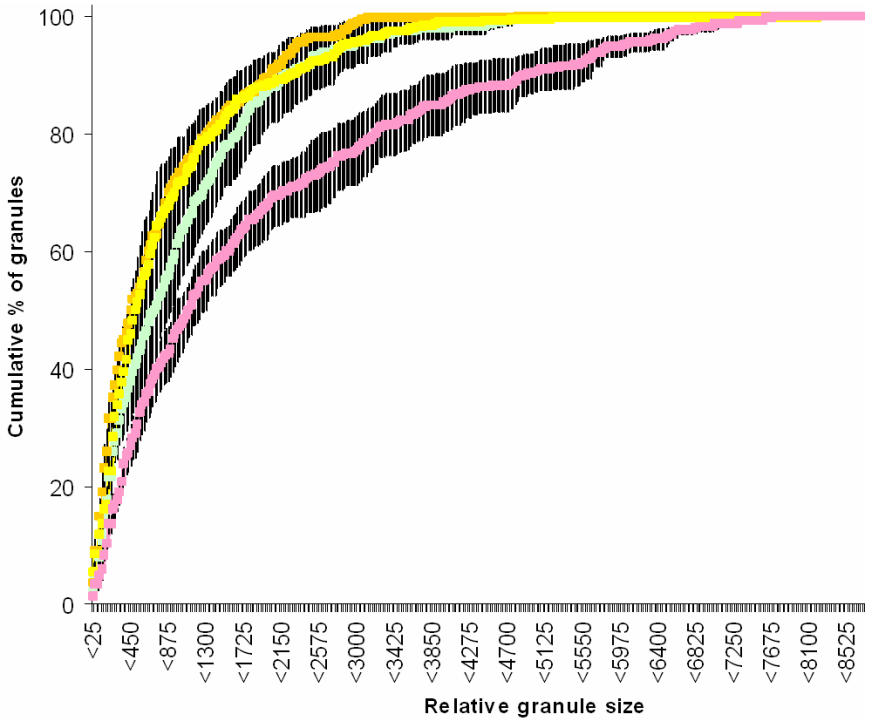


**Figure 60. Micrograph images of iodine stained starch granules.** A) Starch granules derived from tubers of the different genotypes. B) Segmentation of image to determine the relative area of each two dimensional starch granule. The software allows for the manual separation of granules connected to each other in the image. C) Starch granule size distribution. Line 7 (green), line 16 (yellow), line 39 (brown) and the WT control (pink). Error bars represent standard error (n=4-5). Micrograph images were taken by M. Ast, University of Kaiserslautern.

To determine whether the change in granule size was accompanied by changes in glucan structure, the chain length distribution of soluble and insoluble glucan fractions were determined. Structural analysis of the soluble glucans was complicated by the low amounts present in the tubers, meaning that the control samples had to be pooled for the measurements and thus no statistical tests could be performed. There were indications that the structure was affected in two of the lines. In line 39 there seemed to be an increase in shorter chains in samples taken at the time of sprouting in both the parenchyma below the sprout, and also in parenchyma not associated with a sprout. This was also true for line 16 in the parenchyma not associated with the sprout (figure 61).

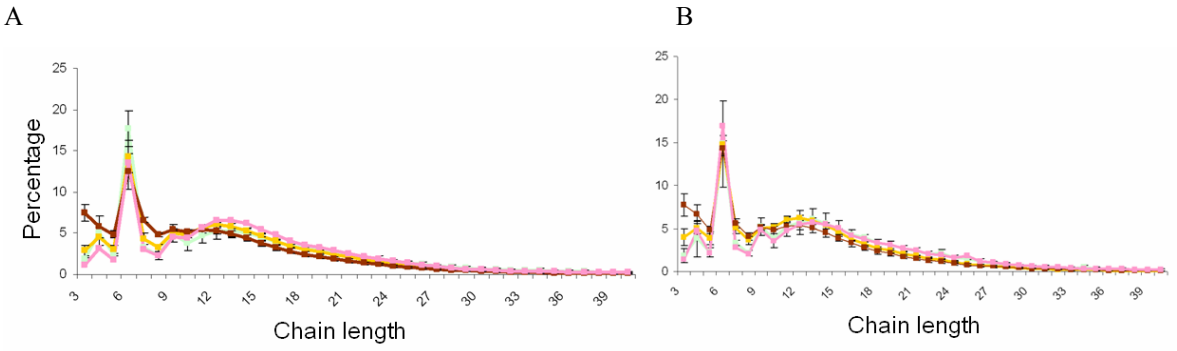


**Figure 61. Relative chain length distribution of soluble glucan.** A) Sprout associated parenchyma and B) parenchyma not associated with a sprout Line 7 (green), line 16 (yellow), line 39 (brown) and the WT control (pink). Error bars represent standard error (n=4-5).

No large differences in the structure of insoluble glucans in any of the time points or tissues analysed could be observed. However, in all three tissues/ time points analysed, there were indications of an increase in shorter chains in line 39 (figure 62).

A

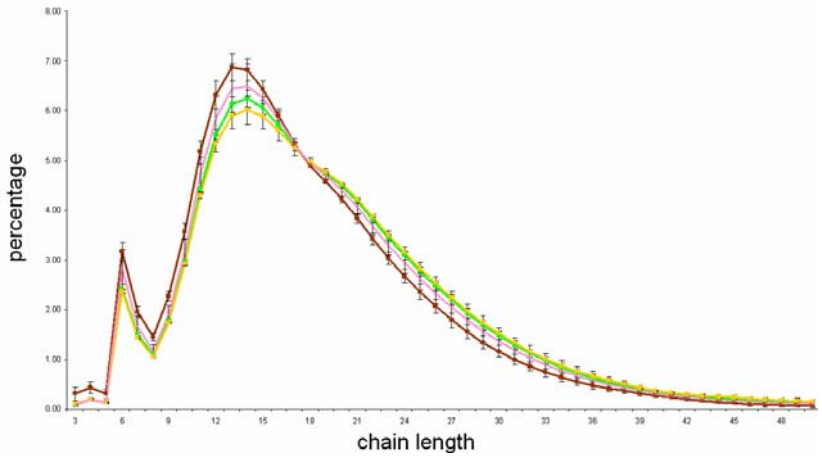


B

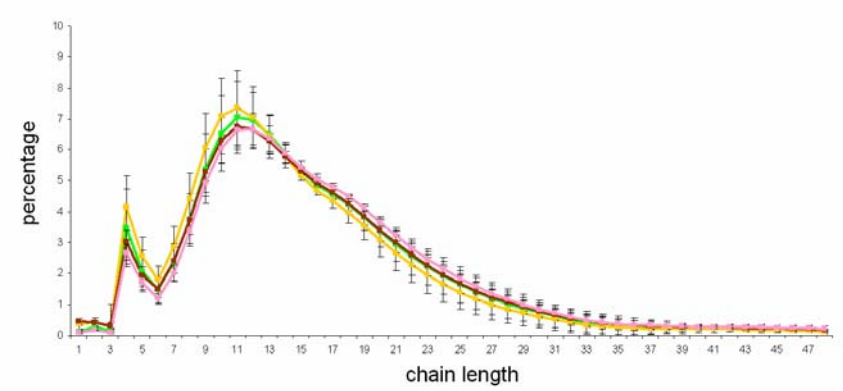


C

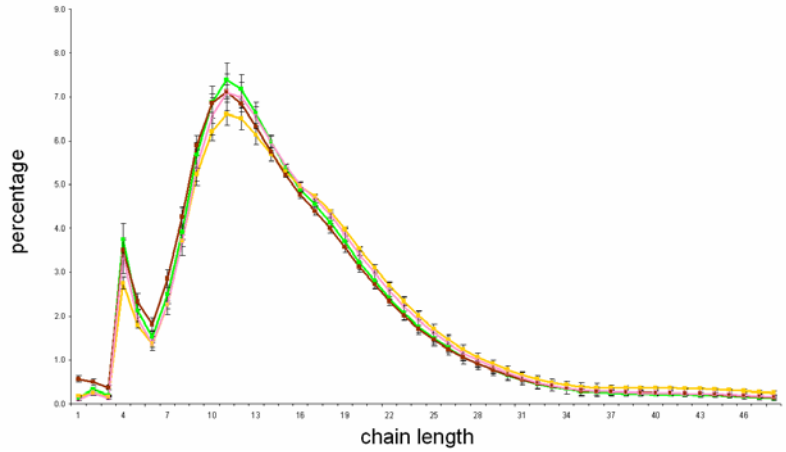


**Figure 62. Relative chain length distribution of insoluble glucan.** A) harvest, B) Parenchyma not associated with the sprout and C) Parenchyma associated with the sprout. Line 7 (green), line 16 (yellow), line 39 (brown) and the WT control (pink). Error bars represent standard error (n=4-5)

## 2.6. Identification and RNAi silencing of alpha-amylase 23 in potato.

The aim of this work was to identify, through microarray data analysis, starch degradation associated genes involved in potato tuber sprouting. Here the identification of a gene, annotated as an alpha-amylase, which was strongly up-regulated at the time of sprouting during the sprout release assay (Hartmann et al., 2011) is shown. The gene was targeted by RNAi and the results are shown.

### 2.6.1. Identification and RNAi silencing of alpha-amylase 23

As mentioned, very little is known about the molecular mechanisms and enzymes involved in starch degradation in potato tubers. This is despite the known negative economic impact of starch degradation during long term storage. In order to identify genes involved in starch degradation under these conditions, expression profiles from tuber discs where sprouting was artificially initiated (Hartmann et al., 2011) was studied. An interesting expression profile was observed for micro.10377.c1, annotated as an alpha-amylase, and was further investigated. The gene was up-regulated at the time of visible tuber sprouting, potentially playing a role in starch mobilisation required for sprout growth (figure 63).

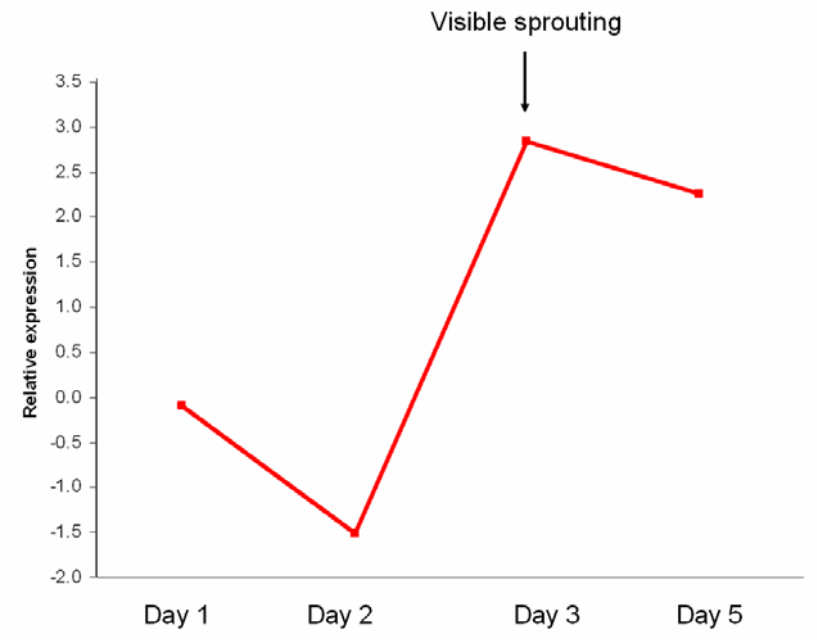


**Figure 63. Relative expression of micro.10377.c1 during the sprout release assay (Hartmann et al., 2011).**

Blast™ results indicated that the EST was derived from alpha-amylase 23 (Genbank accession M79328). To determine the closest homolog of alpha-amylase 23 in Arabidopsis, a phylogentic tree based on the amino acid sequences was created and revealed alpha-amylase is closely related to Arabidopsis alpha-amylase 2 (AAMY2) (figure 64).

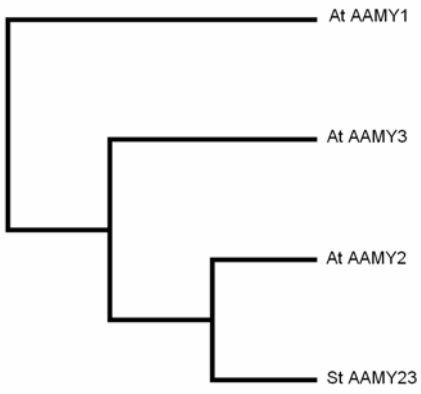


**Figure 64. Phylogenetic tree based on the amino acid sequences of alpha-amylase 23 and Arabidopsis alpha-amylases**. Alpha-amylase 23 from potato (St AAMY23, Accession number AAA91884); and the three alpha-amylases from Arabidopsis, alpha-amylase 1(At AAMY1, accession number AT4G25000), alpha-amylase 2 (At AAMY2, accession number AT1G76130) and alpha-amylase 3 (At AAMY3, accession number AT1G69830). The tree was created using the Geneious™ tree builder.

Arabidopsis AAMY2 is predicted not to have a transit peptide (Yu et al., 2005) and prediction software (SignalP, www.cbs.dtu.dk/services/SignalP) indicated that this is also true for potato alpha-amylase 23. The prediction software, however, did predict a signal peptide.

### 2.6.2. RNAi silencing of alpha-amylase 23.

To study the function of alpha-amylase 23, an RNAi construct targeting the gene was designed and subsequently used for potato transformation (figure 65A). After transformation and regeneration of transgenic plants, total RNA was extracted from leaf material. Northern blot analysis revealed the successful silencing of the gene in several transgenic lines, and lines 12, 15 and 18 were selected for subsequent studies (figure 65B).

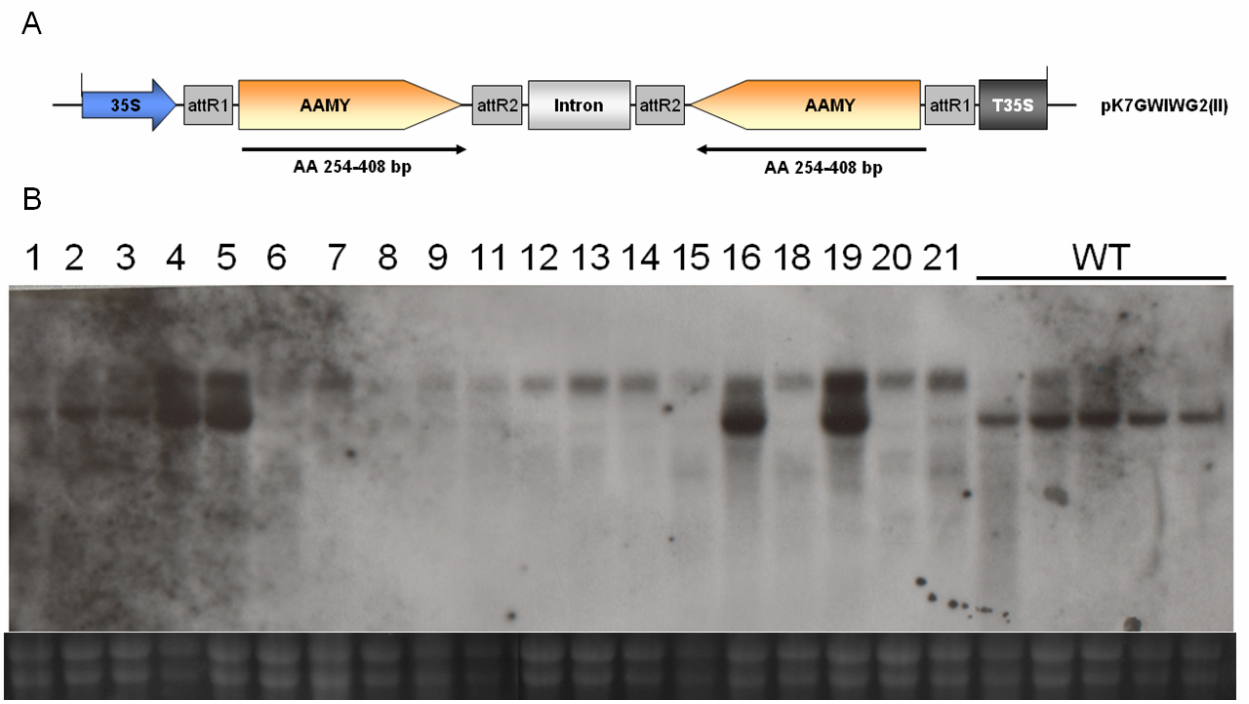


**Figure 65. RNAi silencing of alpha-amylase in potato.** A) RNAi construct for the silencing of alpha-amylase 23 in potato. B) Northern hybridisation showing the successful silencing of alpha-amylase 23. Lines 12, 15 and 18 were selected for further experiments.

### 2.6.3. Metabolic and analysis of tubers at harvest.

Samples taken from tuber material at harvest showed that starch, sucrose, glucose and fructose content were not significantly altered at harvest and there was also not a significant change in tuber yield. There were indications of an increase in the number of tubers, but this was not consistent over three harvests in all the lines (figure 66).

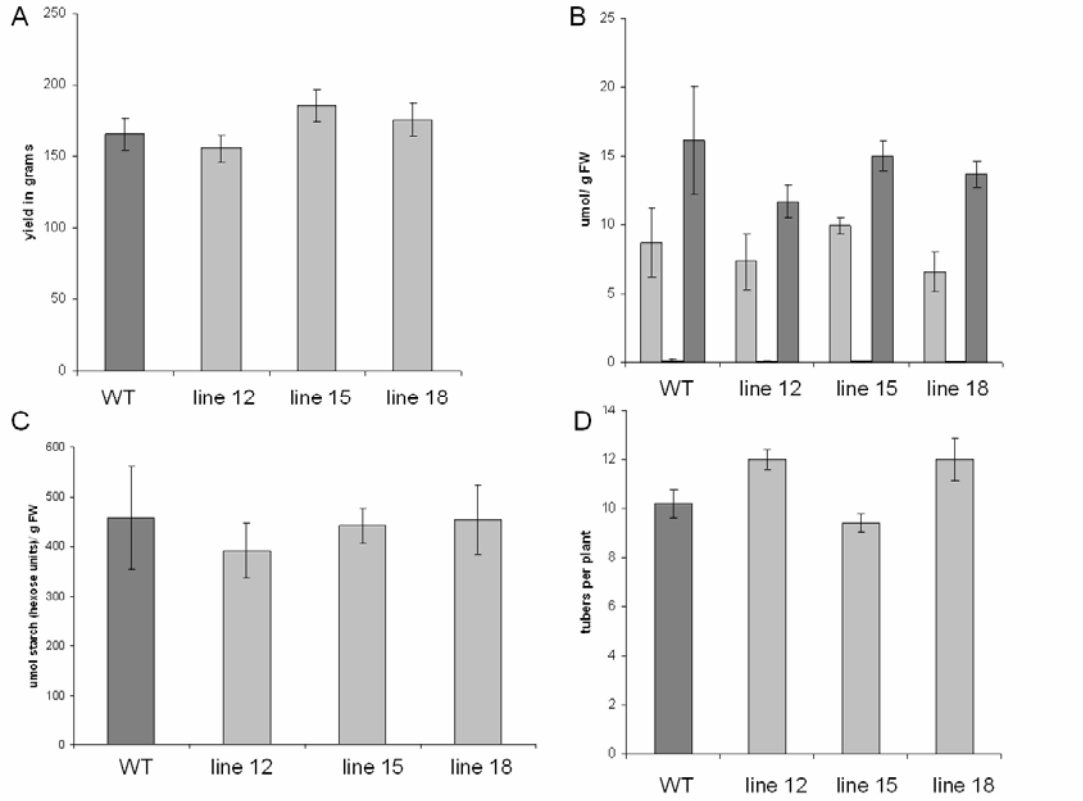


**Figure 66. Transgenic and WT tubers at harvest.** A) Tuber yield, B) Levels of major soluble sugars. Glucose (light grey), Fructose (black) and Sucrose (dark grey). C) Starch content and D) number of tubers per plant. Error bars represent standard error (n = 4-5).

### 2.6.4. Analysis of reduced alpha-amylase 23 expression on tuber sprouting

Transgenic tubers sprouted later than the wild type control. The control lines had the first visible sprouts ninety-two days after harvest and 100% sprouting was reached after one hundred and five days. Lines 12 and 15 showed that first visible sprouts between ninety-two and ninety five days after harvest and reached 100% sprouting at one hundred and sixteen and one hundred and twelve days respectively. Line 18 started sprouting after one hundred and three days and reached 100% sprouting after one hundred and twenty days

(figure 67A and C). The delay in sprouting was accompanied by a significant reduction in the accumulation of glucose in the parenchyma tissue associated with a sprout (figure 67B) (for sampling method, see figure S1). These samples were taken at the time when the wild type sprouted and provides strong evidence that the delay in sprouting is due to a reduction in the rate of starch breakdown. Surprisingly, this was not the case for sucrose which had a similar content to the wild type (figure 66D).

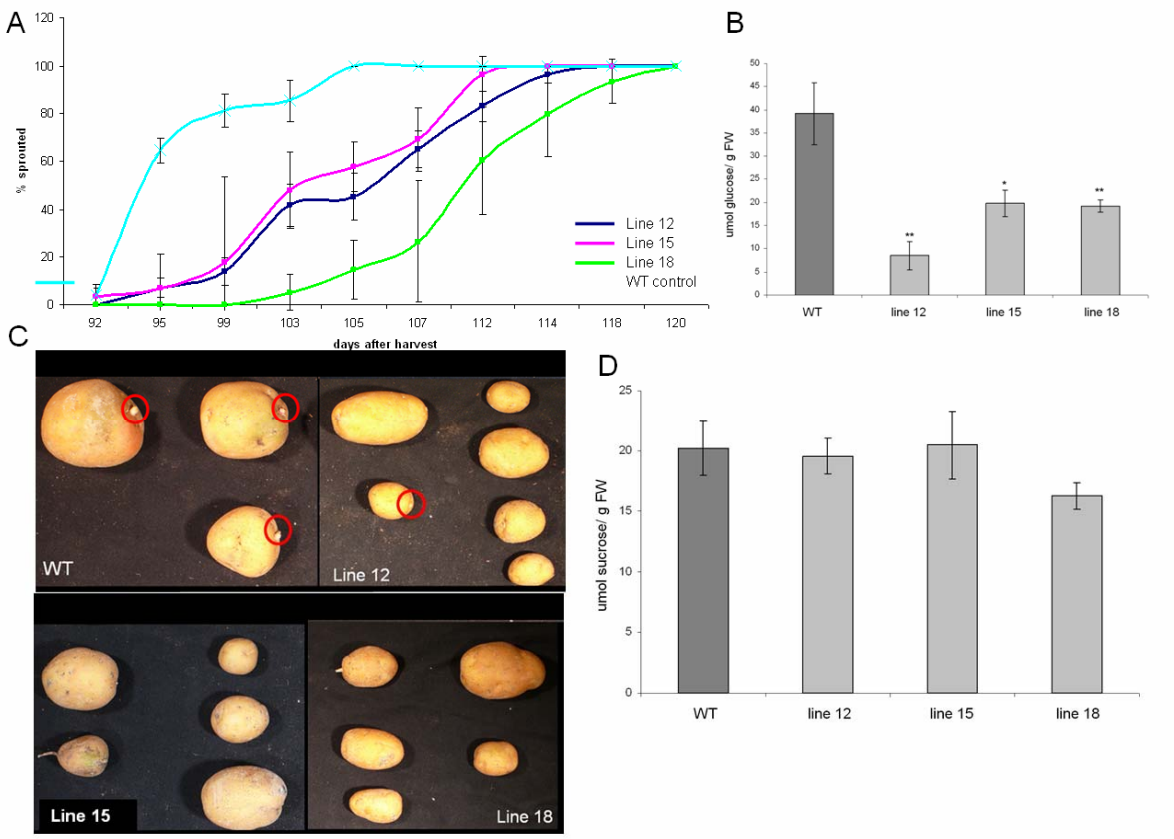


**Figure 67. Tuber sprouting and the accumulation of glucose in the parenchyma associated with a sprout.** A) Figure indicating the delay in sprouting in transgenic line. WT (light blue), line 15 (pink), line 12 (dark blue) and line 18 (green). B) Glucose content of parenchyma associated with a growing sprout. Error bars represent standard error (n=4-5). * indicates p-≤ 0.01 and ** p -≤ 0.001. C) Picture showing the delay in sprouting in the transgenic line (Picture taken one hundred days after an independent harvest ). D) Sucrose content of parenchyma associated with a growing sprout. Error bars represent standard error (n=4-5).

### 2.6.5. Effect on cold induced sweetening.

To determine whether this apparent reduction in the rate of starch degradation also had an influence on cold induced sweetening, potato tubers were stored at 8°C for two weeks.

This showed that in the transgenic lines there was indeed a significant reduction in the accumulation of hexoses, providing further evidence for the involvement of alpha-amylase 23 in tuber starch degradation (figure 68).

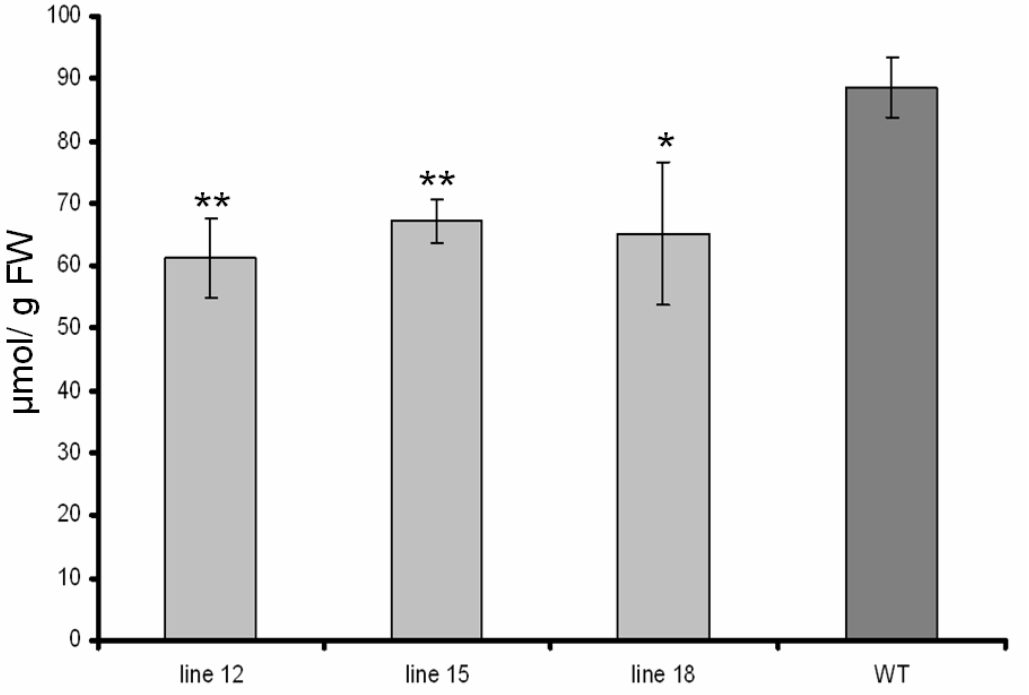


**Figure 68. Accumulation of hexoses under cold conditions.** Error bars represent standard error (n=4-5). * indicates $p \leq 0.01$ and ** $p \leq 0.001$

## 3. Discussion

### 3.1. Comparative transcriptome analysis coupled to X-ray CT reveals sucrose supply and growth velocity as major determinants of potato tuber starch biosynthesis.

#### 3.1.1. Starch biosynthesis in potato leaves follow carbohydrate accumulation and show similarities to tuber starch biosynthesis.

The similarities in gene expression patterns of the same isoforms suggests that starch biosynthesis in leaves and tubers are remarkably similar. This is despite the fact that in leaves hexose phosphates and ATP, needed for starch biosynthesis, is derived from the calvin cycle, and in tubers from imported glucose 6-phosphate and ATP. In leaves, and tubers, there was strong regulation of both GPT2 and NTT, the transporters responsible for glucose 6-phosphate and ATP transport, respectively (Zhang et al., 2008). This hinted towards their possible involvement in source leaf starch biosynthesis. However, not all cell types in leaves are photosynthetically active and to rule out that the observed expression of GPT and NTT in leaf extracts was due to contaminating epidermis cells, which contains almost no chloroplasts, cell-specific RNA analysis was performed. The results, which showed epidermal tissue contributed very little to the observed expression pattern, supports the hypothesis that GPT and NTT might indeed be required for starch biosynthesis in photosynthetic tissue. However, other cell types such as companion and bundle sheath cells could still contribute to the observed expression pattern. It can also not be excluded that the transporters are exporting substrates from the plastid.

Most of the starch synthase genes analysed had the expected expression pattern of increasing with the accumulation of carbohydrate in both leaves and tubers. This was not the case for granule bound starch synthase (GBSS) in leaves where expression was highest two hours into the day. Smith et al. (2004) argue and provide evidence that since the enzyme is present within the granule, the protein is degraded together with starch at

night and must very quickly be re-synthesised in the morning. In tubers, starch synthase IV (SSIV) expression was the highest in stage 1 of tuber induction, after which expression declined, fitting with its proposed role in starch granule initiation (Roldán et al., 2007; Szydlowski et al., 2009).

### 3.1.2. Diurnal oscillation of GBSS in potato tubers can be linked to differences in sucrose supply.

It is known that starch biosynthetic genes are diurnally regulated by several factors, with sucrose and the circadian clock seemingly being the most important. Bläsing et al. (2005) showed that between 30-50% of genes in Arabidopsis rosettes show diurnal changes in their transcripts and that this was especially true for genes involved in redox regulation, nutrient acquisition and assimilation, and starch and sucrose metabolism. Comparative analysis of nutrient feeding and diurnal transcription profiles indicate that sugars make a major contribution to diurnal regulation. Furthermore, Osuna et al. (2007) analysed gene expression in carbon-deprived Arabidopsis seedlings after the addition of sucrose. Genes involved in central carbon metabolism, and more specifically starch biosynthesis, showed a response to sucrose and this did lead to an increase in starch content. This was also shown in our study when leaf discs were floated on sucrose in darkness. A second major regulator of diurnal gene expression seems to be the circadian clock. Bläsing et al. (2005) identified a subset of 373 genes known to be circadian regulated (Harmer, 2000). The gene set was used in a principle component analysis which showed that sucrose and the circadian clock are the predominant factors in regulating diurnal gene expression and that light, nitrogen and water deficiency makes a smaller contribution. Starch degradation related genes also have a strong diurnal rhythm in Arabidopsis which was maintained under continuous light, but not continuous darkness (Lu et al., 2005).

As mentioned, sucrose and the circadian clock seem to be important regulators of diurnal gene expression and this is especially true for GBSS. Tenorio et al. (2003) showed that GBSS is strongly regulated by the circadian clock and that expression is markedly lower in mutants lacking clock genes LHY and CCA-OX respectively. In a detailed study done

on GBSS in snapdragon (*Antirrhinum majus*) it was shown that GBSS is diurnally regulated in leaves even under continuous light and it was concluded that the regulation is due to the circadian clock. This was not the case in snapdragon roots though, where expression was the same in the middle of the day and in the middle of the night (Merida et al., 1999). Also, in rice leaves GBSS continues its diurnal cycling under continuous light suggesting circadian regulation, but expression can be induced by nitrogen starvation or sucrose feeding and repressed by darkness, indicating the importance of sucrose in its regulation (Dian et al., 2003). Moreover, sucrose floating experiments with potato leaves show that GBSS expression can be induced by sucrose (Visser et al., 1991). This increase, as well as the increase of other starch biosynthetic genes, was confirmed by microarray analysis of tuber leaves floated in sucrose.

Our results show that GBSS expression in tubers can be linked to diurnal changes in sucrose supply from the source, although caution should be exercised in the interpretation of the significance of this in terms of enzyme activity. As mentioned earlier, the level of GBSS protein does change substantially during the day in Arabidopsis leaves and the reason for this is probably the location of GBSS within the granule (Smith et al., 2004). This is also true for algae *Chlamydomonas reinhardtii* suspension cultures where GBSS expression and enzyme activity correlates with starch levels. The authors state that the correlation is probably due to the fact that the analysis was conducted in suspension cultures, where new cells are produced constantly leading to continuous production of new GBSS protein (Ral et al., 2006). This however is not necessarily true for GBSS in other tissues or for other enzymes of starch biosynthesis and several studies have shown that diurnal changes in expression do not lead to changes in protein levels (Geigenberger and Stitt, 2000; Lu et al., 2005). However, it still remains an interesting finding that GBSS expression in tubers follows a diurnal rhythm which declines when sucrose supply from the leaves are reduced.

### 3.1.3. Starch biosynthetic gene expression is influenced by tuber growth velocity

Since tuber initiation and growth rates are not synchronised, it was important to determine the growth velocity of individual tubers. To this end X-ray CT was used to determine the volume of individual tubers at different time points and calculate the growth velocity. This is, to our knowledge, the first time that the growth velocities of tubers were determined in a natural environment. Growth velocity could not be directly correlated to the expression of starch biosynthetic genes, but changes between growing and non-growing tubers could be observed. This would suggest that the relationship between growth velocity and starch biosynthetic gene expression is qualitative rather than quantitative. To determine which processes are correlated to growth velocity, functional group enrichment analysis was performed of features positively or negatively correlating to growth velocity. As would have been expected, cell wall- and starch metabolism and storage protein associated processes did positively correlate to growth velocity. It was slightly surprising that there was also an enrichment of energy metabolism associated transcripts, possibly due to generally higher metabolic activity in faster growing tubers. These data indicate that tubers that look visually similar have large differences in gene expression depending on their growth stage.

## 3.2. The mode of sucrose degradation determines the fate of assimilates.

As mentioned, one of the major aims of this work was to elucidate the metabolic pathways and signals responsible for the increase in respiration at the expense of starch biosynthesis in U-IN-2. Here the results obtained from transcriptional and metabolic analysis of various transgenic lines is discussed in the context of U-IN-2.

### 3.2.1. Global analysis reveals that over expression of apoplasmic or cytosolic invertase leads to very different metabolite and transcript patterns.

In two separate principle component analyses used to determine the global relationship between the transcription profiles of either U-IN-1, U-IN-2 and the Desireé control; or CW-ISO, NTTP and Solara control, the genotypes could be clearly separated using either the individual replicates, or the mean expression values for each genotype. These findings

are in disagreement with earlier reports which stated that it was not possible to separate genotypes using transcript profiling (Urbanczyk-Wochniak et al., 2003). The platform used for the transcriptional analysis in the study by Urbanczyk-Wochniak et al. (2003) was not as extensive as the POCI platform used here, making the current study more sensitive, which is probably the reason for the better separation. Metabolic analysis of U-IN-2 revealed no significant change in total free amino acid contents, which is in contrast to earlier studies (Trethewey et al., 1998; Farre et al., 2008). Possible reasons for this could be differences in growth and fertilisation conditions. The time of sample taking would probably have a big effect on amino acid contents. As mentioned, respiration in U-IN-2 accelerates during storage, which would mean an increase in activity of glycolysis and the TCA cycle, leading to higher production of amino acids over time.

The fact that photosynthetic transcripts were reduced U-IN-1 is somewhat perplexing. A reason could of course be light contamination of the control tubers, but this is highly unlikely. Large pool sizes were used and no material from the tuber surface area was taken for RNA extractions. Metabolite analysis also did not reveal a significant increase in ribulose 1,5 bisphosphate, which could be seen as a marker metabolite for Calvin cycle activity . Also, photosynthetic transcripts were not severely altered in U-IN-2, which was compared to the same control, indicating that the relative reduction in photosynthetic gene expression in U-IN-1 is not due to an increase in the control. It would indicate that genes associated with photosynthesis are expressed in heterotrophic tissue. A reason for the reduced expression in U-IN-1 could be the increase in glucose in the apoplasmic space, which is known to inhibit photosynthetic gene expression (Heineke et al., 1992). Other processes regulated in U-IN-1 could also be explained by the increase in apoplasmic glucose. For instance, glucose feeding of tobacco leaf discs lead to accelerated senescence (Wingler, 1998), suggesting that expression of senescence associated genes might be regulated by sugar signals. This hypothesis is further supported by the observation that silencing of cell-wall invertase in tomato leaves resulted in a significantly increased sucrose to hexose ratio in the apoplasmic space and a delay in senescence (Kocal et al., 2008). In Arabidopsis it has been shown that senescence leads to the degradation of microtubules (Keech et al., 2010), explaining the reduction in gene

expression associated with the cytoskeleton. It is worth mentioning that these changes were not observed in U-IN-2, providing evidence that the signal causing these changes must be extracellular.

In addition to the finding in U-IN-1, analysis of expression profiles from CW-ISO and NTTP revealed an increase in the expression of genes associated with photosynthesis. Similar to what was observed in U-IN-1, metabolite analysis also did not reveal a significant change in ribulose 1,5 bisphosphate. Thus, it does seem that photosynthetic gene expression in tubers can be altered without the presence of photosynthetic activity, possibly due to misinterpretation of sugar signals. In sugarcane, ubiquitous vacoular expression of sucrose isomerase (Wu and Birch, 2007) led to an increase in photosynthesis which led to an increase in total carbohydrate content without any yield penalty. The authors argued that the increase was due to increased sink strength, which is widely accepted to determine sugarcane yield (McCormick et al., 2006). Our findings indicate though that it cannot be excluded that sucrose isomerase expression in leaves had a direct effect on photosynthesis. However, in an earlier study where sucrose isomerase was expressed in tobacco leaves (Börnke et al., 2002), there was no change in the expression of ribulose 1,5 bisphosphate carboxylase/oxygenase small subunit (rbsC), and it was concluded that sucrose isomerase expression does not have an effect on photosynthesis associated gene expression in leaves.

A likely explanation for the observed increase in expression of photosynthesis associated gene expression could be a response to sugar starvation, since the trehalulose produced cannot be metabolised. A similar finding has been documented in Arabidopsis dark-grown suspension cells, where there was increased expression of chlorophyll a/b-binding protein and genes from photosystem I and II, upon sucrose starvation (Contento et al., 2004). The authors stated that the increased expression of photosynthetic genes is an attempt by the plant to overcome sugar starvation, despite the suspension cultures being non-photosynthetic. Although our observations of altered photosynthetic gene expression in tubers needs to be verified from independent samples to exclude the possibility of it being an artefact of light contamination, it is very likely that the changes are due sugar

starvation. Further evidence that the sucrose isomerase expressing lines, but CW-ISO in particular, is trying to overcome sucrose starvation is the general increase in expression of starch degrading genes.

### 3.2.2 Alterations in substrate supply changes cell wall and fatty acid biosynthesis.

To further enhance our understanding of what happened in U-IN-1 and U-IN-2, pathway specific analysis of transcripts and metabolites were performed using Mapman software (Thimm et al., 2004). The first pathways analysed were cell wall and fatty acid biosynthesis, since global analysis revealed a down-regulation of transcripts associated with these in both U-IN-1 and U-IN-2. Reduced expression of cell wall biosynthesis associated genes would be in line with reduced production of UDP-glucose by Susy. It would be expected that cell wall biosynthesis is also active during stolon growth and meristematic activity, a time when Susy activity is low. The observation that a Susy isoform, normally associated with stolons (Ferreira et al., 2010), is active in U-IN-2 would suggest that this isoform of Susy is active specifically under these conditions, producing the required UDP-glucose. In U-IN-2 this is probably not very successful considering the high invertase expression levels reached with the B33 promoter (Sonnewald et al., 1997; Hajirezaei et al., 2000), and invertase's much lower $K_m$ for sucrose (Avigad, 1982). The increase in expression of MI-1PS, the rate-limiting enzyme in the myo-inositol pathway (Loewus and Loewus, 1980; Loewus et al., 1980), and cytosolic PGM and UGPase, would also suggest the activation of an alternative pathways for the production of UDP-glucuronate and UDP glucose, respectively.

In constrast to U-IN-1 and U-IN-2, there was an increase in the expression of genes associated with cell wall biosynthesis in CW-ISO and NTTP. There was also increased expression of Susy 4, the major isoform in tubers (Zrenner 1995, Ferreira 2010 Fu and Park 1995), accompanied by a significant increase of fructose in both sucrose isomerase expressing lines. This might indicate that there is an increase in Susy activity, producing UDP glucose, used for cell wall biosynthesis, and fructose, which accumulates in the cell. Comparing the expression in NTTP to that of CW-ISO also clearly showed that the

observed changes were more pronounced in CW-ISO, as was shown in the functional group enrichment analysis. Apart from misinterpretation of sugar signals it is not clear why there would be an increase in expression of Susy4 in CW-ISO and NTTP.

Global analysis revealed a reduction in fatty acid metabolism associated genes in U-IN-1 and U-IN-2, and closer investigation of the fatty acid biosynthetic pathway strengthened this argument. It has been proven beyond reasonable doubt that all the Acetyl-CoA in the plastid is produced there, since it cannot be transported across the plastid membrane (Kohlhaw and Tan-Wilson, 1977; Patel and Clark, 1980; Rangasamy and Ratledge, 2000). The reduction in fatty acid biosynthetic gene expression, despite increased levels of PEP, would indicate that the pool of PEP is not available for Acetyl-CoA synthesis in the plastid.

### 3.2.3. Although specific changes are associated with apoplasmic or cytosolic invertase, high invertase activity seemingly reduces starch biosynthetic capacity.

Based on a global inspection of functional groups there was no obvious change in gene expression related to starch metabolism. There was, however, a strong enrichment of storage protein related transcripts amongst the most-down regulated features in U-IN-2, a process closely associated with starch accumulation (Zrenner et al., 1995), and metabolic data from this and previous studies show that there was a reduction in starch content in U-IN-2. The regulation of invertase gene expression and activity differs greatly between isoforms (Roitsch and González, 2004), with some being activated through a feed-forward mechanism by glucose (Roitsch et al., 1995), which would explain the observed increase. It is however surprising that there was so much difference in the regulation between the two genotypes, showing that the response to glucose for some genes requires the signal to come from outside the cell, similar to what was discussed earlier.

Glucose 6-phosphate (G6P), the metabolite imported into the plastid for starch biosynthesis, can be produced from all three products of sucrose degradation. Under normal conditions, Susy activity is correlated to the rate of starch biosynthesis in potato

tubers (Zrenner et al., 1995). Thus, G6P produced from fructose via fructokinase and phosphoglucose isomerase, and from UDP-Glucose, via UDP-Glucose pyrophosphorylase and cytosolic phosphoglucomutase, would be the primary route. In U-IN-1 and U-IN-2 reduced production of UDP-Glucose would mean that another pathway for starch biosynthesis should be activated, or at least increased, and that is via the phosphorylation of glucose by hexokinase. This is indeed the case with hexokinase 5 expression strongly increased in U-IN-2. Sequence similarity to hexokinase 5 from tobacco indicated that it is most probably bound to the mitochondrial membrane (Giese, 2004).

Reduced expression of fructokinase 2 in U-IN-1, one of the most important isoforms in tubers could be explained by the increase in fructose, which is known to be a strong inhibitor of fructokinase (Renz and Stitt, 1993). The product of fructokinase, fructose 6-phosphate (F6P) also serves as an inhibitor of fructokinase activity, a possible reason for slightly reduced expression of fructokinase 2 in U-IN-2. The reduction in expression of fructokinase 3, which in Arabidopsis and tomato has been shown to be located in the plastid (German, 2004; Damari-Weissler et al., 2006) provides further evidence for reduced substrate supply to the plastid. It should be mentioned though that in an earlier study an increase in fructokinase activity in U-IN-2 was found, with no change in U-IN-1 (Hajirezaei et al., 2000), whilst a second study found no significant reduction in fructokinase activity in U-IN-2 (Junker et al., 2004). Not only does this point to the high variability of fructokinase activity in tubers, but also that caution should be exercised when interpreting expression data and its correlation to actual enzyme activity.

G6P and glucose 1-phosphate (G1P), although not present in equal amounts, normally show a constant ratio since cytosolic phosphoglucomutase catalyses a freely reversible reaction (Kossmann and Lloyd, 2000; Periappuram et al., 2000). The fact there was an imbalance in the ratios of these metabolites would indicate that the G6P is not present freely in the cytosol where it can be converted to G1P. After the production of G6P it must be imported into the plastid, and this occurs via the glucose-6-phosphate transporter, or GPT. In both genotypes there was a strong reduction in the expression of GPT, which

points to a reduced ability to transport G6P to the plastid. This was despite a significant increase in G6P content in U-IN-2 and could be a result of signalling mechanisms blocking GPT transport under specific conditions. As mentioned, there is evidence that in potato G1P can also be transported to the plastid (Fettke et al., 2010), but since the transporter has not yet been identified it is not possible to determine its importance, even at transcriptional level.

Both GPT and Susy positively correlate with storage metabolism, while invertase expression is associated with energy metabolism. Therefore, it was speculated that GPT expression would negatively correlate with invertase expression. This was indeed the case with a strong negative correlation observed between GPT2 and cell wall invertase in comparative transcriptome analysis from tubers under various conditions and genotypes. Aiming to identify possible regulators, genes showing a positive correlation to either invertase or GPT expression were identified. Amongst the genes positively correlating to invertase, several transcription factors could be identified. These include auxin response factor 2 (ARF2) and one ABA-response element binding factor (AREB-like protein). In Arabidopsis ARF2 has been suggested not to function within the auxin signalling pathway but to act as negative regulator of cell growth and senescence (Okushima et al., 2005). Amongst others Arabidopsis mutants lacking expression of ARF2 are characterised by a significantly delayed senescence. Hence, elevated expression of ARF2, especially in U-IN-1 tubers, might explain partly the observed induction of senescence associated genes and possibly acts as negative regulator of GPT. Ectopic expression of SlAREB1, the closest homolog to the identified AREB-like protein, in tomato fruits revealed its involvement in regulating sugar metabolism during fruit development (Bastías et al., 2011). Transgenic fruits expressing SlAREB1 were characterized by increased hexose contents and increased expression of vacuolar invertase. Assuming a similar function in potato tubers, increased expression of the AREB-like protein could be involved in stimulating invertase expression.

It does appear from our transcription data that the reason, or at least part of the reason, for reduced starch content in U-IN-2 is that the G6P available cannot be imported to the

plastid, as stated in an earlier study (Farre et al., 2008). Farre et al. (2008) could show by subcellular fractionation experiments that in both invertase expressing genotypes, but especially in U-IN-2, the ratio of cytosolic to plastidial pools of G6P was increased. Interestingly, searching for GPT co-regulated genes did not reveal any transcription factor. However a number of starch associated genes showed a strong co-regulation to GPT. These included the plastidic ATP/ADP translocator (NTT) (Tjaden et al., 1998), plastidial phosphoglucomutase (pPGM) (Tauberger et al., 2000), ADP-glucose pyrophosphorylase (AGPase) (Müller-Röber et al., 1992) and granule bound starch synthase (Visser et al., 1991), all required for normal starch biosynthesis. Our results indicate that under specific "invertase like" conditions, there is a block in GPT mediated G6P transport to the plastid. Moreover, this inverse correlation between invertase and GPT was also observed in the sugar floating experiments, providing independent proof that such a negative correlation does exist.

### 3.2.4. Reduced substrate supply to the plastid may lead to a reduced redox potential and thereby an altered plastid metabolism

G6PDH expression and activity, which show strong correlation (Hauschild and von Schaewen, 2003), are activated by a low NADPH/ NADP ratio (Wright et al., 1997). The activation of the pentose phosphate pathway in U-IN-2 would indicate that the plant is compensating for reduced reductive power in the plastid caused by limited G6P supply, producing erythrose 4-phosphate as a product. A reduced NADPH/ NADP ratio would also further explain reduced expression of fatty acid biosynthetic genes. Activation of G6PDH would bring the pathway in direct competition with starch biosynthesis regarding the substrate G6P, for which G6PDH has a high affinity under non-reducing conditions (Wenderoth et al., 1997). It should be kept in mind though that an increase in pentose phosphate pathway activity would still represent only a minor flux compared to starch biosynthesis. Moreover, plastidial G6PDH makes up a very small fraction of the total G6PDH activity (von Schaewen et al., 1995), and a strong relative increase in the expression of plastidial G6PDH should be seen in that light. Despite this, the observed activation, at transcriptional level at least, of the pentose phosphate pathway in U-IN-2

does provide evidence of yet another pathway activated at the expense of starch biosynthesis.

The increase in shikimate was surprising in view of the apparent reduced uptake of carbon by the plastid. The pathway, which is unique to plants and micro-organisms, produces chorismate, substrate for the biosynthesis of aromatic amino acids tyrosine, phenylalanine and tryptophan, and is also the precursor for lignin biosynthesis. All but one identifier for the bifunctional enzyme 3DHQ DH/ shikimate-5-DH was strongly down-regulated in U-IN-2. Remarkably, the one up-regulated identifier showed high homology to a tobacco gene which was silenced by RNAi (Ding et al., 2007). The silencing led to an unexpected increase in shikimate and the authors could not explain the result.

Although the observed phenotype remains baffling, there are at least three redox dependent steps in the shikimate pathway, 3-dehydroquinate dehydrogenase (3DHQ DH) producing NADPH, shikimate-5-dehydrogenase (shikimate-5-DH) consuming NADPH and chorismate synthase, requiring reduced flavin mononucleotide (FMN) for activity (Macheroux et al., 1999). This would mean that under non-reducing plastidic conditions shikimate would accumulate due to a block in the pathway at this enzymatic step, leading to a depletion of the down-stream metabolites. DAHP synthase, the first committed step in the pathway seems to be under various control mechanisms which differ greatly among *species*. For instance, it has been shown in Arabidopsis leaves that the enzyme requires $Mn^{2+}$ and reduced thioredoxin to be active (Entus et al., 2002), which would mean decreased activity under non-reducing conditions. Although regulatory mechanisms acting on DAHP synthase seem to be extensive and not understood, a study by Pinto et al. (1988) provides, to some extent, insight into the observed phenotype in U-IN-2. Their studies on potato cell cultures, treated with sub-lethal doses of glyphosate, showed that inhibition of EPSP synthase can lead to an increase in the activity of DAHP synthase (Pinto et al., 1988). This suggests an inverse regulation of DAHP synthase and EPSP synthase activity, which would lead to shikimate accumulation and reduction of metabolites further downstream in the pathway.

In CW-ISO, a similar phenomenon was observed, where the accumulation of shikimate and reduction in aromatic amino acids was accompanied by an increase in the expression of plastidic isoforms of G6PDH. The gene expression patterns observed in CW-ISO for the shikimate pathway, however, were very different to U-IN-2. Furthermore, functional enrichment analysis revealed an increase in the expression of fatty acid metabolism associated transcripts, arguing against non-reducing conditions in the plastid of CW-ISO.

Taken together it seems as though the shikimate pathway is subject to multi-level regulation of which redox state is an important contributor and the most likely explanation for the observed changes in U-IN-2.

### 3.2.5 Sugar signalling, possibly by way of the SnRK1 complex, and substrate channelling appear to be the reason for increased respiration.

The most striking aspect of U-IN-2 is the increase in respiration, which comes at the expense of starch content, especially in stored tubers (Trethewey et al., 1998; Hajirezaei et al., 2000; Bologa et al., 2003). An increase in respiration should come through the activation of glycolysis and the tricarboxylic acid (TCA) cycle. Expression data did not indicate a clear, uniform up- regulation of TCA cycle enzymes, and TCA cycle intermediates were either increased or unchanged, except of fumarate. Importantly, fructose-2,6-bisphosphate, produced by the kinase domain of the bifunctional enzyme F-2,6-BPase, is a potent activator of glycolysis by inhibiting FBPase and inducing pyrophosphate: Fru-6-P 1-phosphotransferase (PFP), while phosphofructokinase (PFK) is insensitive to it (Nielsen et al., 2004). Although increased expression of F-2,6-BPase does not necessarily mean increased levels of fructose-2,6-bisphosphate, especially since it is a bifunctional enzyme with both a kinase and phosphatase domain, increased fructose-1,6-bisphosphatase would fit to the observed increase in respiration.

Phosphorylation of fructose-6-phosphate by PFP rather than PFK is preferred under conditions of low ATP availability. Due to their bulky nature potato tubers have a low

internal oxygen concentration. Bologa et al. (2003) could show that an oxygen gradient from the tuber surface towards the centre exists. Moreover, they showed that this gradient was even steeper in U-IN-2. The authors stated that the reason for this is the less energy sufficient sucrose degradation by invertase compared to Susy, as explained earlier. However, this could also be a secondary effect of increased tuber respiration due to other factors. In either case, conditions of hypoxia would lead to the activation of anaerobic respiration, as was shown by Bologa et al. (2003). There was no clear increase in the expression of marker genes for anaerobic respiration, but there was an accumulation of alanine, a marker metabolite (Davies, 1980), which is in line to earlier studies on U-IN-2. This would point towards anaerobic respiration taking place at least to some extent, although from our data it does not seem as though this is the predominant form of respiration

Despite the many studies done on U-IN-2, the reason why there would be an increase in respiration is still unclear. A previous study has suggested that the increase is due to sugar signalling and that the absence of cytosolic sucrose, rather than an increase in glucose, is sensed (Trethewey et al., 2001). This was supported by a study which expressed invertase specifically in the cytosol of companion cells, or reduced cytosolic sucrose by expression of sucrose isomerase (CW-ISO). The results indicated that a depletion of cytosolic sucrose, and not increased hexose metabolism, lead to the increase in respiration (Hajirezaei, 2003). Gene expression analysis did not reveal a clear increase in the expression of either glycolysis or the TCA cycle in CW-ISO, but there was huge increase in fumarate, intermediate of the TCA cycle.

Taken together the results would indicate that it is highly likely that sugar signalling is primarily responsible for increased respiration, although the mechanisms behind it still need to be resolved. To investigate the mechanisms underlying the increased respiration in U-IN-2, our studies into genes only altered in U-IN-2, and not U-IN-1, identified a catalytic trehalose phosphatase, the enzyme catalysing the dephosphorylation of trehalose 6-phosphate. Assuming that increased expression of the gene would lead to a higher enzyme activity, a decreased accumulation of trehalose-6-phosphate in U-IN-2 tubers

would be expected. This would result in activation of SnRK1 and hence most likely enhanced catabolic metabolism including respiration. Elevated respiration of trehalose phosphatase overexpressing transgenic potato tubers has recently been published (Debast et al., 2011), supporting our hypothesis. Since this trehalose phosphatase is not induced in U-IN-1 tubers, it could explain the observed difference between both genotypes with respect to respiratory activities.

Recent studies in Arabidopsis and potato have shown that there is a correlation between increased respiration and glycolytic enzyme association with the mitochondrial membrane, suggesting the channelling of carbon towards the mitochondria occurs under specific conditions. Moreover, it could be shown that this increased association of glycolytic enzymes to the mitochondrial membrane also exists in U-IN-2 when compared to control tubers (Graham et al., 2007). The entry point to this proposed channel is currently not well understood, especially in plants. In mammalian systems, however, it has been proposed that different hexokinase isoforms are important to channel G6P into different metabolic routes, and that mitochondrial-bound hexokinase would channel the carbon towards the mitochondria and glycolysis (Wilson, 2003). It could be that a similar mechanism exists in plants where hexokinase 5, in response to specific sugar signals, channels glucose through phosphorylation towards glycolysis and respiration, as proposed in figure 69.

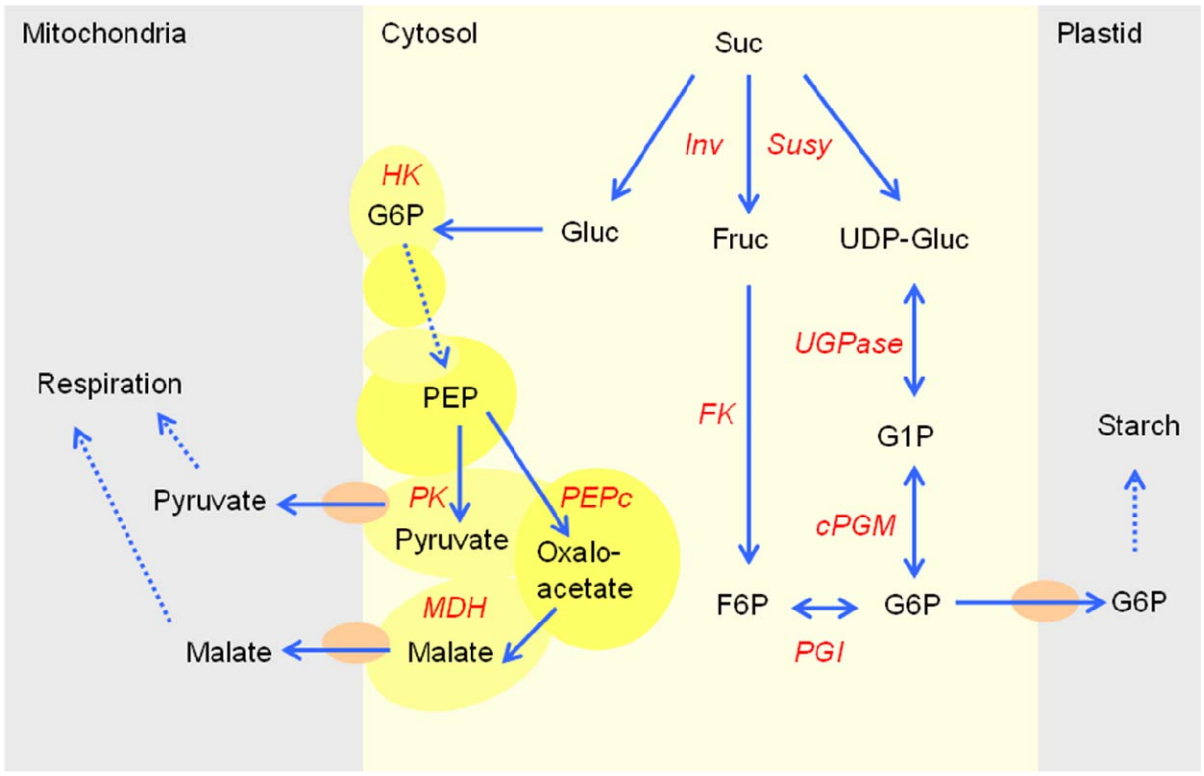


**Figure 69. Proposed channeling of glucose towards the glycolysis and respiration with hexokinase as the entry point.**

Further evidence for this is the imbalance in the ratio between G6P and G1P, indicating that the G6P is caught in the complex and not accessible to cPGM. A possible means to overcome this problem would be to introduce a second complex of proteins involved in sucrose cleavage and the production of G6P, anchored to the plastid membrane via GPT. Future work will be aimed at testing this hypothesis.

### 3.1.4. Comparative analysis of transcription profiles reveals genes possibly regulating starch biosynthesis.

Attempting to identify regulatory genes involved in starch biosynthesis, comparative transcriptome analysis was used to select for genes expressed during active starch biosynthesis. Functional enrichment analysis of the selected genes revealed a strong relative increase of transcripts associated with starch biosynthesis and storage proteins. Despite the caution which should be exercised in the interpretation of the significance of this result due to the small number of features used in the functional enrichment study,

the overwhelming enrichment of these features would indicate that the comparative transcriptome analysis was successful in selecting the desired genes. A transcription factor, annotated as a bZIP protein was identified and closer inspection revealed that it belongs to the S group of transcription factors (Jakoby et al., 2002; Wiese et al., 2004). It is the largest group in Arabidopsis and transcription is up-regulated by light and in sink tissues, making it very likely that they are involved in the regulation of starch and sugar metabolism in tubers. The group is known to have an open reading frame upstream (uORF) of the gene coding sequence which mediates a sucrose induced repression in translation of the subsequent bZIP gene (Wiese et al., 2004). This uORF is highly conserved in plants and has also been reported for potato (Wiese et al., 2004). The published uORF from potato was used to identify five more bZIP transcription factors from the potato genome. The POCI microarray could be used to determine the expression profiles for three of these genes and revealed that two, St_bZIP2 and St_bZIP8, had very similar patterns and correlated to starch biosynthesis. St_bZIP52, however, had a seemingly opposite pattern and negatively correlated to starch in most of the transcription profiles. The results would indicate that bZIP transcription factors from the S-group is very likely to be involved in the regulation of starch biosynthesis and other related processes in potato tubers and warrant further investigation.

### 3.3. Changes in the expression of starch degrading enzymes lead to alterations in tuber sprouting and other related processes.

#### 3.3.1. Simultaneous silencing of isoamylases ISA1, ISA2 and ISA3 by multi-target RNAi in potato tubers leads to decreased starch content and an early sprouting phenotype.

Although RNAi silencing of genes in plants is done routinely this is, to our knowledge, the first example of the silencing of three gene targets using a single silencing construct in plants. Silencing of the different targets appeared to occur in a non-random fashion, since in the majority of cases either all three genes were silenced or none. This could be a secondary effect of cross silencing between the three relatively closely related targets. Furthermore, it has been shown that silencing of either ISA1 or ISA2 in potato leads to

the reduction in expression of the other gene, indicating that the transcript amount of these two genes, are coordinated (Bustos et al., 2004). It is doubtful whether a similar mechanism would exist for ISA3, since it functions independently from the other two proteins. Figures S2-S4 show the alignments of the three gene fragments of the RNAi construct and the three isoamylase genes, which proved inconclusive as to whether cross-hybridisation could be expected or not. The longest cross hybridising fragment identified was between the ISA1 RNAi fragment and ISA3, which stretched nineteen bases. This is unlikely to induce a silencing signal (for review on RNAi silencing see Melnyk et al. (2011)), but possible varietal differences between the background variety, Solara, and variety from which the analysed sequence is derived might mean that a longer stretch of hybridisation might be possible. Thus, sequencing of the endogenous isoamylases of the transgenic plants will be required to determine whether the observed effect is due to cross-silencing or not.

Despite no clearly visible effects on the aerial parts of the plants, and no change to tuber yield, there was a significant reduction in tuber starch content. It is unlikely that this is due to reduced source capacity, since it has been shown that this does not have an effect on tuber starch yield (Zrenner et al., 1996). It is more likely that the reduction is primarily the result of altered starch biosynthesis in the tuber due to the important function of ISA1/ISA2 in amylopectin synthesis (Delatte et al., 2005; Streb et al., 2008). There was a significant increase in smaller starch granules in the transgenic lines, a similar result as to what was found in potato plants with silenced ISA1 or ISA2 (Bustos et al., 2004).

One of the most striking aspects of the transgenic plants was the reduced dormancy period and earlier sprouting. This happened despite the silencing of ISA3, an important starch degrading enzyme (Streb et al., 2008), which led to reduced starch degradation during storage. There were also more sprouts per tuber, indicating that sprouting was less coordinated than in the wild type scenario. A less organised starch structure, due to reduced activity of isoamylase, would lead to increased solubility. This would lead to easier, and less coordinated, starch degradation, fitting to the observed changes regarding sprouting. To investigate whether glucan structure was altered, chain length distribution

analyses of the lines were performed. In this study no clear structural changes to the insoluble glucans could be observed. There was, however, indications of small structural changes in line 39 in all the tissues/ time points analysed. Bustos et al. (2004) did similar structural studies on antisense ISA1 or ISA2 lines and could also not observe changes. Small amounts of soluble glucans in the transgenic tubers could be detected, increasing during storage. Structural analysis of soluble glucans revealed that in line 39 there might be a change, although this is merely an observation and could not be statistically proven.

Despite the lack of obvious structural changes to the starch molecule, the reduced DW/ FW ratio would suggest that at the macromolecular level at least there were changes due to less dense packing of starch, which led to increased water content of granules. Furthermore, since these studies were performed on lines which had only reduced expression of the target genes and were not null mutants, it can be expected that changes occurred non-homogenously, resulting in starch granules with varying structure.

I propose that due to reduced activity of ISA1/ISA2, but not the complete absence, changes to the glucan and granule structure occurs. This would lead to certain parts of the granule being more soluble and accessible to the degrading enzymes, leading to the production of sufficient amounts of sucrose during storage to initiate early sprouting. Sprouting would also be less coordinated, the reason for an increase in sprouts per tuber. The accumulation of soluble glucans during storage was surprising, and probably stems from a different source than those produced during starch biosynthesis, and that is the accumulation of partly degraded glucans due to reduced ISA3 activity.

### 3.3.2. Silencing of a specific alpha-amylase isoform leads to reduced cold sweetening and a delay in sprouting.

By studying microarray expression data an alpha-amylase gene highly up-regulated at the time of sprouting in the sprout release assay (Hartmann et al., 2011) was identified. Blast™ results revealed that the identified gene codes for alpha-amylase 23 (Genbank accession M79328). Although subcellular localisation prediction software revealed that

the protein does not have a plastid transit peptide, it does have a predicted signal peptide, indicating the possible secretion of the protein. According to recent findings, protein secretion could lead to plastidic targeting of proteins (for review see Faye and Daniel (2006)), but whether this would lead to plastidic targeting of alpha-amylase 23, however, needs to be further investigated.

The role of alpha-amylase 23 in potato was analysed by silencing it with RNAi and analysing the results. Transgenic potato tubers sprouted later than the control and there was a reduction of glucose in the parenchyma tissue associated with a growing sprout. Moreover, after cold treatment of tubers for fourteen days there was reduced accumulation of hexoses in the transgenic tubers, implicating the gene in tuber starch degradation. Additionally, a highly homologous alpha-amylase from apple (figure S5) is strongly expressed under cold conditions in leaves (Wegrzryn et al., 2000), providing further evidence that the gene is involved in starch degradation under cold stress. Since enzyme activity was not measured it is not clear yet whether the silenced protein does possess enzyme activity or whether it has a regulatory function, and this will need to be further investigated. It is never the less a significant finding that reduced expression of an alpha-amylase gene leads to a delay in sprouting and cold sweetening, possibly due to reduced starch degradation. Furthermore, the discovery of the gene by studying transcription profiles proves the value of this type of analysis in identifying genes important for specific processes.

## 4. Summary

This study aimed at identifying regulatory mechanisms underlying starch biosynthesis in potato under various conditions, in different tissues, in transgenic plants with altered central carbon metabolism and in tubers growing at different velocities. For this a new technique was developed to measure tuber growth *in vivo*. Furthermore, it was aimed to influence starch degradation in terms of its role in sprouting and cold induced sweetening by reducing the expression of specific genes and analysing the results.

Comparative transcriptome analysis between leaves and tubers indicate that transient and storage starch biosynthesis might not be all that different with the same isoforms being differentially expressed in both tissues. There was also a diurnal rhythm of GBSS expression in tubers which could be correlated to sucrose supply from the leaves. This provided evidence not only of the diurnal regulation of starch biosynthetic gene expression in tubers, but also showed the importance of sucrose supply in regulating gene expression. Since tuber initiation and growth is not synchronised, it was important to determine the growth velocity of individual tubers. To this end X-ray CT was used to determine the volume of individual tubers at different time points and calculate the growth velocity. This was the first time that the growth velocities of tubers were determined in a natural environment. Tuber growth velocity could not be correlated to starch biosynthetic gene expression, although it was clear that gene expression is different between growing and non-growing tubers. The relationship between gene expression and growth velocity seems to be qualitative rather than quantitative and the data provides important information towards the identification of factors determining potato tuber growth.

Further transcriptome based analysis on plants with genetically altered central carbon metabolism reveal that the accumulation of either apoplasmic (U-IN-1) or symplasmic (U-IN-2) hexoses lead to different sugar signals activating different metabolic and physiological processes. U-IN-1 had reduced expression of photosynthesis associated genes which is probably due to the accumulation of glucose in the apoplasmic space,

leading to early senescence. In plants expressing sucrose isomerase in either the apoplasmic space (CW-ISO) or vacuole (NTTP), there was an increase in the expression of photosynthetic genes possibly in response to a sugar starvation signal.

In both U-IN-1 and U-IN-2 there was a reduction of cell wall biosynthetic gene expression, explained by reduced production of UDP-glucose. Strong evidence for substrate channeling which shifts metabolic flux towards respiration is provided and the involvement of the Srnk1 complex is suggested. Furthermore, a strong negative correlation between GPT and cell wall invertase, possibly mediated by transcription factors, suggest that under "invertase like" conditions plastid transporters are down-regulated, leading to insufficient substrate supply. Reduced supply, resulting in a changed redox state, could explain the indirect effects of reduced fatty acid biosynthetic gene expression and the accumulation of shikimate in U-IN-2.

Comparative transcriptome analysis selecting for genes associated with starch biosynthesis was used to identify putative regulators of starch biosynthesis. A bZIP transcription factor from the S-group strongly correlated with starch biosynthesis. Moreover, a uORF associated with this gene was idenfied, as well as five other bZIP transcription factors in the potato genome containing this uORF. The region is known to regulate gene translation in response to the sucrose status. Expression profiles of the other uORF containing bZIP genes support their putative involvement in the regulation of starch and sugar metabolism in potato tubers and warrants further investigation.

In plants where all three isoamylases were simultaneously silenced, there were no clear visible effects on the aerial parts of the plants, and no change to tuber yield, but there was a significant reduction in tuber starch content, likely due to the important function of ISA1/ISA2 in amylopectin synthesis. A reduction in the DW/ FW ratio was observed, indicating that there might be less dense packaging of starch, leading to higher water content of granules. There was an increase in small starch granules but no clear structural changes could be observed to either the soluble or insoluble glucans in terms of chain length distribution and it is proposed that due to reduced activity of ISA1/ISA2, but not

the complete absence, changes to the glucan and granule structure occurs. This would lead to certain parts of the granule being more soluble and accessible to the degrading enzymes, leading to the production of sufficient amounts of sucrose during storage to initiate early sprouting. Sprouting would also be less coordinated, the reason for an increase in the number of sprouts per tuber. The accumulation of soluble glucans during storage was surprising, and it is believed that it stems from a different source than those produced during starch biosynthesis, which is the accumulation of partly degraded glucans due to reduced ISA3 activity.

Through microarray data analysis alpha-amylase 23 was identified to be strongly up-regulated upon sprouting and it was shown that silencing of the gene leads to a delay in sprouting, accompanied by reduced accumulation of glucose in the parenchyma associated with a sprout. Transgenic lines also had reduced cold induced sweetening. This hints towards the direct involvement of the enzyme in starch degradation. Further analyses are required to determine whether the enzyme actively degrades starch, or whether it has a regulatory function. The absence of a predicted plastid transit peptide would indicate that the protein is not targeted to the plastid, but the presence of a signal peptide might mean plastid targeting through alternative mechanisms. The discovery of the gene's involvement in sprouting and other related processes is not only exciting in terms of unravelling potato starch degradation, but also shows the value of microarray data analysis in identifying important genes.

## Zussamenfassung

In der vorliegenden Arbeit sollten regulatorische Mechanismen, denen die Stärke-Biosynthese in der Kartoffel unter verschiedenen Bedingungen, in verschiedenen Geweben, in transgenen Pflanzen mit verändertem Kohlenstoff-Metabolismus und in Kartoffelknollen mit unterschiedlichen Wuchsgeschwindigkeiten unterliegt, identifiziert werden. Hierfür wurde eine neue Methode zur Messung des Knollenwachstums *in vivo* entwickelt. Darüber hinaus wurde beabsichtigt, den Stärke-Abbau durch Reduktion der Expression spezifischer Gene zu beeinflussen und die Ergebnisse in Bezug auf seine Rolle bei der Knollenkeimung und dem „cold-induced sweetening“ zu untersuchen.

Vergleichende Transkriptom-Analyse von Blättern und Knollen deutet darauf hin, dass Speicher- und transiente Stärke-Biosynthese möglicherweise nicht so verschieden sind wie bisher angenommen, da die gleichen Isoformen in beiden Geweben differentiell exprimiert sind. Für die Expression von GBSS konnte ein Tagesrhythmus gezeigt werden, der mit der Saccharose-Versorgung über die Blätter korrelierte. Dies erbrachte nicht nur den Nachweis der Tagesverlauf-abhängigen Regulation von Genen der Stärke-Biosynthese in der Knolle, sondern belegte auch die Bedeutung der Saccharose-Versorgung bei der Regulation der Genexpression. Selbst an derselben Pflanze sind Knollen-Inititation und Knollenwachstum nicht synchronisiert, daher war es wichtig, die Wuchsgeschwindigkeit einzelner Knollen zu bestimmen. Aufnahmen mit einem Röntgen-CT wurden verwendet, um das Volumen einzelner Knollen zu verschiedenen Zeitpunkten zu messen und daraus die Wuchsgeschwindigkeit zu berechnen. Dies erlaubte zum ersten Mal die Bestimmung der Wuchsgeschwindigkeit von Knollen in einer natürlichen Umgebung. Obwohl die Genexpression von wachsenden und nicht-wachsenden Knollen sich eindeutig unterschied, konnte keine Korrelation zwischen Knollenwachstum und Stärke-Biosynthese festgestellt werden. Die Beziehung zwischen Genexpression und Wuchsgeschwindigkeit scheint eher qualitativer als quantitativer Natur zu sein und die hier gezeigten Daten stellen wichtige Information für die weitere Identifikation von Faktoren, die das Knollenwachstum bestimmen, bereit.

Weitere Transkriptom-basierte Analyse von Pflanzen mit verändertem zentralen Kohlenstoff-Metabolismus enthüllte, dass die Akkumulation von apoplastischen (U-IN-1) oder symplastischen (U-IN-2) Hexosen zu verschiedenen Zucker-Signalen führt, die wiederum verschiedene metabolische und physiologische Prozesse aktivieren. U-IN-1 zeigte eine reduzierte Expression von Photosynthese-assoziierten Genen, was wahrscheinlich auf die Akkumulation von Glucose im Apoplasten zurückzuführen ist und früh einsetzende Seneszenz verursachte. In Pflanzen, die eine Saccharose Isomerase im Apoplasten (CW-ISO) oder der Vacuole (NTTP) exprimierten, konnte ein Anstieg der Expression von Photosynthese-Genen nachgewiesen werden, möglicherweise als Antwort auf ein Zuckermangel-Signal.

Sowohl bei U-IN-1 als auch bei U-IN-2 zeigte sich eine Reduktion der Expression von Genen der Zellwand-Biosynthese, was sich durch die reduzierte Bildung von UDP-Glucose erklären lässt. Zudem gab es starke Belege für ein „Substrat-Channeling“ in U-IN-2, das den Metabolismus in Richtung verstärkter Respiration verschiebt, sowie Hinweise auf die Beteiligung des Snrk1-Komplexes an diesem Prozess. Zusätzlich lässt eine starke negative Korrelation zwischen GPT und Zellwand-Invertase - möglicherweise vermittelt durch Transkriptionsfaktoren - vermuten, dass plastidäre Transportproteine unter „Invertase-ähnlichen“ Bedingungen herunterreguliert werden, so dass es zu unzureichender Substratversorgung kommt. Reduzierte Versorgung und dadurch bedingte Veränderung des Redox-Status könnte auch die indirekten Effekte, reduzierte Expression von Fettsäure-Biosynthese-Genen und Akkumulation von Shikimat in U-IN-2, erklären.

Die vergleichende Transkriptom-Analyse wurde darüber hinaus verwendet um Gene, die mit Stärke-Biosynthese assoziiert sind zu selektieren und dadurch mögliche Regulatoren dieses Prozesses zu identifizieren. Ein bZIP Transkriptionsfaktor aus der S-Gruppe korrelierte stark mit Stärke-Biosynthese. Überdies wurde ein uORF identifiziert, der mit diesem Gen assoziiert ist, und es wurden fünf weitere bZIP Transkriptionsfaktoren im Kartoffelgenom ermittelt, die ebenfalls über diesen uORF verfügen. Die uORF Region ist bereits bekannt dafür, die Translation von Genen in Abhängigkeit vom Saccharose-Status zu regulieren. Die Expressionsprofile der ermittelten bZIP Transkriptionsfaktoren

mit diesem uORF unterstützen eine mögliche Beteiligung bei der Regulation des Stärke- und Zuckermetabolismus und berechtigen eine eingehendere Untersuchung.

Bei Pflanzen, in denen alle drei Isoamylasen gleichzeitig herunterreguliert waren, konnten keine sichtbaren Effekte auf die oberirdischen Teile der Pflanzen und den Knollenertrag festgestellt werden. Statt dessen gab es eine signifikante Absenkung des Stärkegehalts der Knollen, wahrscheinlich bedingt durch die wichtige Rolle von ISA1/ISA bei der Amypektin-Synthese. Eine Reduktion des FW/ DW- Verhältnisses wurde ebenfalls beobachtet, unter Umständen ein Hinweis auf ein weniger dichtes Stärkegeflecht, so dass der Wassergehalt der Stärkekörnchen höher ist. Trotz einer erhöhten Anzahl kleiner Stärkekörnchen konnten weder bei den löslichen noch den unlöslichen Glukanen klare strukturelle Veränderungen bezüglich der Verteilung der Kettenlänge ermittelt werden. Vermutlich führte die durch nicht-vollständige Herunterregulierung noch vorhandene Rest-Aktivität von ISA1/ISA2 zu den Veränderungen der Glukan- und Stärkekorn-Struktur. Durch die strukturellen Modifikationen wären einige Teile eines Stärkekorns löslicher und für abbauende Enzyme leichter zugänglich, so dass wohl die in ausreichenden Mengen gebildete Saccharose das beobachtete verfrühte Auskeimen der Knollen bedingt. Zusätzlich wurde die Koordination der Keimung gestört und es kam zu einer erhöhten Anzahl an Keimen pro Knolle. Bei der Lagerung der transgenen Knollen kam es zu einer überraschenden Akkumulation von löslichen Glukanen, deren Quelle wohl nicht in der Stärke-Biosynthese, sondern in unvollständigem Abbau wegen reduzierter ISA3-Aktivität zu finden ist.

Analyse von Microarray-Daten zeigte, dass Alpha-Amylase 23 während der Keimung stark hochreguliert wird. Herabregulierung des Gens führte zu verzögerter Keimung und reduzierter Akkumulation von Glucose im Parenchym direkt unter dem Keim. Das „cold-induced sweetening“ in den transgenen Knollen war ebenfalls vermindert. Beides deutet auf einen direkte Beteiligung des Enzyms am Stärke-Abbau. Weitere Analysen sind nötig um zu klären, ob das Enzym aktiv Stärke abbaut oder eine regulatorische Funktion übernimmt. Das Fehlen eines plastidären Transit-Peptids könnte einerseits bedeuten, dass

das Protein nicht im Chloroplasten lokalisiert ist, andererseits könnte das vorhandene Signalpeptid für eine Lokalisierung im Plastiden über alternative Mechanismen sprechen. Die Entdeckung, dass dieses Gen an der Keimung und weiteren zugehörigen Prozessen beteiligt ist, ist nicht nur ein spannender Schritt in der Entschlüsselung des Stärke-Abbaus, sondern zeigt auch die Bedeutung von Microarray-Daten bei der Identifikation wichtiger Gene.

## 5. Materials and methods

### 5.1. Plant material and experimental conditions.

All plants used in the study were maintained and propagated in tissue culture on MS medium (Murashige and Skoog, 1962) containing 2% (w/v) sucrose with a 16 hour light and 8 hour dark regime. After transfer to the greenhouse the selected lines were cultivated in individual 4 litre pots.

The specific conditions for each experiment is described here:
For transcriptional analysis of potato leaves over a diurnal period, plants were grown in a growth chamber under a 14 hour light and 10 hour dark cycle at 50% humidity and 60 µmol quanta $m^{-2}$ $s^{-1}$. Plants for the tuber induction and X-ray CT and those used for leaf discs floating studies were grown in the greenhouse with 16 hours of supplemental light (150 µmol quanta $m^{-2}$ $s^{-1}$) and 8 hours of darkness. The temperature regime followed the light/ dark cycle with 21°C and 18°C. For leaf floating experiments leaf discs (#12 cork borer) were harvested two hours into the light period and immediately transferred to Petri dishes containing the different solutions. Leaf discs were kept in darkness through the entire experiment. Plants used for analysing the diurnal rhythm in tuber gene expression were grown in a phyto-chamber with 16 hours of light (350 µmol quanta $m^{-2}$ $s^{-1}$) and 8 hours of darkness. For the analysis of growing tubers of sucrose isomerase and yeast invertase expression plants, *Solanum tuberosum* L. cv. Desiree and Solara; and transgenic lines U-IN-1-33, U-IN-2-17 (Sonnewald et al., 1997), SP-B33-CW-ISO-26 (Börnke et al., 2002) and B33-NTTP-PD-SD-6 (Börnke, unpublished) were transferred to the greenhouse and cultivated in individual 4 litre pots at 50% humidity with 16 hours of supplemental light (150 µmol quanta m-2 s-1) and 8 hours of darkness. The temperature regime followed the light/ dark cycle with 21°C and 18°C. For analysis of plants with reduced expression of all three isoamylases or reduced expression of alpha-amylase 23, *Solanum tuberosum* L. cv. Solara and transgenic lines triple-RNAi-ISA-7, -16 and -39, or transgenic line St-RNAi-aamy-12, -15 and -18 were transferred to the greenhouse with 16 hours of supplemental light (150 µmol quanta $m^{-2}$ $s^{-1}$) and 8 hours of darkness. The

temperature regime followed the light/ dark cycle with 21°C and 18°C. Tubers were harvested after 12 weeks and samples were taken using a cork borer, flash frozen in liquid nitrogen and stored at -80° C. For sampling at the time of sprouting tubers were stored in darkness at room temperate and subsequently sampled. Sampling of parenchyma tissue associated with a sprout was performed as described in figure S1. For cold induced sweetening studies, potato tubers were stored at 8°C for 14 days in darkness and sampes taken with a corkborer as described above.

### 5.2. RNA extraction

RNA extraction were performed as described previously (Logemann et al., 1987).

### 5.3. Sample preparation and microarray hydridisation

Sample preparation and microarray hybridisation has been described (Hartmann et al., 2011).

### 5.4. Data extraction and analysis

For data analysis, text files generated by feature extraction software were imported into Genespring$^{TM}$ (version GX7.3 for chapter 2.1 and version 11.0 for chapters 2.2 to 2.4). For hybridisations performed in chapter 2, the following normalisation steps were performed: (1) data transformation: measurements less than 5.0 were set to 5.0; (2) per chip: normalisation to the 50th percentile; (3) per gene: the signal of each feature was normalised to the median of the control samples.

For hybridisations performed in chapters 2.2 to 2.4, the following normalisations were performed:(1) data transformation: measurements less than 1.0 were set to 1.0; (2) per chip: normalisation to the 75th percentile; (3) per gene: the signal of each feature was normalised to the median of the control samples. For Mapman analysis an Anova test was performed to select the features which were significantly altered from the control ($p \leq 0.05$, variance assumed as equal). For sugar feeding experiment, RNA samples were obtained from two different experiments which meant that the replicates did not cluster according to treatment due to experimental noise. To circumvent this problem, clustering

was repeated after reducing the experimental noise by way of an one-way Anova ($p \leq 0.05$, variance assumed as equal). For both PCA analysis and pathway specific analysis in chapters three and four, the fold change, relative to the control, was calculated and used for subsequent analysis. Furthermore, to make the data compatible for Mapman analysis, the log2 value was calculated. PCA analysis was performed using MarkerviewTM software (version 1.1.0.7) and the Pareto clustering algorithm was used. For the functional assignment a volcano plot ($p \leq 0.05$, variance assumed as equal; features changed more than two-fold changed relative to the control) was performed and selected features were divided into up- and down-regulated groups. The percentage of features from a specific functional group was expressed relative to the percentage of features from that group on the entire chip. Functional groupings were used as described previously (Hartmann et al., 2011). For analysis with Mapman software the POCI mapping file was downloaded from the Mapman website (https://www.gabipd.org/projects/MapMan/). In certain cases the mappings were changed to allow the separation of genes coding for proteins expressed in different subcellular compartments, and also to separate features derived from different genes. To identify features expressed in U-IN-2, but not in U-IN-1, a volcano plot ($p \leq 0.05$, variance assumed as equal; features changed more than two-fold changed in U-IN-2 relative to the control) was used to select differentially expressed features and these were exported to Microsoft Excel$^{TM}$. Features which were also regulated in U-IN-1 (relative log2 expression value more than 0.5, or less than -0.5) were excluded (Supplemental data S2)

For the selection of features co-expressed with either GPT2 (micro.1076.c1) or cell wall invertase (micro.11340.c1), selected datasets were imported into Genespring and a new experiment was created. Three normalization steps were applied: (1) data transformation: measurements less than 1.0 were set to 1.0; (2) per chip: normalisation to the 75th percentile; (3) per gene: the signal of each feature was normalized to the median of its value across the dataset. Features with a correlation coefficient (Pearson correlation, t-test unpaired) of >0.95 were selected for micro.1076.c1 and micro.11340.c1 respectively (Supplemental data S1).

To select features correlating to growth velocity, relative expression values in tubers growing at different velocities were exported from Genespring$^{TM}$ 11 and imported into Microsoft excel$^{TM}$. The correlation coefficient (Pearson) was calculated and features with a correlation coefficient of >0.5 or <-0.5 were subsequently used to determine the relative functional group enrichment.

For comparative analysis of various transcription profiles towards the selection of regulators of starch biosynthesis, volcano plots were applied to select for features more than two-fold differentially up-regulated when the following conditions were compared to each other: stage 5 to stage 1 of tuber induction; glucose floating and water and sucrose floating and water; growing tubers to non-growing tubers. Finally features up-regulated in all comparisons were selected using a Venn diagram to create the final list of genes.

Heatmaps were created from the same file used for Mapman pathways. Data was imported into Muti experiment viewer (http://www.tm4.org/mev/) and colour thresholds set at -1.3 as the lower threshold, 0 for neutral and 1.3 as the upper threshold.

**5.5. Metabolite extraction and measurement and analysis.**

Metabolite extraction and measurement of organic acids, phosphorylated intermediates, amino acids, carotenoids (Horst et al., 2010; Kogel et al., 2010), major soluble sugars and starch (Müller-Röber et al., 1992) was performed as described previously. For soluble glucan measurement in chapter 5, tuber material was homogenised in geno grinder (SPEX). The material was kept frozen at all times and to around 600 mg material 3 ml of ice-cold 1.12 M perchloric was added and mixed well. 2.7 ml of suspension was transferred to a fresh tube and centrifuged for 10 minutes (3000g) at 4°C. 2.2 ml of supernatant was transferred to a fresh tube, kept on ice, and subsequently neutralised using neutralisation buffer (2 M potassium hydroxide, 0.4 M MES buffer and 0.4 M potassium chloride) and centrifuged for 10 minutes (3000g) at 4°C. The supernatant was transferred to a fresh tube and used to determine soluble glucan content. Soluble glucans were determined by measuring the amount of glucose released by treatment with a-

amylase and amyloglucosidase (Smith and Zeeman, 2006). To determine sucrose supply rate to a tuber in chapter 2, sucrose content of stolon-ends was determined. A stolon-end is defined as the 15 millimetres of a stolon directly above the connection to the tuber.

For both PCA analysis and pathway specific analysis, the fold change, relative to the control, was calculated and used for subsequent analysis. Furthermore, to make the data compatible for Mapman analysis, the log2 value was calculated.

### 5.6 Soluble and insoluble glucan structure analysis

Soluble and insoluble glucan structure analysis was performed as described previously (Streb et al., 2008).

### 5.7. Quantitative real-time PCR

For all Quantitative real-time PCR (qPCR) analysis at least three biological repeats were used unless stated otherwise. Expression levels of genes were determined by real-time quantitative RT- PCR and the corresponding primers for the amplification of targets between 75 and 150 bp were designed using Primer3plus software [55]. Total RNA (five µg) from each of the developmental time points was treated with DNaseI (Fermentas GmbH) before undergoing reverse transcription using oligo d(T) primers and RevertAid™ H minus first strand cDNA synthesis kit (Fermentas GmbH) to generate a first strand cDNA template. Potato ubiquitin primers were used as a control as described previously [26]. One µl of 1:10 diluted cDNA for each time point were amplified with gene- specific primers in three technical replicates on a Mx3000P Q-PCR system (Stratagene) in combination with the Brilliant II SYBR Green Q-PCR Master Mix Kit (Stratagene). The thermal profile was as follows: 1 cycle 10 min at 95°C for DNA polymerase activation followed by 35 cycles of 10 s at 95°C, 15 s 60°C and 20 s 72°C. Relative gene expression was calculated using the Pfaffl method (Pfaffl, 2001). The primer sequences used are shown in table 2.

**Table. 2. The primer sequences used for qPCR were as follows.**

| Gene | POCI identifier | Forward primer | Reverse primer |
|---|---|---|---|
| Ubi3 | - | 5'-TTC CGA CAC CAT CGA CAA TGT- 3' | 5'-CGA CCA TCC TCA AGC TGC TT- 3' |
| GBSS | micro.920.c2 | 5' – CAG ACT TGA GGA GCA- GAA AGG - 3' | 5' – GTG AGC CAA AGG GAC ATT GA - 3' |
| GPT2 | micro.1076.c1 | 5' –CCT TGT TTC CTG TTG CTG TG- 3' | 5' –AAA GCA GGC TCT CCA CTC TT- 3' |
| Susy4 | micro.196.c8. | 5' –CTG CTG TTT ATG GGT TCT GG- 3' | 5' –GGC ACA CCT TCA TTC ACT CA- 3' |
| NTT | micro.1831.c2. | 5' -GAGCAGCAGCCAA- GATAA CAC- 3' | 5' –GTT CTG CATT GCA CCC ACA- 3' |
| ISA1 | Micro.15626.c1 | 5′-GGC AAA TGG AGA GGA CAA CA -3′ | 5′- ATG GGA ACA CCT TGG GAA AC -3′ |
| ISA2 | Micro.12035.c1 | 5′- TTA TCC TTC CGC CAC CTC -3′ | 5′- CTT CAA CTG GAG TTC CCT TCT-3′ |
| ISA3 | Micro.10651.c1 | 5′- GAC GCT TGC CCT TCA TTC -3′ | 5′- CTC CTG TGC GGT TCT TCT GT -3′ |

## 5.8. Description of X-ray CT

With X-ray CT the 3D volume information of objects can be reconstructed using X-ray projections of the object from different aspects. The geometry used for the investigation was the axial 3D-CT, where a conical X- ray beam projects the object onto a flat 2D image detector. Using axial 3D-CT, projections of the object are taken under different viewing angles, rotating the object perpendicular to the central X-ray beam. The reconstructed volume data set consists of volumetric elements, called voxels, containing grey levels which represent information about the X-ray attenuation characteristics depending on the mass attenuation coefficient and the density distribution of the material (Feldkamp, 1984; Hanke et al., 2008). The mass attenuation coefficient itself is dependent on the applied X-ray spectrum and the effective atomic number of the X-rayed material. The calculation of tuber volumes of potted potato plants embedded in soil requires the segmentation of tubers from other materials in the X-ray CT volume data. Therefore a careful selection of exposure conditions is necessary to achieve sufficient data quality. This comprises X-ray parameters and filters as well as the condition of the soil. The parameters were defined as such: The X-ray source was FXE-225.45,

accelerating voltage 200 kV, total emission 200 μA, the filter 1 mm Cu, detector Perkin Elmer, 1024 × 1024 pixel 200 μm, scan period 50 minutes and aresolution of 141 μm. After segmentation voxel elements, which have a known volume and specific grey level for tubers, were used to determine tuber volume by calculating how many voxels are present in a reconstructed tuber image. The lower and upper threshold grey values were set at 2938 and 3963 after which mistakes were corrected for manually. Tuber volume calculations were performed using Image J software http:// rsbweb.nih.gov/ij.

### 5.9. RNAi construct design and potato transformation

To generate the RNAi construct targeting three different isoamylase genes, individual PCR reactions for each gene was conducted using Isa 1 (5′- CAC C CT CGT GGA ATG CTG TAA ATG -3′ and 5′- GTC ACT CCC CAT GCC AAC TTG GTA AAG GC -3′), Isa2 (5′- GTT GGC ATG GGG AGT GAC CAA TCT CCT CC-3′ and 5′-GTC ACT CCC CAT GCC AAC TTG GTA AAG GC -3′) and Isa3 (5′- GCA GCT GAG C CAA TCT CTG AAT CAC CAG CAC C-3′ and 5′- GCA AAG AAC ACT AGC AAG ATC -3′) specific primers. Primers contained tags at either the 3′ of 5′end which would make it possible for the different PCR fragments created to hybridise in a subsequent PCR reaction, producing a single DNA fragment. This fragment was used for sub-cloning into an entry vector pENTR-D-TOPO, and cloned into pK7GWIWG2(II) using gateway technology (Invitrogen). To generate a RNAi construct targeting alpha-amylase 23, a PCR amplified fragment (5' – CAC CAG CAG TCC TTC AGG AAG CAG
TCA A-3′and 5′- ACT TCT GCC AGA CTG CAT AGC GA -3′) was sub-cloned into the entry vector pENTR-D-TOPO and also cloned into pK7GWIWG2(II). The vectors were used for potato transformation as described previously (Hartmann et al., 2011).

### 5.10. Northern blot

For northern-blot analysis, 20 to 30 μg of total RNA was separated on 1.5% formaldehyde-containing agarose gels and blotted onto nylon membranes (GeneScreen; New England Nuclear) by capillary blotting overnight. The membranes were prehybridized and hybridized at 65°C. cDNA fragments obtained from PCR for ISA1 (5′-

CCC GGG GCT GTT GAT AGT GGA CGT GGA GGT G -3′ and 5′-AAA ATT CAC CCT TAG GAG CTA GCG -3′), ISA2 (5′- CCA TGG GTC TAA GGA AGC TGG AAT TGG AAG A -3′ and 5′-CCA TAT CCT TCA TCG ATT TAA TGG -3′), ISA3 (5′-CCA TAT CCT TCA TCG ATT TAA TGG -3′ and 5′- GAT ATG GCT AAA CTT CAG GAA GAA GC -3′) and alpha-amylase 23 (5' – CAC CAG CAG TCC TTC AGG AAG CAG TCA A-3′and 5′- ACT TCT GCC AGA CTG CAT AGC GA -3′) were used as probes and radioactively labeled with [32P]dCTP by means of the High Prime Kit (Roche). After stringent washing, radioactive membranes were exposed to X-ray films (Kodak) overnight at -80°C. Hybridization with a cDNA fragment of the small subunit of ribulose 1,5-bisphosphate carboxylase (accession no. X02353) served as a loading control.

### 5.11. Granule size distribution measurements

Micrographs of iodine stained starch granules were taken (20X magnification) and the surface area of individual granules calculated using imaging and segmentation software ImageJ (http://rsbweb.nih.gov/ij). A detailed protocol on how to determine the area of two dimensional structures using ImageJ software is available online (naranja.umh.es/~atg/tutorials/VGIV-MeasuringCellsImageJ.pdf).

## 6. References

**Bastías A, López-Climent M, Valcárcel M, Rosello S, Gómez-Cadenas A, Casaretto JA** (2011) Modulation of Organic Acids and Sugar Content in Tomato Fruits by an Abscisic Acid-Regulated Transcription Factor. Physiologia plantarum **141:** 215-226

**Baunsgaard L, Lütken H, Mikkelsen R, Glaring MA, Pham TT, Blennow A** (2005) A Novel Isoform of Glucan, Water Dikinase Phosphorylates Pre-Phosphorylated Alpha-Glucans and Is Involved in Starch Degradation in Arabidopsis. The Plant journal : for cell and molecular biology **41:** 595-605

**Beck E, Ziegler P** (1989) Biosynthesis and Degradation of Starch in Higher Plants. Annual review of plant physiology and plant molecular biology **40:** 95-117

**Bläsing O, Gibon Y, Günther M, Höhne M, Morcuende R, Osuna D, Thimm O, Usadel B, Scheible W-R, Stitt M** (2005) Sugars and Circadian Regulation Make Major Contributions to the Global Regulation of Duirnal Gene Expression in Arabidopsis. Plant cell **17:** 3257-3281

**Bologa KL, Fernie AR, Leisse A, Loureiro ME, Geigenberger P** (2003) A Bypass of Sucrose Synthase Leads to Low Internal Oxygen and Impaired Metabolic Performance in Growing Potato Tubers 1. Plant physiology **132:** 2058-2072

**Börnke F, Hajirezaei M, Heineke D, Melzer M, Herbers K, Sonnewald U** (2002) High-Level Production of the Non-Cariogenic Sucrose Isomer Palatinose in Transgenic Tobacco Plants Strongly Impairs Development. Planta **214:** 356-364

**Börnke F, Hajirezaei M, Sonnewald U** (2002) Potato Tubers as Bioreactors for Palatinose Production. Journal of biotechnology **96:** 119-124

**Bustos R, Fahy B, Hylton CM, Seale R, Nebane NM, Edwards A, Martin C, Smith AM** (2004) Starch Granule Initiation Is Controlled by a Heteromultimeric Isoamylase in Potato Tubers. Proceedings of the National Academy of Sciences of the United States of America **101:** 2215-2220

**Chia T, Thorneycroft D, Chapple A, Messerli G, Chen J, Zeeman SC, Smith SM, Smith AM** (2004) A Cytosolic Glucosyltransferase Is Required for Conversion of Starch to Sucrose in Arabidopsis Leaves at Night. The Plant Journal **37:** 853-863

**Contento AL, Kim S-J, Bassham DC** (2004) Transcriptome Profiling of the Response of Arabidopsis Suspension Culture Cell to Suc Starvation. Plant physiology **135:** 2330-2347

**Damari-Weissler H, Kandel-Kfir M, Gidoni D, Mett A, Belausov E, Granot D** (2006) Evidence for Intracellular Spatial Separation of Hexokinases and Fructokinases in Tomato Plants. Planta **224:** 1495-1502

**Davies D** (1980) Anaerobic Metabolism and the Production of Organic Acids. *In* PK Stumpf, EE Conn, eds, The Biochemistry of Plants, Vol 2. Academic Press, pp 581-609

**de Sousa CaF, Sodek L** (2003) Alanine Metabolism and Alanine Aminotransferase Activity in Soybean (Glycine Max) During Hypoxia of the Root System and Subsequent Return to Normoxia. Environmental and Experimental Botany **50:** 1-8

**Debast S, Nunes-Nesi A, Hajirezaei M-R, Hofmann J, Sonnewald U, Fernie AR, Börnke F** (2011) Altering Trehalose-6-Phosphate Content in Transgenic Potato Tubers Affects Tuber Growth and Alters Responsiveness to Hormones During Sprouting. Plant physiology **156:** 1-19

**Delatte T, Trevisan M, Parker ML, Zeeman SC** (2005) Arabidopsis Mutants Atisa1 and Atisa2 Have Identical Phenotypes and Lack the Same Multimeric Isoamylase, Which Influences the Branch Point Distribution of Amylopectin During Starch Synthesis. The Plant journal : for cell and molecular biology **41:** 815-830

**Delatte T, Umhang M, Trevisan M, Eicke S, Thorneycroft D, Smith SM, Zeeman SC** (2006) Evidence for Distinct Mechanisms of Starch Granule Breakdown in Plants. The Journal of biological chemistry **281:** 12050-12059

**Dian W, Jiang H, Chen Q, Liu F, Wu P** (2003) Cloning and Characterization of the Granule-Bound Starch Synthase Ii Gene in Rice: Gene Expression Is Regulated by the Nitrogen Level, Sugar and Circadian Rhythm. Planta **218:** 261-268

**Ding L, Hofius D, Hajirezaei M-R, Fernie AR, Börnke F, Sonnewald U** (2007) Functional Analysis of the Essential Bifunctional Tobacco Enzyme 3-Dehydroquinate Dehydratase/Shikimate Dehydrogenase in Transgenic Tobacco Plants. Journal of experimental botany **58:** 2053-2067

**Edner C, Li J, Albrecht T, Mahlow S, Hejazi M, Hussain H, Kaplan F, Guy C, Smith SM, Steup M, Ritte G** (2007) Glucan, Water Dikinase Activity Stimulates Breakdown of Starch Granules by Plastidial Beta-Amylases. Plant physiology **145:** 17-28

**Engels C, Marschner H** (1986) Allocation of Photosynthate to Individual Tubers of Solanum Tuberosum L. Journal of Experimental Botany **37:** 1795-1803

**Entus R, Poling M, Herrmann KM** (2002) Redox Regulation of Arabidopsis 3-Deoxy-D -Arabino- Heptulosonate 7-Phosphate Synthase 1. Society **129:** 1866-1871

**Farrar J** (1992) The Whole Plant: Carbon Partitioning within and between Organisms. *In* C Pollock, J Farrar, A Gordon, eds, Carbon Partition within and between Organisms. Bios Scientific, Oxford, pp 163-179

**Farre EM, Fernie AR, Willmitzer L** (2008) Analysis of Subcellular Metabolite Levels of Potato Tubers (Solanum Tuberosum) Displaying Alterations in Cellular or Extracellular Sucrose Metabolism. Metabolomics : Official journal of the Metabolomic Society **4:** 161-170

**Faye L, Daniel H** (2006) Novel Pathways for Glycoprotein Import into Chloroplasts. Plant biotechnology journal **4:** 275-279

**Feldkamp LA** (1984) Practical Cone-Beam Algorithm Sfrdr I _ F. America **1:** 612-619

**Ferreira SJ, Senning M, Sonnewald S, Kessling P-M, Goldstein R, Sonnewald U** (2010) Comparative Transcriptome Analysis Coupled to X-Ray Ct Reveals Sucrose Supply and Growth Velocity as Major Determinants of Potato Tuber Starch Biosynthesis. BMC genomics **11:** 93

**Fettke J, Albrecht T, Hejazi M, Mahlow S, Nakamura Y, Steup M** (2010) Glucose 1-Phosphate Is Efficiently Taken up by Potato (Solanum Tuberosum) Tuber Parenchyma Cells and Converted to Reserve Starch Granules. The New phytologist **185:** 663-675

**Fincher GB** (1989) Molecular and Cellular Biology Associated with the Endosperm Mobilization in Germinating Cereal Grains. annual review of plant physiology and plant molecular biology **40:** 305-346

**Fu H, Park WD** (1995) Sink- and Vascular-Associated Sucrose Synthase Functions Are Encoded by Different Gene Classes in Potato. The Plant cell **7:** 1369-1385

**Geigenberger P, Stitt M** (2000) Diurnal Changes in Sucrose, Nucleotides, Starch Synthesis and Agps Transcript in Growing Potato Tubers That Are Suppressed by

Decreased Expression of Sucrose Phosphate Synthase. The Plant journal : for cell and molecular biology **23:** 795-806

**German M** (2004) Cloning, Expression and Characterization of Lefrk3, the Fourth Tomato (Lycopersicon Esculentum Mill.) Gene Encoding Fructokinase. Plant Science **166:** 285-291

**Graham JWA, Williams TCR, Morgan M, Fernie AR, Ratcliffe RG, Sweetlove LJ** (2007) Glycolytic Enzymes Associate Dynamically with Mitochondria in Response to Respiratory Demand and Support Substrate Channeling. The Plant cell **19:** 3723-3738

**Greiner S, Rausch T, Sonnewald U, Herbers K** (1999) Ectopic Expression of a Tobacco Invertase Inhibitor Homolog Prevents Cold-Induced Sweetening of Potato Tubers. Nature biotechnology **17:** 708-711

**Hajirezaei M-R** (2003) Decreased Sucrose Content Triggers Starch Breakdown and Respiration in Stored Potato Tubers (Solanum Tuberosum). Journal of Experimental Botany **54:** 477-488

**Hajirezaei M-R, Börnke F, Peisker M, Takahata Y, Lerchl J, Kirakosyan A, Sonnewald U** (2003) Decreased Sucrose Content Triggers Starch Breakdown and Respiration in Stored Potato Tubers (Solanum Tuberosum). Journal of Experimental Botany **54:** 477-488

**Hajirezaei MR, Takahata Y, Trethewey RN, Willmitzer L, Sonnewald U** (2000) Impact of Elevated Cytosolic and Apoplastic Invertase Activity on Carbon Metabolism During Potato Tuber Development. Journal of experimental botany **51 Spec No:** 439-445

**Hanke R, Fuchs T, Uhlmann N** (2008) X-Ray Based Methods for Non-Destructive Testing and Material Characterization. Nuclear Instruments and Methods in Physics Research Section A: Accelerators, Spectrometers, Detectors and Associated Equipment **591:** 14-18

**Harmer SL** (2000) Orchestrated Transcription of Key Pathways in Arabidopsis by the Circadian Clock. Science **290:** 2110-2113

**Hartmann A, Senning M, Hedden P, Sonnewald U, Sonnewald S** (2011) Reactivation of Meristem Activity and Sprout Growth in Potato Tubers Require Both Cytokinin and Gibberellin. Plant physiology **155:** 776-796

**Hauschild R, von Schaewen A** (2003) Differential Regulation of Glucose-6-Phosphate Dehydrogenase Isoenzyme Activities in Potato 1. Plant physiology **133:** 47-62

**Heineke D, Sonnewald U, Büssis D, Günter G, Leidreiter K, Wilke I, Raschke K, Willmitzer L, Heldt HW** (1992) Apoplastic Expression of Yeast-Derived Invertase in Potato : Effects on Photosynthesis, Leaf Solute Composition, Water Relations, and Tuber Composition. Plant physiology **100:** 301-308

**Hejazi M, Fettke J, Haebel S, Edner C, Paris O, Frohberg C, Steup M, Ritte G** (2008) Glucan, Water Dikinase Phosphorylates Crystalline Maltodextrins and Thereby Initiates Solubilization. The Plant Journal **55:** 323-334

**Horst RJ, Doehlemann G, Wahl R, Hofmann J, Schmiedl A, Kahmann R, Kämper J, Voll LM** (2010) A Model of Ustilago Maydis Leaf Tumor Metabolism. Plant signaling & behavior **5:** 1446-1449

**Hovenkamp-Hermelink JHM, Jacobsen E, Ponstein aS, Visser RGF, Vos-Scheperkeuter GH, Bijmolt EW, Vries JN, Witholt B, Feenstra WJ** (1987) Isolation of an Amylose-Free Starch Mutant of the Potato (Solanum Tuberosum L.). Theoretical and Applied Genetics **75:** 217-221

**Hussain H, Mant A, Seale R, Zeeman S, Hinchliffe E, Edwards A, Hylton C, Bornemann S, Smith AM, Martin C, Bustos R** (2003) Three Isoforms of Isoamylase Contribute Different Catalytic Properties for the Debranching of Potato Glucans. Society **15:** 133-149

**Jakoby M, Weisshaar B, Dröge-Laser W, Vicente-Carbajosa J, Tiedemann J, Kroj T, Parcy F** (2002) Bzip Transcription Factors in Arabidopsis. Trends in plant science **7:** 106-111

**Junker BH, Wuttke R, Tiessen A, Geigenberger P, Sonnewald U, Willmitzer L, Fernie AR** (2004) Temporally Regulated Expression of a Yeast Invertase in Potato Tubers Allows Dissection of the Complex Metabolic Phenotype Obtained Following Its Constitutive Expression. Plant molecular biology **56:** 91-110

**Kammerer B, Fischer K, Hilpert B, Schubert S, Gutensohn M, Weber A, Flügge UI** (1998) Molecular Characterization of a Carbon Transporter in Plastids from Heterotrophic Tissues: The Glucose 6-Phosphate/Phosphate Antiporter. The Plant cell **10:** 105-117

**Kaplan F, Guy CL** (2005) Rna Interference of Arabidopsis Beta-Amylase8 Prevents Maltose Accumulation Upon Cold Shock and Increases Sensitivity of Psii Photochemical Efficiency to Freezing Stress. The Plant journal : for cell and molecular biology **44:** 730-743

**Keech O, Pesquet E, Gutierrez L, Ahad A, Bellini C, Smith SM, Gardeström P** (2010) Leaf Senescence Is Accompanied by an Early Disruption of the Microtubule Network in Arabidopsis. Plant physiology **154:** 1710-1720

**Kloosterman B, De Koeyer D, Griffiths R, Flinn B, Steuernagel B, Scholz U, Sonnewald S, Sonnewald U, Bryan GJ, Prat S, Bánfalvi Z, Hammond JP, Geigenberger P, Nielsen KL, Visser RGF, Bachem CWB** (2008) Genes Driving Potato Tuber Initiation and Growth: Identification Based on Transcriptional Changes Using the Poci Array. Functional & integrative genomics **8:** 329-340

**Kloosterman B, Vorst OFJ, Hall RD, Visser RG, Bachem CWB** (2005) Tuber on a Chip: Differential Gene Expression During Potato Tuber Development. Plant biotechnology journal**:** 505-519

**Kocal N, Sonnewald U, Sonnewald S** (2008) Cell Wall-Bound Invertase Limits Sucrose Export and Is Involved in Symptom Development and Inhibition of Photosynthesis During Compatible Interaction between Tomato and Xanthomonas Campestris Pv Vesicatoria. Plant physiology **148:** 1523-1536

**Kogel K-H, Voll LM, Schäfer P, Jansen C, Wu Y, Langen G, Imani J, Hofmann J, Schmiedl A, Sonnewald S, von Wettstein D, Cook RJ, Sonnewald U** (2010) Transcriptome and Metabolome Profiling of Field-Grown Transgenic Barley Lack Induced Differences but Show Cultivar-Specific Variances. Proceedings of the National Academy of Sciences of the United States of America **107:** 6198-6203

**Kohlhaw GB, Tan-Wilson A** (1977) Carnitine Acetyltransferase: Candidate for the Transfer of Acetyl Groups through the Mitochondrial Membrane of Yeast. Journal of bacteriology **129:** 1159-1161

**Kossmann J, Lloyd J** (2000) Understanding and Influencing Starch Biochemistry. Critical reviews in biochemistry and molecular biology **35:** 141-196

**Kossmann J, Visser RG, Mueller-Roeber B, Willmitzer L, Sonnewald U** (1991) Cloning and Expression Analysis of a Potato Cdna That Encodes Branching Enzyme:

Evidence for Co-Expression of Starch Biosynthetic Genes. Molecular And General Genetics **230:** 39-44

**Kötting O, Kossmann J, Zeeman SC, Lloyd JR** (2010) Regulation of Starch Metabolism: The Age of Enlightenment? Current opinion in plant biology **13:** 321-329

**Kötting O, Santelia D, Edner C, Eicke S, Marthaler T, Gentry MS, Comparot-Moss S, Chen J, Smith AM, Steup M, Ritte G, Zeeman SC** (2009) Starch-Excess4 Is a Laforin-Like Phosphoglucan Phosphatase Required for Starch Degradation in Arabidopsis Thaliana. The Plant cell **21:** 334-346

**Kruger NJ** (1997) Carbohydrate Synthesis and Degradation. *In* DT Longmann, D Turpin, D Lefebre, D Layzell, eds, Plant Metabolism. Harlow, pp 83-104

**Lloyd JR, Blennow A, Burhenne K, Kossmann J, Germany JRL** (2004) Repression of a Novel Isoform of Disproportionating Enzyme ( Stdpe2 ) in Potato Leads to Inhibition of Starch Degradation in Leaves but Not Tubers Stored at Low Temperature 1. Enzyme **134:** 1347-1354

**Lloyd JR, Landschu V, Kossmann J** (1999) Tubers Leads to Accumulation of Grossly Modified Amylopectin. Society **521:** 515-521

**Loewus FA, Loewus MW** (1980) Myo-Inositol-1-Phosphatase from the Pollen of Lilium Longiflorum Thunb. Plant physiology **70:** 765-770

**Loewus MW, Loewus Fa, Brillinger GU, Otsuka H, Floss HG** (1980) Stereochemistry of the Myo-Inositol-1-Phosphate Synthase Reaction. The Journal of biological chemistry **255:** 11710-11712

**Logemann J, Schell J, Willmutzer L** (1987) Improved Method for the Isolation of Rna from Plant Tissues Plant Tissues. Analytical biochemistry **20:** 16-20

**Lohaus G, Winter H, Riens B, Heldt HW** (1995) Further Studies of the Phloem Loading Process in Leaves of Barley and Spinach - Comparison of the Metabolite Concentration in the Apoplastic Compartment with Those in the Cytosolic Compartment and in the Sieve Tubes. Botanica Acta **108**

**Lorberth R, Ritte G, Willmitzer L, kossmann j** (1998) Inhibition of a Starch-Granule-Bound Protein Leads to Modified Starch and Repression of Cold Sweetening. nature biotechnology **16:** 473-477

**Lu Y, Gehan JP, Sharkey TD** (2005) Daylength and Circadian Effects on Starch Degradation and Maltose Metabolism 1. Society **138:** 2280-2291

**Lütken H, Lloyd JR, Glaring Ma, Baunsgaard L, Laursen KH, Haldrup A, Kossmann J, Blennow A** (2010) Repression of Both Isoforms of Disproportionating Enzyme Leads to Higher Malto-Oligosaccharide Content and Reduced Growth in Potato. Planta **232:** 1127-1139

**Ma JK-C, Drake PMW, Christou P** (2003) The Production of Recombinant Pharmaceutical Proteins in Plants. Nature reviews. Genetics **4:** 794-805

**Macheroux P, Schmid J, Amrhein N, Schaller A** (1999) A Unique Reaction in a Common Pathway: Mechanism and Function of Chorismate Synthase in the Shikimate Pathway. Planta **207:** 325-334

**McCormick A, Cramer M, Watt D** (2006) Sink Strength Regulates Photosynthesis in Sugarcane. New Phytologist **171:** 759-770

**Melnyk C, Molnar A, Baulcombe DC** (2011) Intercellular and Systemic Movement of Rna Silencing Signals. The EMBO journal **30:** 3553-3563

**Merida A, Rodriguez-Galan JM, Vincent C, Romero JM** (1999) Expression of the Granule Bound Starch Synthase I (Waxy) Gene from Snapdragon Is Developmentally and Circadian Clock Regulated. Plant physiology **120:** 401-409

**Miyashita Y, Dolferus R, Ismond KP, Good AG** (2007) Alanine Aminotransferase Catalyses the Breakdown of Alanine after Hypoxia in Arabidopsis Thaliana. The Plant journal : for cell and molecular biology **49:** 1108-1121

**Müller-Röber B, Sonnewald U, Willmitzer L** (1992) Inhibition of the Adp-Glucose Pyrophosphorylase in Transgenic Potatoes Leads to Sugar-Storing Tubers and Influences Tuber Formation and Expression of Tuber Storage Protein Genes. The EMBO journal **11:** 1229-1238

**Murashige T, Skoog F** (1962) A Revised Medium for Rapid Growth and Bio Assays with Tobacco Tissue Cultures. Physiologia Plantarum **15:** 473-497

**Nielsen TH, Rung JH, Villadsen D** (2004) Fructose-2,6-Bisphosphate: A Traffic Signal in Plant Metabolism. Trends in plant science **9:** 556-563

**Niittylä T, Comparot-Moss S, Lue WL, Messerli G, Trevisan M, seymour MD, Gatehouse JA, Villadsen D, Smith SM, Chen J, Zeeman SC, Smith AM** (2006)

Similar Protein Phosphatases Control Starch Metabolism in Plants and Glycogen Metabolism in Mammals. Journal of Biological Chemistry **281:** 11815-11818

**Niittylä T, Messerli G, Trevisan M, Chen J, Smith AM, Zeeman SC** (2004) A Previously Unknown Maltose Transporter Essential for Starch Degradation in Leaves. Science (New York, N.Y.) **303:** 87-89

**Obembe OO, Popoola JO, Leelavathi S, Reddy SV** (2011) Advances in Plant Molecular Farming. Biotechnology advances **29:** 210-222

**Okushima Y, Mitina I, Quach HL, Theologis A** (2005) Auxin Response Factor 2 (Arf2): A Pleiotropic Developmental Regulator. The Plant journal : for cell and molecular biology **43:** 29-46

**Osuna D, Usadel B, Morcuende R, Gibon Y, Bläsing OE, Höhne M, Günter M, Kamlage B, Trethewey R, Scheible W-R, Stitt M** (2007) Temporal Responses of Transcripts, Enzyme Activities and Metabolites after Adding Sucrose to Carbon-Deprived Arabidopsis Seedlings. The Plant journal : for cell and molecular biology **49:** 463-491

**Patel TB, Clark JB** (1980) Lipogenesis in the Brain of Suckling Rats. Studies on the Mechansim of Mitochondrial-Cytosolic Carbon Transfer. The Biochemical journal **188:** 163-168

**Periappuram C, Steinhauer L, Barton DL, Taylor DC, Chatson B, Zou J** (2000) The Plastidic Phosphoglucomutase from Arabidopsis. A Reversible Enzyme Reaction with an Important Role in Metabolic Control. Plant physiology **122:** 1193-1199

**Pfaffl MW** (2001) A New Mathematical Model for Relative Quantification in Real-Time Rt-Pcr. Nucleic acids research **29:** e45

**Pinto JE, Dyer WE, Weller SC, Herrmann KM** (1988) Glyphosate Induces 3-Deoxy-D-Arabino-Heptulosonate 7-Phosphate Synthase in Potato (Solanum Tuberosum L.) Cells Grown in Suspension Culture. Plant physiology **87:** 891-893

**Rahman S, Nakamura Y, Li Z, Clarke B, Fujita N, Mukai Y, Yamamoto M, Regina A, Tan Z, Kawasaki S, Morell M** (2003) The Sugary-Type Isoamylase Gene from Rice and Aegilops Tauschii : Characterization and Comparison with Maize and Arabidopsis. Structure **506:** 496-506

**Ral JP, Colleoni C, Wattebled F, Dauvilleé D, Nempont C, Deschamps P, Li Z, Morrel MK, Chibbar R, Purton S, d´Hulst C, Ball S** (2006) Circadian Clock Regulation of Starch Metabolism Establishes Gbssi as a Major Conributor to Amylopectin Synthesis in *Chlamydomonas Reinhardtii*. Plant physiology **142:** 305-317

**Rangasamy D, Ratledge C** (2000) Compartmentation of Atp:Citrate Lyase in Plants. Plant physiology **122:** 1225-1230

**Renz A, Stitt M** (1993) Substrate Specificity and Product Inhibition of Different Forms of Fructokinases and Hexokinases in Developing Potato Tubers. Planta **190:** 166-175

**Ritte G, Lloyd JR, Eckermann N, Rottmann A, Kossmann J, Steup M** (2002) Water Dikinase. Reactions**:** 1-6

**Roitsch T, Bittner M, Godt DE** (1995) Induction of Apoplastic Invertase of Chenopodium Rubrum by D-Glucose and a Glucose Analog and Tissue-Specific Expression Suggest a Role in Sink-Source Regulation. Plant physiology **108:** 285-294

**Roitsch T, González M-C** (2004) Function and Regulation of Plant Invertases: Sweet Sensations. Trends in plant science **9:** 606-613

**Roldán I, Wattebled F, Mercedes Lucas M, Delvallé D, Planchot V, Jiménez S, Pérez R, Ball S, D'Hulst C, Mérida A** (2007) The Phenotype of Soluble Starch Synthase Iv Defective Mutants of Arabidopsis Thaliana Suggests a Novel Function of Elongation Enzymes in the Control of Starch Granule Formation. The Plant journal : for cell and molecular biology **49:** 492-504

**Rolland F, Baena-Gonzalez E, Sheen J** (2006) Sugar Sensing and Signaling in Plants: Conserved and Novel Mechanisms. Annual review of plant biology **57:** 675-709

**Scheidig A, Frohlich A, Schulze S, Lloyd JR, Kossmann J** (2002) Downregulation of a Chloroplast-Targeted Beta-Amylase Leads to a Starch-Excess Phenotype in Leaves. The Plant Journal **30:** 581-591

**Schwall GP, Safford R, Westcott RJ, Jeffcoat R, Tayal A, Shi YC, Gidley MJ, Jobling SA** (2000) Production of Very-High-Amylose Potato Starch by Inhibition of Sbe a and B. Nature biotechnology **18:** 551-554

**Smith AM, Zeeman SC** (2006) Quantification of Starch in Plant Tissues. Nature protocols **1:** 1342-1345

**Smith AM, Zeeman SC, Smith SM** (2005) Starch Degradation. Annual review of plant biology **56:** 73-98

**Smith SM, Fulton DC, Chia T, Thorneycroft D, Chapple A, Dunstan H, Hylton C, Zeeman SC, Smith AM** (2004) Diurnal Changes in the Transcriptome Encoding Enzymes of Starch Metabolism Provide Evidence for Both Transcriptional and Posttranscriptional Regulation of Starch Metabolism in Arabidopsis Leaves 1. Society **136:** 2687-2699

**Sonnewald U** (2001) Control of Potato Tuber Sprouting. Trends in plant science **6:** 333-335

**Sonnewald U, Hajirezaei M-R, Kossmann J, Heyer A, Trethewey RN, Willmitzer L** (1997) Increased Potato Tuber Size Resulting from the Apoplastic Expression of a Yeast Invertase. Nature biotechnology **15**

**Stark DM, Timmerman KP, Barry GF, Preiss J, Kishore GM** (1992) Regulation of the Amount of Starch in Plant Tissues by Adp Glucose Pyrophosphorylase. Science (New York, N.Y.) **258:** 287-292

**Streatfield SJ** (2006) Mucosal Immunization Using Recombinant Plant-Based Oral Vaccines. Methods **38:** 150-157

**Streb S, Delatte T, Umhang M, Eicke S, Schorderet M, Reinhardt D, Zeeman SC** (2008) Starch Granule Biosynthesis in Arabidopsis Is Abolished by Removal of All Debranching Enzymes but Restored by the Subsequent Removal of an Endoamylase. The Plant cell **20:** 3448-3466

**Sweetlove LJ, Burrell MM, Rees T** (1996) Increased Adpglucose Pyrophosphorylase *. Planta **498:** 493-498

**Sweetlove LJ, Kossmann J, Riesmeier JW, Trethewey RN, Hill SA** (1998) The Control of Source to Sink Carbon Flux During Tuber Development in Potato. The Plant Journal **15:** 697-706

**Szydlowski N, Ragel P, Raynaud S, Lucas MM, Roldán I, Montero M, Muñoz FJ, Ovecka M, Bahaji A, Planchot V, Pozueta-Romero J, D'Hulst C, Mérida A** (2009) Starch Granule Initiation in Arabidopsis Requires the Presence of Either Class Iv or Class Iii Starch Synthases. The Plant cell **21:** 2443-2457

**Takeda Y, Hizukuri S** (1981) Studies on Starch Phosphate. Part 5. Reexamination of the Action of Sweet-Potato Beta-Amylase on Phosphorylated (1->4)-a-D-Glucan. Carbohydrate research **89:** 174-178

**Tauberger E, Fernie aR, Emmermann M, Renz a, Kossmann J, Willmitzer L, Trethewey RN** (2000) Antisense Inhibition of Plastidial Phosphoglucomutase Provides Compelling Evidence That Potato Tuber Amyloplasts Import Carbon from the Cytosol in the Form of Glucose-6-Phosphate. The Plant journal : for cell and molecular biology **23:** 43-53

**Tenorio G, Orea A, Romero JM, Mérida A** (2003) Oscillation of Mrna Level and Activity of Granule-Bound Starch Synthase I in Arabidopsis Leaves During the Day/Night Cycle. Plant molecular biology **51:** 949-958

**Thimm O, Bläsing O, Gibon Y, Nagel A, Meyer S, Krüger P, Selbig J, Müller La, Rhee SY, Stitt M** (2004) Mapman: A User-Driven Tool to Display Genomics Data Sets onto Diagrams of Metabolic Pathways and Other Biological Processes. The Plant Journal **37:** 914-939

**Tjaden J, Mohlmann T, Kampfenkel K, Neuhaus GHaE** (1998) Altered Plastidic Atp/Adp-Transporter Activity Influences Potato (Solanum Tuberosuml.) Tuber Morphology, Yield and Composition of Tuber Starch. The Plant Journal **16:** 531-540

**Trethewey RN, Fernie aR, Bachmann a, Fleischer-Notter H, Geigenberger P, Willmitzer L** (2001) Expression of a Bacterial Sucrose Phosphorylase in Potato Tubers Results in a Glucose-Independent Induction of Glycolysis. Plant, Cell and Environment **24:** 357-365

**Trethewey RN, Geigenberger P, Riedel K, Hajirezaei MR, Sonnewald U, Stitt M, Riesmeier JW, Willmitzer L** (1998) Combined Expression of Glucokinase and Invertase in Potato Tubers Leads to a Dramatic Reduction in Starch Accumulation and a Stimulation of Glycolysis. The Plant journal : for cell and molecular biology **15:** 109-118

**Urbanczyk-Wochniak E, Luedemann A, Kopka J, Selbig J, Roessner-Tunali U, Willmitzer L, Fernie AR** (2003) Parallel Analysis of Transcript and Metabolic Profiles: A New Approach in Systems Biology. EMBO reports **4:** 989-993

**Viola R, Roberts AG, Haupt S, Gazzani S, Hancock RD, Marmiroli N, Machray GC, Oparka KJ** (2001) Tuberization in Potato Involves a Switch from Apoplastic to Symplastic Phloem Unloading. The Plant cell **13:** 385-398

**Visser RG, Somhorst I, Kuipers GJ, Ruys NJ, Feenstra WJ, Jacobsen E** (1991) Inhibition of the Expression of the Gene for Granule-Bound Starch Synthase in Potato by Antisense Constructs. Molecular & general genetics : MGG **225:** 289-296

**von Schaewen a, Langenkämper G, Graeve K, Wenderoth I, Scheibe R** (1995) Molecular Characterization of the Plastidic Glucose-6-Phosphate Dehydrogenase from Potato in Comparison to Its Cytosolic Counterpart. Plant physiology **109:** 1327-1335

**Wegrzryn T, Reilly K, Cipriani G, Murphy P, Newcomb R, Gardner R, Macrae E** (2000) A Novel a-Amylase Gene Is Transiently Upregulated During Low Temperature Exposure in Apple Fruit. European Journal of Biochemistry**:** 1313-1322

**Wenderoth I, Scheibe R, von Schaewen A** (1997) Identification of the Cysteine Residues Involved in Redox Modification of Plant Plastidic Glucose-6-Phosphate Dehydrogenase. The Journal of biological chemistry **272:** 26985-26990

**Wiese A, Elzinga N, Wobbes B, Smeekens SC** (2004) A Conserved Upstream Open Reading Frame Mediates Sucrose-Induced Repression of Translation. Plant Cell **16:** 1717-1729

**Wilson JE** (2003) Isozymes of Mammalian Hexokinase: Structure, Subcellular Localization and Metabolic Function. Journal of Experimental Biology **206:** 2049-2057

**Wingler A** (1998) Regulation of Leaf Senescence by Cytokinin, Sugars, and Light . Effects on Nadh-Dependent Hydroxypyruvate Reductase. Plant Physiology **116:** 329-335

**Wright DP, Huppe HC, Turpin DH** (1997) In Vivo and in Vitro Studies of Clucose-6-Phosphate Dehydrogenase from Barley Root Plastids in Relation to Reductant Supply for No , Assimilation '. Plant Physiology**:** 1413-1419

**Wu L, Birch RG** (2007) Doubled Sugar Content in Sugarcane Plants Modified to Produce a Sucrose Isomer. Plant biotechnology journal **5:** 109-117

**Xu X, Pan S, Cheng S, Zhang B, Mu D, Ni P, Zhang G, Yang S, Li R, Wang J, Orjeda G, Guzman F, Torres M, Lozano R, Ponce O, Martinez D, De la Cruz G, Chakrabarti SK, Patil VU, Skryabin KG, Kuznetsov BB, Ravin NV, Kolganova TV, Beletsky AV, Mardanov AV, Di Genova A, Bolser DM, Martin DMa, Li G, Yang Y,**

**Kuang H, Hu Q, Xiong X, Bishop GJ, Sagredo B, Mejía N, Zagorski W, Gromadka R, Gawor J, Szczesny P, Huang S, Zhang Z, Liang C, He J, Li Y, He Y, Xu J, Zhang Y, Xie B, Du Y, Qu D, Bonierbale M, Ghislain M, Del Rosario Herrera M, Giuliano G, Pietrella M, Perrotta G, Facella P, O'Brien K, Feingold SE, Barreiro LE, Massa Ga, Diambra L, Whitty BR, Vaillancourt B, Lin H, Massa AN, Geoffroy M, Lundback S, Dellapenna D, Robin Buell C, Sharma SK, Marshall DF, Waugh R, Bryan GJ, Destefanis M, Nagy I, Milbourne D, Thomson SJ, Fiers M, Jacobs JME, Nielsen KL, Sønderkær M, Iovene M, Torres Ga, Jiang J, Veilleux RE, Bachem CWB, de Boer J, Borm T, Kloosterman B, van Eck H, Datema E, Te Lintel Hekkert B, Goverse A, van Ham RCHJ, Visser RGF** (2011) Genome Sequence and Analysis of the Tuber Crop Potato. Nature **475:** 189-195

**Yu T-S, Zeeman SC, Thorneycroft D, Fulton DC, Dunstan H, Lue W-L, Hegemann B, Tung S-Y, Umemoto T, Chapple A, Tsai D-L, Wang S-M, Smith AM, Chen J, Smith SM** (2005) Alpha-Amylase Is Not Required for Breakdown of Transitory Starch in Arabidopsis Leaves. The Journal of biological chemistry **280:** 9773-9779

**Zeeman SC, Umemoto T, Lue WL, Au-Yeung P, Martin C, Smith aM, Chen J** (1998) A Mutant of Arabidopsis Lacking a Chloroplastic Isoamylase Accumulates Both Starch and Phytoglycogen. The Plant cell **10:** 1699-1712

**Zhang L, Häusler RE, Greiten C, Hajirezaei M-R, Haferkamp I, Neuhaus HE, Flügge U-I, Ludewig F** (2008) Overriding the Co-Limiting Import of Carbon and Energy into Tuber Amyloplasts Increases the Starch Content and Yield of Transgenic Potato Plants. Plant biotechnology journal **6:** 453-464

**Zrenner R, Krause KP, Apel P, Sonnewald U** (1996) Reduction of the Cytosolic Fructose-1,6-Bisphosphatase in Transgenic Potato Plants Limits Photosynthetic Sucrose Biosynthesis with No Impact on Plant Growth and Tuber Yield. The Plant journal : for cell and molecular biology **9:** 671-681

**Zrenner R, Salanoubat M, Willmitzer L, Sonnewald U** (1995) Evidence of the Crucial Role of Sucrose Synthase for Sink Strength Using Transgenic Potato Plants (Solanum Tuberosum L.). The Plant Journal **7:** 97-107

## Supplemental data.

**Table S1. Phosphorylated intermediates and organic acids in Desireé, U-IN-1 and U-IN-2 tubers.**

Average ± standard deviation. Bold indicates significance compared to WT ($p \leq 0.05$) (n=3-4).

| **Organic acids and phosporylated intermediates (nmol/ g FW)** | **Desireé** | **U-IN-1** | **U-IN-2** |
|---|---|---|---|
| Phosho-enol-pyruvate | 22.8 ± 1.3 | 26.2 ± 4.9 | **40.7 ±3.8** |
| Glucose 6-phosphate | 117.2 ± 9.1 | 116.0 ±13.5 | **355.5 ± 55.2** |
| Glucose 1-phosphate | 20.2 ± 5.3 | 14.3 ±4.7 | 23.3 ± 1.7 |
| Succinate | 83.5 ± 23.8 | **32.2 ±7.9** | 108.2 ±13.4 |
| Fumarate | 31.5 ± 3.8 | 28.8 ±9.1 | **10.3 ± 2.3** |
| Shikimate | 7.0 ± 2.9 | 5.1 ±2.4 | **65.5 ±10.1** |
| UDP-N-acetylglucosamine | 4.1 ± 1.5 | 4.3 ±2.3 | 4.2 ± 0.8 |
| 3-Phophoglycerate | 102.1 ± 9.2 | 112.6 ± 8.6 | **203.1 ± 7.9** |
| Trehalose 6-phosphate | 0.9 ± 0.2 | **0.3 ± 0.2** | **0.5 ± 0.1** |
| Sucrose 6-phosphate | 0.5 ± 0.1 | 0.4 ± 0.2 | **0.1 ±0.0** |
| Fructose 6-phosphate | 22.7 ± 3.1 | **47.2 ± 11.6** | **126.0 ± 18.1** |
| Fructose 1,6-bisphosphate | 0.6 ±0.2 | 0.4 ± 0.1 | **1.5 ± 0.3** |
| Erythrose 4-phosphate | 18.8 ± 3.7 | 21.0 ± 4.1 | **58.2 ±6.6** |
| Glucose 1,6-bisphosphate | 2.8 ± 0.6 | 3.9 ± 1.7 | 2.6 ±1.4 |
| Ribulose 1,5-bisphosphate | 1534.5 ± 160.6 | 1481.7 ± 269.8 | 1665.4 ± 426.9 |
| Dihydroxyacetone-phosphate | 8.3 ± 2.4 | 9.8 ± 5.4 | **28.3 ± 2.6** |
| 2-Oxoglutarate | 6.6 ± 2.6 | 8.0 ± 1.4 | **9.5 ± 2.1** |
| Citrate | 7087.9 ± 720.7 | 7637.1 ± 1137.4 | **8272.5 ± 420.4** |
| Malate | 1989.1 ±229.5 | 1757.7 ± 230.1 | **3131.7 ± 29.2** |
| Inorganic pyrophosphate | 8.4 ± 2.2 | **1.8 ± 0.7** | 10.6 ± 0.7 |

**Table S2. Amino acids in Desireé, U-IN-1 and U-IN-2 tubers** . Average ± standard deviation. Bold indicates a significance compared to WT ($p \leq 0.05$) (n=3-4).

| Amino acid (nmol/ g FW) | Desireé | U-IN-1 | U-IN-2 |
|---|---|---|---|
| Aspartic acid | 490.2 ± 68.4 | 378.8 ±12.1 | **1066.0 ± 39.0** |
| Glutamic acid | 830.1 ±108.8 | 724.7 ±22.0 | 1130.1 ± 37.8 |
| Serine | 447.0 ±74.2 | 301.6 ±22.3 | **865.8 ± 16.4** |
| Glutamine | 1594.0 ±289.0 | 1004.4 ± 116.1 | 2451.4 ± 67.5 |
| Glycine | 147.8 ±29.8 | 95.5 ± 3.4 | 145.3 ± 13.6 |
| Histidine | 566.9 ±98.7 | 323.9 ±7.8 | **264.7 ± 2.4** |
| Threonine | 7131.6 ±1345.4 | 5741.5 ± 74.0 | 7820.1 ± 530.7 |
| Arginine | 429.0 ±81.5 | 248.3 ±20.0 | 283.3 ± 7.2 |
| Alanine | 361.6 ±76.2 | **164.6 ± 9.3** | **1099.8 ± 180.3** |
| Proline | 71.3 ±126.9 | **55.6 ±5.6** | 69.8 ± 13.4 |
| Tyrosine | 1845.4 ±9.1 | **1046.1 ± 64.5** | **826.3 ± 89.5** |
| Valine | 2365.7 ±308.7 | **1068.5 ± 31.9** | **876.3 ± 41.8** |
| Methionine | 1248.8 ±227.7 | 648.6 ± 15.4 | 681.7 ± 55.3 |
| Isoleucine | 1830.0 ±336.4 | **799.4 ±15.0** | **463.2 ± 27.6** |
| Lysine | 264.6 ±39.6 | **122.1 ± 9.1** | **45.8 ± 3.0** |
| Leucine | 464.4 ± 68.7 | 310.7 ± 14.6 | 242.3 ± 25.9 |
| Phenylalanine | 1222.4 ± 207.0 | 688.5 ± 11.4 | 1295.0 ± 98.6 |
| Total | 21310.9 ± 4518.9 | **13861.8 ± 425.2** | 19804.1 ± 1000.2 |

**Table S3. Major carbohydrates in Desireé, U-IN-1 and U-IN-2 tubers**. Average ± standard deviation. Bold indicates significance compared to WT ($p \leq 0.05$) (n = 7-8).

| **Major metabolite (µmol/ g FW)** | **Desireé** | **U-IN-1** | **U-IN-2** |
|---|---|---|---|
| Starch | 483.1± 73.5 | 469.8± 28.9 | **393.3± 41.6** |
| Sucrose | 6.8± 1.7 | **1.6± 1.4** | **0.2± 1.2** |
| Glucose | 2.0± 1.1 | **7.3± 0.3** | **49.0± 0.2** |

**Table S4.Carotenoid contents in growing Desireé, U-IN-1 and U-IN-2 tubers**.Average ± standard deviation. Bold indicates significance compared to WT ($p \leq 0.05$) (n=3-4).

| **Carotenoids (pmol/ g FW)** | **Desireé** | **U-IN-1** | **U-IN-2** |
|---|---|---|---|
| cis-Neoxanthin | 189.5± 13.5 | **145.3± 16.3** | 190.9 ±70.3 |
| Violaxanthin | 943.7± 76.7 | **186.3±15.7** | **568.2 ±95.2** |
| Antheraxanthin | 760.0± 91.8 | **624.2±11.6** | 798.4 ±52.9 |
| Lutein | 255.5± 7.9 | **140.2±8.6** | 231.3 ±34.4 |
| Zeaxanthin | 643.6± 124.8 | **912.2±61.2** | **1200.0 ± 116** |
| Beta Carotine | 6.8± 3.3 | 2.9±0.5 | **19.2 ± 1.4** |

**Table S5. Features correlating with invertase in potato tubers under various conditions**. $p \geq 0.95$.

| POCI identifier | Similarity | Description |
|---|---|---|
| MICRO.11340.C1_1543 | 1.00 | cell wall apoplastic invertase [Vitis vinifera] |
| STMJG56TV_464 | 0.98 | NA |
| MICRO.6998.C3_730 | 0.98 | putative protein |
| 063E04AF.esd_592 | 0.97 | mitogen-activated protein kinase |
| STMJC52TH_686 | 0.97 | auxin response factor 2 |
| bf_arrayxxx_0025a04.t7m.scf_360 | 0.97 | NA |
| MICRO.5974.C1_1055 | 0.97 | ATPUP3; purine transporter |
| MICRO.5158.C1_535 | 0.97 | NA |
| MICRO.15048.C1_959 | 0.97 | putative non-phototropic hypocotyl 3-like protein |
| MICRO.4882.C2_1040 | 0.97 | kinase |
| POCA901TP_857 | 0.97 | Zinc finger, Dof-type |
| bf_mxlfxxxx_0063b10.t3m.scf_672 | 0.97 | myosin XI |
| MICRO.7638.C1_1367 | 0.97 | Glycoside hydrolase, starch-binding |
| bf_mxlfxxxx_0024h12.t3m.scf_335 | 0.97 | Os04g0687900 |
| MICRO.12678.C1_147 | 0.97 | NA |
| MICRO.6764.C1_277 | 0.97 | Agamous-like MADS-box protein AGL8 homolog |
| MICRO.819.C2_1427 | 0.97 | BEL1-related homeotic protein 11 |
| bf_stolxxxx_0050a10.t7m.scf_477 | 0.97 | NA |
| bf_swstxxxx_0052h02.t3m.scf_432 | 0.97 | NA |
| MICRO.8707.C1_599 | 0.97 | unknown protein |
| MICRO.8790.C2_101 | 0.96 | MYB transcription factor MYB48-2 |
| bf_mxflxxxx_0025e05.t3m.scf_364 | 0.96 | ATPUP2 |
| bf_arrayxxx_0020g05.t7m.scf_478 | 0.96 | NA |
| MICRO.3733.C1_1621 | 0.96 | AREB-like protein |
| MICRO.12678.C2_142 | 0.96 | NA |
| MICRO.313.C1_1145 | 0.96 | Zinc finger, Dof-type |
| MICRO.354.C2_2000 | 0.96 | amino acid permease |
| STMGU42TV_738 | 0.96 | ser-thr protein kinase |
| bf_ivrootxx_0045g03.t3m.scf_584 | 0.96 | DNA methyltransferase |
| MICRO.905.C1_1771 | 0.96 | abscisic insensitive 1B |
| MICRO.6998.C1_710 | 0.96 | Zinc finger, RING-type |
| MICRO.10013.C1_758 | 0.96 | unknown |
| MICRO.746.C4_61 | 0.96 | calmodulin binding |
| MICRO.17390.C1_461 | 0.96 | Homeodomain-related |

| | | |
|---|---|---|
| bf_suspxxxx_0004c09.t3m.scf_41 | 0.96 | unknown protein |
| MICRO.5809.C1_1442 | 0.96 | AOBP (ascorbate oxidase promoter-binding protein) |
| MICRO.10812.C1_790 | 0.96 | NA |
| MICRO.6432.C4_684 | 0.96 | NA |
| MICRO.3895.C2_662 | 0.96 | Zinc finger, B-box |
| MICRO.9283.C1_738 | 0.96 | NA |
| MICRO.15137.C1_995 | 0.95 | Pathogenesis-related transcriptional factor and ERF |
| MICRO.6865.C1_814 | 0.95 | putative permease I |
| bf_mxlfxxxx_0016c12.t3m.scf_565 | 0.95 | NA |
| MICRO.3305.C1_808 | 0.95 | arginase 1 |
| MICRO.15773.C1_618 | 0.95 | farnesylated protein (ATFP6) |
| MICRO.13163.C1_882 | 0.95 | hypothetical protein OsI_033557 |
| MICRO.773.C7_129 | 0.95 | Zinc finger, B-box |
| MICRO.1889.C14_348 | 0.95 | CYP72A56 |
| bf_mxflxxxx_0067e11.t3m.scf_533 | 0.95 | NA |
| MICRO.331.C112_270 | 0.95 | NA |
| STDB001N20u.scf_478 | 0.95 | unnamed protein product |
| MICRO.4807.C5_788 | 0.95 | ubiqutin ligase |
| MICRO.1573.C2_978 | 0.95 | N3 like protein |
| MICRO.8707.C2_607 | 0.95 | unknown protein |

**Table S6. Features correlating with GPT2 in potato tubers under various conditions**. $p \geq 0.95$.

| POCI identifier | Similarity | Description |
|---|---|---|
| MICRO.1076.C1_1353 | 1.00 | glucose-6-phosphate/phosphate translocator 2 |
| 174G02AF.esd_341 | 1.00 | glucose-6-phosphate/phosphate translocator 2 |
| ACDA04204G04.T3m.scf_149 | 0.99 | NA |
| MICRO.71.C6_669 | 0.98 | Adenosylhomocysteinase |
| cSTA23K1TH_449 | 0.98 | Glycoside hydrolase, family 1 |
| MICRO.8706.C2_834 | 0.98 | cellulose synthase catalytic subunit |
| MICRO.1831.C5_44 | 0.98 | Plastidic ATP/ADP-transporter |
| MICRO.15669.C1_665 | 0.98 | kinase |
| cSTA32N23TH_281 | 0.98 | Armadillo |
| TBSK02558FF02.t3m.scf_460 | 0.98 | NA |
| TBSK03704FE08.t3m.scf_65 | 0.98 | proline-rich protein |
| MICRO.4029.C1_965 | 0.98 | glucose-6-phosphate/phosphate-translocator precursor |
| MICRO.3904.C1_979 | 0.98 | Os02g0200800 [Oryza sativa |
| MICRO.1850.C2_999 | 0.98 | granule-bound starch synthase isoform II |
| MICRO.15327.C1_616 | 0.97 | unknown protein |
| MICRO.385.C1_2301 | 0.97 | inorganic pyrophosphatase |
| BF_TUBSXXXX_0063G12_T3M.SCF_11 | 0.97 | AOAT2 |
| MICRO.10461.C2_757 | 0.97 | protein binding / ubiquitin-protein ligase/ zinc ion binding |
| ACDA02792A08.T3m.scf_24 | 0.97 | S-adenosyl-L-homocysteine hydrolase-like |
| bf_mxlfxxxx_0054b04.t3m.scf_168 | 0.97 | Os03g0729200 |
| 021C09AF.esd_326 | 0.97 | fructokinase-like |
| bf_arrayxxx_0002h07.t7m.scf_270 | 0.97 | NA |
| MICRO.5608.C1_1764 | 0.97 | hypothetical protein OsI_030111 |
| MICRO.920.C5_1 | 0.97 | starch (bacterial glycogen) synthase |
| MICRO.6116.C1_431 | 0.97 | proline-rich protein |
| MICRO.16694.C1_264 | 0.97 | protein binding / signal transducer |
| MICRO.11617.C1_3 | 0.97 | rapid alkalinization factor 5 |
| MICRO.1743.C2_1865 | 0.96 | Phosphoglucomutase, chloroplast precursor |
| MICRO.2364.C1_109 | 0.96 | 40S ribosomal protein S4-like protein |
| MICRO.5092.C1_534 | 0.96 | ATP binding |
| cSTA26M21TH_336 | 0.96 | nuclear RNA binding protein-like |
| MICRO.71.C7_1722 | 0.96 | S-adenosyl-L-homocysteine hydrolase-like |
| bf_stolxxxx_0048b11.t7m.scf_353 | 0.96 | NA |
| MICRO.1878.C1_537 | 0.96 | Glycoside hydrolase, family 1 |
| MICRO.2198.C1_1938 | 0.96 | ADPglucose pyrophosphorylase large subunit |

| | | |
|---|---|---|
| TBSK04995FA03.t3m.scf_32 | 0.96 | NA |
| bf_arrayxxx_0090e03.t7m.scf_21 | 0.96 | Granule-bound starch synthase 2, chloroplast precursor |
| MICRO.12298.C1_255 | 0.96 | NA |
| bf_lbchxxxx_0058c04.t3m.scf_7 | 0.96 | NA |
| MICRO.10329.C1_832 | 0.96 | Prefoldin |
| MICRO.908.C1_1037 | 0.96 | hydrolase |
| MICRO.920.C2_1499 | 0.96 | Granule-bound starch synthase 1 |
| MICRO.17251.C1_487 | 0.96 | unnamed protein product |
| TBSK04766FF02.t3m.scf_132 | 0.96 | patatin storage protein |
| MICRO.5190.C1_1884 | 0.96 | galactokinase like protein |
| MICRO.8302.C1_701 | 0.96 | NA |
| MICRO.960.C1_679 | 0.96 | Os04g0474800 |
| 090G05AF.esd_88 | 0.95 | NA |
| 149E07AF.esd_570 | 0.95 | ripening-related protein-like |
| MICRO.960.C2_1012 | 0.95 | Glycoside hydrolase, family 1 |
| MICRO.10963.C2_84 | 0.95 | pectinesterase (EC 3.1.1.11) precursor (clone PE1) |
| bf_arrayxxx_0075c09.t3m.scf_514 | 0.95 | fructokinase |
| MICRO.4512.C1_1002 | 0.95 | (-)-isopiperitenol dehydrogenase |
| MICRO.1520.C14_346 | 0.95 | patatin protein group D-1 |
| MICRO.1831.C3_694 | 0.95 | Plastidic ATP/ADP-transporter |
| MICRO.4029.C2_1110 | 0.95 | glucose-6-phosphate/phosphate-translocator precursor |
| MICRO.1818.C1_940 | 0.95 | unknown protein |
| MICRO.694.C1_1662 | 0.95 | pectate lyase |
| MICRO.2447.C1_705 | 0.95 | EDS5-like protein |
| bf_arrayxxx_0052c01.t3m.scf_662 | 0.95 | patatin precursor |

**Table S7. Phosphorylated intermediates and organic acids in NTTP, CW-ISO and WT control**.

Average ± standard deviation. Bold indicates a significant compared to WT ($p \leq 0.05$) (n=3-4).

| Metabolite (nmol/ g FW) | Solara | NTTP | CW-ISO |
|---|---|---|---|
| Phospho-enol-pyruvate | 17.1 ± 2.9 | 14.3 ± 3.2 | 17.9 ± 2.4 |
| Glucose 6-phosphate | 140.1 ± 4.0 | **111.7 ± 3.7** | **168.7 ± 21.4** |
| Glucose 1-phosphate | 11.9 ± 3.9 | 12.1 ± 2.9 | 11.9 ± 4.4 |
| Succinate | 34.1 ± 4.6 | 40.5 ± 6.3 | 34.5 ± 1.5 |
| Fumarate | 35.4 ± 7.2 | 31.9 ± 9.2 | **226.3 ±27.3** |
| Shikimate | 0.3 ± 0.5 | **3.0 ± 0.7** | **13.4 ± 4.1** |
| UDP-N-acetylglucosamine | 1.9 ± 0.4 | 1.9 ± 1.2 | 1.5 ± 1.0 |
| 3-Phosphoglycerate | 90.9 ± 8.5 | 84.0 ± 11.4 | 99.4 ± 8.2 |
| Trehalose 6-phosphate | 0.4 ± 0.1 | 0.5 ± 0.1 | 0.2 ± 0.1 |
| Sucrose 6-phopshate | 0.7 ± 0.2 | 0.5 ± 0.1 | **0.4 ± 0.1** |
| Fructose 6-Phosphate | 31.0 ± 8.7 | **52.2 ± 7.2** | 36.6 ± 2.5 |
| Fructose 1,6-bisphosphate | 0.8 ± 0.3 | 1.2 ± 0.3 | 0.6 ± 0.1 |
| Erythrose 4-phosphate | 23.0 ± 3.0 | **17.8 ± 2.2** | **29.4 ± 4.1** |
| Glucose 1,6-bisphosphate | 2.7 ± 0.7 | 3.3 ± 2.5 | 4.9 ± 1.9 |
| Ribulose 1,5-bisphosphate | 1104.8 ± 67.1 | 1151.8 ± 356.3 | 1356.3 ± 251.2 |
| Dehydroxyacetone-phosphate | 8.3 ± 4.1 | **14.6 ± 2.6** | 13.6 ± 2.1 |
| 2-Oxoglutarate | 26.6 ± 6.1 | **15.6 ± 4.4** | **13.9 ± 3.7** |
| Citrate | 7046.4 ± 1083.7 | 7051.1±1243.2 | 6639.3±797.4 |
| Malate | 3794.2 ± 357 | 4126.9 ± 397.7 | **4401.3 ± 280.9** |

**Table S8. Amino acids in Solara, NTTP and CW-ISO.** Average ± standard deviation. Bold indicates significance compared to WT ($p \leq 0.05$) (n=3-4).

| Amino acid (nmol/ g FW) | Solara | NTTP | CW-ISO |
|---|---|---|---|
| Aspartic acid | 226.9 ± 5.5 | 321.2 ± 65.8 | **280.0** ± 40.4 |
| Glutamic acid | 612.3 ± 35.3 | 842.2 ± 170.9 | 610.4 ± 78.8 |
| Serine | 250.5 ± 51.1 | 125.9 ± 16.0 | **412.7** ± 51.2 |
| Glutamine | 721.3 ± 67.1 | **229.1** ± 22.2 | **3641.1** ± 696.6 |
| Glycine | 138.9 ± 47.1 | 80.5 ± 11.7 | 108.4 ± 18.0 |
| Histidine | 171.5 ± 19.4 | **107.5** ± 22.2 | **97.6** ± 11.3 |
| Threonine | 1975.2 ± 108.1 | **1144.1** ± 388.4 | **5972.5** ± 1007.6 |
| Arginine | 142.8 ± 7.67 | 113.1 ± 33.3 | 164.8 ± 32.8 |
| Alanine | 96.5 ± 20.6 | 54.3 ± 8.0 | **137.5** ± 32.0 |
| Proline | 78.4 ± 8.1 | 53.7 ± 5.6 | 95.6 ± 9.3 |
| Tyrosine | 193.2 ± 25.0 | **96.0** ± 14.8 | **14.9** ± 0.80 |
| Valine | 697.2 ± 30.5 | **434.3** ± 99.3 | 636.6 ± 188.0 |
| Methionine | 411.1 ± 26.3 | **218.3** ± 45.6 | 244.9 ± 69.6 |
| Isoleucine | 226.5 ± 11.3 | 170.2 ± 37.9 | **68.0** ± 10.9 |
| Lysine | 36.5 ± 1.8 | 39.5 ± 9.6 | 23.6 ± 2.6 |
| Leucine | 61.9 ± 5.6 | 65.0 ± 18.2 | 55.5 ± 7.0 |
| Phenylalanine | 650.6 ± 70.5 | **327.8** ± 65.4 | **88.5** ± 9.1 |
| Total amino acid | 6187.7 ± 1140.2 | 4210.7 ± 1462.3 | **14033.8** ± 3480.3 |

**Table S9. Major carbohydrates in Solara, NTTP and CW-ISO tubers**. Average ± standard deviation Bold indicates significance compared to WT ($p \leq 0.05$) (n = 7-8).

| Metabolite (µmol/ g FW) | Solara | NTTP | CW-ISO |
|---|---|---|---|
| Starch | 303.2 ± 22.4 | 290.8 ± 48.3 | **265.8 ± 31.9** |
| Glucose | 3.0 ± 0.7 | **7.6 ± 0.8** | **0.5 ± 0.4** |
| Fructose | 0.4 ± 0.4 | **5.8 ± 0.5** | **1.6 ± 0.4** |
| Sucrose | 13.6 ± 1.0 | **3.2 ± 0.4** | **3.3 ± 0.3** |

**Table S10. Carotenoid contents in Solara, NTTP and CW-ISO.** Average ± standard deviation. Bold indicates significance compared to WT ($p \leq 0.05$) (n=3-4).

| Carotenoid (pmol/ g FW) | WT Solara | NTTP | CW-ISO |
|---|---|---|---|
| cis-Neoxanthin | 210.1 ± 5.8 | **170.6 ± 23.1** | **286.8 ± 23.1** |
| Violaxanthin | 1150.6 ± 9.5 | **970.5 ± 67.9** | **2608.7 ± 246.1** |
| Antheraxanthin | 2568.4 ± 28.5 | **1870.9 ± 128.1** | **1066.1 ± 139.8** |
| Lutein | 603.6 ± 9.1 | **536.7 ± 17.0** | 616.4 ± 43.2 |
| Zeaxanthin | 2725.7 ± 77.5 | 2817.7 ± 330.6 | **442.2 ± 58.7** |
| β-Carotene | 23.3 ± 3.5 | **11.3 ± 1.2** | **14.3 ± 2.0** |
| Total | 7281.8 ± 65.1 | **6377.8 ± 423.1** | **5034.5 ± 84.1** |

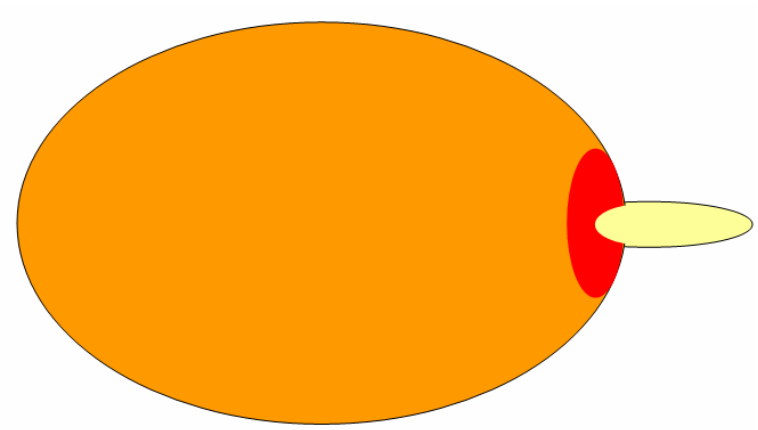

**Figure S1. Schematic representation of a potato tuber to illustrate the sampling of material described as parenchyma associated with the sprout.** A cork borer was used to extract the tissue indicated in red. It can be assumed that this region also contain vascular tissue.


**Figure S2. Alignment of nucleotide sequences of ISA1 RNAi target region with the ISA2 and ISA3 coding sequences.**


**Figure S3. Alignment of nucleotide sequences of ISA2 RNAi target region with the ISA1 and ISA3 coding sequences.**

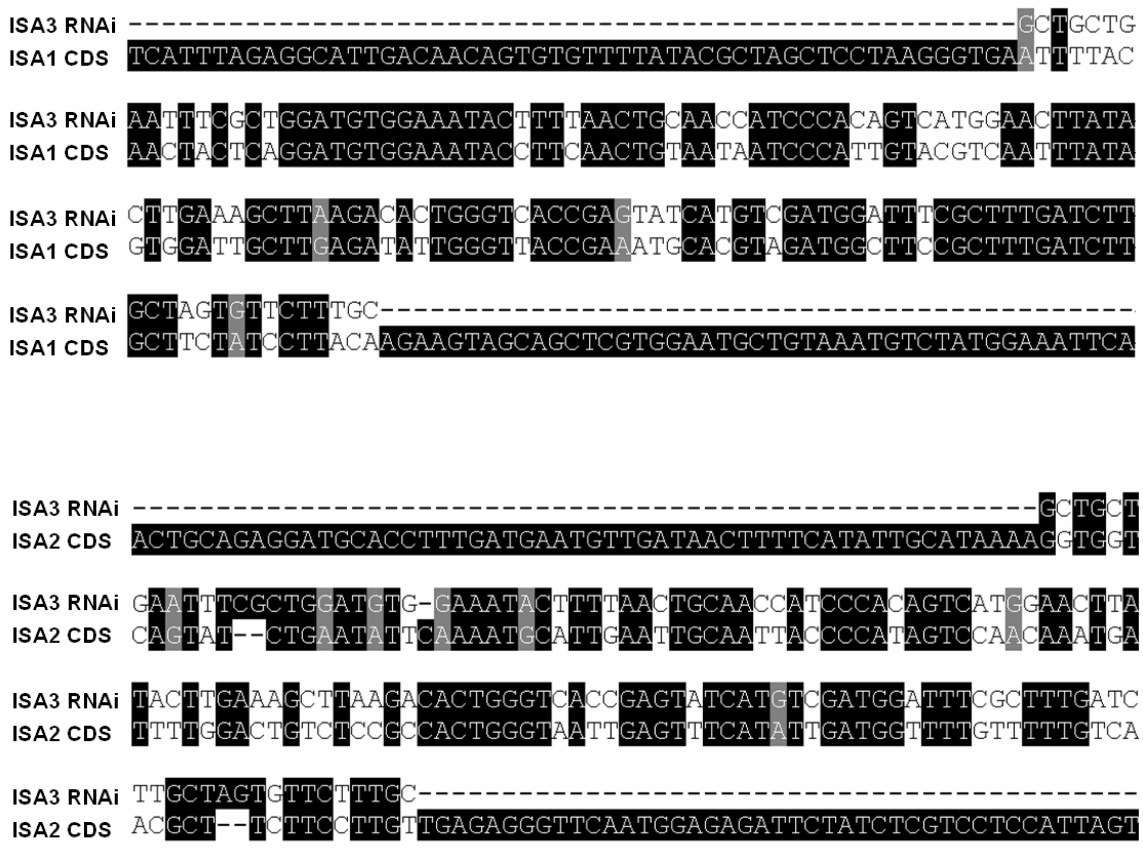


**Figure S4. Alignment of nucleotide sequences of ISA3 RNAi target region with the ISA1 and ISA2 coding sequences.**

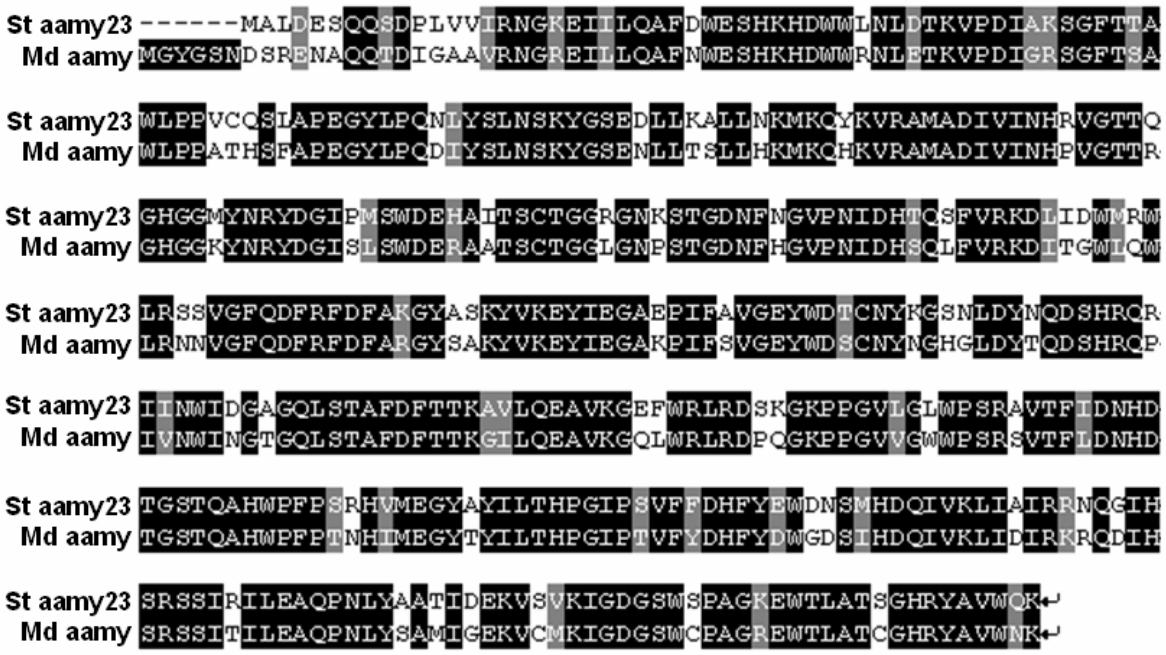


**Figure S5. Amino acid sequence alignment of potato alpha-amylase 23 (St aamy 23) and apple alpha-amylase (Md aamy, accession number AF153828).** Sequence similarity is 76% based on pairwise alignment.

**Acknowledgements**

Since there are so many invaluable contributions, it would be impossible to acknowledge everyone who helped with the work presented in this dissertation, but the following people deserve special mention. Uwe, thank you for all the enthusiasm, help, discussions and the ability to always fit me into your busy schedule. Your contribution to my career and life goes beyond what is written in this thesis and I will be forever greatful. I would like to thank my collegues and friends for making my time in Germany an enriching and wonderfully pleasant experience. Special thanks go to Stephen for always selflessly helping out. Several people outside the *Lehrstuhl* also contributed and again it would be difficult to mention everyone, but I do want to single out the group of Professor Samuel Zeeman at the ETH in Zurich for hosting me in Switzerland and providing the facilities and expertise for glucan structural analysis.

I am blessed with a truly wonderful family and would like to thank them for always supporting me. Special thanks go to my parents for their unconditional love and support. Finally, Mia, thank you very much for sharing a life with me and I look forward to our next adventure together. And thanks for always laughing at my lame jokes (case and point) ☺.

**Curriculum Vitae**

**Personal information:**

Name: Stephanus Johannes Ferreira

Date of birth: 10 December 1981

Place of birth: Upington, South Africa

Nationality: South African

**Education:**

2008-Present: Friedrich-Alexander-Universität Erlangen-Nürnberg, Erlangen, Germany

2001-2007: Stellenbosh University, Stellenbosch, South Africa

1996-2000: Upington High School, Upington, South Africa

1989-1995: Laerskool Oranje-Noord, Upington, South Africa

**Publications:**

**Comparative transcriptome analysis coupled to X-ray CT reveals sucrose supply and growth velocity as major determinants of potato tuber starch biosynthesis.** S.J. Ferreira, M. Senning, S. Sonnewald, P.-M. Kessling, R. Goldstein and U. Sonnewald. *BMC Genomics 11:93*, 2010.

**The reduction of starch accumulation in transgenic sugarcane cell suspension culture lines.** S.J. Ferreira, J. Kossmann, J.R. Lloyd and J.-H. Groenewald. *Biotechonology Journal 3:11*, 2008.